UNIVERSITY OF LIVERPOOL

In vitro Models to Describe the Pharmacokinetics and Pharmacodynamics of New and Existing Antifungal Agents

Thesis submitted in accordance with the requirements of the University of Liverpool for the degree of Doctor of Philosophy

Helen Joan Box

March 2017

Disclaimer

The data in this thesis is a result of my own work. The material collected for this thesis has not been presented, nor is currently being presented, either wholly or in part for any other degree or other qualification. All of the research, unless otherwise stated, was performed in the Department of Pharmacology, Institute of Translational Medicine, the University of Liverpool. All other parties involved in the research presented here, and the nature of their contribution, are listed in the Acknowledgements section of this thesis.

Acknowledgements

First and foremost, I would like to express my utmost gratitude to my academic supervisors, Prof. William Hope and Dr. Joanne Livermore. The guidance, support, encouragement and at times tough-love (!) you have shown me throughout my PhD will be forever appreciated. William, the opportunities and experiences you presented me with during these years went above and beyond. Jo, what else can I say but that you are simply incredible. We will remain the closest of friends for a long time to come.

I would like to thank Joanne Goodwin and Sarah Whalley, not only for their analytical expertise and contribution, but for their unwavering friendship and support. Virginia, I am so lucky to have shared this experience with such an inspiring woman…Thank you! I would also like to extend my gratitude to Dr. Timothy Felton for his wisdom and advice throughout, you are the kindest of geniuses.

Adam and Laura. Rats. We've had a ball. This experience would not have been the same without you. We have lolled, lived and learnt together right the way through. You never failed to bring me back from the downs and were most often, solely responsible for the ups! More recently Nickers, thank you for the howls and for sharing your fabulous outlook on life. Hannah and Soph, my girls! We have travelled through our early academics together as the best of friends, I am so lucky to have you both!

To my mum and dad, you are the most amazing people to me. I can only aspire to develop the selflessness and strength you have shown me as parents. I just can't thank you enough. Last but not least to all my family and friends. My Pegsters, Lizzie and David, school friends, Bores, aunties and cousins. Rosie... I don't know how you have put up with me or where I would be without you. The love and support through this process from all of you will never be forgotten.

Table of Contents

Table of Figures

Table of Tables

Abstract

Invasive mould infections are global contributors to morbidity and mortality in immunocompromised patient populations. There are increasing reports of pathogenic fungi that confer both acquired and intrinsic resistance to current antifungal therapies. The development of novel antifungal agents is essential to broaden the therapeutic options for invasive fungal disease. A knowledge of the pharmacokinetics and the pharmacodynamics of a drug can facilitate an understanding of the optimal exposures required for efficacy. The relationship between dose-exposure and response can be defined from experimental data using PK-PD modelling.

Experimental work was completed using static and dynamic *in vitro* cellular models of invasive fungal infections. Drugs were measured using high performance liquid chromatography and mass spectrometry. Fungal specific antigens were detected using enzyme-linked immunosorbent assays. PK and PD datasets were linked using a PK-PD nonparametric modelling program.

Static studies demonstrated clear dose-response relationships for isavuconazole (ISA), voriconazole (VRC) and novel agent, F901318 against pathogenic fungi. Exposure-response relationships were defined for these agents in dynamic models. Mathematical models demonstrated satisfactory fits to each dataset. PD indexes associated with maximal antifungal effect, in terms of AUC:MIC were determined from model outputs for each agent against isolates of *Aspergillus* (ISA), *S. apiospermum* and *F. solani* (VRC and F901318).

The treatment options available for invasive fungal infections are not ideal. Rising resistance to current antifungal therapies warrant a better understanding of the

optimal exposures that will treat an invasive disease effectively. This thesis describes the development and use of *in vitro* models of invasive fungal disease for the delineation of these key relationships. These analyses may provide decision support for clinicians when determining an effective dosing regimen in the clinic. The datasets generated may also provide information on dosages that may be suitable to take into Phase III clinical trial for novel agents.

CHAPTER I

Introduction

1.1 INVASIVE FUNGAL INFECTIONS

Invasive fungal infections (IFI) are an ever-present clinical concern for patients with a compromised immune system. Patients undergoing transplantation or receiving chemotherapy are most at risk of invasive disease (Galimberti, Torre et al. 2012). The most common IFI are caused by *Candida* spp. closely followed by *Aspergillus* spp. However, the widespread use of chemotherapy and immunosuppressive agents has seen an evolution in the spectrum of organisms that can cause invasive infection (Kontoyiannis and Lewis 2006). Species of *Scedosporium* and *Fusarium* have been increasingly recognised as emerging fungal pathogens. Invasive infections with these organisms are often associated with devastating clinical outcomes (Nucci 2003). Due to the increasing frequency of reported cases and their innate resistance to first-line agents, *Scedosporium* and *Fusarium* species now represent two of the most clinically important moulds contributing to 16% and 22% of non- *Aspergillus* mould infections worldwide, respectively (Figure 1.1) (Park, Pappas et al. 2011, Smith and Kauffman 2012, Slavin, van Hal et al. 2015).

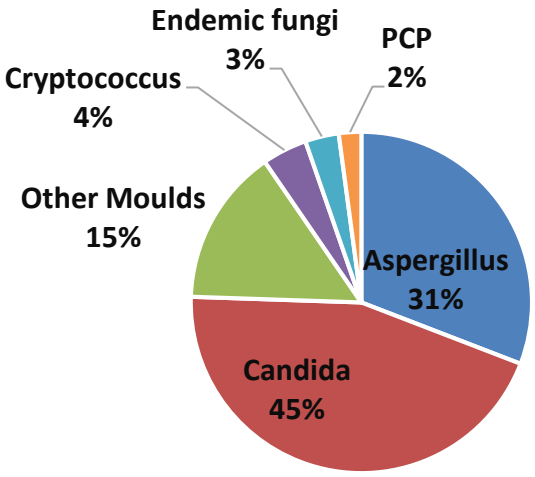

Figure 1. 1

The contribution of specific fungal pathogens to global invasive fungal infections. Data taken form Park et al. 2011 (Park, Pappas et al. 2011)

The discovery and development of novel antifungal drugs is essential to broaden the spectrum of therapeutic options available for the treatment of IFI. An understanding of how both new and existing antifungal regimens can be designed in order to treat organisms appropriately is central to combatting resistance. The pharmacokinetics (PK) of a drug can be described as what happens to an agent as it passes through the human body. The pharmacodynamics (PD) of a drug is how the agent exerts its desired effect within the human body. The target in the case of antimicrobial agents is a specific organism causing an infection. A knowledge of the relationship between the pharmacokinetics and pharmacodynamics (PK-PD) of a drug against specific organisms may facilitate our understanding of the optimal dose and subsequent exposure that will treat a disease effectively. This may, in turn, provide decision support when determining an effective therapeutic course.

Aspergillus spp. are ubiquitous filamentous fungi commonly found in soil or in areas where decomposition is in progress such as compost heaps. *Aspergillus* is a thermotolerant organism and can therefore thrive in a broad range of environments, from tropical to polar conditions (Galimberti, Torre et al. 2012). The majority of human infections are caused by *A. fumigatus*, *A. terreus*, *A. flavus* and *A. niger* (Dimopoulos, Frantzeskaki et al. 2012). The rise in frequency of infection with *Aspergillus* spp. is closely correlated with the increased use of immunosuppressant therapy for the treatment of various conditions. Corticosteroids have been shown to be in use in around 30% of patients with *Aspergillus* infection, 63% of whom developed invasive disease (Perfect, Cox et al. 2001). The incidence and mortality of infection is relative to the degree of immunosuppression and the underlying illness. In patients with acute leukaemia, the incidence of invasive infection is around 13% with an attributable mortality rate (AMR) of around 12%.(Pagano, Caira et al. 2007). A multi-

centre study of patients receiving haematopoietic stem cell transplants (HSCT) observed a frequency of infection with *Aspergillus* spp. in around 7-10% of patients. In this study mortality rates reached around 60% (Marr, Carter et al. 2002). In solid organ transplant patients, a similar mortality rate is observed with a slightly higher incidence of 11%-14% (Segal 2009). Consequently, *Aspergillus* species have become an increasingly recognised human pathogen in immunocompromised hosts and infections with this organism have become a recurring clinical complication in patients receiving immunosuppressive drugs.

Underlying disease or characteristic	**No. (%) of patients (n=1209)**
Pulmonary disorder	477(40)
Corticosteroid use	381(32)
Neutropenia	61 (5)
Haematopoietic stem cell transplant	39 (3)
Solid-organ transplant	100 (8)
Cystic Fibrosis	127 (11)
HIV infection	138 (11)

Table 1. 1

A summary of risk factors for *Aspergillus* infection. Data from 24 centres and 1209 patients over a one year time period was obtained for the formations of the Aspergillosis Case Surveillance Form. (Perfect, Cox et al. 2001)

Scedosporium spp. and related organisms within the *Scedosporium-Pseudallescheria* species complex are ubiquitous filamentous moulds that can be found in temperate climates and areas of extensive pollution (Cortez, Roilides et al. 2008). These organisms are often described as rare and emerging fungal pathogens as an increase in the frequency of infection has been observed over recent years. *S. apiospermum* is the predominant species causative of human infections followed by *S. prolificans* (Lamaris, Chamilos et al. 2006, Heath, Slavin et al. 2009). Their emergence as a pathogenic species may be correlated with the increased use of antifungal prophylaxis (Park, Pappas et al. 2011, Auberger, Lass-Flörl et al. 2012). *S. apiospermum* has previously been described as the asexual reproductive form (anamorph) of *P.boydii*. More recently, these organisms have been reclassified as separate species although very closely related on both a morphological and molecular level (Gilgado, Cano et al. 2008). Infections caused by these organisms are not transmitted between individuals (Campa-Thompson, West et al. 2014). Disease states may range from cutaneous and sub-cutaneous tissue infections to invasive, disseminated disease (Troke, Aguirrebengoa et al. 2008). Although disseminated infection has been reported in immunocompetent patients in the case of near drowning incidents, immunocompromised individuals are the predominant population at risk for developing invasive scedosporiosis (Smith and Kauffman 2012).

Fusarium spp. are important plant pathogens that grow on a wide range of substrates including soil, plant debris and in water. These ubiquitous saprophytes are able to persist in water reservoirs in the form of water-structure biofilms. *Fusarium* species are recognised as a significant contributor to water-borne infections in hospital patients (Nucci and Anaissie 2007). Hyaline hyphae are formed in tissue and as for *Scedosporium* spp. can often be mistaken for those formed by *Aspergillus* spp.

(Esnakula, Summers et al. 2013). Human infection with *Fusarium* spp. can present as a range of clinical manifestations from superficial to locally invasive and disseminated infection. A review of the literature of 300 cases of *Fusarium* infection revealed that approximately 12 species of *Fusarium* spp. are associated with human infection. *F. solani* is the most common human pathogen accounting for approximately 50% of cases, followed by *F. oxysporum* which is responsible for approximately 20% of cases overall and almost all cases of fusarial onchomycosis. *F. verticilloidis* and *F. moniliforme* accounted for approximately 10% of cases individually. In a multicentre review of patients with haematological malignancy and invasive fusariosis, 83% of patients were persistently neutropenic and around 39% had undergone a haematopoietic stem cell transplant (HCST). Mortality rates of up to 80% have been observed in these groups of patients. Prolonged neutropenia and the use of high dose corticosteroids were predictive of poor outcome (Nucci, Anaissie et al. 2003). These findings were confirmed in a second multi-centre investigation in HSCT recipients with fusariosis. In this study persistent neutropenia was also observed to be the single prognostic factor relating to death (Nucci, Marr et al. 2004)

1.11 Pathophysiology

The pathophysiology of invasive mould disease is similar for *Aspergillus, Scedosporium* and *Fusarium* species.

The development of an invasive infection is dependent on the underlying state of the host immune system (Table 1.1). The production of pro-inflammatory cytokines and phagocytosis of conidia by alveolar macrophages is a first-line defence for the clearance of inhaled conidia (Segal 2009). The subsequent prevention of conidial germination and hyphal damage via neutrophilic aggregation and the formation of NADPH oxidase are principal clearing mechanisms in place for invading pathogenic fungi (Dagenais and Keller 2009). In the presence of steroids such as in chemotherapy patient populations, the secretion of inflammatory mediators is diminished (Alekseeva, Huet et al. 2009, Bellanger, Millon et al. 2009).

In the absence of these key pulmonary defence mechanisms microscopic fungal spores may be inhaled into the lung which can then colonise to cause a primary infection (Figure 1.2 A). With minimal clearance by the host immune system, the conidia swell and begin to germinate into hyphae (Kwon-Chung and Sugui 2013). The process of angioinvasion by the hyphae then begins (Kousha, Tadi et al. 2011), eventually leading to dissemination of the fungi and fungaemia (Denning 1991) (Figure 1.2 B).

A

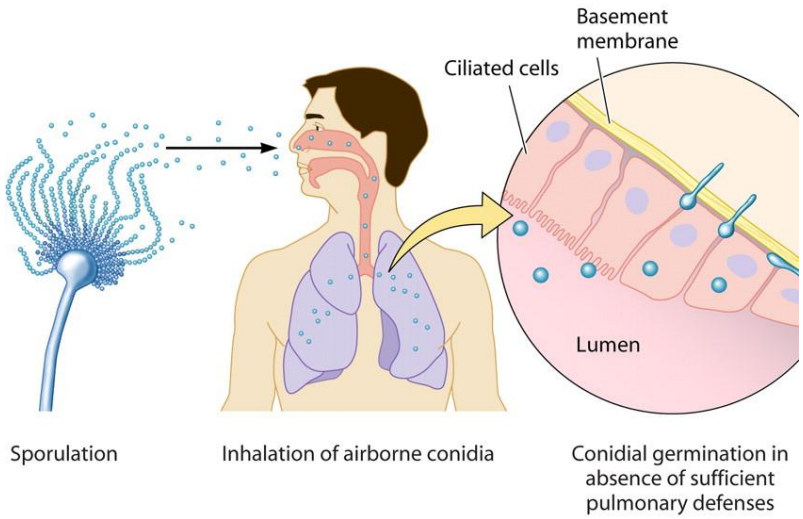

B

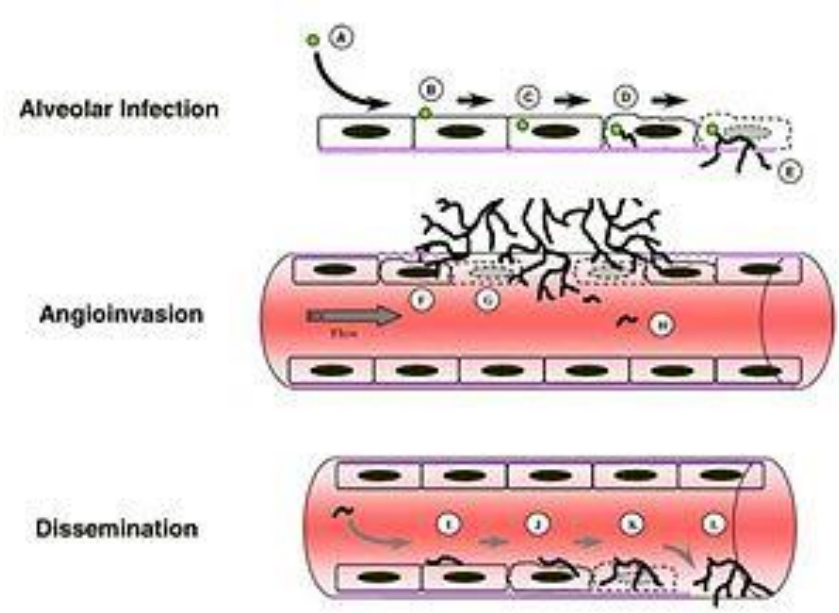

Figure 1. 2

(A) Pathophysiology of a primary fungal lung infection and (B) Pathophysiology of an invasive and disseminated infection fungal infection. Taken from Dagenais et al. (2009) and Richardson et al. (2009).

Specific virulence factors involved in the pathophysiology of *S. apiospermum* and *F. solani* infections have not been extensively studied. Several factors have been well characterised for *Aspergillus* species which may contribute towards an overall understanding of how a primary infection is contracted and how this may develop into an invasive and disseminated disease.

Sialic acid residues are present on the surface of the conidia of several pathogenic species of *Aspergillus* and are particularly abundant on those produced by *A. fumigatus* (Wasylnka, Simmer et al. 2001). These residues may facilitate the binding of conidia to the basal lamina of the alveolar epithelium and may play a role in the establishment of primary lung disease. Conidia then produce toxins that can inhibit the mucociliary clearance mechanism. This may inhibit the expulsion of pathogens from the lung and facilitate the entry of additional conidia into the lower airways (Margalit and Kavanagh 2015).

The production of reactive oxygen species (ROS) by the alveolar macrophages is an important antimicrobial defence against respiratory pathogens (Jahn, Koch et al. 1997). Dihydroxynaphthalene (DHN)-melanin is a pigment present in the cell walls of *Aspergillus* species. This pigment has a protective role against ultra-violet light, enzymatic lysis and oxidation, including that induced by ROS (Chotirmall, Mirkovic et al. 2014). More recently, DHN-melanin has demonstrated the ability to inhibit the acidification of *Aspergillus* containing phagolysomes post engulfment by the alveolar macrophages (Thywiben et al. 2011). Superoxide dismutase enzymes (SOD), responsible for the detoxification of superoxide, have been implicated as virulence factors for several pathogenic fungi including *A. fumigatus*, *Candida* spp. and some species of *Cryptococcus* (Fréalle, Noël et al. 2005). Lima et al. (2007) investigated production of SOD by the hyphae of *S. apiospermum* and it was suggested that the

production of SOD may play a protective, immuno-evasive role in the pathophysiology of *S. apiospermum* infection (Lima, Larcher et al. 2007).

In order for the hyphae of *Aspergillus* spp. to invade through the surrounding blood vessels the organism secretes a range of proteolytic enzymes for the destruction of host tissue and nutrient acquisition (Hohl and Feldmesser 2007). Elastin is an important component of the lung tissue. Clinical isolates from patients with invasive disease have demonstrated increased elastase activity in comparison to environmental isolates, suggesting a key role for elastase in the pathogenicity of invasion (Blanco, Hontecillas et al. 2002) Silva et al. investigated peptidase release for isolates of *P. boydii* and *S. apiospermum*. This investigation established that peptidase enzymes were extracellularly released by the mycelium of these fungi. IgM and IgG are involved in the activation of complement cascades and play a significant role in the host antimicrobial response (Horton and Vidarsson 2013). Lima et al. demonstrated that metallopeptidase enzymes extracted from *P. boydii* were able to cleave the IgG molecules *in vitro* and may contribute towards the pathogenesis of invasion. Fibronectin is implicated in the activation of alveolar macrophages and monocytes (Lackner and Guarro 2013). Laminin represents a key component of the basement membranes of the lung. The release of metallopeptidases by *P. boydii* was demonstrated to be associated with the break-down of these proteins. This may allow the fungi to suppress the activation of macrophages by fibronectin and may also contribute towards angioinvasion of *P. boydii*.

The virulence factors associated with the pathogenesis of *Fusarium* spp. in humans are understudied. *Fusarium* species inherently produce mycotoxins such as the trichothecenes. These compounds have been demonstrated to decrease the proliferation and production of both lymphocytes and macrophages. They also inhibit

neutrophilic aggregation. This suppression of humoral and cellular immunity may play a key role in the pathophysiology of invasive disease (Nelson, Dignani et al. 1994).

1.12 Diagnosis

1.121 *Imaging*

The use of computed tomography (CT) is amongst the most conventional forms of diagnoses for invasive mould disease. The earliest radiological manifestation is a nodule however in the case of an aspergilloma the fungal mass may be separated from the wall of the lung producing a crescent- shaped airspace known as the "air crescent sign" (Franquet, Muller et al. 2001, Smith and Kauffman 2012). The mass usually moves around within the lung as the patient changes position known as the "Monod sign". Invasive disease may present on a CT scan as a "halo" sign (HS) that can be seen as an opaque area surrounded by a halo, ground-glass like attenuation which represents an area of alveolar haemorrhage. The frequency of observation very much depends on the immune status of the individual and the progression of the disease. This is a good indication of IFI in at risk patient populations and is thought to be present in around 50-90% of cases. However, lower frequencies of HS can be observed in the later stages of disease (Georgiadou, Sipsas et al. 2011). Imaging is not species specific and similar signs may be observed in patients infected with a range of respiratory pathogens. This may result in a delay in diagnosis. Therefore, alongside imaging other diagnostic techniques must be used to determine the disease- causing pathogen (Morrissey, Chen et al. 2013).

1.122 *Microbiology and histopathology*

The culture and identification of sputum, bronchoalveolar lavage (BAL) and serum samples are traditional methods of diagnosis for invasive aspergillosis. Samples are cultured in a suitable medium such as Sabouraud dextrose medium (SAB) and are then identified by microscopy. Microscopic examination allows for the identification of a specific pathogen, an advantage over imaging alone.

Microscopic visualisation of fungi in a sample may also be used to confirm the presence of an infection where there is uncertainty of the results obtained from other tests. Direct microscopic examination is time-efficient and results can be obtained in 1-2 hours (Schelenz, Barnes et al. 2015). The morphological characteristics and microscopic markers of IFI are similar between clinically important moulds (Table 1.2). The patient may also be infected with more than one pathogen. Training and expertise for medical mycologists is essential for the determination of organism and species. It is therefore suggested that microscopy is used in parallel to other diagnostic tests to obtain a definitive diagnosis (McClenny 2005). As *Aspergillus* species are ubiquitous in nature they can often contaminate specimens and culture medium which may produce false-positive results. The sensitivity of culture and microscopic identification is increased in patients with an advanced disease. However this may be hampered if only a small sample is obtained from the patient. This can be improved by repeat sampling however is often difficult in critically ill patients (Hayes and Denning 2013).

Organism(s)	Microscopic markers	
	Hyphae	**Other features**
A. fumigatus	2.5-8 µm wide, septate, hyaline, acute angle branching, tree or fan-like branching. Stipes may resemble those of zygomycetes.	Conidial head uniseriate, columnar, conidia in chains or detached and dispersed. Single or paired conidia may resemble yeast cells
A. niger	See *A. fumigatus*	Conidial head biseriate, radiate, conidia in chains or detached and dispersed. Single or paired conidia may resemble yeast cells
A. terreus	See *A. fumigatus*	Small, round, hyaline conidia (‘accessory’ conidia) attached to the vegetative hyphae
***Accremonium, Fusarium, Paecilomyces* spp.**	See *A. fumigatus*	Phialides and phialoconidia, specific to the genus, may be found in closed tissue
Scedosporium apiospermum	See *A. fumigatus*	Typical annelloconidia and annellides may be found in closed tissue
Zygomycetes	10–30 µm wide, aseptate, non-radiating, 90° angle branching. Folds in hyphae may simulate septae	N/A
Dermateaceous moulds	Hyphae with brown pigmentation; walls often not parallel; may appear moniliform (like a ‘string of beads’)	Brown pigment seen in KOH exam with brightfield illumination; stained with Fontana—Masson and often with Hematoxylin and Eosin

Table 1. 2

Microscopic markers of clinically relevant pathogenic mould species (McClenny 2005)

Histopathological staining of biopsy samples may also be used in order to diagnose an IFI. A panel of stains may be used in order to both identify and exclude the presence of specific organisms. The Grocott methenamine silver (GMS) stain or Periodic Acid Schiff (PAS) are used for the assessment of fungi and are recommended in patients with a suspected fungal infection (Schelenz, Barnes et al. 2015). Both *Scedosporium* and *Fusarium* species demonstrate the ability to sporulate in tissue (adventitial sporulation), which may be a key indicator of scedosporiosis or fusariosis in biopsy samples or blood cultures. *Fusarium* species may be identified by the presence of characteristic 'banana-shaped' macroconidia. However, these structures may often be confused with yeasts (Lackner and Guarro 2013). Although histopathology is a useful tool in the determination of invasive infection, it may be difficult to determine the presence of a specific fungal pathogen due to the morphological similarities in septated fungi (Thornton, Johnson et al. 2012). Obtaining a biopsy sample for histopathological analysis may also be complicated and in some cases fatal for patients who are critically ill.

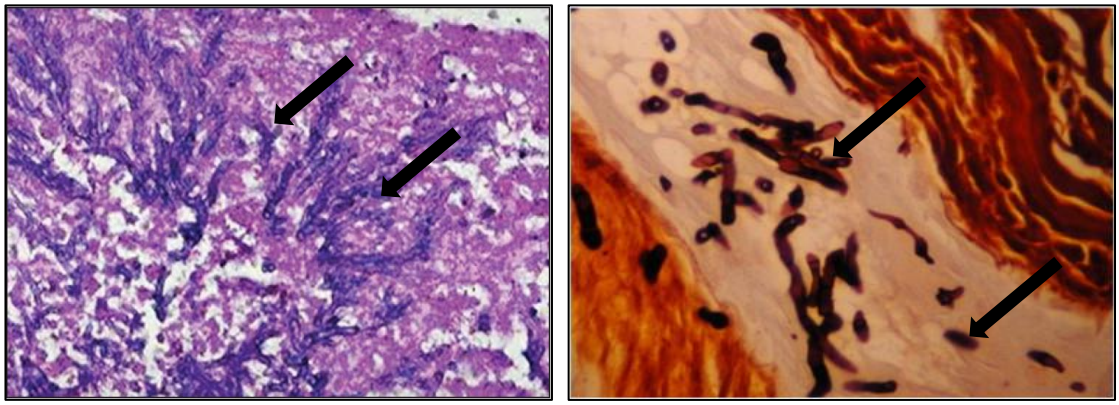

Figure 1. 3

Histological images of tissue infected with A) *S. apiospermum* and B) *F. solani*. Arrows highlight the septated, branching hyphae associated with invasion. Adapted from A) Agatha et al. (2014) and B) Galimberti et al. (2012).

1.123 Serological and molecular testing

The development of molecular based techniques and serological assays for the diagnosis of IFI has been a major advancement. Molecular based diagnostics such as PCR or a galactomannan assay may be performed on bronchoalveolar lavage fluid (BAL) and blood samples. The diagnostic strategy associated with a molecular platform is detailed in Figure 1.3.

The detection of circulatory biomarkers that are indicative of disease has been particularly useful in the diagnosis of aspergillosis (Verdaguer, Walsh et al. 2006, Galimberti, Torre et al. 2012). Galactomannan is an exo-antigen that is a key component of the fungal cell wall. It is released by *Aspergillus* species during cell growth and has been demonstrated to be a relatively specific biomarker for aspergillosis. The double sandwich enzyme immunoassay (ELISA) for the detection of galactomannan has been clinically available in Europe and the USA for over a decade. This assay now provides the gold standard for the diagnosis of aspergillosis and may also be indicative of disease progression. The Platelia *Aspergillus* kit marketed by Bio-Rad laboratories utilises a galacatofuranose- specific rat monocolonal antibody in order to detect galactomannan at varying concentrations in blood and BAL cultures. A cut off absorbance value (450nm) of 1.5 was originally recommended by the manufacturer for the classification of a positive result. However further research has demonstrated the reduction of this to the FDA approved value of 0.5 significantly boosts the assay sensitivity to 97.4%. It is important to note that in this study an increase in sensitivity was at the expense of specificity which was reduced from 97.5% to 90.4% (Maertens, Klont et al. 2007). The accuracy of the galactomannan assay is very much dependent on disease progression and has a rate of

misdiagnosis in itself. A recent multicentre study of European ICU patients observed an 87% accurate diagnosis in patients with definitive invasive aspergillosis compared to a positive galactomannan culture seen in only 18% of patients in the early stages of disease (Taccone, Van den Abeele et al. 2015). Although galactomannan has been clinically validated as a relatively accurate biomarker of both early and late-stage aspergillosis (Marr, Balajee et al. 2004), there are limitations to its use in pharmacodynamic studies. Firstly, the assay read-outs demonstrate a relatively limited dynamic range. False negative results have also been reported. These may be due to the requirement of a heat pre-treatment step that denatures potential reactive serum proteins however may also denature protein-bound galactofuranose antigens (Verweij and Mennink-Kersten 2006). Studies have also suggested that prior exposure to antifungals may reduce the sensitivity of the Platelia *Aspergillus* assay (Marr, Laverdiere et al. 2005). This has a direct implication on the diagnosis of patients receiving prophylactic antifungal therapy using this assay.

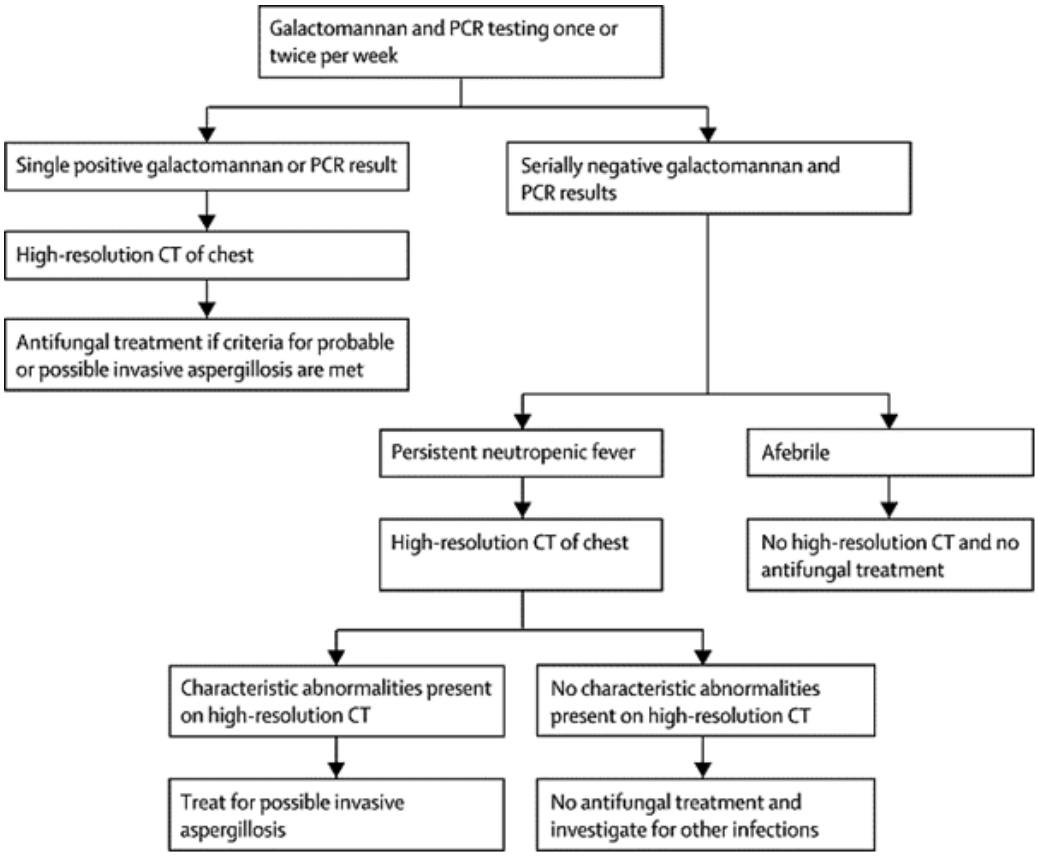

Figure 1. 4

Diagnostic strategy using molecular based techniques as the primary diagnostic platform . Figure taken from Morrissey et al. (2013)

More recently, Thornton *et al*. have described the generation of an *Aspergillus*-specific monoclonal antibody (JF5). This has been incorporated into a point-of-care diagnostic immuno-chromatographic lateral flow device for the detection of circulating antigens released by *Aspergillus* spp. (Thornton 2008). The use of this device has been validated in patient sera and BAL samples (Thornton, Johnson et al. 2012). Studies suggest that antigens bound by JF5 may be used as a surrogate marker for the diagnosis of invasive aspergillosis (Thornton 2008) (Figure 1.4).

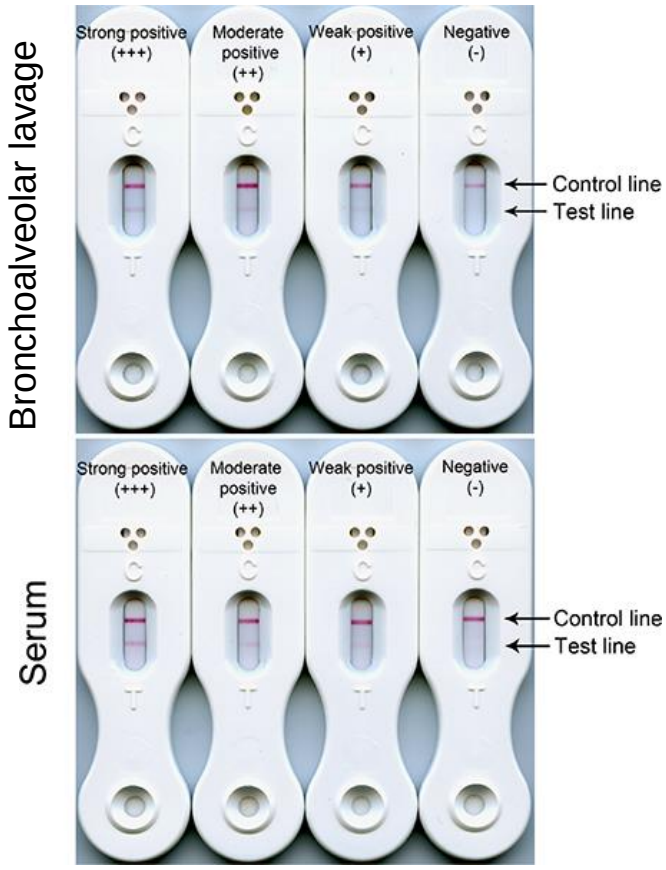

Figure 1. 5

Control lines and test lines from patient serum and BAL samples using the lateral flow device produced by Thornton et al. Figure taken from Thornton et al. (2008)

Scedosporium and *Fusarium* spp. are galactomannan negative therefore no serological assays for their detection are clinically available. Recently Thornton *et al*. have utilised in-house developed immunoglobulin (IgM) and IgG1 k-light chain monoclonal antibodies (MAbs) in a double antibody sandwich enzyme-linked immunosorbent assay (DAS-ELISA) in order to detect *P. boydii* and its related species. The MAbs are specific to *P. boydii* and *S. apiospermum* and do not react with *S. prolificans, A. fumigatus* and many other clinically relevant pathogenic fungi (Thornton 2009). Similarly, a single antibody ELISA utilising mouse-derived monoclonal antibodies is also under development for the detection of *Fusarium* species. ED-7 is an IgM specific monoclonal antibody and binds to an extracellular 200kDa heat stable glycoprotein antigen specific for *Fusarium* spp. The detection of ED-7 in both hospital and sink biofilms has allowed for the tracking of environmental isolates of *Fusarium* species (Thornton and Wills 2015, Al-Maqtoofi and Thornton 2016). Despite the relatively limited dynamic ranges these assays currently provide, the detection of these antigens in a clinical setting may provide a potential platform for the molecular diagnosis of infection with *S. apiospermum* and *Fusarium* species.

1.13 Clinical Presentation

Relatively few specific clinical symptoms are typically seen in the early stages of pulmonary aspergillosis (Taccone, Van den Abeele et al. 2015). Fever, cough, sputum production and dyspnoea are common symptoms however these are nonspecific (Soubani and Chandrasekar 2002). Upon vascular invasion patients may present with significant pleuritic chest pain due to the development of pulmonary infarcts. In late stage disseminated disease the nervous system may be implicated, manifesting with seizures, focal neurological signs, cerebral infarctions and intracranial haemorrhage (Denning 1998). Deterioration may occur extremely rapidly. The clinical spectrum in immunocompetent hosts spans keratitis, endopthalmitis, sinusitis, soft tissue infections and lung infection. CNS involvement in healthy individuals is generally a result of an invasive and disseminated sinus or lung infection. In immunosuppressed hosts the spectrum of infection is similar, however invasive and disseminated disease may affect several organs (Tortorano, Richardson et al. 2014). The clinical presentation of invasive scedosporiosis is generally non-specific and similar to that of aspergillosis. Disseminated *S. apiospermum* infection often involves the central nervous system and the brain is also a common primary site of infection (Castiglioni, Sutton et al. 2002). Symptoms of CNS involvement can include headaches, incontinence, drowsiness and vomiting (Park, Pappas et al. 2011). The clinical manifestation of invasive infection with *Fusarium* spp. is very similar to that of invasive aspergillosis and scedosporiosis and is often non symptomatic. Invasive infection can present as skin, lung or sinus lesions. As with *Aspergillus* spp., patients with a lung infection may present with a cough, fever and pleuritic chest pain (Marom, Holmes et al. 2008, Tortorano, Richardson et al. 2014).

1.2 ANTIFUNGAL AGENTS FOR THE TREATMENT OF INVASIVE FUNGAL INFECTIONS

The treatment of IFI may be challenging for several reasons. The continuous emergence of resistant strains of pathogenic fungi represents a major clinical issue when determining an effective treatment regimen. Contributing to this, many isolates of *Fusarium* and *Scedosporium* may demonstrate innate resistance to clinically used antifungals (Nucci and Anaissie 2007, Cuenca-Estrella, Alastruey-Izquierdo et al. 2008). The patient populations these infections most commonly affect often have underlying conditions and may already be taking a significant amount of medication including antifungal prophylaxis. This may reduce the safe therapeutic options available to patients due to altered pharmacokinetic profiles in these populations and potential drug interactions. As discussed, the species- specific diagnosis of invasive mould infections may be a lengthy process. Empirical decisions on therapy may have been made during this time, driving resistance and limiting the effective therapeutic options available for the patient.

The use of higher dosages or combination therapy for the treatment of invasive fungal infections represent alternative therapeutic options for patients (Cuenca-Estrella, Alastruey-Izquierdo et al. 2008). Importantly, the development of novel antifungal agents will allow for a greater diversity in treatment options. There are four main classes of drugs currently available for the treatment of IFI. These include the echinocandins, the triazoles, polyene classes of agents and flucytosine (Figure 1.7). More recently, the discovery of novel classes such as the orotomides may broaden the spectrum of antifungals for the treatment of IFI.

1.21 Pharmacokinetics and Pharmacodynamics (PK-PD) of Antifungal Agents

Pharmacokinetics and pharmacodynamics (PK-PD) data for antifungal agents can provide a valuable insight into the optimal exposures of drug associated with antifungal activity against an organism.

1.211 The assessment of antifungal resistance and determination of susceptibility breakpoints

With the diversity of pathogenic mould species increasing, it is necessary for clinicians to have a knowledge of how effective an antifungal agent may be against a specific organism. The epidemiological cut off value (ECOFF) for an organism defines the concentration at which a drug is no longer effective against a population of isolates. They are derived from large epidemiological studies wherein extensive determination of the minimum inhibitory concentrations (MIC) against large numbers of strains is conducted in order to delineate concentrations at which strains have a high probability of resistance (Howard, Lass-Flörl et al. 2013). ECOFF values may then be used alongside PK-PD data obtained from several preclinical and clinical studies in order to define the clinical susceptibility breakpoint for an agent. Clinical susceptibility breakpoints are used to differentiate concentrations at which an agent may demonstrate therapeutic success (susceptible strains) from those where treatment failure is likely (resistant strains) (Martinez, Coque et al. 2015). The use of standardised methodologies for MIC testing and the determination of both ECOFF and clinical breakpoints has proven invaluable to clinicians worldwide (Espinel-Ingroff, Chowdhary et al. 2013). When an antimicrobial agent has been in use for an extended period of time breakpoints are often revised in order to compensate for the emergence and evolution of resistant strains. Large surveillance studies are key to the revision of breakpoints for various antifungal agents as they allow for the identification of trends

in pathogen incidence and resistance profiling (Masterton 2008). Active since 1997, the SENTRY Antimicrobial Surveillance Program is one of the largest programs to date. SENTRY provides comprehensive information on the frequency of pathogen emergence and their susceptibilities to antifungal agents that is central to the establishment of susceptibility breakpoints for antimicrobial agents (Pfaller, Messer et al. 2013).

The relationship between the concentration-time profile for an agent and its clinical efficacy is key for the revision and setting of clinical susceptibility breakpoints. This can be termed the exposure-response relationship between an organism and a drug. The exposure- response relationships of an agent and the MIC are often linked together to derive indices that best correlate to clinical efficacy. These are termed PK-PD indices as they incorporate both the pharmacokinetics of an agents and its pharmacodynamics against an organism. For many agents the clinical outcome is well correlated with the ratio between the area under the concentration time curve (AUC) and the MIC of the organism (AUC:MIC). For other agents outcome may be better related to the proportion of a dosing interval that the concentration of drug exceeds the MIC (%T>MIC) or the maximal concentration of drug reached (C_{max}) over the MIC (C_{max}:MIC) (Mouton, Brown et al. 2012). The determination of these parameters requires analysis of the antimicrobial kill kinetics and is largely dependent on whether an agent exhibits concentration or time-dependent killing (Tam and Nikolaou 2011).

A prior knowledge of the pharmacokinetics and pharmacodynamics of a drug may mean that no more information than the MIC is needed in order to determine an appropriate dosage. However, many find that the interpretation of PK-PD data via

clinical breakpoints is extremely useful when determining if a treatment regimen will be successful (Turnidge and Paterson 2007).

1.212 Current models for the analysis of antifungal PK-PD

In vivo

Several *in vivo* models of invasive aspergillosis have been developed and utilised for the delineation of exposure-response relationships. Murine models of fungaemia using a tail-vein route of infection have been used to define the efficacy of posaconazole, fluconazole, itraconazole, (Gonzalez, Tijerina et al. 2003), AmB formulations (Capilla, Mayayo et al. 2004) and voriconazole (Capilla, Serena et al. 2003) against isolates of *P. boydii* and *S. apiospermum*.

Inhalational murine models of invasive aspergillosis have been used to define the PK-PD of several antifungal agents against isolates of *Aspergillus* spp. (Mavridou, Bruggemann et al. 2010, Lepak, Marchillo et al. 2013, Seyedmousavi, Mouton et al. 2014). Similar to humans, invasive and disseminated infections cannot be established in the presence of a competent immune system. The use of immunosuppressive agents may increase the complexity of a model however plays an essential role in the establishment of a suitable pulmonary infection. Severe and persistent neutropenia is most commonly achieved using a combination of cyclophosphamide and corticosteroids in order to mimic the immune status of an individual at risk of infection (Paulussen, Boulet et al. 2014).

A limitation of these murine models is the differences in expression of key drug metabolising enzymes between mice and humans such as those implicated in the cytochrome P450 pathway (Muruganandan and Sinal 2008). For antifungal agents cleared via these pathways it may be difficult to obtain accurate pharmacokinetic data.

This is particularly apparent in the case of triazole agents voriconazole and isavuconazole where the clear differences in clearance can be seen between mice and humans (Warn, Sharp et al. 2006, Goddard, Stevens et al. 2010, Calvo, Pastor et al. 2012, Lepak, Marchillo et al. 2013, Seyedmousavi, Bruggemann et al. 2015). Mice also exhibit significantly different levels of plasma esterase enzymes to humans which may present challenges in the development of models of agents that are administered as prodrugs, such as isavuconazonium sulphate, the prodrug of isavuconazole (Bahar, Ohura et al. 2012). Mouse models are generally cost effective as the use of a lower order species requires less technical expertise. Murine studies are also high throughput however are terminal and numerous samples cannot be taken.

Rabbit models of invasive aspergillosis are also well validated for the study of PK-PD. Similar to murine studies these models generally induce immunosuppression for the establishment of disease. This may differ depending on whether a neutropenic or a non-neutropenic model is preferred. A neutropenic model is associated with a more severe infection that may be due to the ability of the hyphae to elongate and invade more efficiently in the absence of neutrophils (Petraitiene, Petraitis et al. 2015). Non neutropenic studies are less severe and may be used for the analysis of an early-stage infection. The route of infection is usually by endotracheal instillation of conidia (Felton, Baxter et al. 2010, Al-Nakeeb, Petraitis et al. 2015, Petraitiene, Petraitis et al. 2015). These models have defined the PK-PD relationships for several antifungals including amphotericin B formulations (Al-Nakeeb, Petraitis et al. 2015), micafungin (Petraitis, Petraitiene et al. 2002) and the triazole agents. A non-linear pharmacokinetic profile for voriconazole is also seen in the rabbit model. As in mice, this is thought to be due to saturation of the cytochrome P450 enzymes used for metabolism (Roffey, Cole et al. 2003).

The guinea pig may be a more reliable model for the determination of PK-PD for such agents against *Aspergillus* spp. and has been validated (Roffey, Cole et al. 2003). However this model is not widely available and is costly.

Current models of infection for invasive infection with *P. boydii* and *S. apiospermum* are mainly murine and use a tail-vein route of infection. For a significant infection to be established severe and persistent neutropenia is essential. A guinea pig model has previously been used to investigate the PK-PD of voriconazole *in vivo*, although this model is not widely available (Capilla and Guarro 2004).

Models of fusariosis have been utilised in order to evaluate the use of PCR versus colony forming unit (CFU) measurement as an estimate of fungal burden (González, Márquez et al. 2013). A neutropenic model has also been used to compare the efficacy of AmB and caspofungin in the prophylaxis and treatment of invasive fusariosis with *F. solani* (Spellberg, Schwartz et al. 2006). A similar model evaluated the efficacy of pentamidine as a potential prophylactic and therapeutic agent for the treatment of *F. oxysporum* infection (Lionakis, Chamilos et al. 2006).

In vitro

There are several *in vitro* models of infection used in the determination of exposure response relationships for antimicrobial agents. These may be static or dynamic in nature. A time-kill static methodology is often used in the early evaluation of antibacterial pharmacodynamics. This is consists of a timed incubation of the organism in the presence of a concentration of an agent. Samples are taken at various time-points in order to distinguish the kill kinetics of the agent. For the assessment of antifungal agents against mould species, this methodology is less commonly used. In the case of an invasive pulmonary infection, hyphae are the morphological structures

present. As conidia are usually absent in infected tissue, it is important that the antifungal efficacy is determined against actively growing hyphae as opposed to conidia (Krishnan, Manavathu et al. 2005). *In vitro* models of invasive aspergillosis using cellular bilayers as a model of the human alveolus have defined the PK-PD relationships of voriconazole (Al-Saigh, Elefanti et al. 2012, Jeans, Howard et al. 2012, Jeans, Howard et al. 2012), itraconazole (Al-Nakeeb, Sudan et al. 2012) and posaconazole (Howard, Lestner et al. 2011) against isolates of *A. fumigatus*. Cellular bilayers consisting of airway epithelial cells on the top layer and human pulmonary endothelial cells on the bottom layer are inoculated with *Aspergillus* conidia which may then germinate into hyphae. The hyphae then begin to invade through the cellular bilayer to simulate the invasion of the pulmonary artery seen in humans. Upon exposure to varying concentrations of drug in a static environment, the concentration at which maximal antifungal efficacy is achieved can be determined.

The use of kinetic models of infection can allow for the simulation of pharmacokinetic profiles that are representative of human clearances and exposures of drug, whilst determining the antimicrobial effect over the time course. The use of hollow-fibre infection models (HFIM) to examine the PK-PD relationships of antibacterial agents has been well validated. The models typically comprise of two parallel circuits. A central reservoir is 'dosed' with the antibacterial agent. Drug containing media is then pumped out into a waste reservoir and is replaced with fresh media at a rate proportional to the relevant clearance seen in humans. Simultaneously, the drug containing media is circulated through a hollow fibre cartridge containing the bacteria of interest. The cartridge consists of thousands of tubular filters. Pores on the fibres allows for the free diffusion of drugs whilst retaining the bacteria in the cartridge to prevent bacterial elimination (Gloede, Scheerans et al. 2010). These models have

been central to the determination of key PD indices for several antibacterial agents and have informed the dosage selection for both preclinical animal studies and clinical trials (Gloede, Scheerans et al. 2010, Felton, Goodwin et al. 2013, Docobo-Perez, Drusano et al. 2015).

As with a time-kill methodology the applicability of these models to represent an invasive mould infection is questionable. Jeans et al. further developed the static cellular model of invasive aspergillosis for use in a kinetic model using a similar circuitry to that of the HFIM. In replacement of the hollow fibre cartridge was the cellular bilayer model described earlier, housed in a custom made bioreactor that allowed for the continuous flow of media and the direct exposure of fungal hyphae to drug. This model has been particularly useful in the assessment of the efficacy of voriconazole at current dosages in the treatment of triazole resistant *Aspergillus* isolates. As voriconazole demonstrates nonlinear PK and a rapid clearance in mice this model allowed for exposures seen in the clinical to be achieved and was able to define accurate pharmacodynamic target exposures that may be best associated with antifungal efficacy against isolates with an elevated MIC (Jeans, Howard et al. 2012).

1.214 Mathematical modelling for the bridging of in vitro PK-PD data to humans

The use of pharmacokinetic and pharmacodynamic modelling and simulation in order to extrapolate experimental findings to human populations has the potential to revolutionise the drug development process and may be a step towards the individualisation of antimicrobial therapy. The establishment of an *in vitro- in vivo* correlation is essential for the translation of experimental data into a clinical setting.

Pmetrics, short for pharmacometrics, is a library package for R developed for the non- parametric and parametric modelling of PK-PD datasets. This software can

be used in order to establish a link between PK and PD datasets to explore the relationship between dose- exposure and the resultant pharmacodynamic effect (Neely, van Guilder et al. 2012). The model can allow for the prediction of key pharmacokinetic parameters and the elucidation of target PD indices that would otherwise be unobtainable from raw datasets (Kovanda, Petraitiene et al. 2016). Once the PK-PD model has been assessed and validated, the predicted data may then be used in further PK-PD simulations in order to explore the clinical implications of the experimental findings (Felton, Goodwin et al. 2013). Monte- Carlo simulation utilises large clinical pharmacokinetic datasets that are either obtained from patient populations and/ or clinical studies in order to construct a population model. Individual exposures of drug using a defined dosing regimen can then be predicted from datasets obtained either clinically or experimentally for the determination of response to therapy (Neely, Margol et al. 2015, Huurneman, Neely et al. 2016, Rhodes, Kuti et al. 2016). Key limitations in *in vitro* datasets such as differences in protein binding may be accounted for and incorporated into the model design using this methodology. In the bridging of *in vitro* data obtained from infection models to human populations the pharmacokinetic parameter values and variance for each "individual" obtained from PK-PD models may be used in simulations in order to determine what proportion of patients in a population are likely achieve the PD target recommended by the experimental data when given a dose of drug (Jeans, Howard et al. 2012). It is therefore possible to elucidate whether clinical success is likely to be achieved using a certain dosing regimen or if a dosage adjustment is necessary. This approach has been used to predict the likelihood of PD target attainment for several agents on the basis of preclinical *in vivo* and *in vitro* data. Jeans et al. successfully defined target AUC:MIC values for the treatment of azole- resistant aspergillosis. When placed in a

clinical context via Monte- Carlo simulation it was clear that target exposures could not be achieved using current dosing recommendations and that a dosage escalation would be necessary for the treatment of resistant isolates (Jeans, Howard et al. 2012). Using a similar methodology, Felton et al. examined the impact of bolus dosing versus extended infusion of piperacillin/ tazobactam on the emergence of resistance in a model of *Pseudomonas aeruginosa.* In this case, it was concluded that bolus doses of drug were equivalent in both antibacterial effect and in suppressing the emergence of resistance (Felton, Goodwin et al. 2013).

1.213 The use of PK-PD analyses in drug development

The interest of large pharmaceutical companies in the discovery and development of novel antifungal agents has diminished in the past years. This is largely due to a lack of financial incentive and the challenges associated with demonstrating efficacy and safety. Clinical trials for novel antimicrobial agents are notoriously difficult as patient populations are refined to those who have exhausted alternative therapies. There is also a high risk in the use of an experimental agent in at-risk patient populations due to underlying illness and the complex physiological state of the patient. In this case, the analysis of data may be complicated and prevent the determination of an endpoint to describe success or failure. These trials may therefore fail due to lack of evidence to prove the safety and efficacy of the agent. This may lead to late- stage withdrawal of a candidate drug. Regulatory bodies are then presented with the question of whether to withdraw a drug from the market based on a failed trial, the consequences of which for patients with no alternative options may be fatal. These reasons collectively present an unfeasible development pathway for the

development of novel antimicrobial agents and owe to the lack of interest in the antimicrobial field from the pharma industry (Rex, Eisenstein et al. 2013). More recently, it has been suggested that, if necessary, regulatory approval should exist in stages. Termed “adaptive licensing”, clinical access to agents may be granted earlier on in development for orphan diseases based on a portfolio of smaller studies and clinical trials. This evidence based approach would allow access to the agent under restricted circumstances as more evidence to further its development accumulates. It is thought that lowering the barriers associated with the development of novel agents and using a benefit-risk approach to approval may increase financial incentive and allow for the progression of candidate drugs that would otherwise be terminated (Woodcock 2012).

The use of PK-PD analysis has now been incorporated into the drug development pipeline for agents focussed upon the treatment of orphan diseases. It has been recognised that in the setting of an unmet medical need where it is essential that novel agents be introduced into the clinic more rapidly, a framework of one Phase III study and several smaller studies may be sufficient in order to grant an agent orphan drug status by the Food and Drug Administration (FDA). PK-PD analysis forms the basis of these smaller studies and allows for the definition of an appropriate dosage that has been demonstrated as safe (Phase I studies) and effective to be taken into Phase III studies. It is suggested that the late-stage failure of antimicrobial agents is uncommon when the clinical dosages are guided by PK-PD analysis (Rex, Eisenstein et al. 2013) (Figure 1.7).

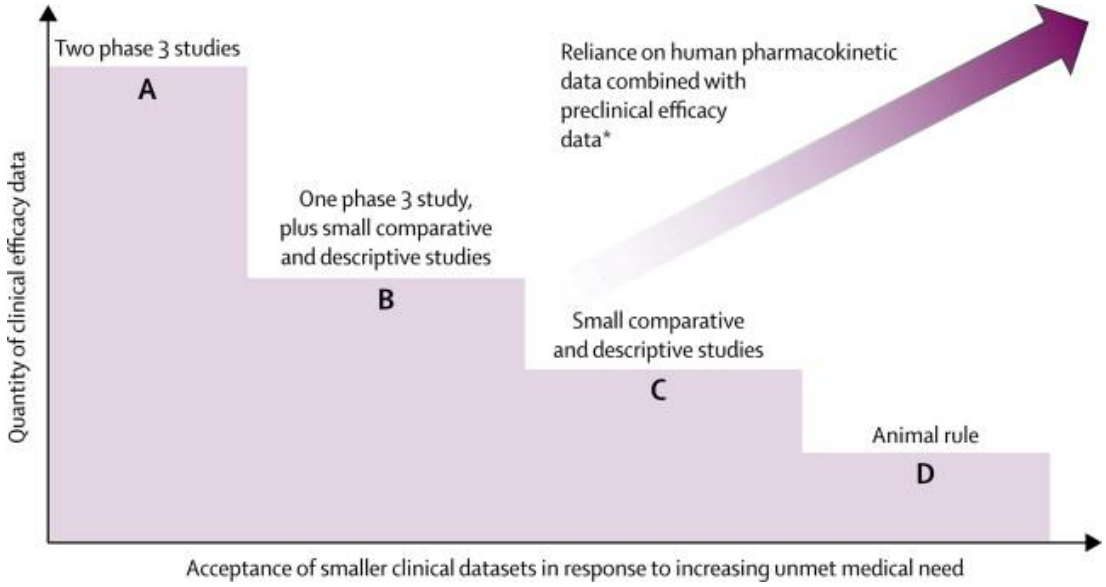

Figure 1. 6

The use of PK-PD studies in the drug development process. The balance between quantity of clinical efficacy data and unmet medical need. Taken from Rex et al. 2013.

1.22 Amphotericin B (AmB)

Formerly, amphotericin B deoxycholate (DAmB) has been standard antifungal therapy for the treatment of many invasive fungal infections. AmB binds directly and irreversibly to ergosterol, a key component of the fungal cell membrane. This results in the disruption of the cell membrane and ultimately, cell death (Gray, Palacios et al. 2012). AmB demonstrates activity against an extensive range of fungal pathogens including *Aspergillus*, *Candida*, *Scedosporium*, *Fusarium* spp. and several of the zygomycetes (Gomez-Lopez, Cuenca-Estrella et al. 2001, Diekema, Messer et al. 2003, Lewis, Wiederhold et al. 2005, Torres-Narbona, Guinea et al. 2007, Rudramurthy, Jatana et al. 2013). Although conventional DAmB is an effective agent in treating these infections, its routine use presents serious safety concerns. Adverse drug reactions associated with DAmB include infusion-related side effects such as pyrexia and chills, and neprotoxicity (Petrikkos 2009). Further to this it is only available in i.v. formulation and demonstrates poor penetration of the blood brain barrier (Dupont 2002). Due to these limitations, alternative lipid formulations of AmB have now been developed. Three formulations are available in most countries: liposomal amphotericin B (L-AmB, AmBisome; Gilead Sciences Inc., Foster city, CA, USA), amphotericin B lipid complex (ABLC; Enzon Pharmaceuticals Inc., Bridgewater, NJ, USA; Cephalon Limited, Welwin Garden City, UK), and amphotericin B colloidal dispersion (ABCD; Three River Pharmaceuticals Inc., Cranberry Township, PA, USA). These formulations demonstrate activity against most yeast and mould species comparable to that of conventional AmB. Despite similar activities, their structures and pharmacokinetics differ significantly (Adler-Moore and Proffitt 2008, Lestner, Howard et al. 2010). Lipid formulations of AmB allow for a superior drug delivery system and improved safety profiles. This can,

therefore, overcome the safety reservations that clinicians often harbour when using AmB therapy (Vyas and Gupta 2006).

1.221 Pharmacokinetics and Pharmacodynamics

ABCD has been demonstrated to be less nephrotoxic than DAmB (Choi, Brummer et al. 2004, Chandrasekar and Sobel 2006). However, there are still toxicity concerns with ABCD. This was demonstrated in a clinical trial carried out by Timmers *et al*. This open-label randomised trial to compare ABCD with fluconazole for antifungal prophylaxis in neutropenic patients demonstrated a high rate of infusion related toxic events (94%) in patients receiving 4mg/kg/day of ABCD. It was concluded that ABCD was not a suitable prophylactic agent for neutropenic patients (Joseph, Jain et al. 2007).

A recent *in vitro* study demonstrated the effectiveness of L-AmB against mould isolates in comparison to DAmB, voriconazole, itraconazole and fluconazole. This study found that L-AmB has *in vitro* activity against *Aspergillus*, *Fusarium* and species of Zygomycetes comparable to, if not superior, to that of both conventional AmB and the triazole agents (Rudramurthy, Jatana et al. 2013). A clinical trial by Walsh et al. evaluating the safety and tolerability of high-dose L-AmB in the treatment of infections with *Aspergillus* spp. and other filamentous fungi further validated these findings. Dosages of up to 15mg/kg were observed to be effective in treating infections whilst also demonstrating good tolerability and safety (Garcia-Effron, Park et al. 2009).

Despite upstanding pre-clinical and clinical data to support the use of higher dosages of L-AmB, several recent clinical trials have demonstrated similar efficacy of low-dose regimens when compared to standard dose in the treatment of IFI

(Kassamali, Danziger et al. , Cornely, Maertens et al. 2007, Bal 2010). The most recent of these trials observed comparable survival rates and clinical improvement in treatment groups receiving low-dose L-AmB (1mg/kg/day) and standard dosages (>2mg/kg/day) (Kassamali, Danziger et al.). A second trial comparing a high-loading dose regimen with standard dosing for the treatment of invasive aspergillosis in severely immunocompromised patients also demonstrated that the use of 10mg/kg/day for 14 days offered little superiority in treatment outcome and an increased frequency of nephrotoxicity compared to patients receiving 3mg/kg/day (Cornely, Maertens et al. 2007). Collectively these studies suggest that the use of higher dosages of L-AmB may increase the incidence of adverse events with no additional antifungal benefit.

Similar antifungal efficacies between formulations were also observed in an *in vitro* model of invasive pulmonary aspergillosis which described the PK-PD relationship of DAmB, L-AmB and ABLC against a green fluorescent protein (GFP) modified isolate of *A. fumigatus*. However, despite similar MIC values, concentrations at which 50% antifungal activity was observed (EC_{50}) estimated from AUC- response relationships for both L-AmB and ABLC were significantly higher than those for DAmB (67.73, 210.2 and 6.4 respectively) (Lestner, Howard et al. 2010).

Animal studies suggest that the use of higher dosages of L-AmB may be more effective in reducing fungal burden in rats and mice (Clemons, Espiritu et al. 2005, Gavalda, Martin et al. 2005, Olson, Adler-Moore et al. 2006, Takemoto, Yamamoto et al. 2010). In a murine model of invasive scedosporiosis with *S. prolificans*, dosage escalation up to 10mg/kg and 20mg/kg observed a significant improvement in survival (70% and 80% survival respectively) compared to control mice (10% survival). However when escalated to 30mg/kg a decreased survival was seen suggesting toxicity at this dosage (around 30% survival) (Bocanegra, Najvar et al. 2005). In an

immunosuppressed murine model of IPA Olsen *et al*. validated the safe use of higher dosages compared to high-dose ABLC. Survival of mice was significantly prolonged in groups receiving 12mg/kg of both drugs. Mice receiving even higher dosages of 15 and 20mg/kg showed a further increase in survival of 80-90% compared to 12mg/kg dosing (57% survival). ABLC demonstrated decreased survival and nephrotoxicity at dosages higher than 12mg/kg suggesting that dosage escalation may be unsafe. The reduced nephrotoxicity seen in mice receiving L-AmB compared to those which received ABLC may provide evidence for the use of L-AmB at higher dosages of 15 or 20 mg/kg (Olson, Adler-Moore et al. 2006). The safety of L-AmB at higher dosages of 10mg/kg was also demonstrated in a murine model of six species of Zygomycetes with efficacy equal to or superior to DAmB. Efficacy of L-AmB at clinical dosages (3mg/kg) was also observed in this study (50-100% survival) (Takemoto, Yamamoto et al. 2010).

1.23 Echinocandins

The echinocandins represent the latest class of antifungal agent to be developed and include caspofungin, micafungin and anidulafungin. Their mechanism of action targets FKS1, a 1,3-β-D glucan synthase enzyme that is responsible for the transcription of 1,3-β-D glucan, an essential component of the fungal cell wall. The susceptibility of an organism to the echinocandins is dependent on the amount of glucan present in the cell wall. This varies between species. With nephrotoxicity concerns for amphotericin B and emerging limitations of azole drugs, the echinocandins have proved to be a favourable treatment option for IFI. Their advantages include desirable safety profiles, broad spectrum efficacy and minimal drug-drug interactions (Vazquez 2005).

The echinocandins are compounds of high molecular weight and have limited oral bioavailability. They are, therefore, administered intravenously (i.v). They are generally metabolised in the liver and metabolism does not implicate the Cytochrome P450 metabolising enzymes. Therefore few drug-drug interactions can be seen with this class of drugs (Chandrasekar and Sobel 2006). Plasma concentrations are dose-proportional, indicating linear pharmacokinetic (PK) profiles after single and multiple dose intravenous administration of the echinocandins (Chandrasekar and Sobel 2006).

As efficacy of the echinocandins has been demonstrated to be related to both overall exposure and the achievement of high peak concentrations of drug it is debatable whether AUC/MIC or C_{max}/MIC is the PK-PD predictive parameter best associated with efficacy (Sinnollareddy, Peake et al. 2012).

The echinocandins are approved for the treatment of aspergillosis as a salvage therapy only when other antifungal strategies have been unsuccessful (Bal 2010).

Determination of pharmacodynamic properties for the echinocandins against *Aspergillus* spp. is challenging. The MIC is often hard to interpret due to the fungistatic nature of the echinocandins. Therefore the minimum effective concentration (MEC50) is determined as a potential pharmacodynamic target. The MEC50 values for all the echinocandins range between 0.007 and 0.12 mg/L for isolates of *A. fumigatus, A. terreus, A. niger* and *A. flavus* (Pfaller, Boyken et al. 2009). In terms of monotherapy the echinocandins have little to poor effectiveness in the treatment of infections with *Scedosporium* spp. or *Fusarium* spp. and are therefore not recommended for the treatment of these infections (Chen, Slavin et al. 2011). There are however some studies where the use of an echinocandin in combination with amphotericin B or triazole agents has demonstrated a synergistic effect in treating fusariosis (Philip, Odabasi et al. 2005, Ruiz-Cendoya, Rodriguez et al. 2008, Shalit, Shadkchan et al. 2009).

1.24 Triazole Agents

The triazole class of antifungal drugs are first-line agents for the treatment and prophylaxis of several invasive and superficial fungal infections. Their mechanism of action targets the cytochrome P-450- dependent 14-α-demethylase enzyme that is necessary for the conversion of lanosterol to ergosterol. Inhibition of this biosynthetic pathway results in an accumulation of toxic methylsterol compounds leading to cell death and inhibition of fungal growth. Depletion of ergosterol also compromises the integrity of the fungal cell membrane contributing to further cell death (Sharma and Bhatia 2011).

Triazoles routinely used in a clinical setting include first generation triazoles itraconazole and fluconazole, and second generation agents, voriconazole, posaconazole and more recently, isavuconazole (Fera, La Camera et al. 2009). As a class they are generally well tolerated. However, drug interactions are a concern to clinicians when prescribing these drugs. Their spectrum of activity spans across a broad range of fungal pathogens including *A. fumigatus*, *S. apiospermum* and *F. solani*. The activity, mechanisms of resistance and susceptibility breakpoints of the triazoles against isolates of *Aspergillus* spp. have been extensively studied and defined (Howard, Webster et al. 2006, Howard, Cerar et al. 2009). However, variable *in vitro* and clinical susceptibilities of these agents is seen against species of *Scedosporium* and *Fusarium* (Alastruey-Izquierdo, Cuenca-Estrella et al. 2008, Cuenca-Estrella, Alastruey-Izquierdo et al. 2008). Therefore susceptibility testing is essential in these cases. The PK-PD properties of the triazoles differ between drugs (Stevens 2012).

1.241 *Itraconazole*

Itraconazole is a lipophilic triazole with high plasma protein binding of >99% yielding low concentrations in parts of the body such as cerebrospinal fluid (CSF) and eye fluid (Willems, van der Geest et al. 2001). As a result, fungal infections of the central nervous system may require dosage adjustments or alternative antifungal therapy for successful treatment. Itraconazole exhibits a wide tissue distribution (Heykants, Van Peer et al. 1989). This allows concentrations at infection sites to remain high even after drug has been cleared from the plasma. Itraconazole undergoes extensive metabolism in the liver mainly by CYP3A4 to produce its major metabolite, hydroxy-itraconazole. This metabolite also possesses potent antifungal activity and similar PK-PD to the parent compound (Mino, Naito et al. 2013). Itraconazole was originally marketed in a capsule formulation. However there is a marked variability in intestinal absorption using this formulation. To overcome this, an oral solution and i.v formulation with the incorporation of cyclodextrin were later developed (Zhang, Zhou et al. 2011). The pharmacokinetic profile for itraconazole is non-linear and the metabolism is saturated at clinical dosages leading to a long plasma half-life of around 30 hours (Willems, van der Geest et al. 2001).

1.242 *Posaconazole*

Posaconazole was approved in 2005 and 2006 in the US and Europe respectively for the treatment and prophylaxis of IFIs in immunocompromised patients. It is also approved for the treatment of oropharyngeal candidiasis, aspergillosis, fusariosis, chromoblastomycosis and coccidioidomycosis in patients refractory to or intolerant of first-line agents. Posaconazole has a spectrum of activity comparable to that of voriconazole with the exception of zygomycetes for which superior activity is demonstrated (Torres, Hachem et al. 2005). *In vitro* data evaluating

the activity of posaconazole against 55 clinical isolates of *S. prolificans* demonstrated an MIC range of 2-8 mg/L suggesting dosage escalation may be necessary for a successful treatment outcome in patients with scedosporiosis (Meletiadis, Meis et al. 2002, Wiederhold, Kontoyiannis et al. 2004).

For the treatment of fusariosis, posaconazole is currently recommended as salvage therapy and may be an effective treatment option in some cases (Nucci 2003, Raad, Hachem et al. 2006, Tortorano, Richardson et al. 2014). Isolates of *F. solani* demonstrate varying susceptibilities to posaconazole and can be greater than 8 mg/L (Espinel-Ingroff 2001, Paphitou, Ostrosky-Zeichner et al. 2002, Espinel-Ingroff 2003)

1.243 *Voriconazole*

Voriconazole is the first of the second generation triazoles to be developed. It gained FDA approval in May 2002 for the treatment of invasive aspergillosis. It is also indicated for fusariosis and scedosporiosis in patients refractory to or intolerant of other antifungal medications (Ader, Bienvenu et al. 2009). This licence was then extended in 2004 for the treatment of candidemia in non-neutropenic patients, disseminated candidiasis and *Candida* infections of the abdomen, kidney, bladder wall and wounds (Peman, Salavert et al. 2006).

Pharmacokinetics and Pharmacodynamics

The recommended dosing regimen of voriconazole consists of 6 mg/mg q12hr for the first day followed by a 4mg/kg twice daily maintenance dose. Voriconazole is available in both oral and i.v formulations and has a non- linear saturable pharmacokinetic profile in adults. Comparative to this, a linear pharmacokinetic profile has been demonstrated in children with doses of 4 mg/kg correlating to

exposures similar to that of 3 mg/kg in adults (Walsh, Teppler et al. 2004). Steady state plasma concentrations are usually reached around 5 days after oral and intravenous administration. With the use of a loading dose steady state may be achieved within 24 hours (Purkins, Wood et al. 2002, Theuretzbacher, Ihle et al. 2006). Voriconazole demonstrates an oral bioavailability of around 96% when taken after food. When administered orally, maximum plasma concentrations are achieved within 2 hours post administration. The plasma elimination half-life of voriconazole is around 6-7 hours. This is dose dependent and dose escalation can result in a non-proportional accumulation of drug. It is metabolised primarily by CYP2C19 with some contribution from CYP2C9 and CYP3A4. Due to the polymorphic nature of CYP2C19 there can be a high variability in plasma concentrations between individuals (up to 100-fold) as voriconazole clearance may be significantly reduced in patients with a CYP2C19 deficient phenotype (Denning, Ribaud et al. 2002). Inducers and substrates of CYP3A4, CYP2C19 and CYP2C9 may also contribute to a variation in the PK of voriconazole and present a considerable risk of drug-drug interactions between voriconazole and other drugs which interfere with these enzymes (Dolton, Ray et al. 2012). This has previously been seen with rifabutin (CYP3A4 inducer) and efavirenz (CYP3A4 inhibitor and substrate) (Pfizer 2011). A study in critically ill patients with renal impairment demonstrated sub-optimal concentrations of drug when administered the recommended dosage of 3-4mg/kg. This suggests that dosage escalation may be beneficial in these patients. Further studies in the critically ill are necessary to confirm these findings (Myrianthefs, Markantonis et al. 2010).

Voriconazole demonstrates excellent *in* vitro and *in vivo* antifungal activity against clinically important *Aspergillus* species. In an *in vitro* dynamic model of pulmonary invasive aspergillosis, the PK-PD relationships of voriconazole against

wildtype and resistant isolates of *A. fumigatus* were established. When bridged to humans using a nonparametric mathematical model and Monte-Carlo simulation, this study suggested that increased drug exposures may allow for the successful treatment of infections with resistant strains of *Aspergillus* spp. (Jeans, Howard et al. 2012).

A similar study describing the PK-PD of voriconazole against three clinical strains of *A. fumigatus*, *A. flavus* and *A. terreus* suggests that higher drug exposures are necessary in order to effectively inhibit *A. terreus* (Al-Saigh, Elefanti et al. 2012). Both studies suggest that an increased dosage may be an option for clinicians when treating patients suffering from resistant infections.

For the treatment of infections with *Scedosporium* spp. numerous cases have reported successful treatment outcomes. In an analysis of 101 patients suffering from scedosporiosis treated with voriconazole, 61% patients responded to therapy with a 33% recovery rate. A 63% success rate was observed in patients infected with *S. apiospermum* compared to a 44% success rate in those with *S. prolificans* infection suggesting an increased dosage or combination therapy may be a more appropriate option for patients infected with *S. prolificans* (Troke, Aguirrebengoa et al. 2008).

Voriconazole exhibits varying *in vitro* activity against species of *Fusarium* with MICs ranging from 1 mg/L -16 mg/L (Espinel-Ingroff, Johnson et al. 2008). Several retrospective analyses observe voriconazole to be the most commonly used agent in the treatment of disseminated fusariosis (Lortholary, Obenga et al. 2010, Horn, Freifeld et al. 2014). Lorthorlary *et al*. saw a survival rate of 42% in patients with haematological malignancies who had been treated with voriconazole (Lortholary, Obenga et al. 2010). Similar figures were obtained by Horn *et al*. where survival was 44% (Horn, Freifeld et al. 2014) and Nucci *et al*. reported a survival rate

of 43% (Nucci, Marr et al. 2014). These analyses suggested that voriconazole is a potential treatment option for fusariosis, however the exposures necessary to improve response rates are yet to be defined.

Numerous clinical studies have investigated the relationship between plasma concentrations of voriconazole and antifungal efficacy (Ally, Schurmann et al. 2001, Denning, Ribaud et al. 2002, Perfect, Marr et al. 2003, Dolton, Ray et al. 2012, Jacobs, Selleslag et al. 2012). An analysis of samples obtained from 10 clinical trials found no correlation between plasma concentration of voriconazole and efficacy against *Aspergillus* spp. (Lutsar, Hodges et al. 2003). However, further PK-PD analysis of data suggested that a decrease in dosage may lead to a reduction in efficacy in patients with plasma concentrations <5ug/ml. This was further studied in 28 patients receiving voriconazole where a correlation between plasma concentrations of <2.05 mg/L and a reduced clinical response was observed, suggesting that a dosage escalation may be necessary in patients who do not achieve plasma levels >2.05 mg/L (Smith, Safdar et al. 2006).

Walsh et al. carried out the largest evaluation to date of the safety and efficacy of voriconazole in comparison to liposomal amphotericin B for empirical antifungal therapy in a cohort of 837 febrile neutropenic patients. The superiority of voriconazole in reducing fungal breakthrough infections and adverse events such as infusion-related reactions and nephrotoxicity was demonstrated in patients receiving a 6mg/kg loading dose q12h for two doses followed by a 3mg/kg q12h loading dose. Plasma concentrations far exceeding the MIC for the majority of fungal pathogens were detected between dosing intervals. This may suggest that a regimen using lower dosages of voriconazole may be indicated in neutropenic patients and could reduce the risk of toxicity (Walsh, Pappas et al. 2002).

An observational study investigating the relationship between plasma concentrations of voriconazole and clinical response analysed PK-PD data from 825 patients from nine phase II and III clinical trials. A clear relationship between patients who had a higher C_{avg}/MIC value and increased clinical response to voriconazole therapy was seen. Although the use of trough concentration as a PD parameter has its limitations, the trough/MIC concentrations at which clinical efficacy is most likely to occur was demonstrated to be around 2-5 which may help to guide dosing of voriconazole (Troke, Hockey et al. 2011).

Though studies have demonstrated a relationship between the pharmacokinetics and antifungal efficacy of voriconazole, due to its nonlinear PK profile a small change in dosage may have dramatic effects on the resultant plasma levels. It is therefore hard to suggest a dosage that may reach exposures within the therapeutic range. Therapeutic drug monitoring is recommended for patients receiving voriconazole therapy in order to determine appropriate dosage adjustments. Studies have reported that nonparametric population models may be able to predict voriconazole AUC from clinical trough levels. There is the potential here to predict target exposures from as little as one pharmacokinetic sample, for the individualisation of therapy (Hope, VanGuilder et al. 2013, Neely, Margol et al. 2015, Huurneman, Neely et al. 2016)

In vitro and *in vivo* preclinical data for the treatment of invasive pulmonary aspergillosis using a dynamic *in vitro* model and an inhalational neutropenic murine model suggests that an AUC:MIC ratio of 166.9 is required to achieve 50% antifungal effect. The study also estimates that for *Aspergillus* species with MIC values >0.125 mg/L the current dosing regimen of 800 mg/ day may be sub-optimal (Howard, Lestner et al. 2011). In a recent investigation to determine a pharmacodynamic target

for posaconazole against wild-type and resistant isolates of *A. fumigatus*, the highest MIC for which the existing dosing regimen would produce a 1-log kill was 0.25 mg/L. This also suggests that the current dosing regimen may be ineffective for the treatment of infections with resistant isolates for which MIC values are 1-8 mg/L (Lepak, Marchillo et al. 2013).

.

1.534 *Isavuconazole*

Isavuconazole is a novel triazole agent that is approved in the USA for the treatment of aspergillosis, mucormycoses and candidiasis. Isavuconazole exhibits a broad spectrum of activity against several clinically important fungal pathogens including *Candida* spp., *Aspergillus* spp., *Cryptococcus neoformans* and perhaps some species of the Zygomycetes (Thompson and Wiederhold 2010). The incorporation of a side arm into the molecular structure of isavuconazole allows for a higher binding potency for the CYP51 binding pocket. Isavuconazole therefore demonstrates a broader antifungal activity compared to that of other triazole agents (Livermore and Hope 2012).

Pharmacokinetics and Pharmacodynamics

Isavuconazole is administered either orally or intravenously as a water-soluble pro-drug, BAL8557. Therefore the use of potentially nephrotoxic excipients such as cyclodextrin can be avoided. Cleavage into the active compound, BAL4815 via esterase enzymes in the plasma is near complete (around 98%) as negligible amount of pro-drug can be found in the urine post administration (Livermore and Hope 2012). Single and multiple dose studies in healthy volunteers demonstrated isavuconazole to be well tolerated. Isavuconazole exhibits an extensive half-life of 76-100hr with a low

systemic clearance (2.80-5.03 L/h). It is highly protein bound (around 98%) and has a large volume of distribution. Single dose studies suggest a non-linear pharmacokinetic profile however multiple dose studies suggest linearity (Schmitt-Hoffmann, Roos et al. 2006, Schmitt-Hoffmann, Roos et al. 2006)

Isavuconazole possesses potent antifungal activity against *Aspergillus* spp. with MIC values ranging from 0.06-4 mg/L (Guinea, Pelaez et al. 2008, Perkhofer, Lechner et al. 2009, Rudramurthy, Chakrabarti et al. 2011). However it's *in vitro* activity against *Fusarium* spp. and *Scedosporium* spp. is dependent on strain as many isolates of these organisms exhibit resistance to isavuconazole and have MICs exceeding 8 mg/L (MIC range of 2->16 for *S. apiospermum* and *S. prolicans*, 4->16 for *Fusarium* spp.) (Guinea, Pelaez et al. 2008, Thompson and Wiederhold 2010). A Phase III randomised, comparative study (SECURE) demonstrated the non-inferiority of isavuconazole to voriconazole for the treatment of invasive aspergillosis. Patients received dosages of isavuconazium sulphate comparable to 4 mg/kg i.v twice-daily or 200 mg orally twice- daily. Isavuconazole demonstrated a 50% success rate and 62% clinical response rate in this trial and also exhibited an overall comparable safety profile to voriconazole in this patient population (Ullmann A 2014).

1.25 The Orotomides

The discovery and development of novel classes of antifungal agents has been a great challenge over the past decades. The interest from big pharma in the development of antimicrobials with novel targets has diminished due to lack of financial incentive. Therefore, small biotechnology companies have become the main contributors towards the discovery of novel antimicrobial agents. The orotomide class of agents are a novel class of antifungals. F901318 is the first and most advanced agent

of the orotomides and is currently in Phase I of clinical development with F2G Ltd. F901318 was discovered via the screening of a 370,000 compound library for antifungal activity against *A. fumigatus*. Its primary target was determined to be the dihydroorotate dehydrogenase (DHODH) enzyme. The role of DHODH in the *de novo* biosynthesis of pyrimidines is well characterised in both humans and fungi. It is responsible for the conversion of dihydroorotate to orotate. As fungi such as *Aspergillus* spp. cannot salvage pyrimidines from their environment, the *de novo* biosynthesis pathway is the sole source of pyrimidines for these pathogens (Figure 1.7). Specificity of F901318 for fungal DHODH has been demonstrated and the agent exhibits a very poor inhibition of the human enzyme. The mechanism of F901318 is reversed in the presence of pyrimidine compounds however this is only at high concentrations of >5mM of which only a small fraction is present in human serum (Oliver, Law et al. 2015). F901318 also demonstrates *in vitro* activity against *S. apiospermum* and other species within its species complex (Fothergill, Wiederhold et al. 2015). Phase I data also suggests F901318 is safe and well tolerated at the dosages given in its first single ascending dose study in humans (Kennedy, Allen et al. 2015) An understanding of the pharmacokinetic and pharmacodynamic (PK-PD) relationships of new and currently used agents against *S. apiospermum* can provide an insight into the optimal dosages that may be effective in treating these infections (Fothergill, Wiederhold et al. 2015, Oliver, Law et al. 2015).

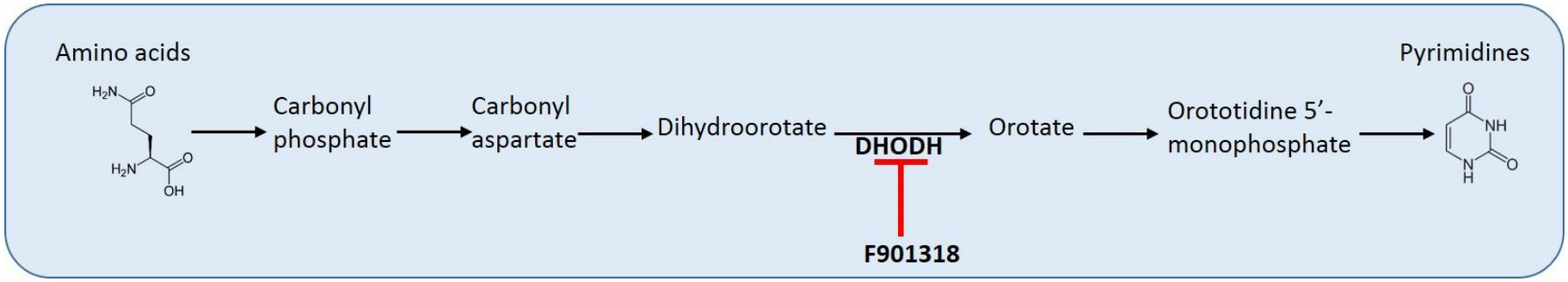

Figure 1. 7

Flow diagram to describe the de novo pyrimidine biosynthesis pathway used in fungi emphasising the mechanism of action of novel agent, F901318.

1.3 AIMS

The general aims of this thesis are comprised of two key components. Firstly, to develop *in vitro* models of invasive fungal infections that can successfully mimic the human PK of antifungal agents. Secondly, to refine these models for the establishment of key PK-PD relationships of new and existing agents that may guide the use of antifungal therapy in the clinic.

Aim 1 is to use the existing *in vitro* cellular models of invasive aspergillosis described by Jeans et al. to define the exposure response relationships between the novel triazole agent, isavuconazole, and both wild-type and triazole resistant isolates of *Aspergillus fumigatus*. These PK and PD datasets will then be bridged together using a one compartmental, non-parametric PK-PD model to establish the importance of key pharmacodynamic indices, such as the AUC and AUC:MIC in the case of triazole agents. This model will then be further developed for isolates of *Aspergillus terreus* in order to provide pre-clinical evidence for the suitability of isavuconazole in treating this species.

Aim 2 is to develop *in vitro* cellular models of scedosporiosis and fusariosis, specific for isolates of *Scedosporium apiospermum* and *Fusarium solani*. These models will first be validated using voriconazole. The study will use novel ELISA methodologies for the tracking of *S. apiospermum* and *F. solani* to define the exposure- response relationships for novel orotomide agent, F901318, against wild-type isolates of these organisms. Pharmacodynamic analysis will be performed using PK-PD modelling software to predict the PD indices best associated with maximal antifungal effect in these models.

CHAPTER II

The Pharmacokinetics and Pharmacodynamics of Isavuconazole against isolates of *Aspergillus fumigatus*

2.1 INTRODUCTION

Invasive pulmonary aspergillosis (IPA) predominantly affects individuals with a significantly impaired immune system. *A. fumigatus* is the most common *Aspergillus* species associated with opportunistic human infection and is a leading cause of infection in immunocompromised patients (Hope, Kruhlak et al. 2007).

The triazole class of agents target the fungal cytochrome P-450- dependent 14-α-demethylase enzyme responsible for the biosynthesis for key fungal cell wall components. It has been widely demonstrated that mutations within this target enzyme confer towards resistance to the triazoles (Parker, Warrilow et al. 2014). As the triazoles form the basis of many antifungal treatment regimens, the increasing emergence of triazole resistance in *Aspergillus* spp. is of growing clinical concern. Therefore research into the development of new and broader spectrum antifungals is necessary in order to combat this problem.

Isavuconazonium sulfate (BAL8557) is a water soluble prodrug that is cleaved by plasma esterase enzymes to form the active triazole moiety, isavuconazole (ISA; BAL4815), plus an inactive compound (BAL8728). ISA has recently been approved for the treatment of invasive aspergillosis and invasive mucormycosis in the United States (Livermore and Hope 2012). ISA demonstrates *in vitro* antifungal activity against the majority of *A. fumigatus*. (Gregson, Goodwin et al. 2013). The safety and efficacy of ISA for the treatment of aspergillosis have been demonstrated in Phase I and III clinical trials (Schmitt-Hoffmann, Roos et al. 2006, Schmitt-Hoffmann, Roos et al. 2006, Desai 2014). ISA has a safety profile comparable to that of voriconazole with fewer adverse events recorded during Phase III trials. An alteration in structure to include a branch side chain allows ISA to exhibit a broader spectrum of activity

compared to voriconazole that is inclusive of the mucorales (Thompson and Wiederhold 2010). The pharmacokinetics and pharmacodynamics (PK-PD) of ISA against isolates of *Aspergillus* spp. have been studied in murine models of disseminated aspergillosis (Warn, Sharp et al. 2009, Lepak, Marchillo et al. 2013, Seyedmousavi, Bruggemann et al. 2015). However, there are significant differences in the clearance of ISA between mice and humans. The terminal half-life in these studies was seen to be approximately 1-2 hours comparable to that of 100 hours in humans (Warn, Sharp et al. 2006, Majithiya JB 2008, Warn PA 2008). These differences in the PK of ISA may be a potential roadblock in the bridging of PK-PD data from mice to humans.

A greater understanding of the pharmacokinetics and pharmacodynamics of new and existing agents against *Aspergillus* spp. can provide valuable insight into the optimal dosages required to treat these infections.

In this thesis *in vitro* static model of the human alveolus was used in order to establish the PK-PD of ISA against one strain of *A. fumigatus* in order to establish both effective and sub optimal concentrations for dynamic studies. The activity of ISA against *A. fumigatus* was then studied further in a dynamic of the human alveolus were also used to define the PK-PD relationships of ISA against two wild-type and two mutant strains of *A. fumigatus*.

2.2 METHODS

2.21 Organism preparation

2.211 *Isolates*

All isolates of *A. fumigatus* were gifted from the Regional Mycology Reference Laboratory, University Hospital of South Manchester and are detailed in Table 3.1.

Species	Isolate	CYP51 mutation
A. fumigatus	GFP- transformant	Widtype
	NIH4215	Wildtype
	F16216	L98H substitution
	F11628	G138C substitution

Table 2. 1 Isolates of *A. fumigatus* used for static and dynamic studies.

2.212 *Culture*

Isolates of *A. fumigatus* were obtained from Wynthenshawe stored at -80^{0}C using the Microbank ™ preservation system (Pro-lab, Merseyside, UK). Isolates were sub-cultured onto a potato dextrose agar (PDA) flask (Sigma-Aldrich, Poole, UK), at 37^{0}C, 5 days prior to each experiment.

2.213 *Inoculum preparation*

Conidial suspensions were prepared by flooding with 20 ml phosphate buffered saline (PBS) (Invitrogen, Paisley, UK) whilst carefully disturbing the surface of the growth using a sterile swab. The resultant suspension was then filtered through sterile gauze (Medisave Ltd., Dorset, UK). Washing was performed twice by centrifuging the

filtrate for 10 minutes at 2500rpm and re suspending the pellet in 20ml PBS. Endothelial basal medium (EBM-2) (Promocell, Heidelberg, Germany) was used for the preparation of the final inoculum. A conidial suspension of 1-3 x 10^4 was prepared using a haemocytometer and was confirmed by quantitative cultures on Sabouraud dextrose agar with chloramphenicol (SAB-C) (Oxoid, Hampshire, UK).

2.22 *In vitro* susceptibility testing

Minimum inhibitory concentrations (MIC) for isavuconazole (ISA) against *A. fumigatus* and *A. terreus* isolates were determined in 5 independent experiments using both the European Committee for Antimicrobial Testing (EUCAST) and Clinical Laboratories Standards Institute (CLSI) methodologies. ISA concentrations for MIC testing ranged from 0.03 mg/L- 8 mg/L.

2.23 Tissue culture

A cell culture model of the human alveolus using 24- well cell culture plate inserts (Appleton Woods, Birmingham, UK) for a static *in vitro* model and 12-well cell culture plate inserts (Greiner Bio-One, Stonehouse, UK) for a dynamic *in vitro* model was used. A cellular bilayer consisting of human pulmonary arterial endothelial cells (HPAECs) (Promocell, Heidelberg, Germany) and human alveolar epithelial cells (A549s) (LGC Standards, Middlesex, UK) was constructed.

HPAECs were cultured using endothelial growth medium (EGM-2) (Promocell, Heidelberg, Germany). This was prepared in accordance with instructions provided by the manufacturer. EBM-2 was supplemented with 2% foetal bovine serum (FBS) (Invitrogen, Paisley, UK), ascorbic acid, heparin, hydrocortisone, human endothelial growth factor, vascular endothelial growth factor 165, human fibroblast factor B and R-3-insulinlike growth factor 1.

A549 cells were cultured using EBM-2 medium containing 10% FBS. Once 70-80% confluency was achieved, cells were washed using Hanks Balanced Salt Solution (HBSS) (Sigma-Aldrich, Poole, UK) and harvested with 6 mL of 0.25% trypsin–ethylenediaminetetraacetic solution (Sigma-Aldrich, Poole, UK). Cells were then centrifuged for 5 minutes at 2000 rpm and re-suspended in the appropriate media to achieve final densities of 1 x 10^6 and 5.5 x 10^5 for HPAECs and A549s respectively. 24-well cell culture inserts (static model) and ThinCert cell culture inserts for 12- well plates (dynamic and histopathology models) were used for the construction of the cellular bilayer. Cell culture inserts were aseptically inverted and placed in a sterile plate. For the construction of the endothelial cell layer 100 uL and 400 µL of HPEAC cell suspension was pipetted onto the underside of the membrane for static and dynamic/histopathology models respectively. Inserts were then incubated (37^0C, 5% C02) for 2 hours to ensure cellular adhesion to the membrane. Inserts were then transferred to their corresponding 24 (static) and 12 (dynamic and histopathology)-well plates containing 0.6 mL and 1.5 mL of EGM-2 media. 100 µL and 400 µL of EBM-2 containing 10% FBS were then added to the top compartment (alveolar) for static and dynamic/ histopathology models respectively. The cell culture plates were then incubated (37^0C, 5% C02) for 24 hours. After 24 hours, media in the alveolar compartments was removed and inserts were transferred to new plates containing the relevant amounts of fresh EGM-2 media. At this time, 100 µL for static models and 400 µL for dynamic/histopathology models of A549 cell suspension was added to the top compartment of each insert and incubated. After 2 hours, media in the alveolar compartment was removed to create an air-liquid interface. EGM-2 media in the bottom compartment was replaced every 48 hours and any media present in the

alveolar compartments was also removed. Inserts were used for experiments 5 days after construction.

2.24 Static *in vitro* models of invasive aspergillosis

Cell culture inserts were transferred to a 24 well plate containing 0.6 mL of EBM-2 media supplemented with 2% FBS. A conidial suspension of 1-2 x 10^4 for *Aspergillus* spp. and 4-8 x 10^5 for *Scedosporium* spp. and *Fusarium* spp. was prepared as described earlier and warmed to 37^0C for 20 minutes. 100 µL of conidial suspension was pipetted into the top compartment for each cell culture insert and incubated at 37^0C, 5% CO_2 for 6 and 12 hours for *Aspergillus* spp. and *Scedosporium*/ *Fusarium* spp. respectively.

Pure isavuconazole, F901318 and voriconazole powders were dissolved in DMSO (Sigma- Aldrich, Poole) to produce stock solutions. Stocks were then serially diluted in EBM-2 media supplemented with 2% FBS in order to achieve the desired concentrations of each drug. These can be seen in Figures 3.2, 4.2 and 5.2. After 6 hours of incubation for experiments using *Aspergillus* spp. and a 12 hour incubation period for experiments using *Scedosporium* spp. and *Fusarium* spp., the inoculum was removed from cell culture inserts which were then placed into 24 well plates containing relevant drug concentrations. Plates were then then incubated at 37°C, 5% CO_2 for 48 hrs. Samples from the endothelial and alveolar compartments were obtained and stored at -80^0C for measurement of drug concentrations and fungal burden.

2.25 Dynamic *in vitro* models of invasive aspergillosis

2.251 *Bioreactors and Construction*

Cell culture inserts were housed in custom-designed stainless steel bioreactors for the duration of the experiment. Bioreactors were specifically engineered to house cell culture inserts whilst allowing media to flow past the endothelial layer of cells. Each bioreactor was connected to the circuit using Marprene® thermoplastic elastometer tubing (Watson Marlow, Cornwall, UK). Silastic®, 1.6 mm bore tubing (Dow Corning) was used to construct the remainder of the circuit. All connections were made using polypropylene barbed luer adapters (Cole Palmer, London UK; West Group, Hants, UK). A central reservoir containing 200 mL of warmed media was connected to the circuit using 1.5-mm bore polytetrafluoroethylene (PTFE) semi-rigid tubing (Diba Labware, Kinesis Ltd., Cambridge, UK) fitted into Omni-Fit Q-series bottle caps (Diba Labware, Kinesis Ltd., Cambridge, UK). All central reservoirs contained magnetic stirring bars and were placed on a stirring plate to create a vortex, thereby ensuring continuous mixing of media components and drug. Duran bottles containing fresh media and empty bottles for the removal of waste were also connected to the circuit in a similar manner. ISA was administered directly to the central compartment. Two 205-U multichannel cassette peristaltic pumps fitted with 1.52 mm bore Marprene manifold tubing (Watson Marlow, Cornwall, UK) were used, ensuring flow of media round the system and allowing for multiple circuits to be run simultaneously.

All components of the model were sterilised by autoclave before use and circuits were assembled in a class II safety cabinet. Once assembled, circuits were transferred to a 37^0C incubator for the remainder of the experiment. Dulbecco's modified Eagle medium (DMEM) containing 4500 mg/L D-Glucose, L-Glutamine and HEPES buffer

(Invitrogen, Paisley, UK) was supplemented with 2% FBS and penicillin-streptomycin solution (Sigma-Aldrich, Poole) to give a final concentration of 100 U/mL penicillin and 0.1 mg/mL streptomycin. This media was used for all experiments. The circuits were primed overnight at a pump speed of 0.5rpm with this media. The bioreactors were then connected to the circuit. The pump responsible for media flow through the bioreactor was run at 1.9 rpm as described by Jeans et al. (Jeans, Howard et al. 2012).

2.252 *Inoculation*

Cell culture inserts were transferred to a 12 well plate containing 1.5 mL EBM-2 media supplemented with 2% FBS per well. A conidial suspension of 1-2 x 10^4 was prepared as previously described in the literature (Jeans, Howard et al. 2012) and incubated at 37^0C for 20 minutes. Four hundred µL of this suspension was then pipetted into the top compartment of each cell culture insert and incubated at 37^0C, 5% CO_2 for 12 hours.

2.253 *Treatment with antifungal agents and sampling*

For each experiment the PK and PD of antifungal agents against each isolate of *A. fumigatus* were determined in three individual circuits. Each circuit was treated with a different dosage of drug. A fourth untreated circuit was used as a control. Bolus dosages of 0mg, 0.3mg, 0.5mg and 1.5mg were administered to separate circuits at time 0. These dosages were chosen on the basis of static *in vitro* data in order to achieve concentrations of drug in the system that correlated to sub-optimal, optimal and levels of drug exceeding the effective antifungal dose (Figure xxx). The relationship between dose and concentration within the system was first tested in control pharmacokinetic experiments, i.e. drug alone in un-infected circuits. ISA was administered directly to the central compartment. Samples for PK and PD were taken

from the same sampling port situated after the bioreactor every 6 hours up to 48 hours post-treatment. A pump speed of 0.5rpm was used to set a clearance rate of ISA of 0.043 mL/min- clearance of ISA in L/h reference. After sampling, media taken out of the system during sampling was replaced with an equal volume of complete DMEM.

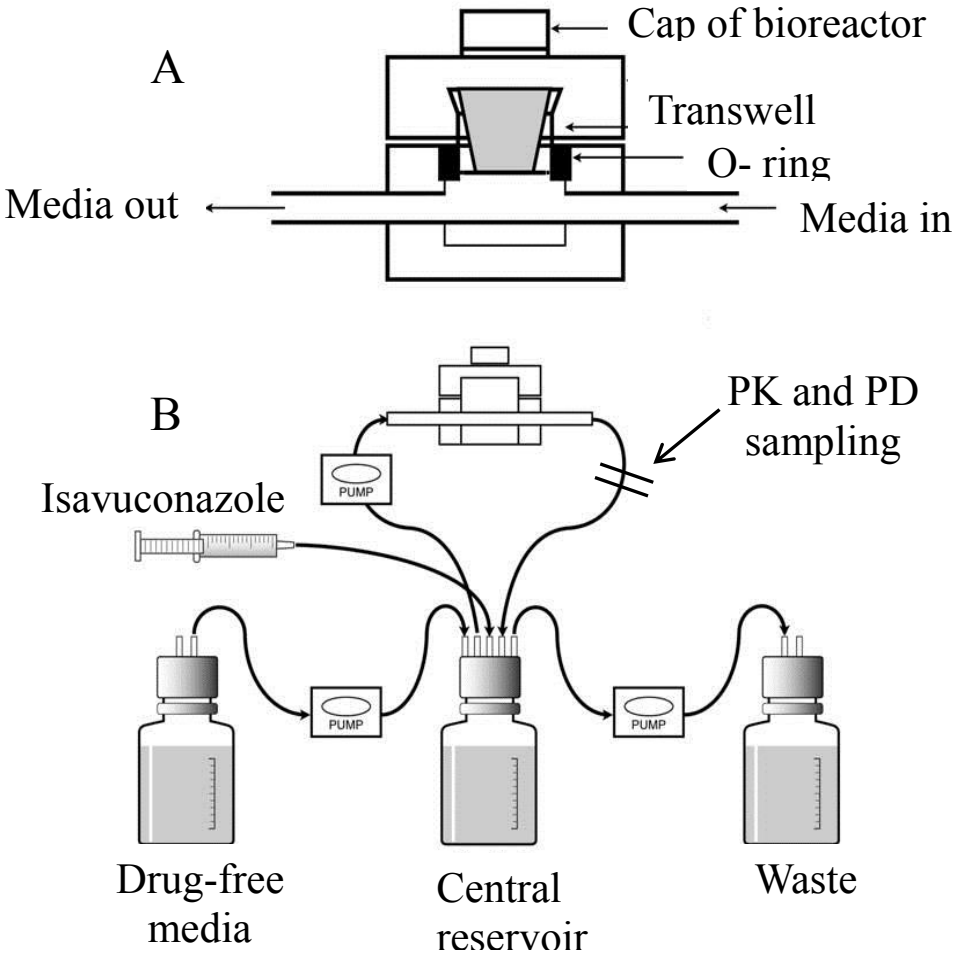

Figure 2. 1 Set-up of the dynamic in vitro model of the human alveolus for ISA against *A. fumigatus*.

2.26 High performance liquid chromatography

High performance liquid chromatography (HPLC) for pharmacokinetic analysis was performed by Joanne Goodwin and Sarah Whalley at the University of Liverpool.

Isavuconazole concentrations in media were measured using HPLC with a Shimadzu Prominence (Shimadzu). The isavuconazole method used a Kinetex 2.6u C18 New Column 75 x 4.6 mm (Phenomenex) and a 40 µL injection volume. A standard curve encompassing 0.005–20 mg/L was constructed from stock solutions of isavuconazole 1000 mg/L in DMSO further diluted in methanol (Fisher Scientific, Loughborough, UK). The internal standard was itraconazole (Sigma-Aldrich, Poole, UK). The mobile phase was 60% 0.1% trifluoroacetic acid (TFA) in water 40% acetonitrile with 0.1% TFA (v/v) with a gradient profile changing to 40% and 60% respectively over 4 minutes with an overall run time of 6 minutes and flow rate of 1 mL/min. Isavuconazole was detected using fluorescence with Ex 250nm, Em 380nm; they eluted after 3.2 and 4.5 mins, respectively. The CV% was <6.4% over the concentration range 0.005 – 20 mg/L. The limit of detection was 0.005 mg/L. The intra and inter-day variation was <6.6%.

2.27 Platelia Aspergillus assay

Galactomannan (GM) was used as a quantitative biomarker in order to evaluate the antifungal efficacy of isavuconazole. Galactomannan levels were measured using a double-sandwich enzyme linked immunosorbent assay (Platelia *Aspergillus;* Bio-Rad). The protocol provided by the manufacturer, was followed with one modification. Due to the relatively small volume of sample that can be obtained using this model, 25 µL of sample treatment solution was added to 75 µL of sample as

opposed to the recommended volume of 100 µL of sample treatment solution to 300 µL of sample.

2.28 Mathematical modelling

A population methodology was used in order to fit a mathematical model to the data from each isolate. A one compartmental model was chosen to represent the number of compartments present in the dynamic model. In order to account for the varying susceptibilities of the isolates used in this study and to improve the fit of the pharmacodynamic model, the MIC was incorporated into equation 2b. Version 1.2.9 of Pmetrics PK-PD analytical software was used. The structural mathematical model consisted of the following two inhomogeneous ordinary differential equations:

$$dX1/dt=B(1)-(SCL/Vc)*X1 \qquad \text{Equation 1}$$

$$dN/dt=Kgmax*(1-(N/POPMAX))*N \qquad \text{Equation 2a}$$

$$*(1-(X1/Vc)^{Hg}/(X1/Vc)^{Hg}+C50g^{Hg})) \qquad \text{Equation 2b}$$

Where: B(1) is the bolus input of isavuconazole, SCL is the clearance of isavuconazole from the circuit, Vc is the volume of the circuit, N is the galactomannan concentration, Kgmax is the maximal rate of growth; POPMAX is the theoretical maximal density within the circuit; Hg is the slope function for the suppression of growth; and, C50g is the concentration of ISA in the circuit where there is half-maximal suppression of growth multiplied by the MIC.

Equation 1 describes the rate of change of ISA concentrations in the circuit. Equation 2 describes the rate of change of galactomannan in the circuit and contains terms that describe fungal growth in the absence of ISA (Equation 2a) and the ISA induced suppression of growth in relation to the MIC (Equation 2b).

The model was fitted to the dataset of untreated and treated circuits obtained from each isolate. Each circuit was treated as an "individual". The Bayesian posterior estimates for each of the parameters in the model were then used to define the concentration-time profile of ISA and the resultant effect on galactomannan concentrations.

As the AUC:MIC has consistently been demonstrated as the pharmacodynamic indices best associated with the antifungal efficacy of ISA (Lepak, Marchillo et al. 2013) the parameter estimates from the model were used to estimate the AUC that developed in each circuit, and consequently the AUC:MIC ratio for each isolate and experimental condition. A sigmoid inhibitory maximal effect (Emax) model was used in order to establish the relationship between AUC and AUC:MIC and antifungal efficacy. The model consisted of the following structure:

$$\text{Effect} = \text{Baseline} - (\text{Emax} * X^{H})/(EC_{50}{}^{H} * X^{H}),$$

Where Baseline is the fungal burden in the absence of drug, Emax is the

asymptotic reduction in fungal burden induced by antifungal drug exposure, X

is a measure of drug exposure (i.e., the AUC or AUC/MIC ratio), EC50 is the concentration resulting in half-maximal effect, and H is the slope (or Hill) function.

2.3 RESULTS

2.31 Minimum Inhibitory Concentrations

Minimum inhibitory concentrations (MIC) (mode, range and geometric means) for ISA against isolates of *A. fumigatus* using EUCAST and CLSI methodologies are summarised in Table 2.3. For isolates of *A. fumigatus*, the MIC was higher in those isolates with amino acid substitutions in the Cyp51 protein using both methodologies.

			EUCAST			CLSI		
Species	**Isolate**	**Cyp51A mutation**	**Mode**	**Range**	**Mean**	**Mode**	**Range**	**Mean**
A. fumigatus	**GFP**	**Wild-type**	**1**	**0.5-2.0**	**1**	**1**	**0.5-1**	**0.81**
A. fumigatus	**4215**	**Wild-type**	**1**	**0.5-2.0**	**1**	**1**	**1-4**	**1.62**
A. fumigatus	**16216**	**L98H**	**2**	**2-4**	**2.64**	**4**	**1-4**	**2.63**
A. fumigatus	**11628**	**G138C**	**4**	**4-8**	**4.92**	**4**	**1-8**	**2.82**

Table 2. 2

Minimum inhibitory concentrations were determined in 10 independent experiments. Means displayed above are geometric means.

2.32 Pharmacokinetics and pharmacodynamics of *A. fumigatus* in static models of invasive aspergillosis

The exposure-response relationship of ISA against a wild-type GFP-transformant of *A. fumigatus* is demonstrated in Figure 3.2. Consistent with previous findings using this model concentrations of ISA required to achieve suppression of galactomannan release were higher for the alveolar compartment than the endothelial compartment. A dose-dependent decline in galactomannan index was observed. Maximal suppression of galactomannan for this isolate was achieved at a concentration of around 0.4 mg/L. This result was comparable to the MIC obtained for this isolate (Table 3.1).

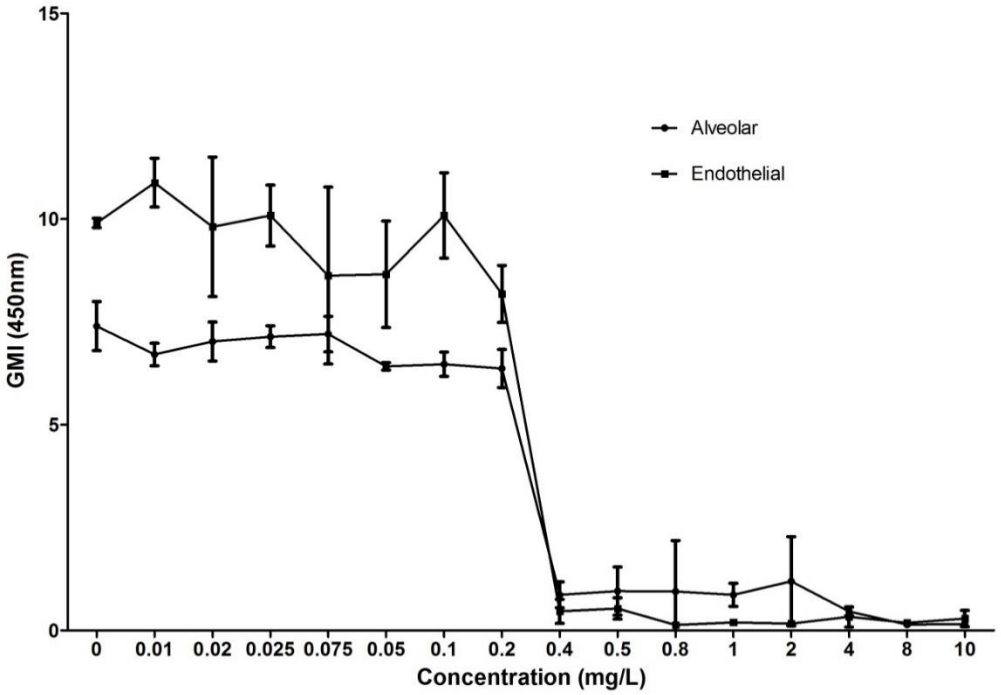

Figure 2. 2

Pharmacokinetics and pharmacodynamics of ISA in a static model against *A. fumigatus* GFP transformant. Error bars represent the standard deviation of three separate transwells. Measured concentrations were all within 10% of administered dosage.

2.33 Pharmacokinetics and pharmacodynamics of ISA against isolates of *A. fumigatus* in dynamic models of invasive aspergillosis

Human-like plasma concentration-time profiles for ISA were generated using the dynamic *in vitro* model (Figures 2.3- 2.6).

The kinetics of galactomannan release was different between isolates. Levels of galactomannan in all untreated circuits started to increase at around 18-24 hours post treatment (Figures 2.3-2.6). A maximum galactomannan index was observed at approximately 24 hours for the GFP transformant, F/11628 and NIH 4215. The strain F/16216 appeared to grow more slowly and maximal galactomannan concentrations were reached at around 36 hours post inoculation (Figure 2.5). The maximum galactomannan concentrations ranged from an index of approximately 6-9.

Clearly defined exposure-response relationships for ISA against each of the isolates were demonstrated. Consistent with results from the static model, a trough concentration of approximately 0.2-0.5 mg/L resulted in near maximal suppression of galactomannan release for the wild-type GFP transformant. Similar results were observed for the wild-type organism NIH 4215. For the two CYP51A variant isolates the exposure-response relationships were different. Only a dosage of 1.5mg ISA against F/16216 resulted in a considerable suppression of galactomannan production. None of the ISA concentrations were able to suppress the release of galactomannan for strain F/11628. Thus the MIC and genotype seemed to be a significant influence on the variation in the observed exposure-response relationships.

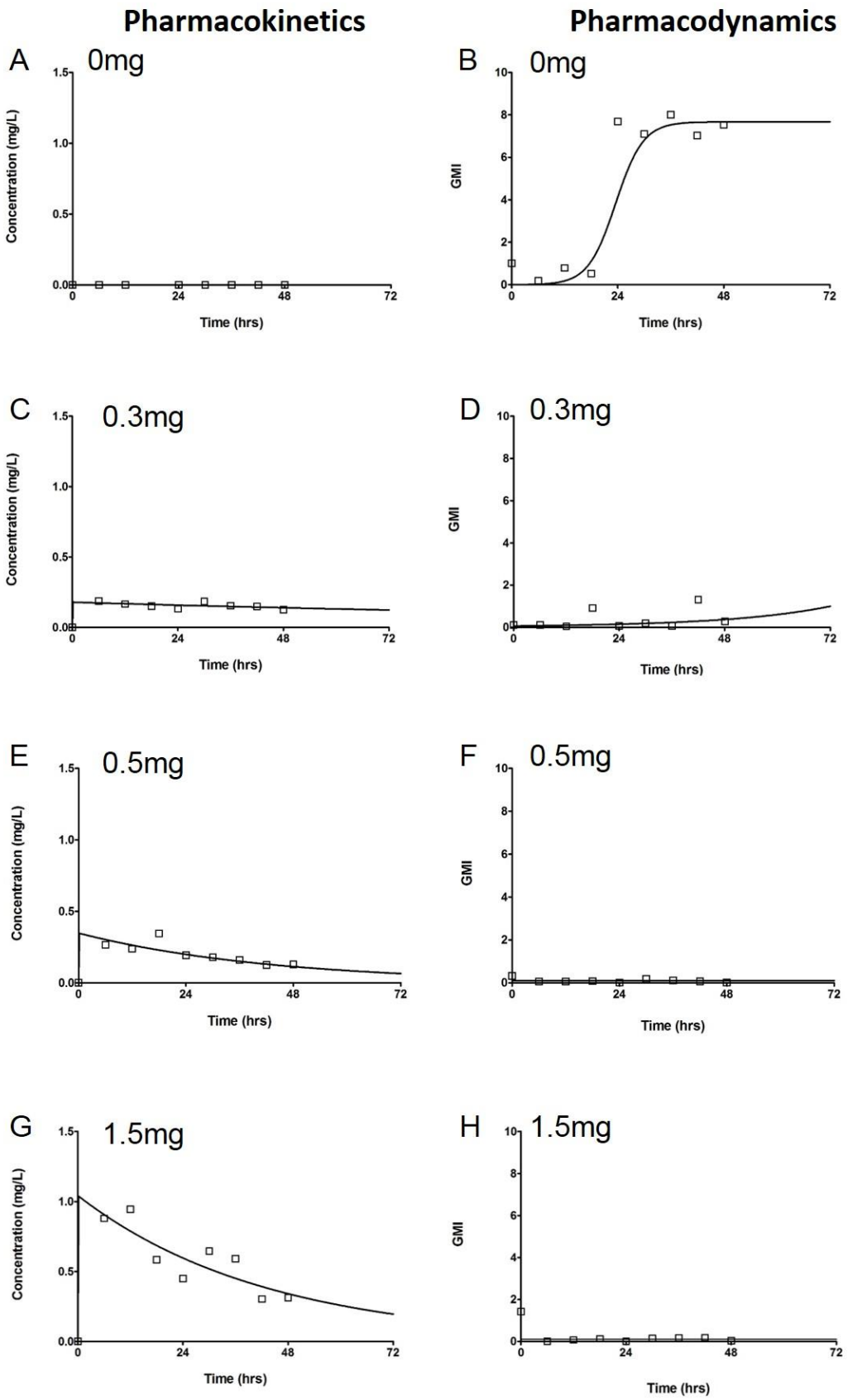

Figure 2.3 Pharmacokinetics and pharmacodynamics of ISA against the GFP transformant of *A. fumigatus*.

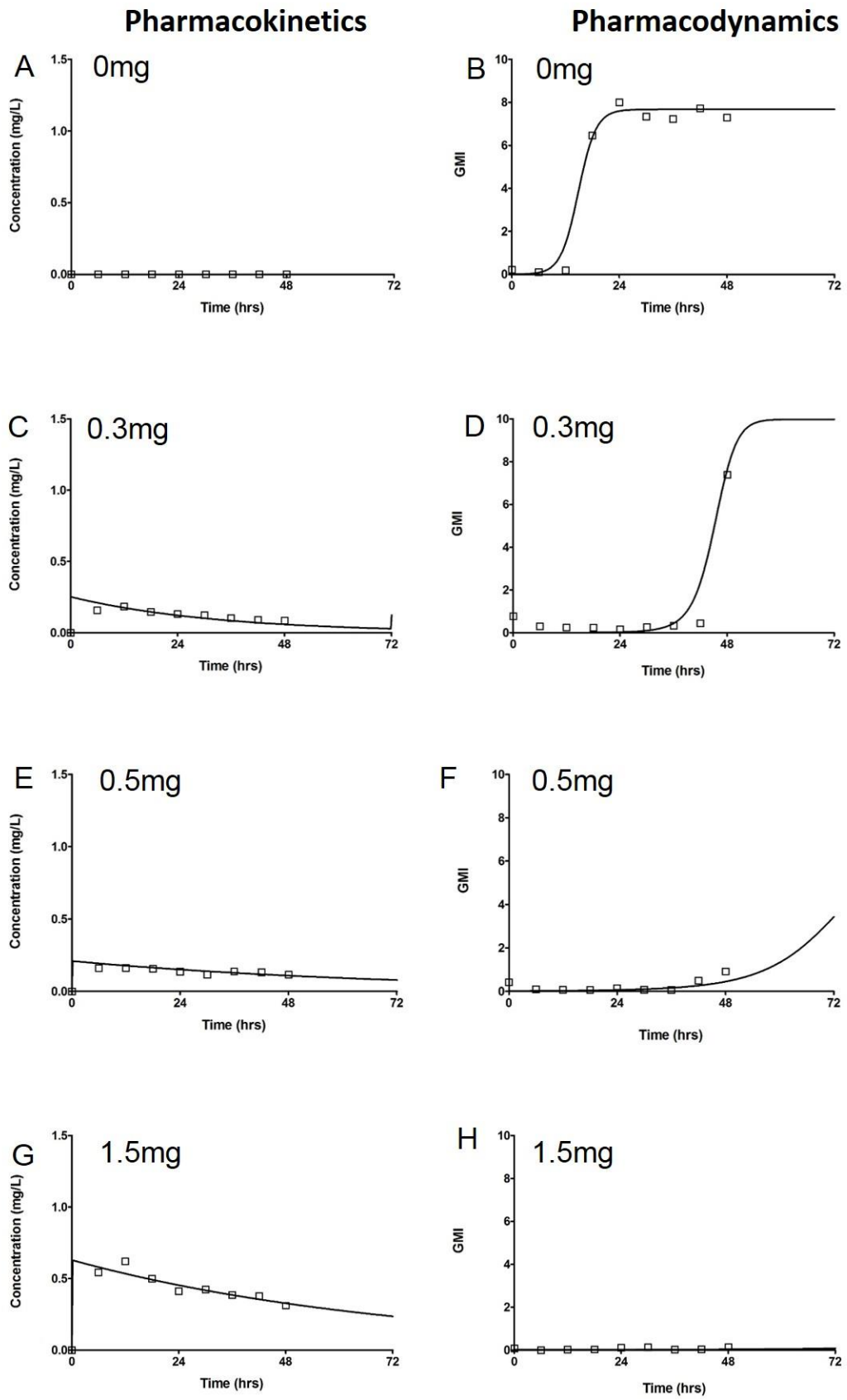

Figure 2.4 Pharmacokinetics and pharmacodynamics of ISA against wild-type isolate NIH4215 of *A. fumigatus.*

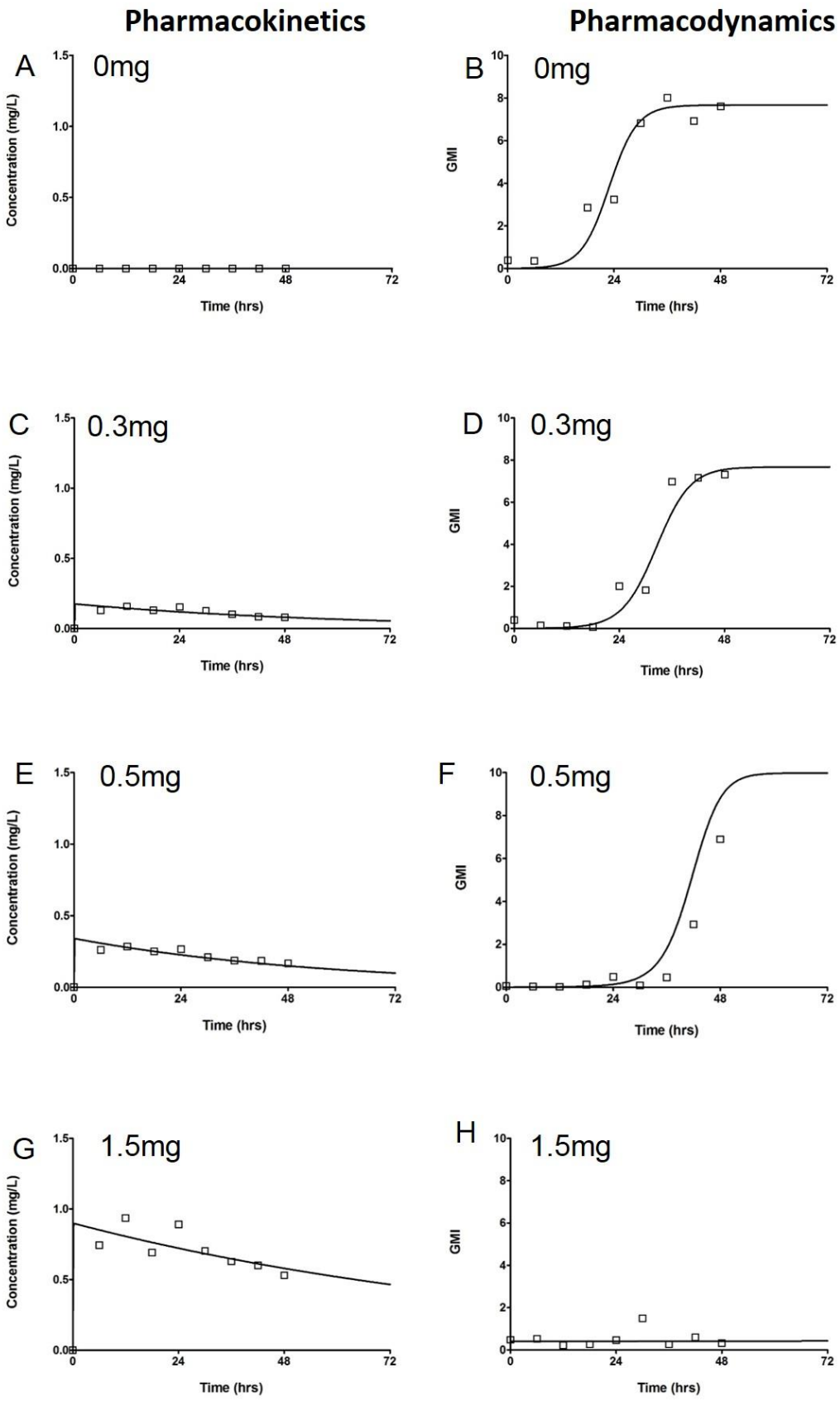

Figure 2.5 Pharmacokinetics and pharmacodynamics of ISA against L98H expressing isolate F/16216 of *A. fumigatus*.

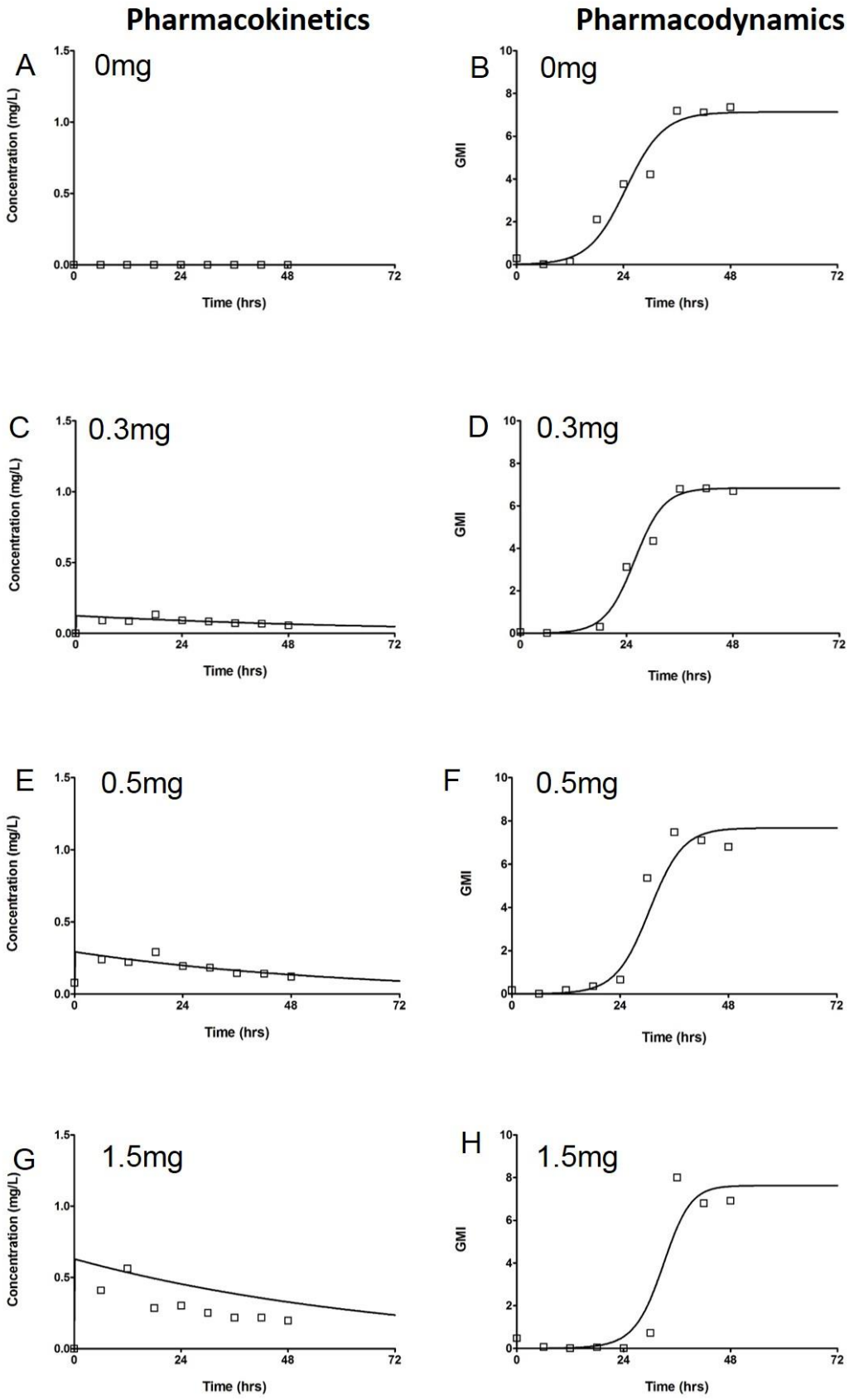

Figure 2.6 Pharmacokinetics and pharmacodynamics of ISA against G138C expressing isolate F/11628.

3.34 Mathematical Modelling of *A. fumigatus* pharmacokinetics and pharmacodynamics

The fit of the mathematical model to the data was highly acceptable. The fit of the Bayesian posterior estimates for each circuit is shown in Figures 2.3-2.6.

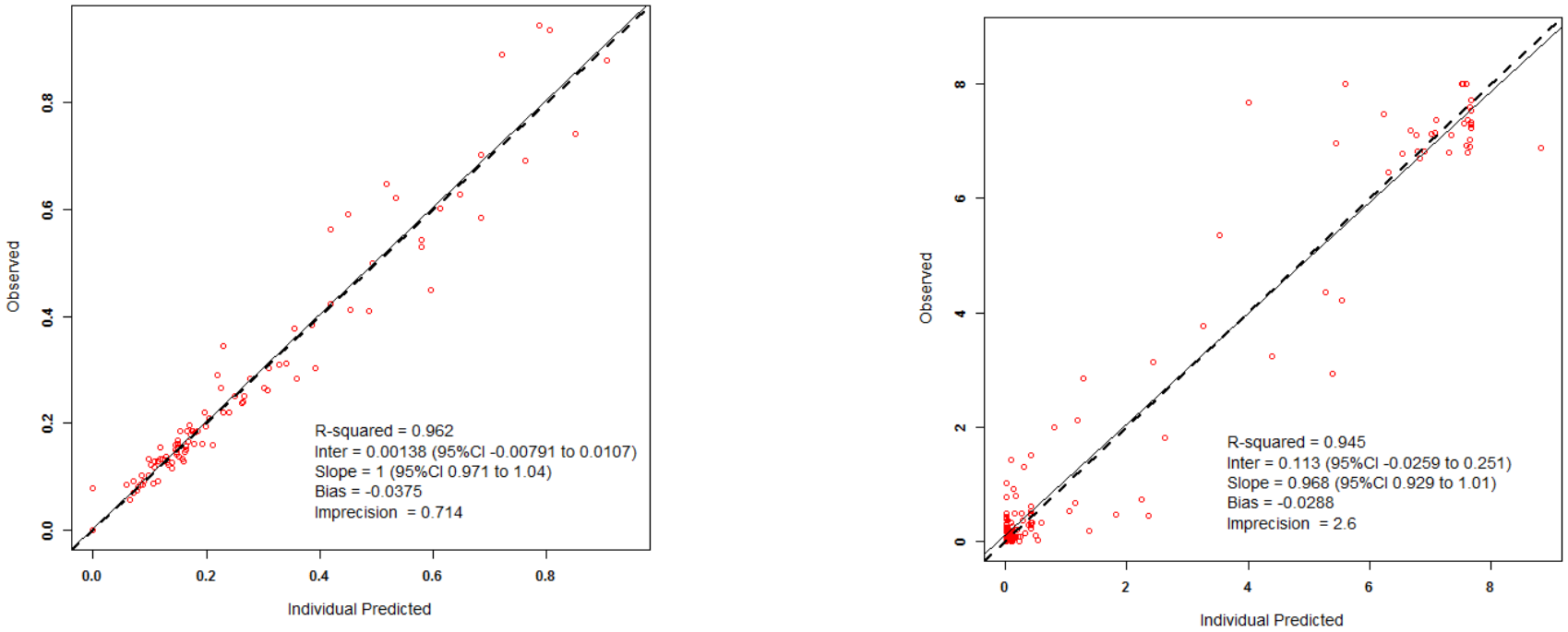

Figure 2.7

Observed vs predicted graphs after the Bayesian step, generated using Pmetrics for (A) pharmacokinetics data from 16 individual circuits and (B) pharmacodynamics data as measured by absorbance obtained from the Platelia *Aspergillus* assay from 16 individual circuits.

Isolate	Dosage (mg)	MIC (mg/L)	Cl (L/hr(	V (L)	F	Kgmax	POPMAX	C50	Hg	IC1
GFP	0.0	1	0.003	0.17	0.10	0.32	7.67	0.13	1.53	0.00
GFP	0.3	1	0.0008	0.16	0.10	0.18	7.73	0.06	1.45	0.07
GFP	0.5	1	0.003	0.14	0.10	0.16	8.13	0.00	1.99	0.10
GFP	1.5	1	0.003	0.14	0.10	0.16	8.12	0.00	1.99	0.10
4215	0.0	1	0.0005	0.49	0.01	0.51	7.67	0.00	1.99	0.00
4215	0.3	1	0.003	0.11	0.09	0.88	9.97	0.06	1.99	0.00
4215	0.5	1	0.003	0.23	0.10	0.24	7.11	0.08	1.49	0.02
4215	1.5	1	0.003	0.23	0.10	0.24	7.11	0.08	1.49	0.02
16216	0.0	2	0.003	0.17	0.10	0.32	7.66	0.13	1.52	0.00
16216	0.3	2	0.003	0.17	0.10	0.32	7.67	0.13	1.53	0.00
16216	0.5	2	0.002	0.13	0.09	0.80	9.98	0.06	1.83	0.00
16216	1.5	2	0.001	0.11	0.06	0.10	5.03	0.00	0.96	0.41
11628	0.0	4	0.003	0.23	0.10	0.24	7.13	0.08	1.50	0.02
11628	0.3	4	0.003	0.24	0.10	0.42	6.83	0.06	0.97	0.00
11628	0.5	4	0.003	0.17	0.10	0.32	7.67	0.13	1.53	0.00
11628	1.5	4	0.004	0.18	0.07	1.00	7.63	0.03	1.06	0.00

Table 2. 3

The median posterior parameter estimates from the mathematical model using data from 12 individual circuits. Cl represents the estimated clearance of ISA from the ciruit; V; the estimated volume of the central compartment; Kgmax, the predicted rate of growth of *A. fumigatus* in the circuit; POPMAX, the maxima obtained from the Platelia *Aspergillus* assay; C50, the concentration of ISA that 50% suppression of galactomannan is obtained; Hg, the slope function to describe *A. fumigatus* growth in both absence and presence of drug; IC1, the initial conditions for the pharmacodynamic dataset, representing background noise of the assay.

Strain	Dose (mg/ q12)	Predicted AUC_{0-48} isavuconazole(mg.hr/L)	Predicted AUC_{0-48} galactomannan
A. fumigatus GFP	0	0.00	187.59
	0.3	4.03	8.35
	0.5	6.36	4.70
	1.5	19.06	4.72
A. fumigatus 4215	0	0.00	254.40
	0.3	4.30	38.29
	0.5	4.27	5.47
	1.5	12.83	1.22
A. fumigatus 16216	0	0.00	192.17
	0.3	3.47	120.96
	0.5	6.68	72.87
	1.5	19.28	19.86
A. fumigatus 11628	0	0.00	166.92
	0.3	2.55	152.18
	0.5	5.79	135.52
	1.5	10.14	118.81

Table 2. 4

Model predicted isavuconazole AUC_{0-48} and galactomannan absorbance values for isolates of *A. fumigatus* for individual circuits achieved using the dynamic model.

2.35 Sigmoid Emax analysis

The fit of the sigmoidal curve demonstrated an association between the AUC_{0-48} for galatomannan release and the AUC_{0-48} of ISA (Figure 3.8, R^2= 0.701). This link was improved upon the incorporation of the MIC as a pharamcodynamic predictor of response (Figure 3.9, R^2= 0.888).

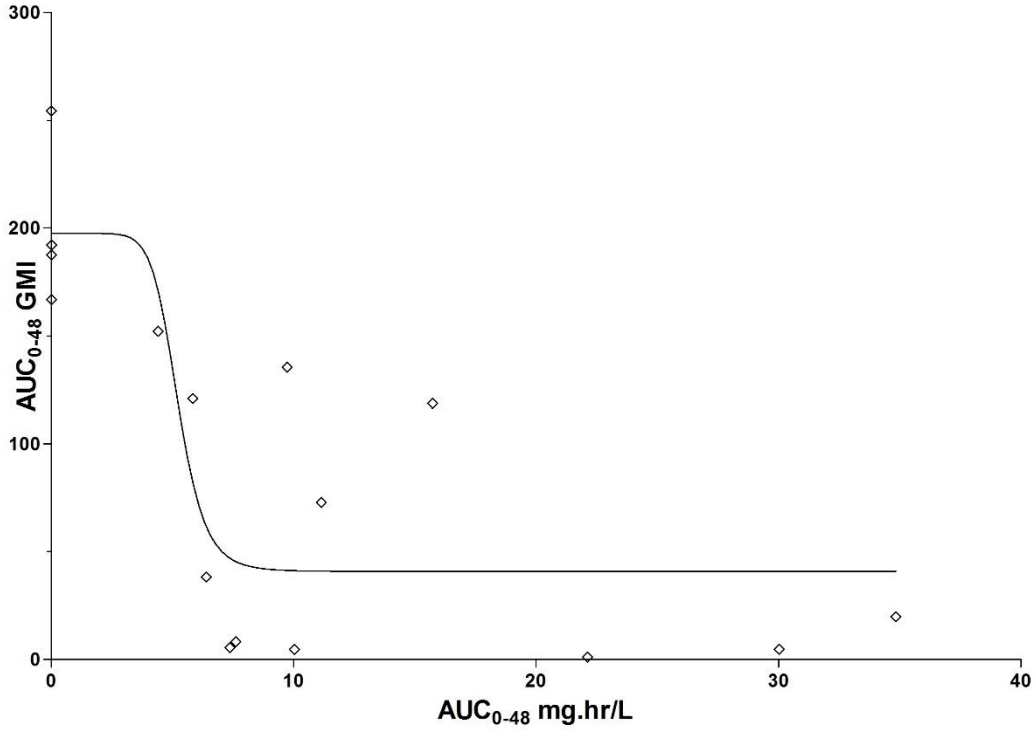

Figure 2.8

Area under the galactomannan curves (0-48hrs) for *A. fumigatus* versus area under the concentration- time curves (mg.hr/L) (0-28). R^2 = 0.709.

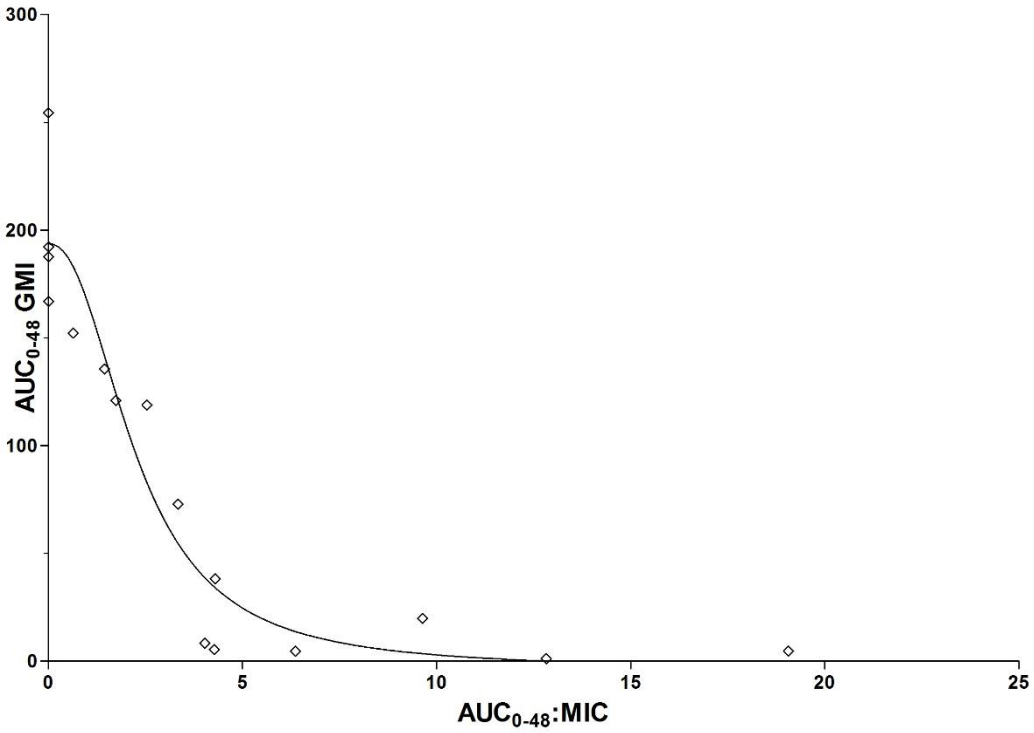

Figure 2.9

Area under the galactomannan curves (0-48hrs) for *A. fumigatus* versus AUC_{0-48}:MIC. $R^2 = 0.911$

2.4 CONCLUSIONS

Invasive pulmonary aspergillosis is associated with relatively high morbidity and mortality (Hope, Kruhlak et al. 2007). Pathogenic isolates of *A. fumigatus* that are resistant to existing antifungal drugs are emerging (Howard and Arendrup 2011). The development of novel antifungal agents is essential in order to improve clinical outcomes and meet evolving clinical requirements. ISA is a novel triazole antifungal agent that is administered as the water soluble prodrug, isavuconazonium sulfate (BAL8557). The efficacy of ISA has recently been established in a Phase III clinical trial (SECURE), which compared the clinical response and mortality of patients with invasive aspergillosis receiving ISA or voriconazole (Ullmann A 2014) . An understanding of the PK-PD relationships of ISA is central to the optimal use of this agent. These analyses describe the use of *in vitro* static and dynamic models of early invasive pulmonary aspergillosis to define the PK-PD relationships of ISA against clinical isolates of *A. fumigatus.*

ISA demonstrated a dose- dependent decline in galactomannan release in a static model of IPA using the wild-type GFP transformant of *A. fumigatus*. These findings were confirmed in the *in vitro* dynamic model.

There were defined differences in the PK-PD relationships between isolates in the dynamic model. Both wild-type strains were readily treatable with ISA at trough concentrations of approximately 0.1-0.3 mg/L. The isolate expressing an L98H substitution in the Cyp51A binding site (F/16216) required a slightly higher concentration of ISA in order to eliminate galactomannan release. A trough concentration of approximately 0.5 mg/L successfully suppressed galactomannan in

this study suggesting these levels may be effective in treating infections with this strain. None of the drug concentrations used were efficient in suppressing galactomannan release in the strain expressing a G138C substitution mutation. These findings are consistent with previous studies to describe the PK-PD of alternative triazole agents for the treatment of infection with the four organisms studied here (Howard, Lestner et al. 2011, Jeans, Howard et al. 2012). This suggests that these isolates may confer pan resistance across the triazole class of agents.

Again, this pharmacodynamic variability observed between strains may be understood and quantified in terms of the MIC and the phenotype of the organism. Higher MIC values for ISA are observed against isolates of *A. fumigatus* carrying Cyp51A amino acid substitutions, L98H and G138C (Gregson, Goodwin et al. 2013). Relatively more ISA, in terms of the AUC, is required to exert an antifungal effect against these strains in this *in vitro* dynamic model. This suggests that both the MIC and the genotype account for a considerable amount of the variance seen. The importance of the MIC in this study is demonstrated in Figures 3.8 and 3.9 where an improved association between AUC:MIC and antifungal effect can be seen comparted to AUC alone. This observation further suggests that the MIC may be a reliable *in vitro* measure to guide antifungal therapy in patients in the setting of invasive aspergillosis. Standardized testing methodology for ISA has been developed by both CLSI and EUCAST, and epidemiological surveys detailing MICs in medically important opportunistic fungal pathogens have been published (Espinel-Ingroff, Chowdhary et al. 2013, Gregson, Goodwin et al. 2013). The MIC value that defines the upper limit of the wild-type distribution according to Howard et al, 2013 is 2 mg/L for *A. fumigatus, A. flavus and A. terreus*. For isolates of *A. niger* it is 4 mg/L. For CLSI the ECOFF is 1 mg/L for *A. fumigatus, A. flavus* and *A. terreus*. The CLSI

ECOFF is 4 mg/L for niger (Espinel-Ingroff, Chowdhary et al. 2013). The results from the Phase III clinical trial (SECURE) suggest that the majority of strains that belong to the wild-type distribution are likely to be treatable and using EUCAST terminology, wild-type *A. fumigatus* is likely to be a "good target" for ISA. There is still some uncertainty as to the breakpoint for ISA using either EUCAST or CLSI methodology (Marr K 2014, Ullmann A 2014)

In this model of early invasive pulmonary aspergillosis, total drug AUC:MIC values of approximately 19.1 and 12.8 using EUCAST methodology, respectively are associated with near maximal antifungal activity for wild-type isolates. These target values are lower than two recently published studies (Lepak, Marchillo et al. 2013, Seyedmousavi, Bruggemann et al. 2015). In the first of these studies, Lepak et al. used a profoundly neutropenic murine model of invasive pulmonary aspergillosis, and report that a much higher median AUC:MIC target of approximately 500 is associated with a static antifungal effect (i.e. prevents net growth or kill as assessed using a qPCR endpoint). This pharmacodynamic target increases almost 2-fold to ~1000 if orders of logarithmic killing are used as the pharmacodynamic endpoint (Lepak, Marchillo et al. 2013). A second study by Seyedmousavi et al. suggests that a much lower pharmacodynamic AUC:MIC target of 24.73 is reasonable (Seyedmousavi, Bruggemann et al. 2015). This target is closer to the value in our study and was estimated using a non-neutropenic model of disseminated aspergillosis. The differences in these estimates of the pharmacodynamic target for ISA may be related to the degree in the severity of each model, the stage of disease that is being mimicked and the background immunosuppression. The model of IPA used by Lepak et al. is a severe neutropenic model. In this murine model the progression of disease is rapid and terminal without the prompt initiation of therapy. In contrast, the non-neutropenic

model of disseminated aspergillosis has a much longer time-course and estimates of drug exposure effect relationships are more complex due to the additional antifungal activity of immunological effectors. The *in vitro* dynamic model used in this study is a model of early invasive disease before there is significant tissue damage. Drug exposure-response relationships are estimated before the onset of the haemorrhagic infarction and pyogranulomatous inflammation that is characteristic of invasive aspergillosis in neutropenic and non-neutropenic hosts, respectively. The three experimental models represent the spectrum of invasive aspergillosis that is observed in the clinic, which ranges from very early disease right through to established disease in profoundly immunosuppressed hosts. Therefore the estimates for pharmacodynamic targets required for therapeutic efficacy from the three models vary accordingly.

An understanding of the PK-PD of ISA and most relevant pharmacodynamic targets is important for decision support in setting *in vitro* susceptibility breakpoints. For phase III clinical trials a loading dose of 200 mg q8h on days 1 and 2 followed by 200 mg/day was used in order to compare the efficacy and safety of ISA to that of VRC. Population pharmacokinetic analysis of this data suggests this regimen produces a mean AUC of approximately 100 mg/h/L and is effective for the treatment of the majority of wild-type isolates of *A. fumigatus*. Given this data, a higher AUC:MIC target such as that suggested by the neutropenic mouse model of IPA may therefore be difficult to achieve for the majority of wild type isolates. An AUC:MIC target of 500 would likely be achievable for strains with an MIC 0.125 mg/L (i.e. 100 divided by 0.125 = 800, which is exceeds the recommended target of 500). However, the likelihood of a successful outcome becomes progressively less with strains with MICs > 0.125 mg/L). Using an AUC:MIC target of 500 would therefore mean that the

breakpoint would divide the wild-type population. This is not consistent with observations from the randomised Phase III clinical trial where there was not a tendency for clinical failure with strains with elevated MICs. In contrast, using a lower pharmacodynamic target of 11-25 would enable the wild type population to be adequately covered in the majority of patients which would be consistent with clinical results. The most profoundly immunosuppressed patients with a high burden of infection may require higher drug exposure for a successful outcome, as suggested by Lepak et al. The determination of this however will require further experience and clinical studies with ISA.

ISA is demonstrated to be a safe and effective agent for the treatment of invasive aspergillosis. The results from this study suggest that the MIC of ISA to clinical isolates of *A. fumigatus* may be an important determinant of the exposure-response relationships. The preclinical PK-PD data and analyses from three different laboratories are somewhat discordant. This may be due to significant differences in the experimental models that are used to characterize these relationships. The results from this study suggest that the majority of wild-type isolates can be treated with the currently used regimens. A definitive breakpoint analysis will require the development population PK model, which is currently in progress. The population PK model and PK-PD bridging studies will then help define the highest MIC that can be treated with the current ISA regimen and indicate the potential benefit of dosage escalation to treat strains that may otherwise be classified as having intermediate susceptibility.

CHAPTER III

The pharmacokinetics and pharmacodynamics of isavuconazole against isolates of *Aspergillus terreus*

3.1 INTRODUCTION

Invasive pulmonary aspergillosis is a lethal infectious syndrome. *Aspergillus* spp. is the most common mould infection in immunocompromised patients. Due to the presence of underlying disease in immunocompromised patient populations and inter-species variability in susceptibility to commonly used antifungal agents, the treatment of these infections are complex.

A. terreus is an important human pathogen associated with global morbidity and mortality in at risk individuals. The incidence of *A. terreus* has increased significantly over recent years and this species now contributes to approximately 3-12% of IPA infections (Slesiona, Gressler et al. 2012). Although *A. terreus* infection is less common than that of *A. fumigatus* clinical outcomes tend to be poor. Mortality rates of up to 85% have been described in patients with haematological malignancy. *A. terreus* is intrinsically resistant to amphotericin B meaning there are relatively few therapeutic options. Voriconazole is the recommended first-line agent however clinical outcome may be variable (Hachem, Kontoyiannis et al. 2004, Steinbach, Benjamin et al. 2004, Pastor and Guarro 2014). The development of novel antifungal agents effective for the treatment of IPA with *A. terreus* is essential to provide additional therapeutic options.

Isavuconazole (ISA), administered as prodrug isavuconazonium sulphate, is the most recent antifungal agent to obtain licensure from the FDA and EMA for the treatment of IPA. ISA demonstrates a favourable safety profile and a broad spectrum of antifungal activity that includes medically important yeasts, moulds and species of the Mucorales (Rybak, Marx et al. 2015). ISA exhibits potent *in vitro* activity against most isolates of *A. terreus* (Pfaller, Messer et al. 2013).

Understanding the pharmacokinetics and pharmacodynamics of ISA against *A. terreus* may help determine the best efficacious dosage for the treatment of IPA caused by this organism. This chapter describes the preliminary development of a previously used *in vitro* model of IPA for use with isolates of *A. terreus*. This model was then utilised for the definition of *in vitro* PK-PD parameters for isavuconazole against three isolates *A. terreus*.

3.2 METHODS

Methods for preparation of inoculum, *in vitro* susceptibility testing, tissue culture, set-up of static and dynamic models and analysis of samples are as described in Chapter II (Sections 2.21-2.27).

3.21 Organism preparation

3.211 *Isolates*

All isolates of *A. terreus* were gifted from the Regional Mycology Reference Laboratory, University Hospital of South Manchester and are detailed in Table 3.1.

Species	Isolate
A. terreus	hus1199
	hus1333
	hus7980

Table 3. 1 Isolates of *A. terreus* used for static and dynamic studies.

3.212 *Culture*

Isolates of *A. terreus* were obtained from Wynthenshawe stored at -80^{0}C using the Microbank ™ preservation system (Pro-lab, Merseyside, UK). Isolates were sub-cultured onto a potato dextrose agar (PDA) flask (Sigma-Aldrich, Poole, UK), at 37^{0}C, 5 days prior to each experiment.

3.22 Mathematical modelling

Data were modelled using the model for isavuconazole described in Chapter II.

3.3 RESULTS

3.31 Minimum Inhibitory Concentrations

Minimum inhibitory concentrations (MIC) (mode, range and geometric means) for ISA against isolates of *A. terreus* using EUCAST and CLSI methodologies are summarised in Table 4.1.

3.32 Pharmacokinetics and pharmacodynamics of ISA against isolates of *A. terreus* in static models of invasive aspergillosis

The exposure-response relationships of ISA against three clinical isolates of *A. terreus* are shown in Figure 4.2. The concentrations of ISA required to achieve suppression of galactomannan release were higher for the alveolar compartment than the endothelial compartment. No suppression of galactomannan was observed in the alveolar compartment for isolates hus1199 and hus7980 at the concentration ranges tested. For isolate hus1333 a dose- dependent decline in galactomannan release was seen in the alveolar compartment however maximal suppression was not achieved. For the endothelial compartment clear differences in the exposure response relationships between isolates were observed. Measured concentrations of approximately 0.2 mg/L were sufficient to maximally suppress galactomannan release for isolates hus1333 and hus7980. Concentrations of ≤1 mg/L were not sufficient to maximally suppress galactomannan release for isolate hus1199 (MIC=8) although a slight decline can be seen at the highest concentrations tested.

		EUCAST			CLSI		
Species	**Isolate**	**Mode**	**Range**	**Mean**	**Mode**	**Range**	**Mean**
A. terreus	**hus1199**	**8**	**4-8**	**6.06**	**4**	**2-4**	**3.48**
A. terreus	**hus1333**	**0.5**	**0.5-0.5**	**7.40**	**4**	**2-4**	**3.03**
A. terreus	**hus7980**	**1**	**0.5-1**	**0.81**	**2**	**1-4**	**1.62**

Table 3. 2

Minimum inhibitory concentrations were determined in 5 independent experiments. Means displayed above are geometric means.

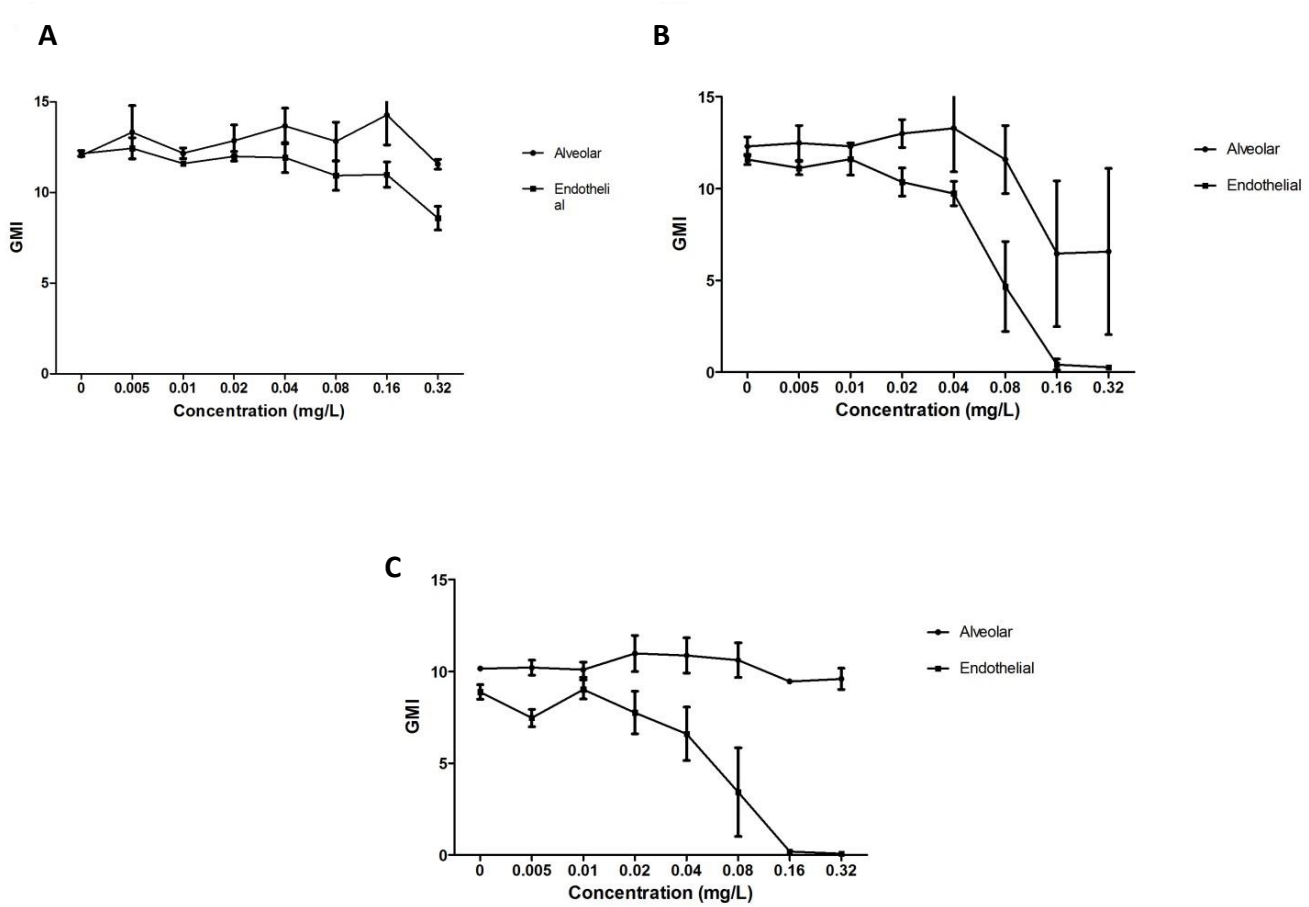

Figure 3. 1 Pharmacokinetics and pharmacodynamics of ISA in a static model against *A. terreus* isolates.

hus1199 (A) hus1199 (B), hus1333 and (C) hus7980. Error bars represent the standard deviation between triplicate samples.

3.33 Pharmacokinetics and pharmacodynamics of ISA against isolates of *A. terreus* in dynamic models of invasive aspergillosis

Human-like plasma concentration-time profiles for ISA were generated using the dynamic *in vitro* model (Figures 4.2- 4.4).

Preliminary data (not shown) suggested the kinetics of galactomannan release may be slower for isolates of *A. terreus* than *A. fumigatus* therefore a 72 hour model (compared to a 48 hour model for *A. fumigatus*) was used to ensure the growth of the organism in untreated circuits. The kinetics of galactomannan release was different between isolates. Concentrations of galactomannan in all untreated circuits started to increase at around 48-60 hours post treatment (Figures 3.2-3.4). A maximum galactomannan concentration was observed by 72 hours for all strains in untreated circuits. In the presence of sub optimal ISA concentrations (Figures 3.2- 3.4 C&D) an earlier release of galactomannan is observed for isolates hus1199, hus1333 and hus7980. For some isolates an anomalous detection of galactomannan was observed at time zero (Figure 3.4H). By 12 hours post treatment galactomannan concentrations were below the threshold of detection in all circuits with the exception of isolate hus7980 in the circuit treated with 1.5mg ISA (Figure 3.4H). The maximum galactomannan concentrations ranged from an index of approximately 7-12.

Clearly defined exposure-response relationships for ISA against each of the isolates were demonstrated. Trough concentrations of approximately 0.2-0.3 mg/L resulted in near maximal suppression of galactomannan release for isolates hus1333 and hus7980. None of the ISA concentrations were able to suppress the release of galactomannan for strain hus1199.

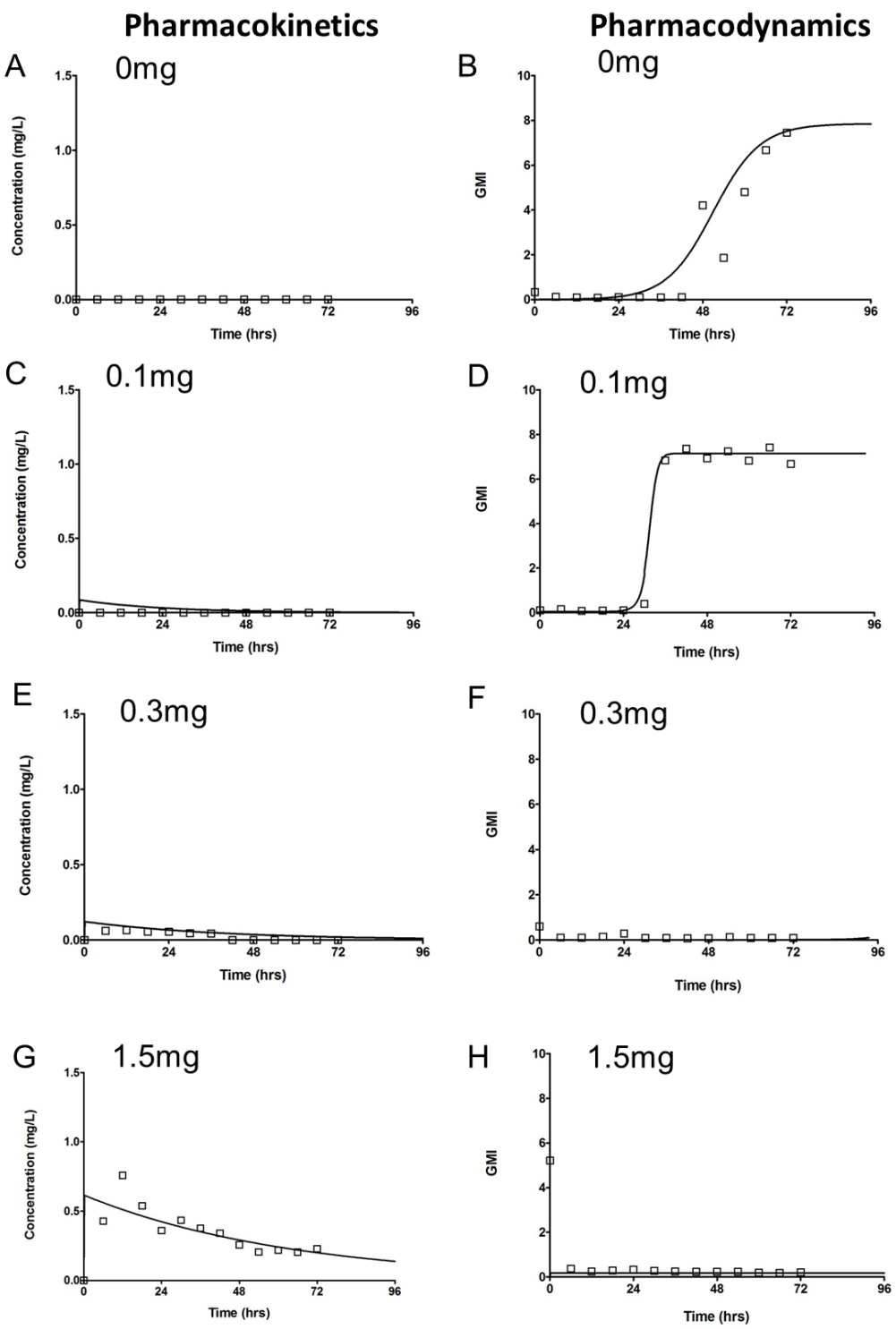

Figure 3. 2 Pharmacokinetics and pharmacodynamics of ISA against *A. terreus* hus1333.

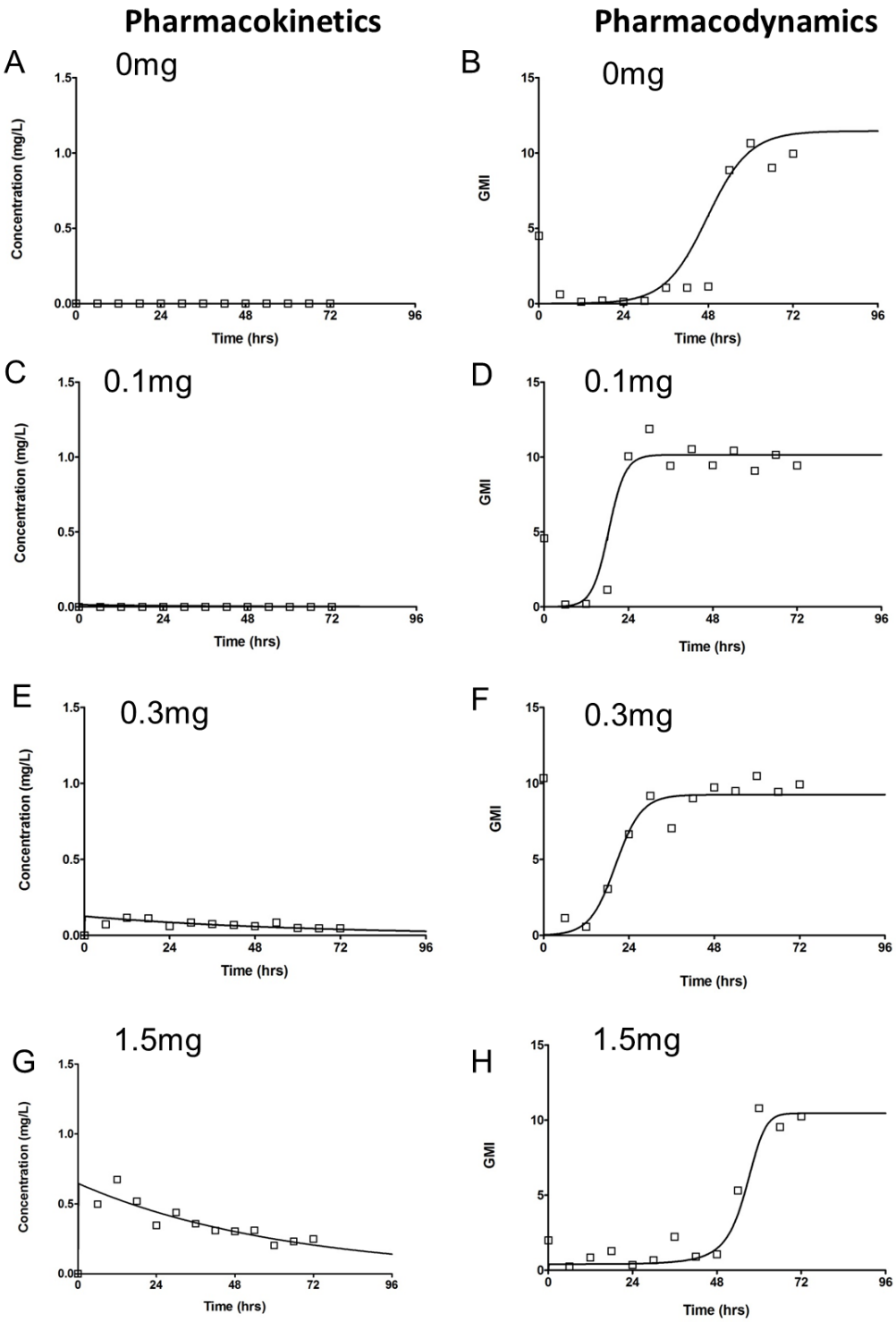

Figure 3. 3 Pharmacokinetics and pharmacodynamics of ISA against *A. terreus* hus1199.

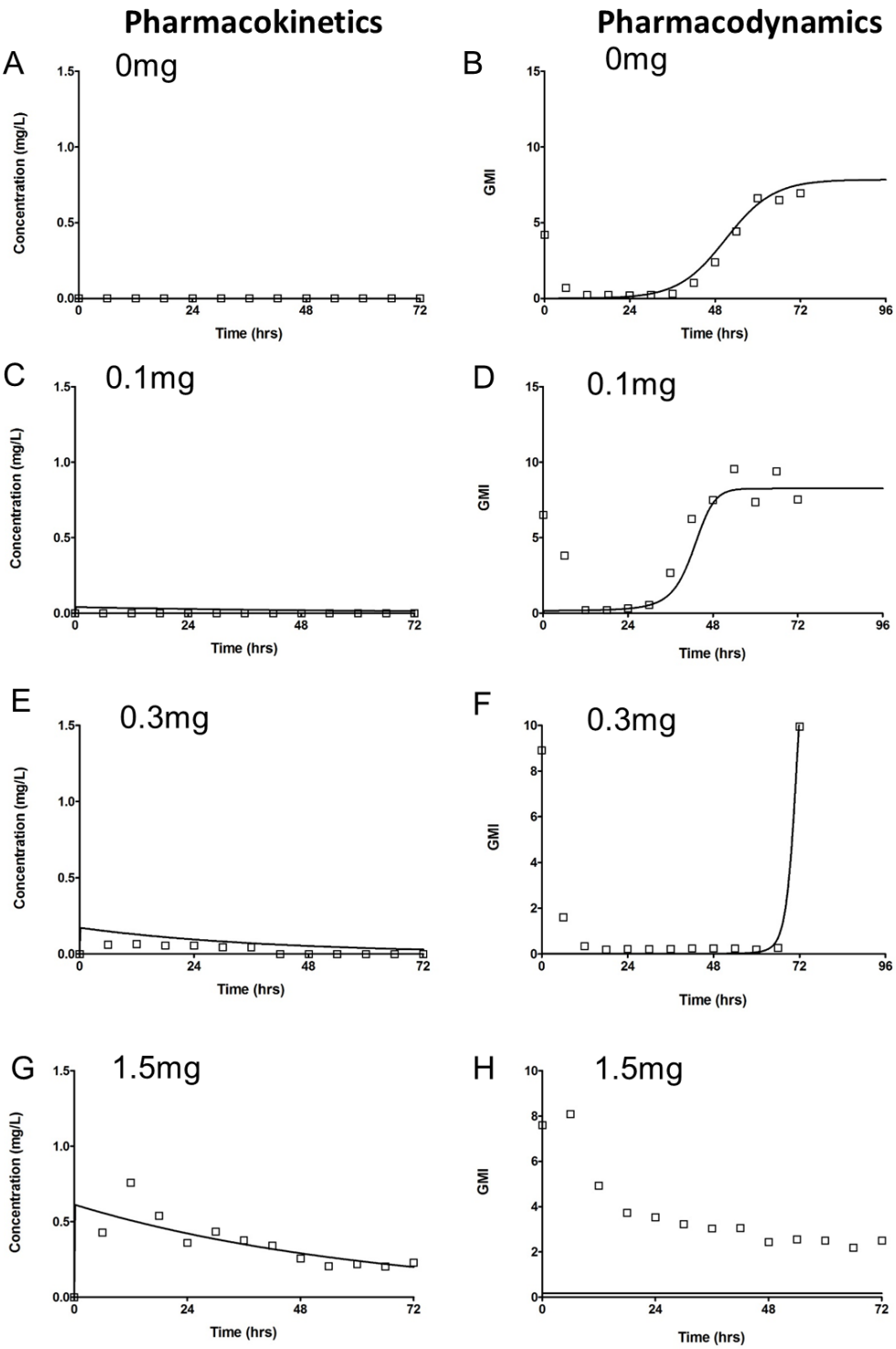

Figure 3. 4 Pharmacokinetics and pharmacodynamics of ISA against *A. terreus* hus7980.

3.34 Mathematical Modelling of *A. terreus* pharmacokinetics and pharmacodynamics

The fit of the mathematical model to the data was highly acceptable (Figure 3.5). The fit of the Bayesian posterior estimates for each circuit is shown in Figures 3.2-3.4. Median posterior parameter estimates for each model can be seen in Table 3.3.

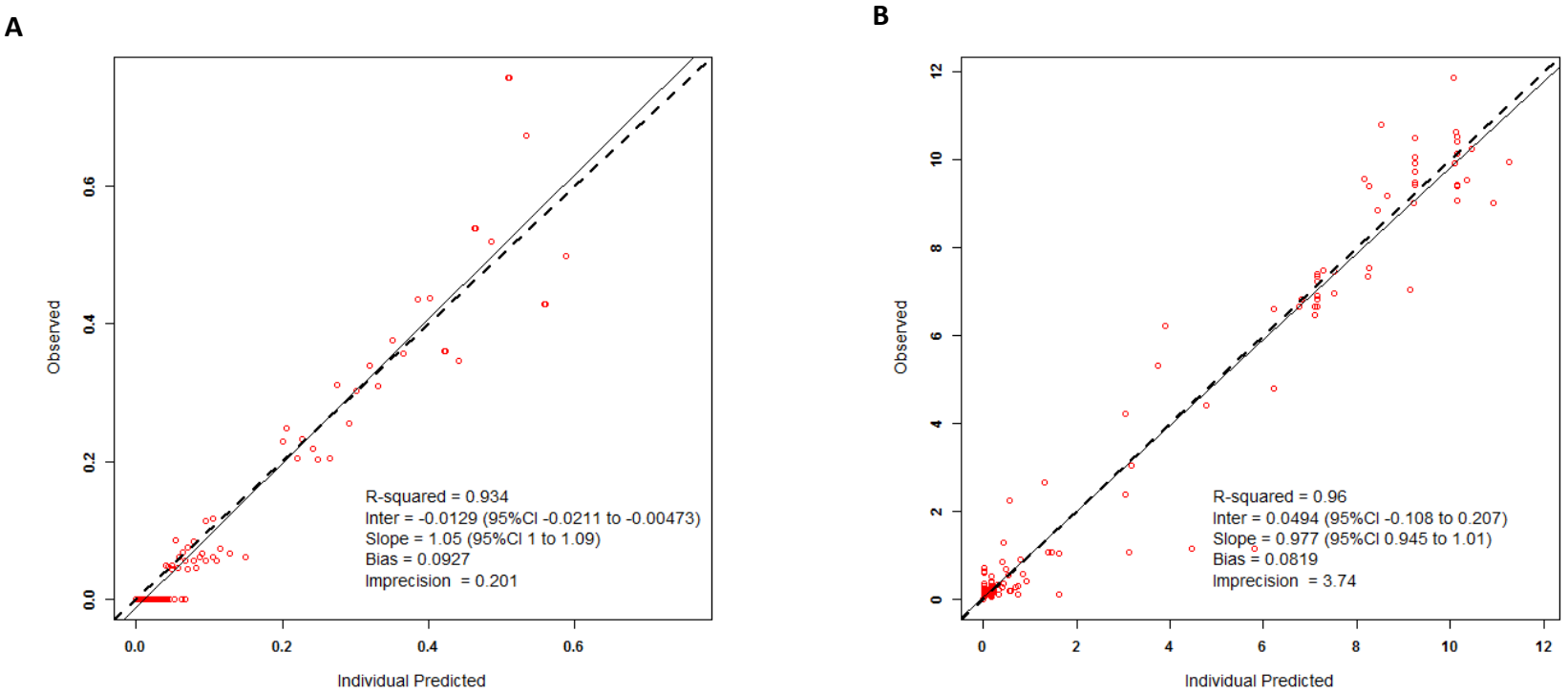

Figure 3. 5

Observed vs predicted graphs after the Bayesian step, generated using Pmetrics for (A) pharmacokinetics data from 12 individual circuits and (B) pharmacodynamics data as measured by absorbance obtained from the Platelia *Aspergillus* assay from 12 individual circuits.

Isolate	Dosage	MIC	Cl	V	F	Kgmax	POPMAX	C50	Hg	IC1
hus1333	0	0.5	0.003	0.10	0.03	0.15	7.85	0.03	1.06	0.00
hus1333	0.1	0.5	0.004	0.10	0.09	1.00	7.15	0.05	7.96	0.04
hus1333	0.3	0.5	0.003	0.13	0.05	0.17	8.22	0.03	6.16	0.01
hus1333	1.5	0.5	0.002	0.13	0.05	0.54	8.28	0.02	7.72	0.17
hus1199	0	8	0.003	0.29	0.06	0.17	11.45	0.07	6.16	0.00
hus1199	0.1	8	0.004	0.17	0.02	0.43	10.15	0.03	1.59	0.00
hus1199	0.3	8	0.002	0.13	0.05	0.28	9.25	0.27	2.19	0.03
hus1199	1.5	8	0.004	0.23	0.10	1.00	10.45	0.03	7.51	0.41
hus7980	0	1	0.003	0.10	0.03	0.15	7.85	0.03	1.06	0.00
hus7980	0.1	1	0.002	0.13	0.05	0.55	8.25	0.02	7.74	0.17
hus7980	0.3	1	0.003	0.12	0.07	1.00	14.95	0.03	7.21	0.01
hus7980	1.5	1	0.002	0.13	0.05	0.55	8.27	0.02	7.72	0.17

Table 3. 3

The median posterior parameter estimates from the mathematical model using data from 12 individual circuits. Cl represents the estimated clearance of ISA from the ciruit; V; the estimated volume of the central compartment; Kgmax, the predicted rate of growth of *A. terreus* in the circuit; POPMAX, the maxima obtained from the Platelia *Aspergillus* assay; C50, the concentration of ISA that 50% suppression of galactomannan is obtained; Hg, the slope function to describe *A. terreus* growth in both absence and presence of drug; IC1, the initial conditions for the pharmacodynamic dataset, representing background noise of the assay.

Strain	Dose (mg/ q12)	Predicted AUC_{0-72} isavuconazole(mg.hr/L)	Predicted AUC_{0-72} galactomannan
A. terreus hus1333	0	0	166.92
	0.1	1.96	284.43
	0.3	4.06	0.39
	1.5	26.59	12.37
A. terreus hus1199	0	0	278.90
	0.1	0.47	543.96
	0.3	5.39	478.29
	1.5	27.68	197.85
A. terreus hus7980	0	0	166.92
	0.1	1.77	257.07
	0.3	5.80	27.08
	1.5	26.52	12.55

Table 3. 4

Model predicted isavuconazole AUC_{0-72} and galactomannan absorbance values for isolates of *A. terreus* for individual circuits achieved using the dynamic model.

3.35 Sigmoid Emax analysis

The fit of the sigmoidal curve demonstrated little association between the AUC_{0-72} for galatomannan release and the AUC_{0-72} of ISA (Figure 3.6, R^2= 0.26). This link was improved upon the incorporation of the MIC as a pharamcodynamic predictor of response (Figure 3.7, R^2= 0.618).

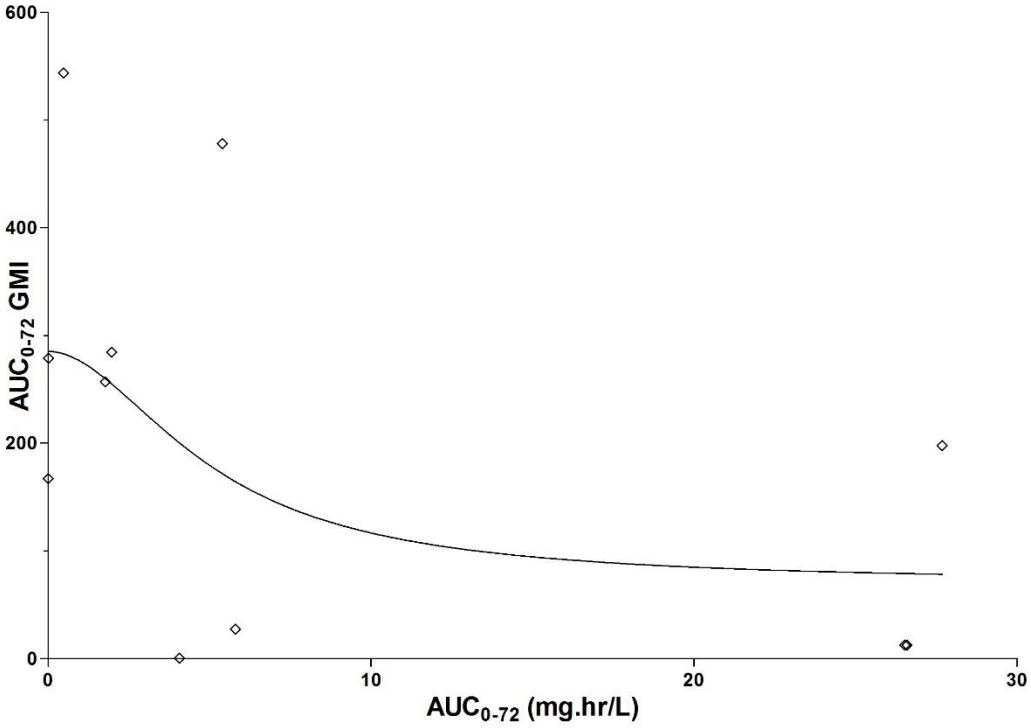

Figure 3. 6

Area under the galactomannan curves (0-72hrs) for *A. terreus* versus the total area under the concentration- time curves for ISA (mg.hr/L). R^2= 0.26

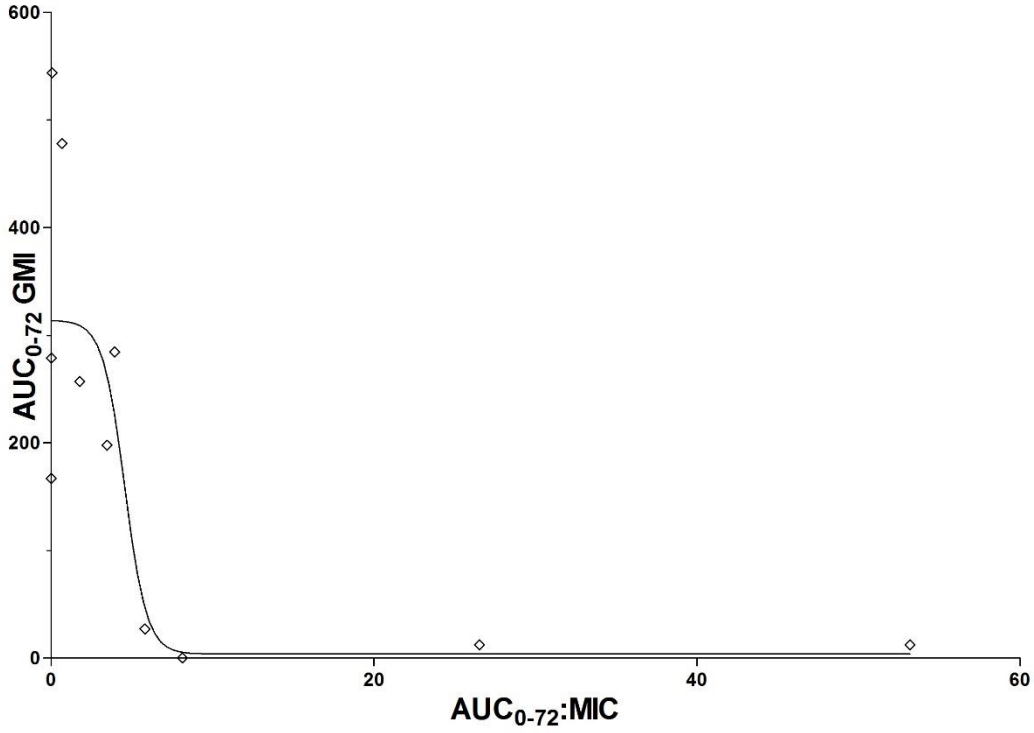

Figure 3. 7

Area under the galactomannan curves (0-72hrs) for *A. terreus* versus AUC:MIC ISA (0-72hrs). R^2= 0.618.

3.4 CONCLUSIONS

Invasive pulmonary aspergillosis caused by *A. terreus* is of emerging clinical concern. The resistance of this species to current antifungal agents is increasing. Therefore it is essential to develop novel agents for the treatment of these infections.

Static studies demonstrate clear pharmacodynamic differences between isolates of *A. terreus* upon increasing exposures to ISA. One isolate demonstrated persistent fungal growth in the presence of drug at the highest concentration used whereas other isolates demonstrated a clear dose-dependent reduction in galactomannan release upon increasing exposure to drug. These results are proportional to the MICs obtained for these isolates. A strain with a higher MIC was untreatable with ISA in this static model whereas there was a dose-dependent antifungal effect against those demonstrating a lower MIC. This suggests that the MIC may make a significant contribution to the pharmacodynamic differences observed between isolates and could therefore serve as a predictive parameter relating to clinical response. These results are consistent with previous studies that have demonstrated the varying susceptibilities of clinical and environmental isolates of *A. terreus* to second generation triazoles such as voriconazole and posaconazole (Graybill, Hernandez et al. 2004, Lass-Florl, Griff et al. 2005, Lass-Flörl, Alastruey-Izquierdo et al. 2009). Whether isolates of *A. terreus* can ultimately be treated with ISA in a clinical setting is yet to be defined. Infections with *A. terreus* formed 2.8% of the total ISA treated patient population in the SECURE phase III trial to establish non-inferiority of ISA to voriconazole. However, the stratification of species-specific treatment outcomes from this study are yet to be published (Maertens, Raad et al. 2016).

A relationship between the MIC and the susceptibility of these isolates to ISA in both dynamic and static cellular models can be observed. There was an improved correlation between the reduction in galactomannan release and increasing AUC:MIC of ISA (R^2= 0.614) (Figure 4.7) in dynamic models, compared to that of the AUC alone (R^2= 0.22) (Figure 4.6). This further supports the potential importance of the MIC as a predictor of treatment success for ISA in this model. The predicted AUC:MIC values associated with maximal suppression of galactomannan were 8.11 and 26.51, comparable to the PD target suggested by Seyedmousavi et al (AUC:MIC of 33.4) (Seyedmousavi, Bruggemann et al. 2015). Consistent with PD target values obtained for *A. fumigatus* using this model (Chapter III) (Box, Livermore et al. 2016) these estimates are markedly lower than at least one study published in the literature (Lepak, Marchillo et al. 2013). However, as detailed in Chapter III, key differences in disease severity, and both routes of infection and administration between models may account for this variability. Population pharmacokinetic models using trough levels predicted that AUC values between 10 and 343 mg.hr/L were achieved in patients with IFIs (Desai 2014). Probability of target attainment (PTA) analyses suggested that at least 90% of this population may be able to achieve an AUC:MIC of 33.4 if MIC is ≤1 mg/L. This supports that an AUC:MIC of 8-26 may be achievable using clinical regimens and that the two susceptible isolates studied in dynamic models may be treatable with ISA without dosage escalation.

Epidemiological surveys performed by EUCAST suggest a clinical breakpoint of 1 mg/L for isolates of *A. terreus* as determined using ECOF values. One of the isolates used in this study demonstrates a higher ISA MIC value up to 8 mg/L and may express potential resistance to azole therapy. Static and dynamic data

presented in this study for these isolates further supports that isolates with MICs above 1 mg/L may not be treatable with ISA. The underlying mechanisms of azole resistance for *A. terreus* have not been well investigated. Molecular characterisation of some azole resistant isolates suggests a potential role for alterations within the Cyp51A protein, similar to those seen in *A. fumigatus* (Arendrup, Jensen et al. 2012). However, further characterisation of isolate hus1199 would be necessary to determine the molecular mechanisms behind the results observed in this study.

The results from this study suggest that wild-type isolates of *A. terreus* may be readily treatable with clinically used dosages of ISA. However, isolates with a higher MIC may require dosage escalation. The use of population PK models described by Desai et al. may be able to bridge these data to clinical populations to derive a susceptibility breakpoint for ISA against *A. terreus* at which higher dosages may be required.

CHAPTER IV

The Pharmacokinetics and Pharmacodynamics of Voriconazole against isolates of *Scedosporium apiospermum and Fusarium solani*

4.1 INTRODUCTION

Scedosporium apiospermum and closely related organisms within the *Pseudallescheria- Scedosporium* species complex are emerging fungal pathogens that can cause disease in both immunocompetent and immunocompromised individuals. In neutropenic patients invasive and disseminated infections may develop that can be fatal (Cortez, Roilides et al. 2008).

S. apiospermum exhibits reduced susceptibility to amphotericin B and flucytosine, echinocandins and triazole antifungal agents (Cuenca-Estrella, Alastruey-Izquierdo et al. 2008). Voriconazole is a first-line agent for the treatment of invasive scedosporiosis (Tortorano, Richardson et al. 2014). However, the emergence of resistant isolates that exhibit reduced *in vitro* susceptibility are concerning (Tortorano, Richardson et al. 2014). The standard regimen of voriconazole for the treatment of invasive fungal infections is 6mg/kg intravenously twice-daily on day 1, followed by 4mg/kg twice daily or 200mg orally. Variable clinical success is seen using this regimen for the treatment of scedosporiosis. The clinical response may be as low as 40-45% in cancer patients and haematopoietic stem cell transplant recipients (Troke, Aguirrebengoa et al. 2008).

A species-specific diagnosis of *Scedosporium* infection is difficult to achieve. The histopathological appearances in tissue are almost identical to those of *Aspergillus* species (Campa-Thompson, West et al. 2014). There are currently no biomarkers that are specific for *Scedosporium* spp. that can be used to establish a diagnosis of invasive disease. A reliable diagnosis therefore depends upon concomitant microbiological culture from tissue samples.

In 2009, Thornton et al. reported the development of two monoclonal antibodies (MAbs), GA3 and HG12, which are directed towards cell wall antigens present in species within the *Scedosporium- Pseudallescheria* complex. The use of these MAbs for the detection of species specific antigens in an enzyme-linked immunosorbent assay has been used for the identification of these pathogens in environment samples. The development of this assay as a clinical product may represent a significant advance in the diagnosis of scedosporiosis (Thornton 2009).

Fusarium spp. are ubiquitous moulds that are emerging as important clinical pathogens in immunocompromised patient populations (Boutati and Anaissie 1997, Nucci and Anaissie 2007). There are now hundreds of species of *Fusarium* that have been identified. The majority of these fungi are plant pathogens (Michielse and Rep 2009). There are approximately eleven known species of *Fusarium* that are pathogenic in humans. *F. solani* is the predominant species that causes human disease, followed by *F. oxysporum* and *F. moniliforme* (Dignani and Anaissie 2004). The lung is the most common site of primary infection in humans and typically affects patients with severe and persistent neutropenia such as those undergoing chemotherapy, and transplant recipients (Garnica, Oliveira da Cunha et al. 2015). Invasive fusariosis demonstrates mortality rates up to 79% in patients with haematological malignancies and 87% in haematological transplant recipients (Nucci 2003, Campo, Lewis et al. 2010).

Imaging and microbiological culture are the main diagnostic techniques used for *F. solani* lung infections. However, these techniques are not species specific. In histopathological sections, *Fusarium* spp. exhibits a morphology similar to that of *Aspergillus* spp. and other filamentous fungi with septate hyphae that exhibit angular dichotomous branching. There are no clinically validated biomarkers available for the

detection of these organisms. As a result, the identification of *Fusarium* spp. to species level requires the study of morphological characteristics from organisms recovered from cultures. This is a time consuming process that involves considerable mycological expertise.

Al-maqtoofi et al. describe the identification of *Fusarium* species via the detection of a water soluble, surface expressed, carbohydrate antigen present on both the conidial spores and hyphae of *Fusarium* spp. This was done using a genus-specific immunoglobulin M (IgM) monoclonal antibody, ED7, directed towards the antigen, by ELISA (Al-Maqtoofi and Thornton 2016). The identification of such species-specific circulatory biomarkers that are indicative of disease state and progression provides a platform for the diagnosis of disease using serological techniques.

There has been much debate on the optimal treatment of invasive fusariosis. Traditional treatment regimens were centred upon amphotericin B formulations. However, variable in vitro susceptibility profiles, poor clinical response rates and poor tolerability all contribute to suboptimal treatment outcomes for fusariosis. With better tolerability and improved clinical outcomes, voriconazole has become a first-line agent for the treatment of invasive infection (Nucci, Marr et al. 2014). However, *in vitro* susceptibilities of voriconazole against isolates of *F. solani* are variable (Alastruey-Izquierdo, Cuenca-Estrella et al. 2008) and overall response rates to voriconazole therapy may be as low as 46% (Perfect, Marr et al. 2003, Stempel, Hammond et al. 2015). The commencement of voriconazole therapy without dosage optimisation, on the assumption of an invasive disease caused by a more susceptible fungi such as *Aspergillus* spp., may result in the sub-optimal treatment of fusariosis.

An understanding of the PD is a first critical step for the optimisation of antifungal therapy. There is a lack of understanding of the dose-exposure-response relationships for first-line agents such as voriconazole against isolates of *Scedosporium* and *Fusarium* species. Previous studies are limited to efficacy and do not measure drug exposure. Murine models cannot accurately simulate human pharmacokinetics of some agents such as voriconazole. It is clear that the available models are far from optimal for the determination of the exposure-response relationships in the treatment of these medically important fungi. The development of novel models that can mimic a human pathway of disease progression and achieve human-like exposures of drug may provide a significant insight into the exposure-response relationships between current antifungal agents and these lethally infectious organisms. The use of these models to further our understanding of the pharmacokinetics and pharmacodynamics of novel agents against *Scedosporium* and *Fusarium* spp. may offer a significant advancement in the development of novel treatment strategies for invasive disease.

In this chapter a previously described model of the human alveolus (Jeans, Howard et al. 2012, Box, Livermore et al. 2016) has been used in order to develop static and dynamic *in vitro* models of *S. apiospermum* and *F. solani* infection for the definition of exposure-response relationships. MAbs, GA3 and HG12, directed towards antigens specific to *P. boydii* and *S. apiospermum* were used as a measure of fungal burden and antifungal drug effect in a model of invasive scedosporiosis. In this model of invasive fusariosis, ED7 was used to for the tracking of *F. solani*. Dynamic models for these pathogens were developed using voriconazole against three clinical isolates of *S. apiospermum* and two isolates of *F. solani*. Once validated these models may be used for the assessment of novel antifungal agents against these organisms.

4.2 METHODS

4.21 Organism preparation

4.211 Pseudallescheria and Scedosporium spp.

Isolates

Isolates of *P. boydii* , *P. ellispoidea* and one isolate of *S. apiospermum* were gifted from the Regional Mycology Reference Laboratory, University Hospital of South Manchester. Isolates of *S. apiospermum* were gifted from the Mycology Reference Laboratory, National Centre for Microbiology, Instituto de Salud Carlos III, Madrid, Spain. Isolates are detailed in Table 4.1.

Species	Isolate	Where obtained
P. boydii	7935	University Hospital, South Manchester
P. eliipsoidea	13144	University Hospital, South Manchester
S .apiospermum	8353	University Hospital, South Manchester
S. apiospermum	CNM-CM6322	Instituto de Salud Carlos III, Madrid, Spain.
S. apiospermum	CNM-CM6386	Instituto de Salud Carlos III, Madrid, Spain.

Table 4. 1 Isolates of *P.boydii*, *P.ellipsoidea* and *S. apiospermum* used for static and dynamic studies.

Culture

Isolates of *S. apiospermum* were stored at -80^{0}C using the Microbank ™ preservation system. Isolates were sub-cultured onto an oatmeal agar flask (Sigma-Aldrich, Poole, UK), at 30^{0}C, 10 days prior to each experiment.

Inoculum preparation

Conidial suspensions were prepared by flooding with 20 ml PBS whilst gently disturbing the surface of the growth using a sterile swab. The resulting suspension was then filtered through sterile gauze. Washing was performed twice by centrifuging the filtrate for 10 minutes at 2500 rpm and re suspending the pellet in 10ml PBS. EBM-2 was used for the preparation of the final inoculum. A conidial suspension of 1-2 x 10^6 was prepared using a haemocytometer and was confirmed by quantitative cultures on SAB-C.

4.212 Fusarium spp.

Isolates

All isolates of *F. solani* used for this thesis were gifted from the Mycology Reference Laboratory, National Centre for Microbiology, Instituto de Salud Carlos III, Madrid, Spain. Isolates are detailed in Table 4.2.

Species	Isolate
F. solani	CNM-CM6951
F. solani	CNM-CM7271
F. solani	CNM-CM7294
F. solani	CNM-CM7328

Table 4. 2 Isolates of *F.solani* used for static and dynamic studies.

Culture

Isolates of *F. solani* were stored at -80^{0}C using the Microbank ™ preservation system. Isolates were sub-cultured onto a SAB-C, at 30^{0}C, 10 days prior to each experiment.

Inoculum preparation

Conidial suspensions were prepared by flooding with 20 ml PBS whilst gently disturbing the surface of the growth using a sterile swab. The resulting suspension was then filtered through sterile gauze. Washing was performed twice by centrifuging the filtrate for 10 minutes at 3500 rpm and re suspending the pellet in 10 ml PBS.

EBM-2 was used for the preparation of the final inoculum. A conidial suspension of 1-2 x 10^6 was prepared using a haemocytometer and was confirmed by quantitative cultures on SAB-C.

4.22 Sequencing of organisms

The identification of *P.boydii* and *S. apiospermum* was done via sequencing of the internal transcribed spacer (ITS) and β-tubulin regions of the fungi. Isolates of *P. boydii* spp. and *S. apiospermum* detailed in chapter IV were sequenced in the PHE Mycology Reference Laboratory, Bristol. Extraction of fungal DNA was performed as follows. 20-40 Acid washed glass beads were suspended in 0.5 mL of sterile distilled water. 2 mm diameter Flinders Technology Associates (FTA) filters were cut from a Whatman FTA classic indicator card (Whatman International) using a sterile puncture and placed into 200 µL Ependorfs (where from). Organisms were grown on oatmeal agar for five days prior to isolation. Mycelium and spores were isolated from the colony by gentle abrasion with a sterile needle. Samples were then added to 1.5 mL Ependorfs containing beads and water. Samples were homogenised using a FastPrep-24 homogeniser for run twice for 30 seconds at 6.5 m/s. Sterile filters were then inoculated with 2 µL of homogenate from each sample for the extraction of DNA. Filters were left to dry for 10 minutes then washed twice with 100 µL sterile distilled water. For amplification, 700 µL of polymerase chain reaction (PCR) reaction mix was prepared and consisted of 70 µL buffer (QIAGEN, UK), 7 µL dNTPs (2.5mM), 70 µL forward primer, 70 µL reverse primers, 420 µL PCR grade H_2O, 3.5 µL HotstarTaq (QIAGEN, UK). PCR reaction mixture was then vortexed for 1 min. 100 µL of PCR reaction mixture was added to each PCR tube containing inoculated filter. PCR reaction conditions were as follows; 15mins 94^0C for one cycle, 40 cycles of 30 sec at 94^0C, 30 sec 50^0C, 90 sec 72^0C, one cycle of 7

mins at 72^{0}C, 4^{0}C for remainder. After the PCR cycle completed, 8 µL was transferred to a new PCR tube and 5 µL of the appropriate forward primer was added for sequencing of the ITS and β-tubulin regions. Sequencing of the amplicons was done by Beckman- Coulter Genomics Inc. Sequences were analysed for identification via the FUNCBS.txt database (http://www.cbs.knaw.nl/Collections/BioloMICSSequences.aspx).

4.23 *In vitro* susceptibility testing

Minimum inhibitory concentrations (MIC) for voriconazole (VRC) against *S. apiospermum* and *F. solani* isolates were determined in 5 independent experiments using both the European Committee for Antimicrobial Testing (EUCAST) and Clinical Laboratories Standards Institute (CLSI) methodologies. Concentrations for MIC testing ranged from 0.06 mg/L to 32 mg/L. The modal value, range and geometric mean were determined. The mode was used in the pharmacodynamic analyses for the determination of AUC:MIC values.

4.24 Static models of invasive scedosporiosis

4.241 Inoculum finding for P. boydii/ S. apiospermum

Cellular bilayers were constructed as described in Chapter II and grown up to confluency for five days in a 24-well plate. On the day of experiment, three sets of *P. boydii* 7935 inocula were harvested and adjusted to densities of $5x\ 10^4$, $2.2x\ 10^5$ and $1.5x\ 10^6$. Inocula were confirmed by quantitative culture after 48 hours incubation. Each row of Transwells were inoculated with a 100µL of each inoculum, yielding six replicates for each concentration of cells. Transwells were incubated at 37^0C, 5% $C0_2$ for 48 hours. Samples from the alveolar compartment were then taken by lavage with PBS and the endothelial media extracted. Samples were stored at -80^0C. Antigen detection was done at University of Exeter by Dr. Christopher Thornton, using the ELISA methodology described for *P. boydii/ S. apiospermum* in Chapter II without the use of goat anti-mouse biotin antibody.

4.242 Optimisation of inoculation period for P. boydii/ S. apiospermum static models

Cellular bilayers were constructed as described in Chapter II and grown up to confluency for five days in a 24-well plate. On the day of experiment, an inoculum of $1\text{-}2\ x\ 10^6$ was harvested from cultures and 100µL of inoculum was pipetted onto the alveolar layer of transwells. Inoculated transwells were incubated at 37^0C, 5% $C0_2$ for 6, 9, 12 and 15 hours post-inoculation. At these time-points the inoculum was removed and Transwells were incubated for a further 48 hours post-removal to monitor the invasion of the fungi. After 48 hours models were harvested to obtain alveolar and endothelial samples. Antigen detection was performed at the University of Exeter in collaboration with Dr. Christopher Thornton, using an ELISA methodology described

for *P. boydii/ S. apiospermum* in section 4.27 without the use of goat anti-mouse biotin antibody.

4.25 Dynamic Model of invasive scedosporiosis

4.251 Bioreactors and Construction

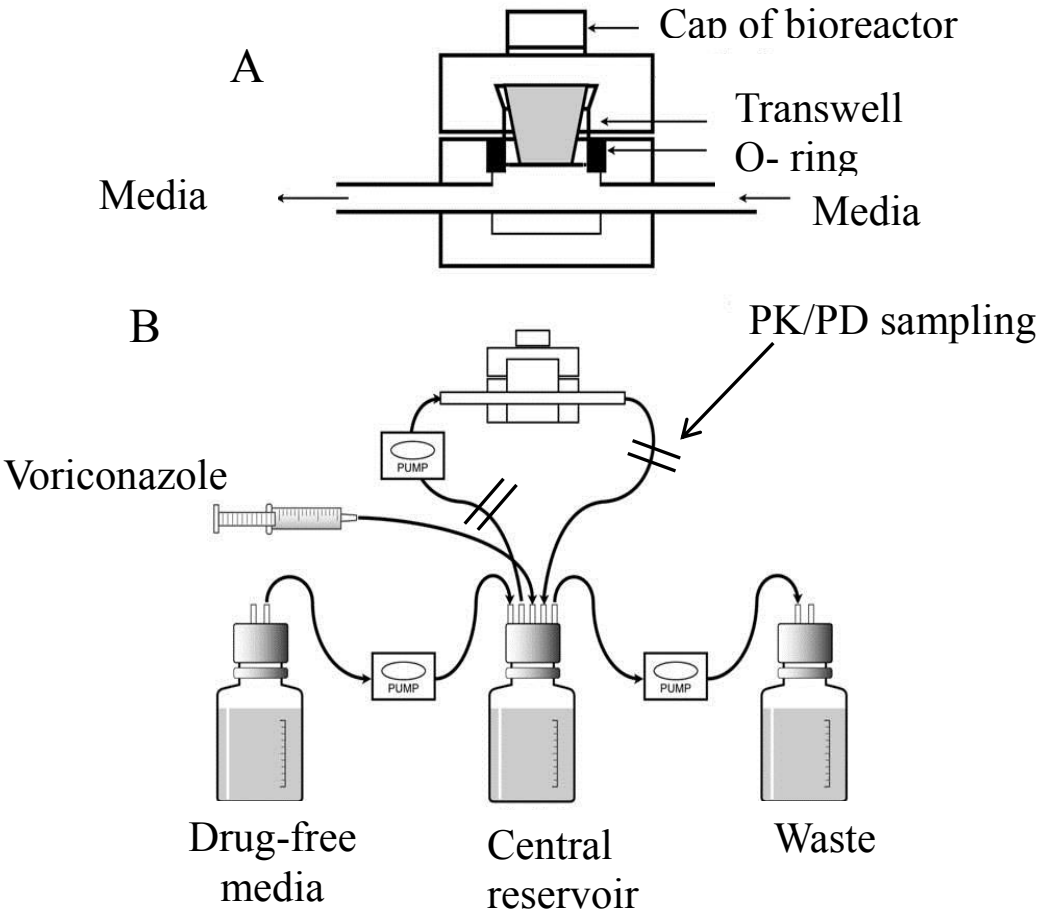

Figure 4. 1 Set-up of the dynamic *in vitro* model of the human alveolus specific for voriconazole against *Scedosporium apiospermum.*

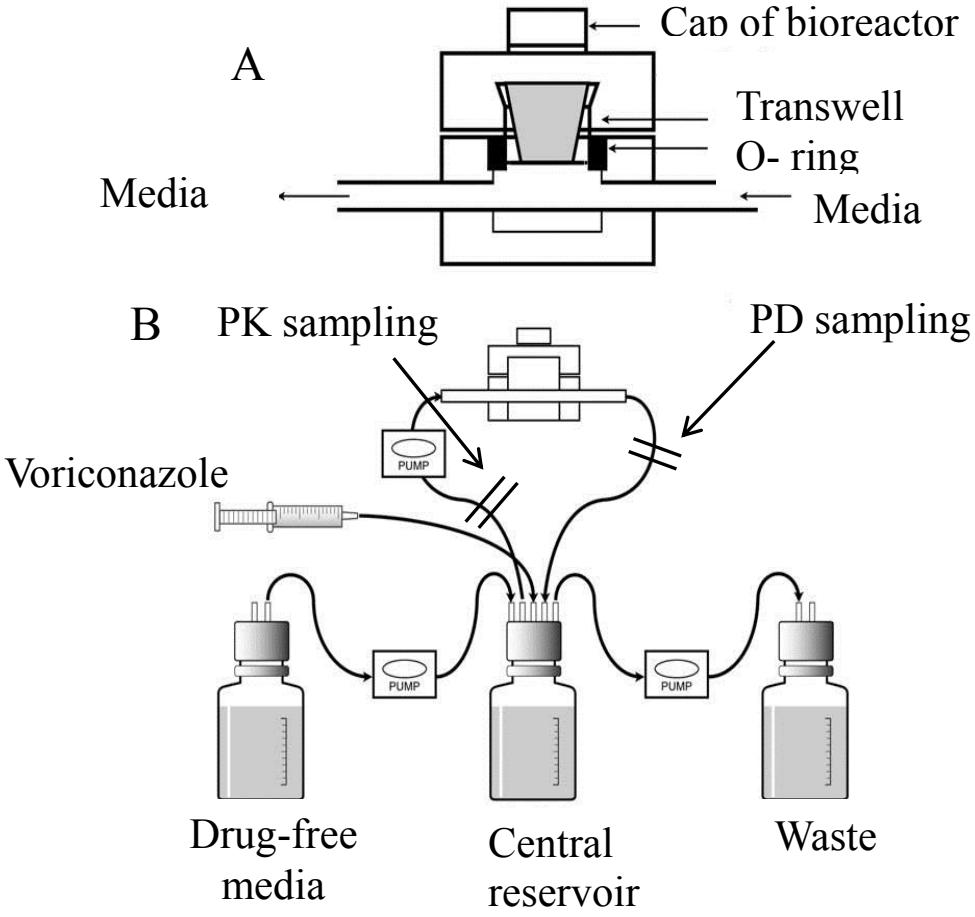

Figure 4. 2 Set-up of the dynamic *in vitro* model of the human alveolus specific for voriconazole against *Fusarium solani.*

4.252 Treatment with Voriconazole and sampling

Voriconazole pure powder was dissolved in DMSO. Dilutions were prepared from known stock concentrations in DMSO in order to achieve the required concentrations for each dynamic system. Each regimen was administered directly into the central compartment as a 100µL bolus. Dosages were selected from previously published data demonstrating the achievement of voriconazole exposures that ranged from sub-optimal to successful in treating organisms of similar susceptibilities in this model (Jeans, Howard et al. 2012). Dosages of 0mg, 0.1mg, 0.2mg, 1mg and 3mg were administered every 12 hours to the central compartments. The pump connected to the fresh media and the waste Durans for the clearance of drug was run at a speed of 1.9 rpm proportional to a flow rate of 10 mL/hour. This was demonstrated previously to generate human-like concentration- time profiles for voriconazole, as described by Jeans et al. (Jeans, Howard et al. 2012).

For each experiment the PK and PD of voriconazole against each isolate of *S. apiospermum* and *F. solani* were determined in four individual circuits. Each circuit was treated with a different dosage of drug. A fifth untreated circuit was used as a control. Four different dosages were used for each drug. Drugs were administered twice-daily. Sampling regimens for both pharmacokinetics and pharmacodynamics profiles were optimised using data generated from control circuits (PK alone and PD alone). Samples for PK and PD were taken up to 96 hours post treatment. After sampling, media taken out of the system was replaced with an equal volume of complete DMEM.

4.26 Mass Spectrometry

Mass spectrometry for pharmacokinetic analysis was performed by Joanne Goodwin and Sarah Whalley at the University of Liverpool.

Voriconazole concentrations were determined using a UHPLC/MS-MS triple-quadrupole 6420 mass spectrometer, (Agilent Technologies, Santa Clara, CA, USA). Instrument parameters were optimized for voriconazole (350.0 → 224.0 m/z). Voriconazole was extracted from DMEM media using acetonitrile and methanol (Fisher Scientific, Loughborough, UK) with IS.

HPLC separation was achieved using a Zorbax Eclipse Plus Rapid 1.8 µm C18 50 x 2.1 mm (Agilent Technologies, Santa Clara, CA, USA) column. The mobile phase consisted of 0.2% formic acid in water and 0.2% formic acid in acetonitrile at a flow rate of 0.5 ml/min for F90318 and 0.1% formic acid in water and 0.1% formic acid in acetonitrile at a flow rate of 0.5 ml/min. The column was maintained at 40 °C. Phenacetin (Sigma-Aldrich, Poole, UK) 100 ng/mL in acetonitrile was used as internal standard for voriconazole. The chromatographic run time for one sample was 3 minutes. The lower limit of quantitation of voriconazole was 0.0025 mg/L. Intraday and interday coefficients of variation were <8.4% at concentrations ranging from 0.0025 to 20 mg/L.

4.27 Enzyme linked immunosorbent assays

4.271 P. boydii and Scedosporium spp.

MAbs were developed and cultured as described by Thornton et al. (2009). 50 µL volumes of HG12 antibody prepared as previously described (Thornton 2009) were used to coat the surface of the wells of Maxisorp microtiter plates (Fisher Scientific, Loughborough, UK). After incubation at 4^0C overnight microtiter plates were washed

four times with PBS containing 0.05% (v/v) Tween20 (PBST). Plates were then washed once with PBS and once with distilled water then left to dry by air in a drying cabinet at 23^0C for 1 hour. Wells were incubated at 23^0C for 10 minutes with 100µL of PBS containing 1% (w/v) bovine serum albumin (BSA) to prevent non-specific protein binding. All following incubations were performed using 50 µL volumes. Wells containing samples were incubated for 2 hours, followed by a 1 hour incubation with goat anti-mouse biotin antibody (IgM µ chain specific) (Sigma Aldrich, Poole, UK) diluted 1 in 1000 in PBST containing 0.5% (w/v) BSA. A further 1 hr incubation with goat anti-mouse polyvalent (IgG, IgA, and IgM) peroxidase conjugate (Sigma-Aldrich, Poole, UK) diluted 1 in 1000 in PBST containing 0.5% (w/v) BSA was then performed. Bound antibody was visualized by incubating wells with tetramethyl benzidine (TMB) substrate solution (Sigma- Aldrich, Poole, UK) for 30 minutes. Reactions were stopped by the addition of 3M H_2SO_4. Absorbance values were determined using a spectrophotometer at 450 nm. Wells were given three 5 minute rinses with PBST between incubations. Control wells were incubated with tissue culture medium (EBM-2) containing 10% (vol/vol) FBS. All incubation steps were performed at 23°C in sealed plastic bags. The threshold for detection of antigen in ELISA was determined previously from control means (2 TCM absorbance values) (Thornton 2001, Thornton 2009). These values were consistently in the range of 0.050 to 0.100. Consequently, absorbance values of >0.100 were considered positive for the detection of antigen.

4.272 Fusarium spp.

MAbs were developed and cultured as described by Thornton et al. (2001). 50 µL volumes of antigen contraining samples were used to coat the surface of the wells of Maxisorp microtiter plates and incubated at 4^0C overnight. Microtiter plates were then

washed four times with PBST. Plates were then washed once with PBS and once with distilled water then left to dry by air in a drying cabinet at 23^0C for 1 hour. Wells were incubated at 23^0C for 10 minutes with 100µL of PBS containing 1% (w/v) BSA to prevent non-specific protein binding. All following incubations were performed using 50µL volumes. A 1 hour incubation with Anti-Mouse Polyvalent Immunoglobulins (G,A,M)−Peroxidase solution (Sigma Aldrich, Poole, UK) diluted 1 in 1000 in PBST was then performed. Bound antibody was visualized by incubating wells with TMB substrate solution for 30 minutes. Reactions were stopped by the addition of 3M H_2SO_4. Absorbance values were determined using a spectrophotometer at 450 nm. Wells were given three 5 minute rinses with PBST between incubations. Control wells were incubated with tissue culture medium (EBM-2) containing 10% (vol/vol) FBS. All incubation steps were performed at 23°C in sealed plastic bags.

4.28 Histology

Cell culture inserts were transferred to a 12 well plate containing 1.5 mL per well of EBM-2 media supplemented with 2% FBS. A conidial suspension of 4-8 x 10^5 was prepared as described earlier and warmed to 37^0C for 20 minutes. 400 µL of conidial suspension was then pipetted into the top compartment of each cell culture insert. Cell culture inserts were serially sacrificed in triplicate until 84 hours post inoculation. Samples from the endothelial compartment were taken and stored at -80^0C for PK and PD analysis. Membranes/inserts/bilayers were formalin-fixed, routinely processed, trimmed, and embedded in paraffin. Care was taken to ensure appropriate tissue orientation for evaluation of cross-sectional and endothelial surfaces. Approximately 5 µm thick, serial sections were cut, mounted on glass slides and stained with Grocott

methenamine silver stain (Newcomer Supply, Middleton, WI) at Charles River Laboratories, Pathology Associates Division, Frederick, MD. All slides were evaluated microscopically by a board-certified anatomic veterinary pathologist (J. Schwartz). Slides were digitally scanned at 40 x and 400 x magnification using an Aperio ScanScope CS (Leica Biosystems) and images captured using Spectrum 10.1.5.2029 software (Leica Biosystems). High magnification cross-section images were acquired using an Olympus BH-2 microscope.

4.25 Mathematical Modelling

A population methodology was used throughout. Version 1.2.9 of the population PK- PD program Pmetrics was used for all fitting. For the estimation of pharmacokinetic polynomial error, the intercept and slope values from a polynomial equation derived using trough, median and C_{max} values from circuits treated with 3mg dosages were used. A one compartmental model was used in order to represent the experimentally simulated bloodstream infection and its subsequent treatment with voriconazole. For pharmacodynamic datasets, data were normalised to a maxima of 1 due to variability in maximum absorbance obtained in control circuits between isolates. Initially a Tlag was used to account for the delayed observation of C_{max} in the model. However, as voriconazole is also given as an oral formulation the delayed C_{max} may be better described using an absorption parameter to represent oral dosing of the drug. Therefore, a parameter to define absorption (Ka) was used to improve the fit of the model as used by Hope et al. in a previous model of orally dosed voriconazole (Hope, VanGuilder et al. 2013). Initial conditions for pharmacodynamic data were set to describe PD values obtained at T_0 due to background noise from the assay. The structural mathematical model consisted of the following two inhomogeneous ordinary differential equations:

$dX1/dt=B(1)-(SCL/Vc)*X1$ Equation 1

$dN/dt=Kgmax*(1-(N/POPMAX))*N$ Equation 2a

$*(1-(X1/Vc)^{Hg}/(X1/Vc)^{Hg}+C50^{Hg}))$ Equation 2b

Where: B(1) is the bolus input of is the bolus input of VRC, SCL is the clearance of drug from the circuit, Vc is the volume of the circuit, N is the antigen concentration, Kgmax is the maximal rate of growth; POPMAX is the theoretical maximal density within the circuit; Hg is the slope function for the suppression of growth; and, C50 is the concentration of drug in the circuit where there is half-maximal suppression of growth.

Equation 1 describes the rate of change of drug concentrations in the circuit. Equation 2 describes the rate of change of antigen in the circuit and contains terms that describe fungal growth in the absence of drug (Equation 2a) and the drug induced suppression of growth (Equation 2b).

The model was fitted to the dataset of untreated and treated circuits obtained from each isolate. Each circuit was treated as an "individual". The fit of the model was assessed using the coefficient of determination (r^2) from a linear regression of the observed vs. predicted plots for both population and individual predictions, the mean and median values of parameters predicted by the model compared to those observed experimentally and the log likelihood. The Bayesian posterior estimates for each of the parameters in the model were then used to define the concentration-time profile of voriconazole and the resultant effect on antigen concentrations. As the AUC:MIC has been shown to be the pharmacodynamic indices best associated with maximal antifungal effect (REF), parameter estimates were used to estimate the AUC that developed in each circuit and consequently the AUC:MIC ratio.

4.3 RESULTS

4.31 Minimum Inhibitory Concentrations

The minimum inhibitory concentrations (mode, range and geometric mean) for voriconazole against isolates of *S. apiospermum*, *P. boydii* and *F. solani* are summarised in Table 4.3.

			EUCAST			CLSI		
Drug	**Species**	**Isolate**	**Mode**	**Range**	**Mean**	**Mode**	**Range**	**Mean**
Voriconazole	***S. apiospermum***	**8353**	**0.5**	**0.5-1**	**0.57**	**0.25**	**0.25-0.25**	**0.25**
Voriconazole	***S. apiospermum***	**6322**	**1**	**1-1**	**1**	**0.25**	**0.25-0.25**	**0.25**
Voriconazole	***S. apiospermum***	**6386**	**1**	**0.5-1**	**0.71**	**0.5**	**0.25-0.5**	**0.44**
Voriconazole	***P. boydii***	**7935**	**0.5**	**0.5-0.5**	**0.5**	**2**	**2-8**	**3.48**
Voriconazole	***P. ellipsoidea***	**13144**	**8**	**8-8**	**8**	**4**	**0.5-4**	**1.74**
Voriconazole	***F. solani***	**CNM-6951**	**16**	**8-16**	**12.12**	**4**	**2-4**	**3.03**
Voriconazole	***F. solani***	**CNM-7328**	**16**	**8-32**	**16**	**16**	**8-16**	**10.56**

Table 4. 3

Minimum inhibitory concentrations were determined in 5 independent experiments. Means displayed above are geometric means.

4.32 *Pseudallescheria boydii- Scedosporium apiospermum* models

4.321 Growth and inocula investigation

Preliminary experiments using *P. boydii* 7935 demonstrated that an inoculum of 1-2x 10^6 and an initial incubation period of 12 hours preceding a 48 hour model post- removal of inoculum yielded the highest absorbance values using ELISA methodology for the detection of antigen in both alveolar and endothelial samples (Figures 4.3 and 4.4). These conditions were therefore used for subsequent experiments using drug. The maximum absorbance value obtained from these preliminary finding experiments was approximately 0.17. Therefore, for further analysis of pharmacodynamic samples the use of a goat anti-mouse biotin antibody (IgM µ chain specific) (Sigma Aldrich, Poole, UK) was incorporated into the ELISA methodology for the amplification of signal and improvement of dynamic range.

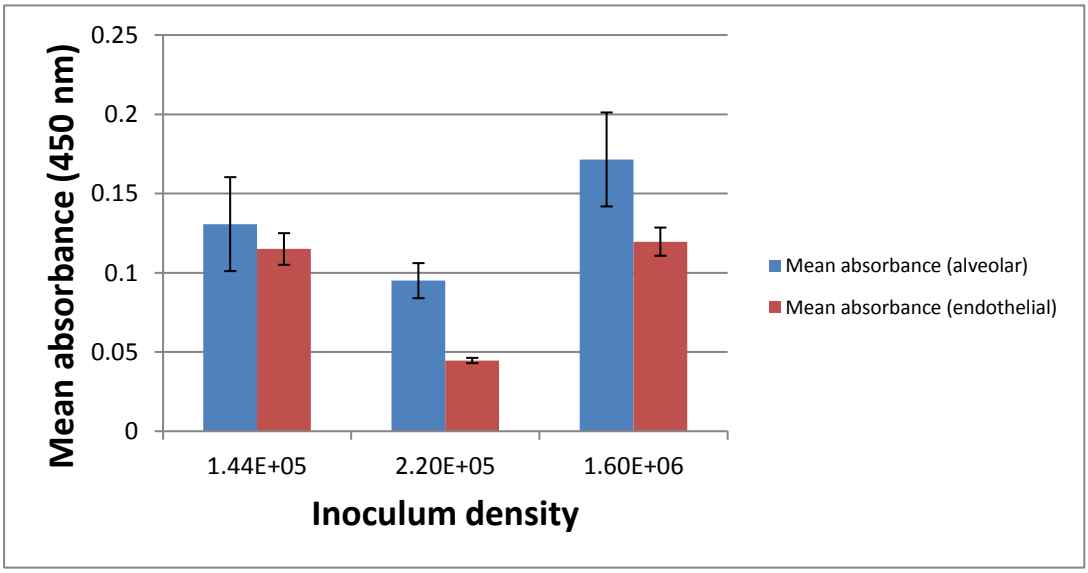

Figure 4. 3

Mean absorbance values from static models to determine optimal inoculcum density of of *P. boydii* for invasion through the cellular bilayer and detection of antigen. All samples were obtained after 48 hours post-removal of inocula. Data presented are the mean absorbance values obtained from six transwells. Error bars represent the standard deviations between transwells for each time-point.

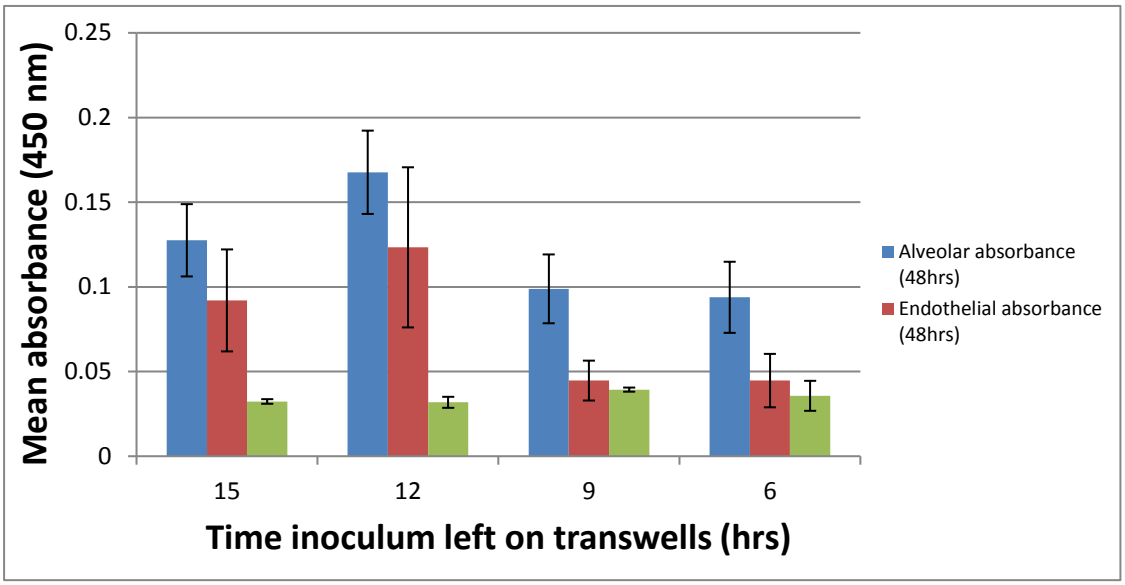

Figure 4. 4

Mean absorbance values from static models to determine optimum time for conidial germination of *P. boydii* 7935. Data presented are the mean absorption of six transwells. Error bars represent the standard deviations between transwells for each time-point.

4.322 In vitro Histopathology model

Germination and invasion of *S. apiospermum* conidia through the cellular bilayer was observed over 84 hours as seen in Figure 4.5 and 4.6. Antigen levels increased over time to a maximum absorbance of approximately 1.5 (absorbance at 450nm). There was little variation in antigen detection between experiments at the same time-point, with relatively low standard deviation values between cellular models (0.0006-0.12) (Figure 4.5). After 12 hours the conidia had begun to germinate into hyphae, invade through the cell layers and were able to colonise the endothelial layer (Figure 4.6). By 72 hours post inoculation complete invasion, biofilm development and destruction of the cell layers were observed (Figure 4.6).

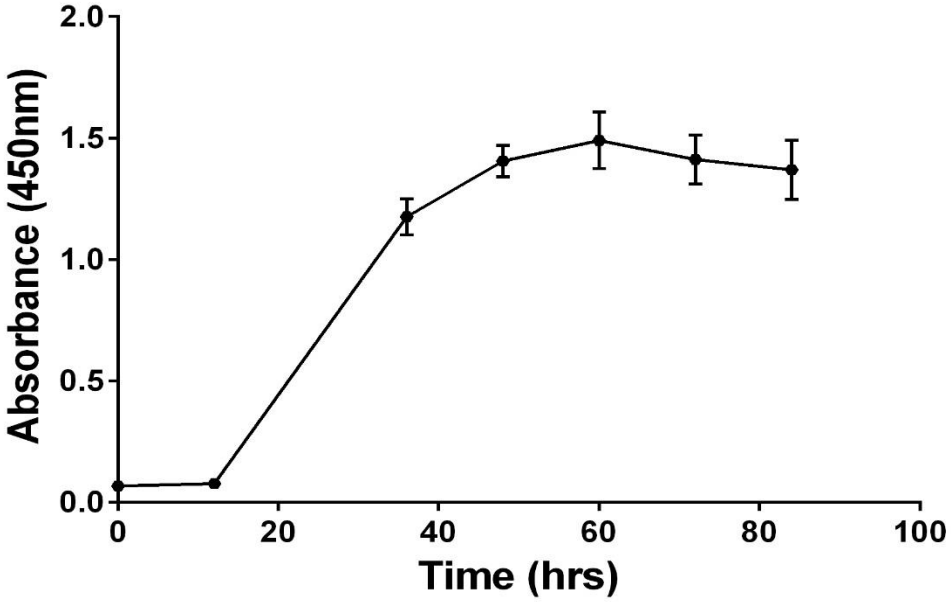

Figure 4. 5

Detection of antigen in the endothelial compartment of transwells infected with *S. apiospermum* isolate 8353 over 84 hours measured using HG12 and GA3 antibodies. Error bars represent the standard deviation between triplicate samples for each time-point.

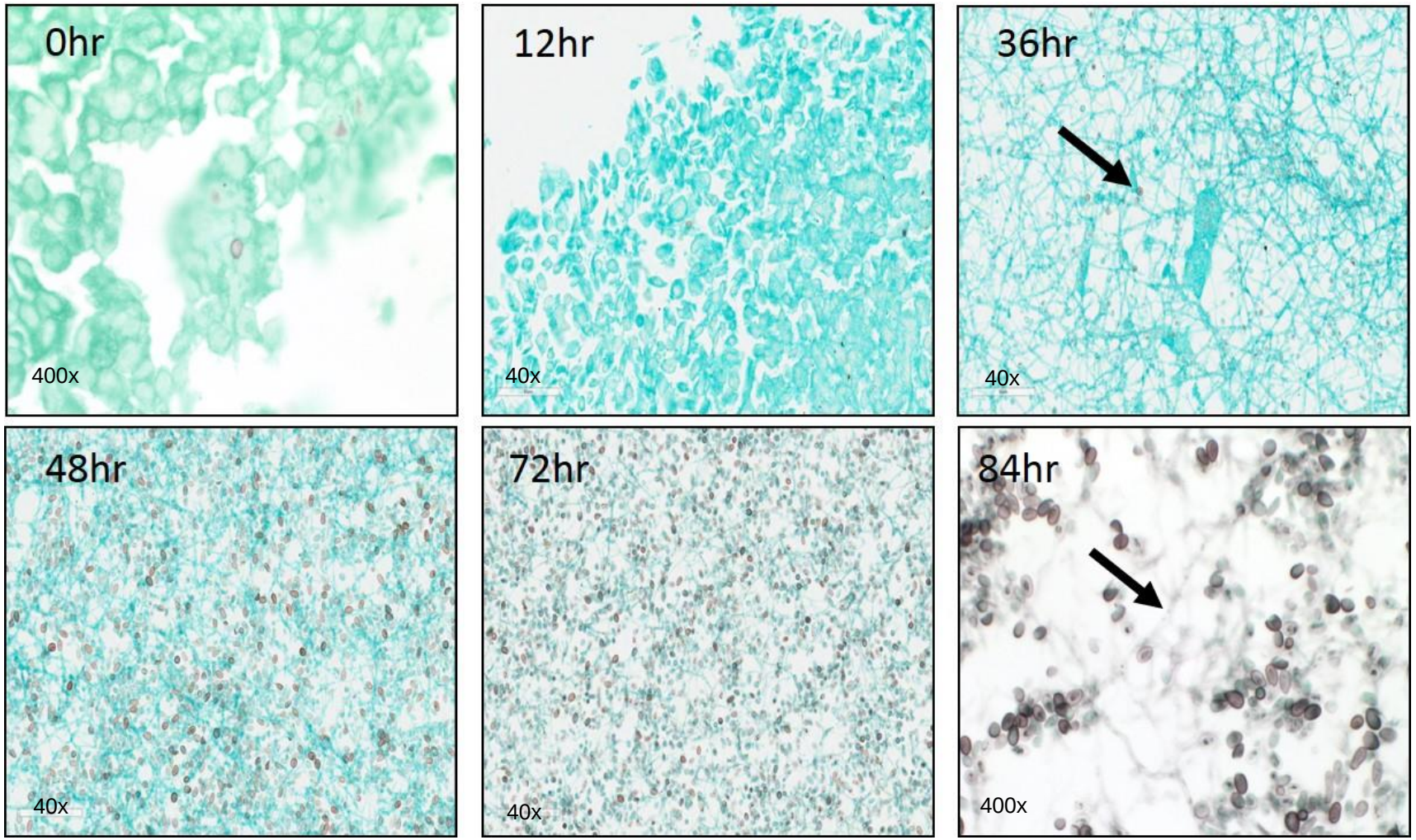

Figure 4. 6 Histopathology of the growth and biofilm development of *S. apiospermum* on the endothelial side of the cellular bilayer over 84 hours.

Arrows point to S. apiospermum conidia (36hr) and hyphae (84hr) on the endothelial cell layer.

4.333 Static models of the human alveolus

The exposure-response relationships for voriconazole are described in Figure 4.7. Antigen detection was consistent for samples obtained from untreated controls in static models. Variability between antigen levels measured in samples exposed to the same concentration of drug was apparent in those obtained from the alveolar compartment. A maximum absorbance value of approximately 1 -1.5 for isolates of *S. apiospermum*, *P.boydii* and *P. ellipsoidea* were achieved as opposed to 0.17 in growth experiments suggesting the use of biotin antibody successfully boosts the range of this ELISA. Voriconazole concentrations of approximately 8 mg/L, 4 mg/L and 2 mg/L were sufficient for maximal suppression of antigen release for *S. apiospermum* isolates 8353, 6322 and 6386 respectively. For isolates of *P.boydii* and *P. ellipsoidea* concentrations of approximately 4 mg/L and 1 mg/L were sufficient for the maximal suppression of growth.

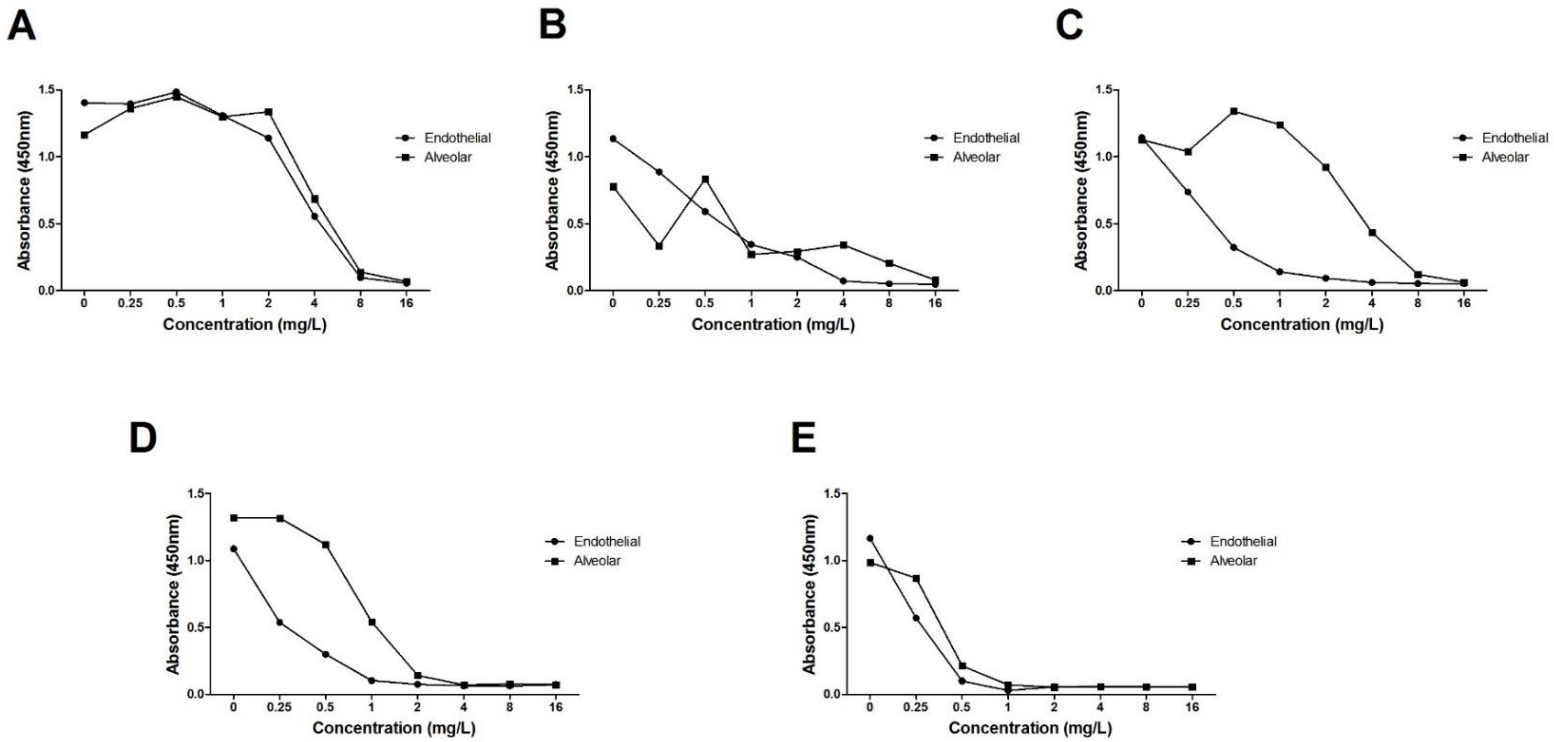

Figure 4. 7

Pharmacokinetics and pharmacodynamics of voriconazole in a static model against *S. apiospermum* isolates (A) 8353, (B) 6322, (C) 6386, *P. boydii* 7935(D) and *P. ellipsoidea* 13144 (E).

5.333 Dynamic models of the human alveolus

Human like concentration-time profiles for VRC were generated using a twice-daily dosing regimen in this model (Table 4.4, Figures 4.8-4.10). Clinically relevant exposures were achieved within the circuits (Table 4.5) however there was a delay in the detection of maximal concentrations within the system of 2-4 hours post dose. This was due to PK sampling after the bioreactor as opposed to straight out of the central compartment. For all isolates there were dose response relationships using a twice-daily dosing regimen. Model- predicted $AUC_{72\text{-}96}$ values of 66.6, 65.5 and 64.5 mg.hr/L for isolates 8353, 6322 and 6386 respectively, were associated with maximal suppression of antigen, using a minimum threshold absorbance of 0.1 measured at 450nm. Subsequently, $AUC_{72\text{-}96}$: MIC ratios calculated using EUCAST methodology generated MIC values that were associated with maximum effect were 133.3, 65.5 and 64.5 for isolates 8353, 6322 and 6386 respectively. The antigen was detected consistently under the flow and clearance conditions set by the model. The kinetics of antigen expression in the untreated circuits was different between isolates. Antigen concentrations for isolates 8353 and 6386 began to increase at around 60-72 hours post-inoculation. Isolate 6322 was slightly slower growing and may be less virulent as antigen levels only began to increase at 84-96 hours post- inoculation.

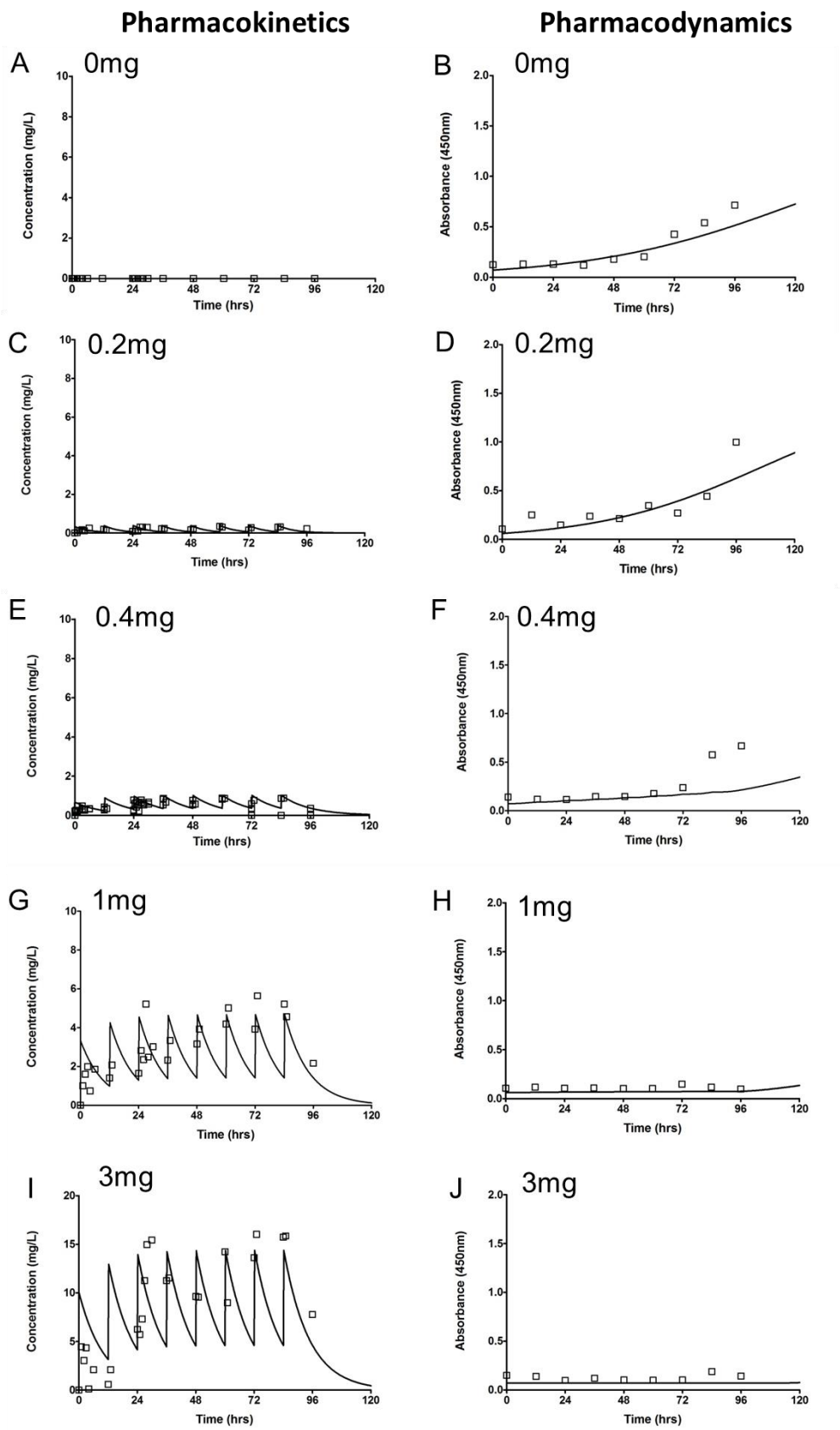

Figure 4. 8 Pharmacokinetics and pharmacodynamics of voriconazole against *S. apiospermum* isolate 8353.

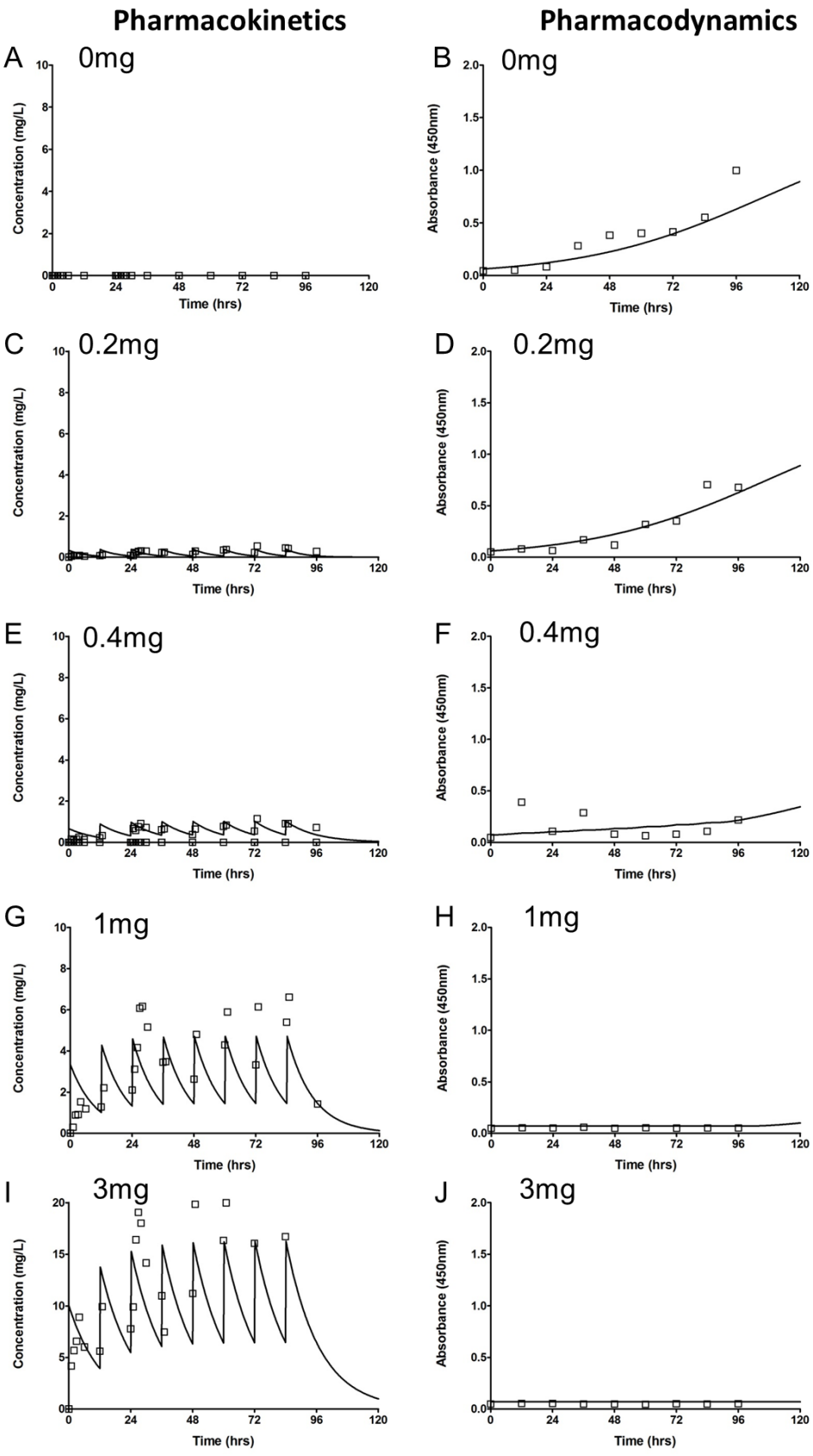

Figure 4. 9 Pharmacokinetics and pharmacodynamics of voriconazole against *S. apiospermum* isolate 6322.

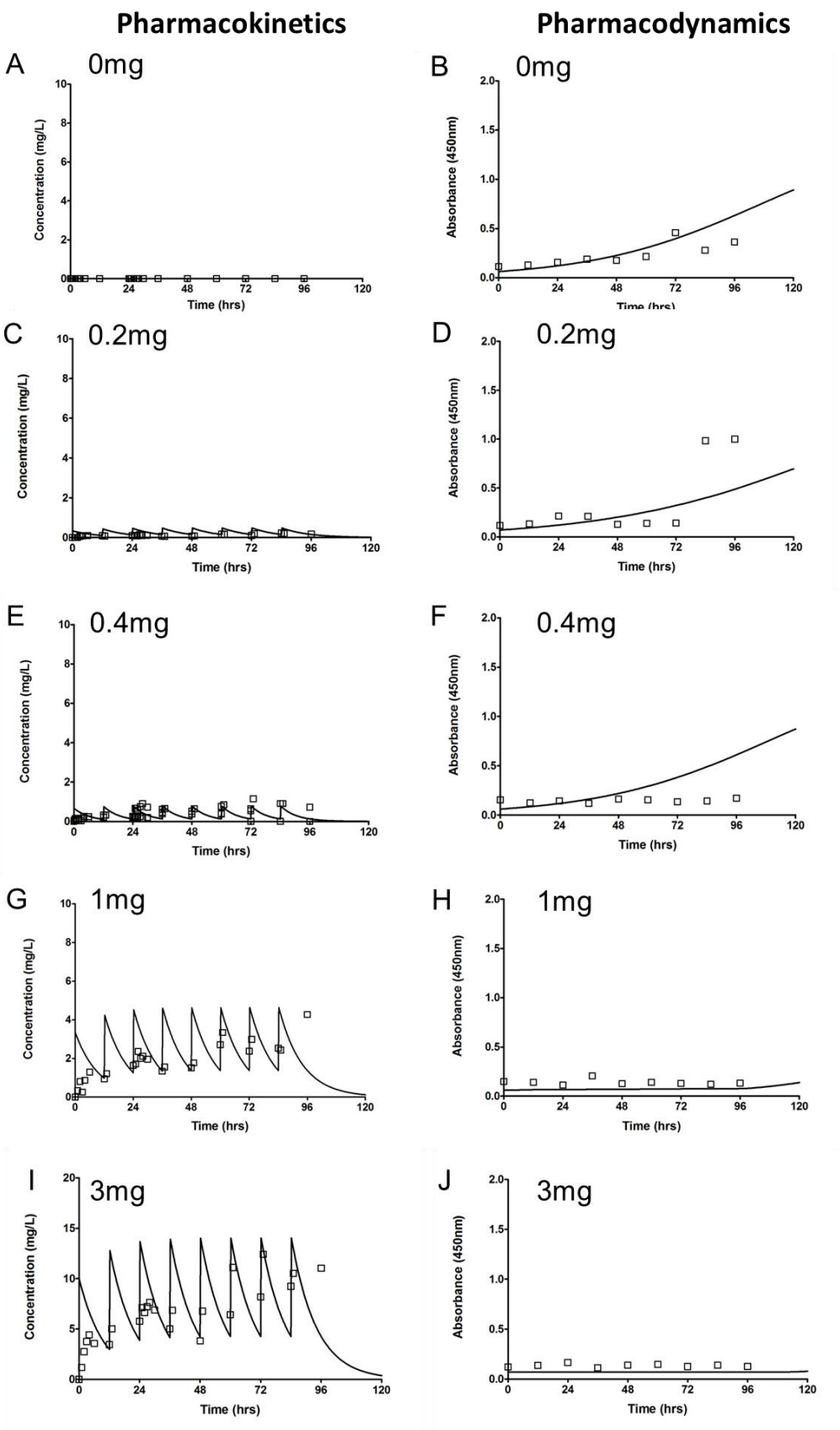

Figure 4. 10 Pharmacokinetics and pharmacodynamics of voriconazole against *S. apiospermum* isolate 6386.

4.334 Mathematical Modelling

The fit of the mathematical models to the data were acceptable. Bayesian R^2 values were 0.715 and 0.73 for pharmacokinetic and pharmacodynamic data respectively (Figure 4.11). The use of Ka as a parameter improved the fit of the model. Despite this, the delay in C_{max} levels due to the late sampling point in the system reduced the r^2. The fits of the Bayesian posterior estimates for each circuit is shown in Figures 4.8-4.10. The posterior median parameter values can be seen in Table 4.4. Predicted $AUC_{72\text{-}96}$ values (mg.hr/L) for voriconazole and total AUC for the antigen are displayed in Table 4.5.

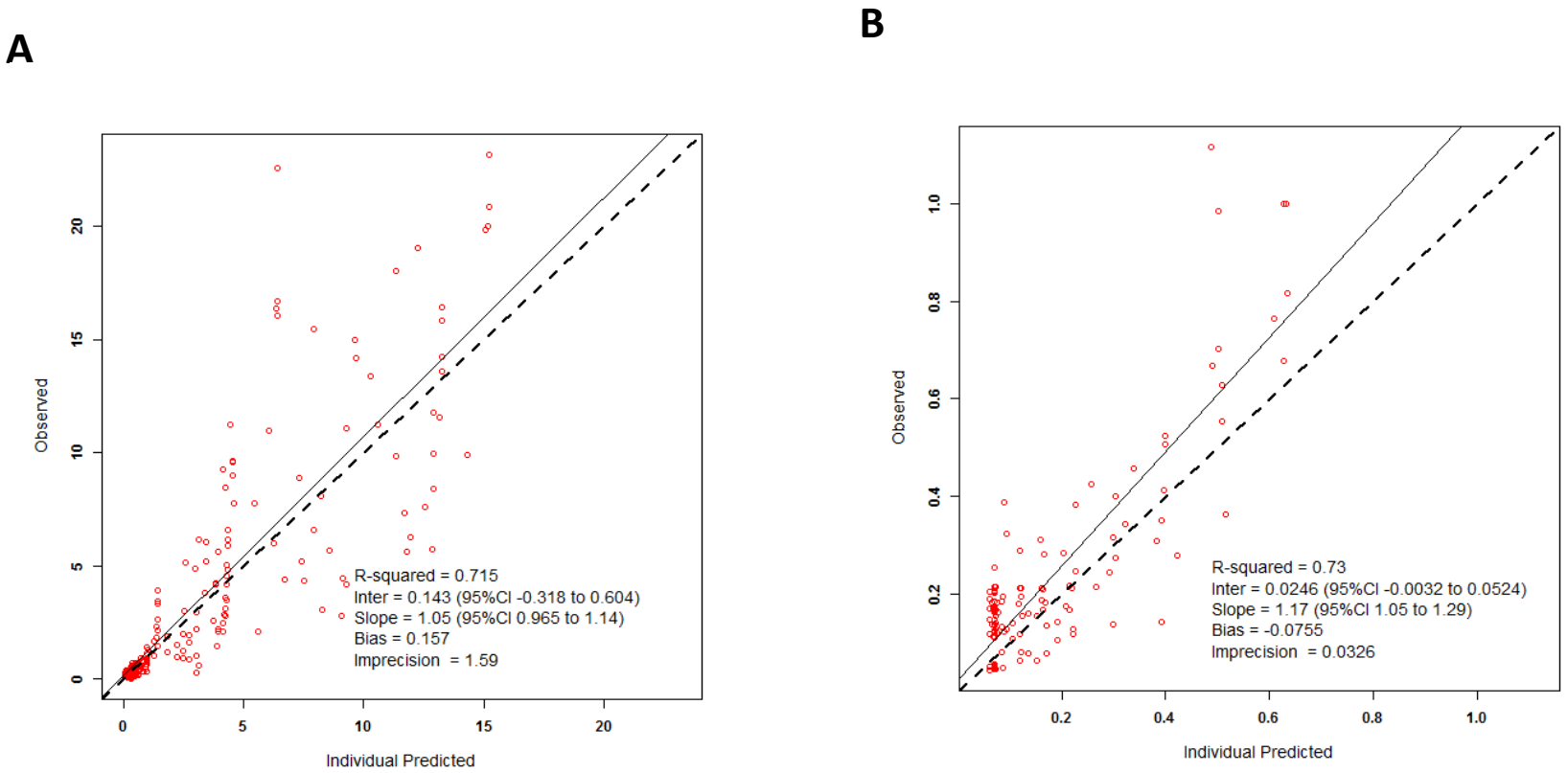

Figure 4. 11

Observed vs predicted graphs after the Bayesian step, generated using Pmetrics for (A) pharmacokinetics data from 15 individual circuits and (B) pharmacodynamics data as measured by antigen from 15 individual circuits.

Isolate	Dose	Ka	Cl	V	Kgmax	POPMAX	C50	Hg	IC1
8353	0	0.90	0.04	0.30	0.03	1.49	1.13	4.84	0.061
8353	0.1	0.88	0.05	0.30	0.03	1.49	1.14	4.83	0.061
8353	0.2	4.03	0.03	0.30	0.02	1.49	0.58	6.03	0.07
8353	1	4.01	0.03	0.30	0.02	1.49	0.59	6.00	0.07
8353	3	4.01	0.02	0.30	0.02	1.49	0.59	6.00	0.07
6322	0	4.01	0.03	0.30	0.02	1.49	0.59	6.00	0.07
6322	0.1	0.88	0.05	0.30	0.03	1.49	1.14	4.83	0.06
6322	0.2	4.03	0.03	0.30	0.02	1.49	0.58	6.03	0.07
6322	1	2.55	0.03	0.30	0.03	1.49	1.13	4.85	0.06
6322	3	4.02	0.03	0.30	0.02	1.49	0.58	6.01	0.07
6386	0	2.54	0.03	0.30	0.03	1.49	1.13	4.85	0.06
6386	0.1	4.02	0.03	0.30	0.02	1.49	0.58	6.01	0.07
6386	0.2	0.88	0.05	0.30	0.03	1.49	1.14	4.83	0.06
6386	1	2.53	0.03	0.30	0.03	1.49	1.13	4.85	0.06
6386	3	4.01	0.03	0.30	0.02	1.49	0.59	6.00	0.07

Table 4. 4

The median posterior parameter estimates from the mathematical model using data from 15 individual circuits. Ka is a description of absorption and describes the estimated time taken for C_{max} concentrations to be reached at the sampling point in the circuit. Cl represents the estimated clearance of VRC from the ciruit; V; the estimated volume of the central compartment; Kgmax, the predicted rate of growth of *S. apiospermum* in the circuit; POPMAX, the maxima obtained from the ELISA assay; C50, the concentration of voriconazole that 50% suppression of antigen is obtained; Hg, the slope function to describe *S. apiospermum* growth in both absence and presence of drug; IC1, the initial conditions for the pharmacodynamic dataset, representing background noise of the assay.

Strain	Dose (mg/ q12)	Predicted AUC_{72-96} voriconazole (mg.hr/L)	Predicted AUC_{0-96} antigen
S. apiospermum 8353	0	0	25.70
	0.1	4.39	25.48
	0.2	15.42	12.98
	1	66.64	6.79
	3	254.91	6.78
S. apiospermum 6322	0	0	22.72
	0.1	4.38	25.48
	0.2	15.42	12.98
	1	65.55	6.69
	3	206.27	6.81
S. apiospermum 6386	0	0	25.76
	0.1	6.95	21.92
	0.2	8.71	24.89
	1	64.46	6.73
	3	197.12	6.78

Table 4. 5

Model predicted voriconazole AUC_{72-96} and antigen AUC_{0-96} for isolates of *S. apiospermum* for individual circuits achieved using the dynamic model.

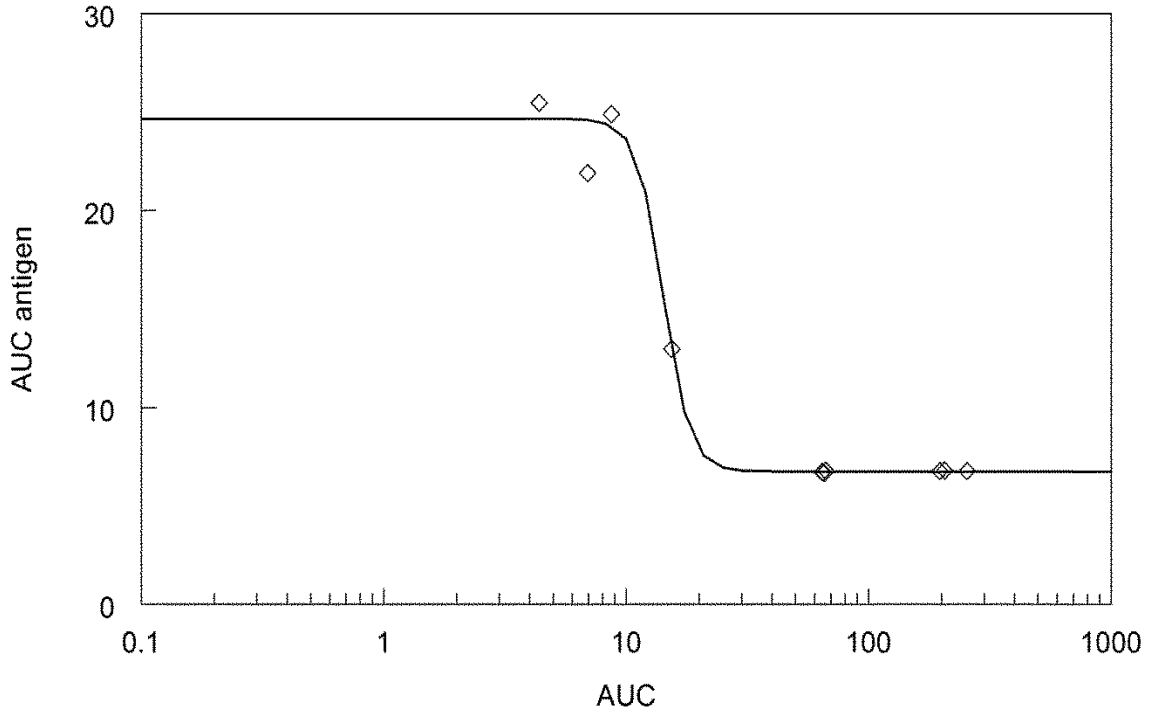

Figure 4. 12

Total AUC for *Scedosporium* specific antigen detected at 450nm, versus $AUC_{72\text{-}96}$ for voriconazole (mg.hr/L). Equations were generated in ADAPT 5 using the maximum likelihood estimator.

AUCantigen= 24.67-(17.92*(AUC)^7.9)/((AUC)^7.9+14.23^7.9).

R^2= 0.986.

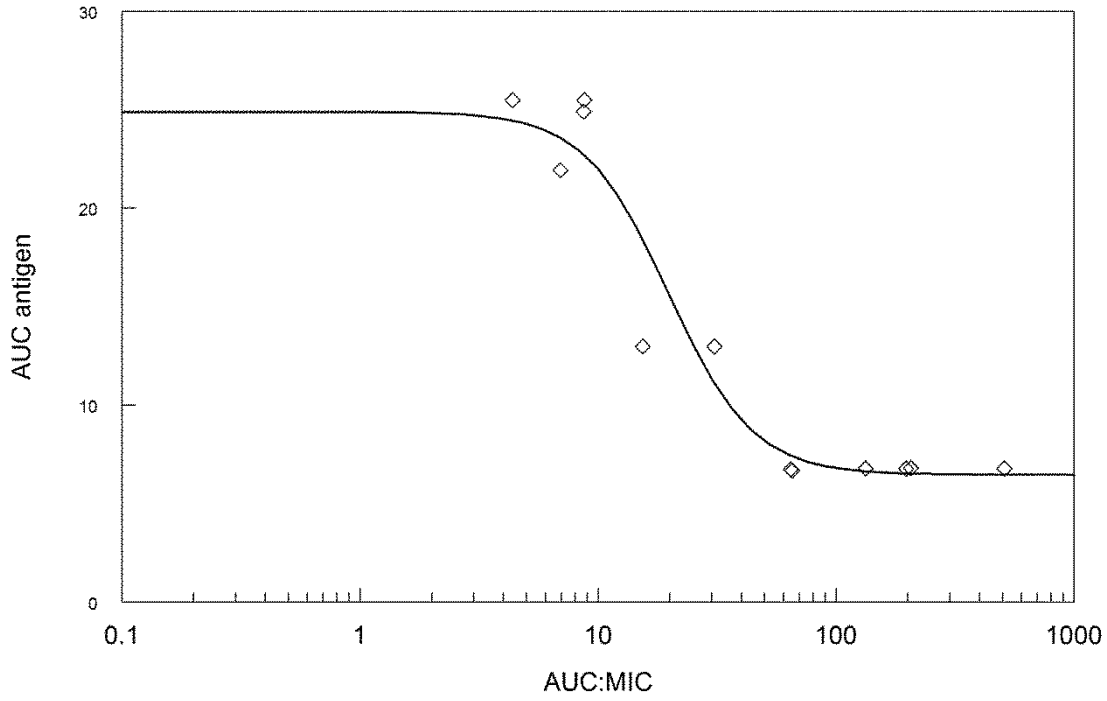

Figure 4. 13

Total AUC for *Scedosporium* specific antigen detected at 450nm, versus $AUC_{72\text{-}96}$: MIC (EUCAST methodology). Equations were generated in ADAPT 5 using the maximum likelihood estimator.

AUCantigen = 24.89-(18.42*(AUC)^2.455)/((AUC)^2.455+19.77^2.455)

R^2= 0.986

5.34 *Fusarium solani* models

5.341 Static models of the human alveolus

The exposure-response relationships for voriconazole are described in Figure 4.14 (A & B). Antigen detection was consistent for samples obtained from the model and seemed to be in proportion to fungal burden seen by eye. Maximum absorbance values of approximately 1 - 1.5 measured at 450nm were obtained for untreated inserts infected with isolates of *F. solani*. Voriconazole concentrations of approximately 8 mg/L were sufficient for maximal suppression of antigen release for isolate 7328. For isolate 6951, antigen was not sufficiently suppressed even at the highest concentration of 16 mg/L.

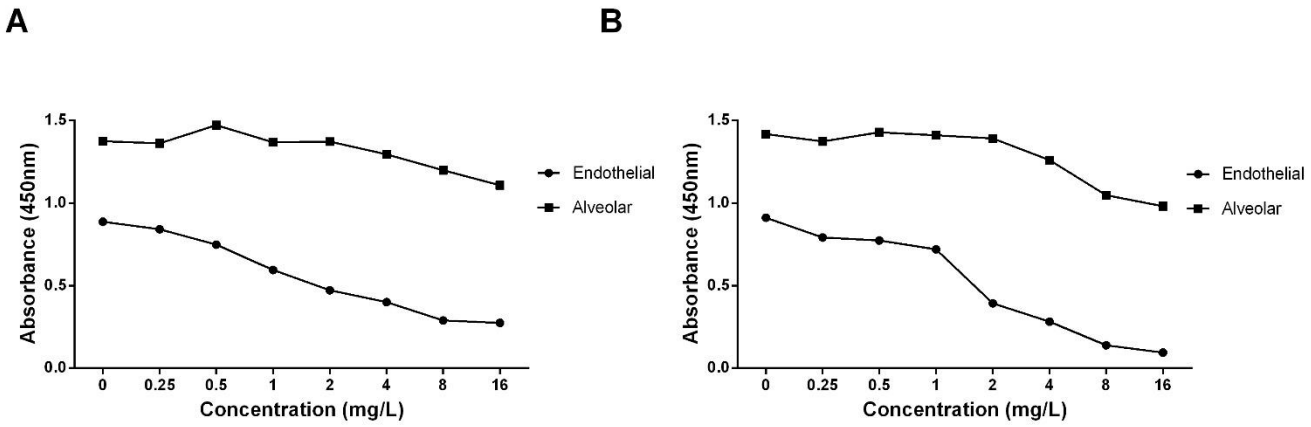

Figure 4. 14 Pharmacokinetics and pharmacodynamics of voriconazole in a static model against *F. solani* isolates.

CNM-6951 (A) and CNM-7328 (B).

5.342 Dynamic models of the human alveolus

The exposure-response relationships for voriconazole against *F. solani* were similar for both isolates studied (Figures 4.15-4.16). Sampling for PK was taken before the bioreactor and C_{max} levels of drug were detected within an hour of dosing in these experiments. Trough concentrations of approximately 1.5 mg/Lwere sufficient in suppressing the release of antigen for all isolate using a cut off value of 0.1. These concentrations are proportional to the MICs obtained for voriconazole against these isolates. Model- predicted AUC_{24-48} values of 64.9- and 85.2 mg.hr/L corresponding to AUC_{24-48}; MIC ratios of 4 and 5 were associated with minimal detection of antigen using a cut-off absorbance value at 450nm of 0.1 for isolates CNM-6951 and CNM-7328 respectively.

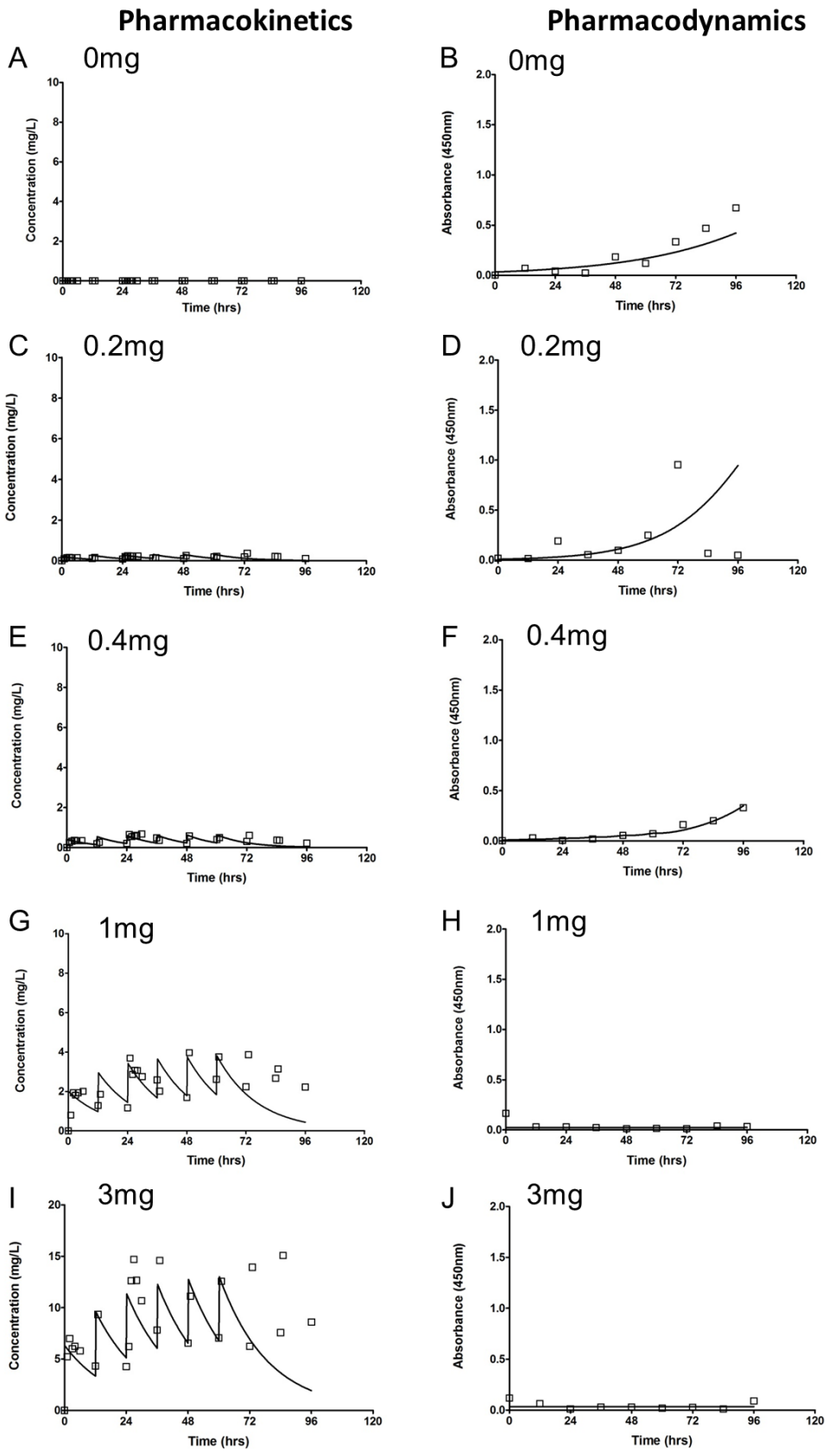

Figure 4. 15 Pharmacokinetics and pharmacodynamics of voriconazole against *F. solani* CNM-6951.

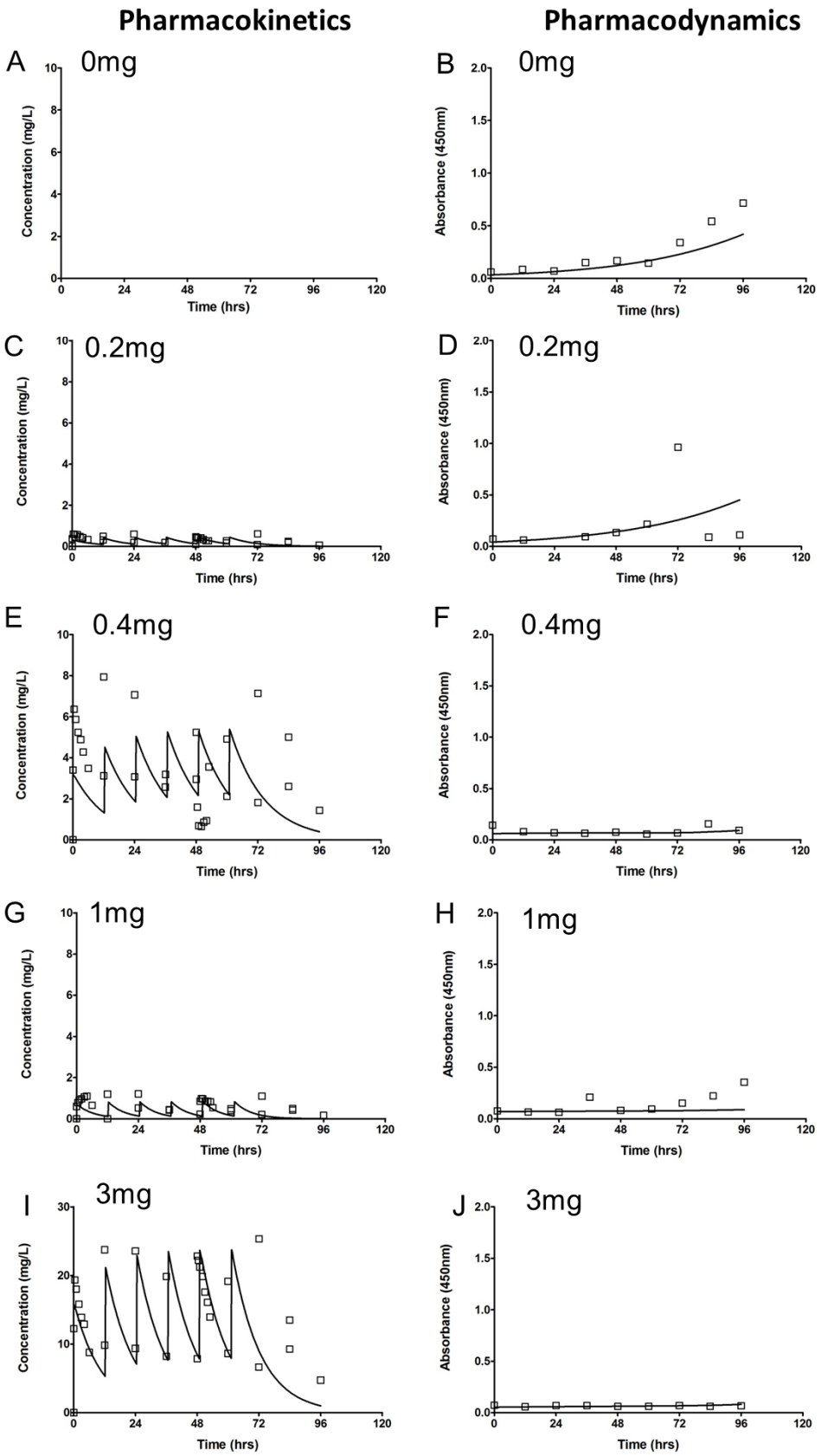

Figure 4. 16 Pharmacokinetics and pharmacodynamics of voriconazole against *F. solani* CMM-7328.

5.343 Mathematical Modelling

The fit of the mathematical models to the data were acceptable. Bayesian R^2 values were 0.958 and 0.691 for pharmacokinetic and pharmacodynamic data respectively (Figure 4.17). The use of absorption (Ka) as a parameter improved the fit of the pharmacokinetic model. The fits of the Bayesian posterior estimates for each circuit is shown in Figures 4.15-4.16. The posterior median parameter values can be seen in Table 4.6. Predicted $AUC_{48\text{-}72}$ values (mg.hr/L) for voriconazole and total AUC for the antigen are displayed in Table 4.7.

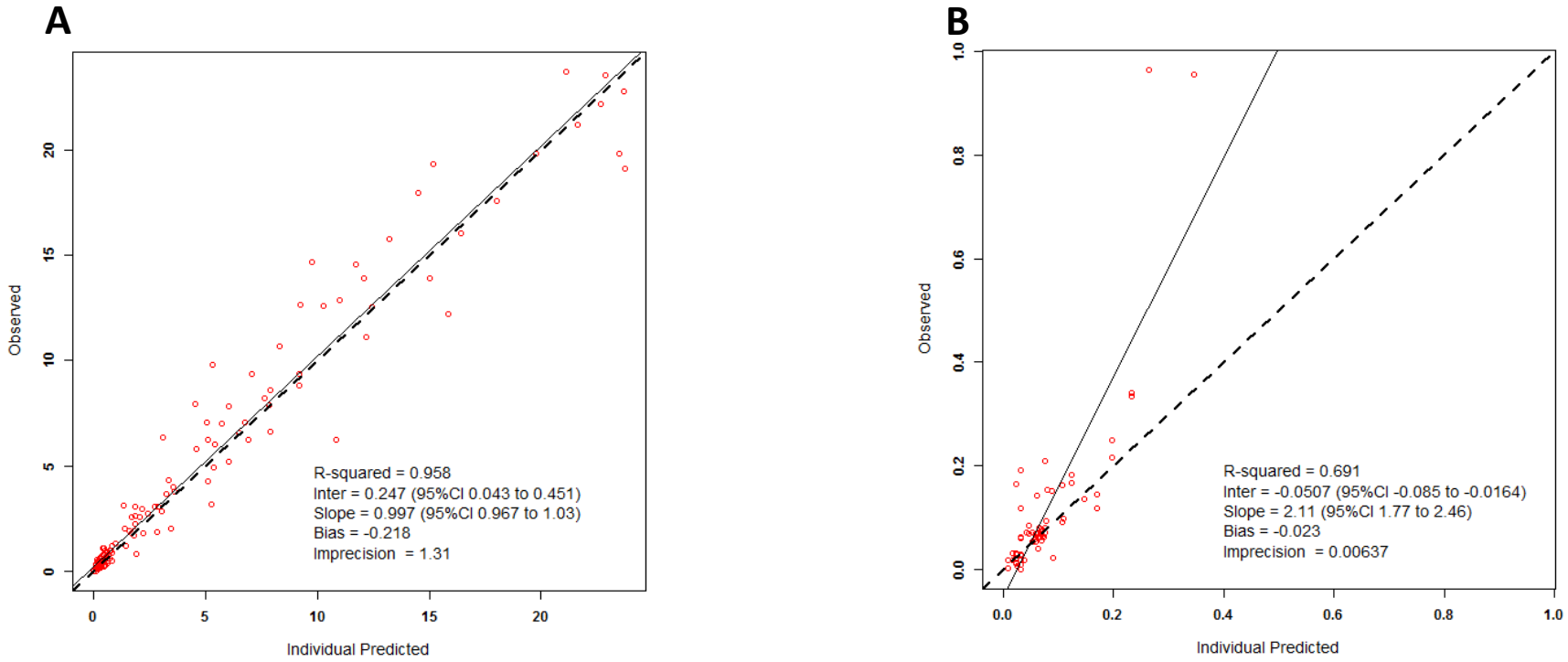

Figure 4. 17

Observed vs predicted graphs after the Bayesian step, generated using Pmetrics for (A) pharmacokinetics data from 10 individual circuits and (B) pharmacodynamics data as measured by absorbance at 450nm from 10 individual circuits.

Isolate	Dose	Cl	V (L)	Kgmax	POPMAX	C50	Hg	IC1
CNM-6951	0	0.03	0.47	0.03	2.98	0.42	5.72	0.033
CNM-6951	0.1	0.03	0.31	0.03	2.48	0.85	3.59	0.042
CNM-6951	0.2	0.04	0.29	0.005	0.55	0.25	7.96	0.070
CNM-6951	1	0.02	0.31	0.01	2.99	1.77	5.68	0.062
CNM-6951	3	0.02	0.19	0.02	0.86	1.99	0.83	0.054
CNM-7328	0	0.03	0.47	0.03	2.98	0.422	6.87	0.033
CNM-7328	0.1	0.04	0.50	0.05	2.99	0.41	8.91	0.009
CNM-7328	0.2	0.04	0.50	0.05	2.99	0.41	8.91	0.009
CNM-7328	1	0.03	0.50	0.03	2.99	0.37	5.20	0.024
CNM-7328	3	0.03	0.50	0.03	2.99	1.95	6.91	0.033

Table 4. 6

The median posterior parameter estimates from the mathematical model using data from 10 individual circuits. Cl represents the estimated clearance of VRC from the ciruit; V; the estimated volume of the central compartment; Kgmax, the predicted rate of growth of *F. solani* in the circuit; POPMAX, the maxima obtained from the ELISA assay; C50, the concentration of voriconazole that 50% suppression of antigen is obtained; Hg, the slope function to describe *F. solani* growth in both absence and presence of drug; IC1, the initial conditions for the pharmacodynamic dataset, representing background noise of the assay.

Strain	Dose (mg/ q12)	Predicted AUC_{48-72} voriconazole (mg.hr/L)	Predicted AUC_{0-72} antigen
F. solani CNM-6951	0	0	15.0.2
	0.1	5.07	21.63
	0.2	10.15	7.99
	1	68.80	2.29
	3	230.63	3.13
F. solani CNM-7328	0	0	14.97
	0.1	5.98	17.48
	0.2	9.27	7.42
	1	86.17	6.71
	3	348.93	6.17

Table 4. 7

Model predicted voriconazole AUC_{48-72} and area under antigen curves (0-72) for individual circuits achieved using the dynamic model.

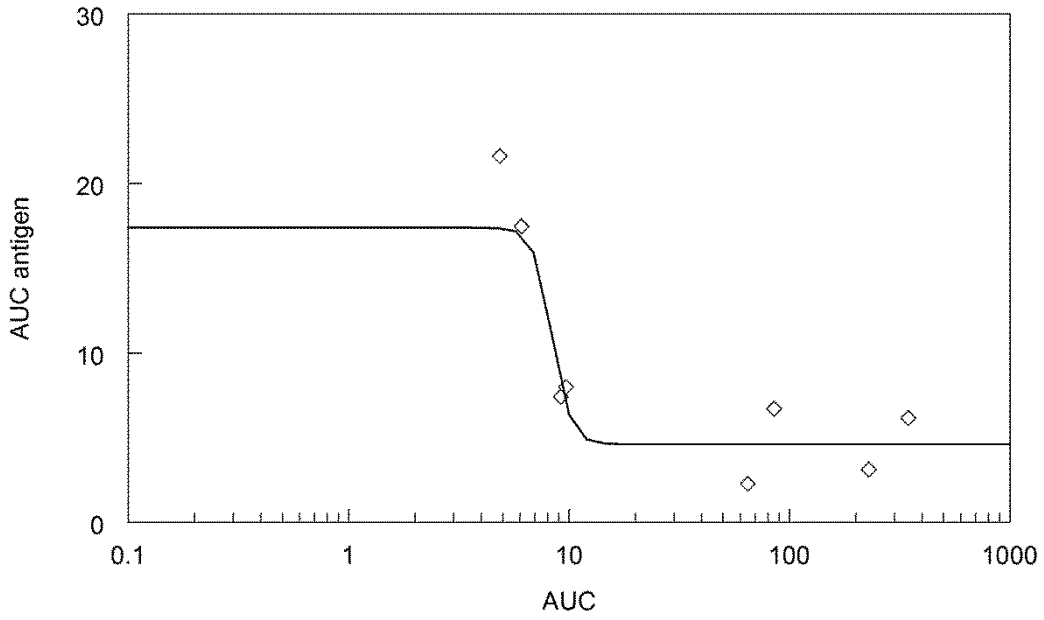

Figure 4. 18

Total AUC for *Fusarium* specific antigen detected at 450nm, versus $AUC_{48\text{-}72}$ for voriconazole (mg.hr/L). Equations were generated in ADAPT 5 using the maximum likelihood estimator.

AUCantigen = 17.41-(12.78*(AUC)^10.53)/((AUC)^10.53+8.387^10.53)

R^2= 0.879

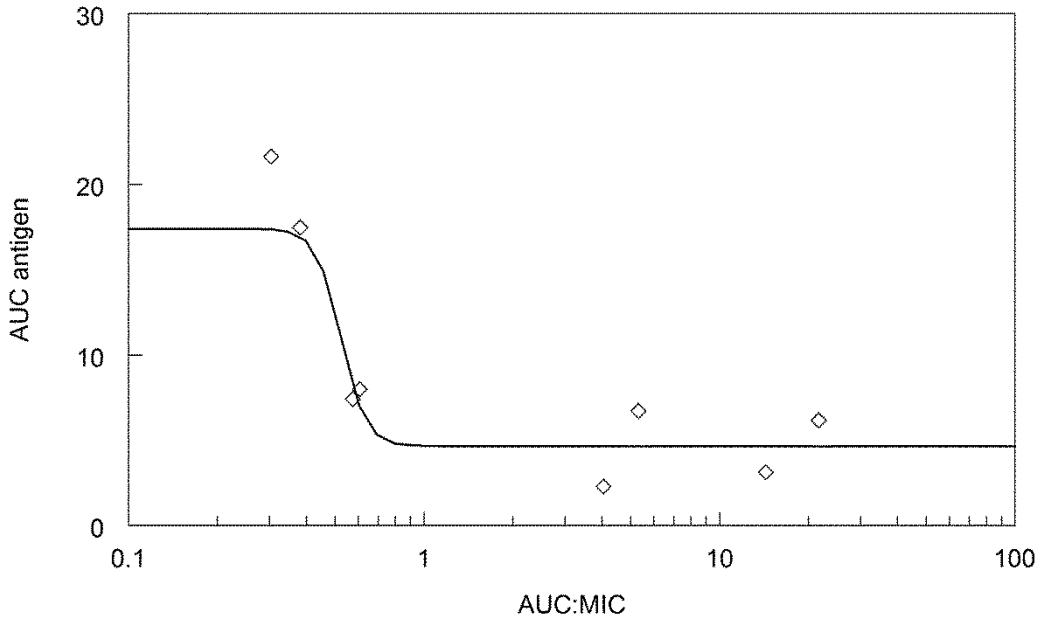

Figure 4. 19

Total AUC for *Fusarium* specific antigen detected at 450nm, versus area under the $AUC_{48\text{-}72}$: MIC (EUCAST methodology). Equations were generated in ADAPT 5 using the maximum likelihood estimator.

AUCantigen = 17.40-(12.74*(AUC)^10.42)/((AUC)^10.42+0.5237^10.42)

R^2= 0.879

4.4 CONCLUSIONS

Scedosporium and *Fusarium* spp. are emerging fungal pathogens. The treatment of these infections is problematic owing to primary resistance to several agents used in first-line therapy. Voriconazole is a first-line agent for the treatment of invasive scedosporiosis; however, the clinical outcome using this agent is variable. Due to the scarcity of randomised comparative data from clinical studies to compare the antifungal efficacy of agents for the treatment of disseminated *F. solani* infection, the optimal treatment strategy for this disease remains unclear. With a favourable toxicity profile to amphotericin B, voriconazole has become a first-line treatment option for invasive fusariosis despite demonstrating high minimum inhibitory concentrations and variable clinical success (Alastruey-Izquierdo, Cuenca-Estrella et al. 2008, Lortholary, Obenga et al. 2010).

The pharmacokinetics and pharmacodynamics (PK-PD) of a drug are central for an understanding of the relationship between dose, exposure and the subsequent antifungal effect of an agent. An understanding of these key relationships may provide insight into the exposures of drug that are best associated with optimal antifungal efficacy. To date, the PK-PD of currently used agents for the treatment of invasive *S. apiospermum* and *F, solani* infections has not been extensively studied. Current animal models are limited to tail-vein models of fungaemia. No models of invasive pulmonary disease for these fungi have been described. The pharmacokinetics of voriconazole in mice are characterised by a rapid clearance of drug. Therefore, clinically relevant exposures cannot be achieved. This chapter describes the development of novel *in vitro* models of early invasive pulmonary disease with *S. apiospermum* and *F. solani* that are able to simulate human-like voriconazole PK. These models were used to define the PK-PD relationships of voriconazole against

clinical isolates of *S. apiospermum* and *F. solani*, using novel antigens directed towards these pathogens as a measure of disease progression.

4.41 Models of *P. boydii* and *S. apiospermum*

4.411Static models of the human alveolus

The detection of the *Scedosporium/Pseudallescheria boydii* specific antigen in both alveolar and endothelial compartments of untreated static models was consistent (Figures 4.5 and 4.7). Maximum absorbance values of approximately 1-1.5 were detected in endothelial samples from these models. These values are comparable to maxima achieved by Thornton et al. and suggest that the fungi were able to invade through the cellular bilayer effectively (Thornton 2009). Upon histological examination of transwells over time, an association between the detection of antigen in the endothelial compartments and fungal burden was seen, indicating that the antigen may be a good marker for disease progression in this model (Figures 4.5 and 4.6).

For drug treated models, voriconazole demonstrated a dose dependent reduction in antigen for all isolates. The concentrations at which maximal antifungal effect was observed in static models were consistent with the respective MIC values, with the exception of two isolates (Figure 4.7, A and B). Here, we must consider the effect of starting inoculum on the observed antifungal effect. The starting inoculum used in these preliminary studies is markedly higher than those used in standardised methodologies set by EUCAST and CLSI which may explain the difference in exposures needed to achieve antifungal effect for a "susceptible" isolate in this model (CLSI 2008, Arendrup, Cuenca-Estrella et al. 2012). For isolates that demonstrated slightly lower absorbance values in untreated controls, exposure- response

relationships can be seen at levels of drug comparable to those seen in the clinic (Pascual, Calandra et al. 2008). It is also important to note that some models demonstrate variable antigen measurement in samples taken from the alveolar compartments. This may be due to the variable amount of fungi that is extracted when flooding the surface of the alveolar layer.

5.412 Dynamic models of the human alveolus

S. apiospermum was markedly slower growing than other filamentous fungi used in this model such as *Aspergillus* spp (Box, Livermore et al. 2016). Little to no growth was seen in the first 48 hours of these experiments. The maximum absorbance values detected in untreated circuits varied between isolates, largely with isolate 6386. This isolate also observed a low maximum absorbance in static studies. A difference in virulence between clinical isolates of *S. prolificans* has previously been documented in murine investigations, despite demonstrating pathogenicity in humans (Ortoneda, Pastor et al. 2002). It may be that some isolates of *S. apiospermum* demonstrate lesser virulence in this cell associated model to others which may account for the differences in antigen detected between models.

When PK samples were taken after the bioreactor, C_{max} levels were reached within 2-4 hours. This is not representative of the bolus dose administered, which may be a limitation of this particular dataset and may be why the model fit is not optimal (R^2= 0.715). However, the pharmacokinetics generated using this model are comparable to those seen in orally dosed patients where peak plasma concentrations are achieved up to 2 hours post-administration (Wang, Xie et al. 2015).

In clinical populations, voriconazole displays a marked variability in drug exposure that is due in part to its non-linear pharmacokinetic behaviour. It is difficult

to predict a dosage that will yield exposures within a therapeutic window without the use of therapeutic drug monitoring (Trifilio, Pennick et al. 2007, Moriyama, Kadri et al. 2015). A number of studies have investigated the importance of voriconazole serum concentrations in relation to both clinical outcome and toxicity in patients at risk or with IFI (Table 4.8). The area under curve: MIC (AUC: MIC) has been described as the pharmacodynamic parameter best associated with therapeutic success in preclinical models of *Aspergillus* spp. (Andes, Marchillo et al. 2003, Mavridou, Bruggemann et al. 2010, Jeans, Howard et al. 2012)..

Clinical data from haematopoietic stem cell transplant patients suggest that $AUC_{0\text{-}24}$ values of around 70 mg.hr/L were achieved using standard dosages of voriconazole. These values are comparable to AUCs associated with maximum suppression of antigen in this model of around 65 mg/L (Table 4.5) (Bruggemann, Blijlevens et al. 2010). This suggests that with currently used regimens, the voriconazole exposures associated with treatment success in this model may be suitable for the treatment of scedosporiosis with these isolates.

The MICs from this study correlate well with the reported MIC_{90} of 1 mg/L for voriconazole against clinical isolates of *S. apiospermum* (Troke, Aguirrebengoa et al. 2008). The concentrations relative to maximal suppression of the antigen in the dynamic model are consistent with the respective MICs suggesting that clinically used regimens may be effective in treating the isolates used in dynamic models.

Predicted AUC: MIC values of 133.3, 65.5 and 64.5 (Figure 4.14) were associated with maximal antifungal effect in this model. These values are similar to those obtained for voriconazole against isolates of *A. fumigatus* in a similar experimental model of aspergillosis where an AUC:MIC value of 45.59 was

associated with a 90% probability of treatment success (Jeans, Howard et al. 2012). Furthermore, a strong association between the AUC:MIC and antigen suppression was demonstrated (Figure 4.14, R^2= 0.986) indicating that the MIC may be predictive of antifungal efficacy for voriconazole in this model.

Although AUC:MIC has been derived as the best pharmacodynamic parameter associated with treatment success, the number of clinical samples required for the determination of AUC is often difficult to obtain from patients. Therefore many clinical studies use trough levels of voriconazole as a surrogate for AUC to predict treatment outcome (Table 4.8). However, a small change in dose based on reported trough levels of drug may have a disproportionate effect on serum levels due to the non-linear pharmacokinetic profile seen with voriconazole. Studies have reported that nonparametric population models may be able to predict voriconazole AUC from clinically obtained C_{min} values. There is the potential here to predict target exposures from as little as one pharmacokinetic sample, for the individualisation of therapy (Hope, VanGuilder et al. 2013, Neely, Margol et al. 2015, Huurneman, Neely et al. 2016)

Troke et al. reported a relationship between increasing trough/ MIC ratio and the probability of clinical success for the treatment of IFI. These analyses estimated a trough/ MIC ratio between 2 and 5 to be associated with maximal clinical outcome in the treatment of IFIs (Troke, Hockey et al. 2011). This correlates well with trough/ MIC ratios calculated from dynamic model data for voriconazole against isolates of *S. apiospermum* which are 5.2, 2.7 and 2 for strains 8353, 6322 and 6386 respectively.

The largest study to date, described by Dolton et al., retrospectively analysed voriconazole TDM data collected from 201 patients from centres across Australia.

Plasma levels of drug were shown to be a significant determinant of clinical success. It was suggested that trough concentrations of ≥ 1.17 mg/L significantly minimised the risk of treatment failure, whilst levels ≥ 5 mg/L saw an increase in the incidence of neurological adverse events (Dolton, Ray et al. 2012). A similar therapeutic window was suggested by Pascual et al. In this cohort, 46% of patients with trough levels ≤ 1mg/ L failed to respond to therapy and all patients experiencing neurological adverse events demonstrated trough levels ≥ 5.5mg/ L (Pascual, Calandra et al. 2008). Troke et al. also performed a retrospective analysis on data from 9 clinical trials confirming low response rates outside of the range of 0.5 mg/L- 5 mg/L (Troke, Hockey et al. 2011).

In this *in vitro* model of scedosporiosis, median trough concentrations of approximately 2.45 mg/L were associated with maximal antifungal effect against all isolates, well within the therapeutic range suggested by these clinical studies for the treatment of IFIs. Although, it is important to note that analyses performed by Troke et al. did not distinguish between the pathogenic causes of IFIs, which may be a key determinant of patient response to voriconazole therapy.

Indication	Lower Limit (mg/L)	Upper Limit (mg/L)	Reference
Treatment	≤ 1.17	≥ 5	(Dolton, Ray et al. 2012)
Treatment	≤ 1	≥ 5.5	(Pascual, Calandra et al. 2008)
Treatment	≤2	≥5	(Troke, Hockey et al. 2011)
Treatment	≤2	≥10	(Denning, Ribaud et al. 2002)
Treatment	≤2	≥6	(Ueda, Nannya et al. 2009)

Table 4. 8

Table to describe the upper and lower limits of plasma trough levels best associated with efficacy and toxicity for voriconazole derived from clinical datasets for the treatment of IFIs.

Due to the scarcity of both preclinical and clinical PK-PD datasets available for voriconazole therapy against *S. apiospermum* there are no clinical breakpoints set (Tortorano, Richardson et al. 2014). Therefore little is known about the optimum treatment of resistant infections within this species. This model is able to generate voriconazole exposures comparable to those seen in the clinic, a marked limitation of murine studies (Andes, Marchillo et al. 2003, Mavridou, Bruggemann et al. 2010). The ability of this model to link clinically relevant drug levels to disease progression using a novel biomarker as a measure of disease progression is a clear advancement in the study of PK-PD relationships for agents against *S. apiospermum*. Although there is no defined association between dosage and plasma voriconazole concentrations in humans, a knowledge of the optimal AUC and trough levels associated with the successful treatment of these infections may guide clinicians in predicting therapeutic failure and the need for dosage escalation. This may be particularly helpful for the definition of PK-PD relationships between voriconazole and resistant isolates of *S. apiospermum*, to further our understanding of the potential susceptibility breakpoints for these organisms.

5.42 Models of *F. solani*

5.421 Static models of the human alveolus

For the treatment of *F. solani* infection, static studies demonstrated that concentrations of ≥16 mg/L were insufficient for the complete suppression of antigen using a cut off value of 0.1. Maximum absorbency values in untreated transwells for each of these experiments were all around 1.5 suggesting that in a static setting these isolates of *F. solani* were able to invade through the cellular bilayer, consistent with the *in vivo* pathogenicity of invasive fusariosis. This similarity in maxima also suggests that each fungal isolate may exhibit a similar release of antigen. A relatively small dynamic range is observed for this assay, more so than the assay used for the tracking of *Scedosporium* spp. This may be due to the lack of a biotin amplification step for this assay leading to a decreased sensitivity for the detection of antigen.

5.422 Dynamic models of the human alveolus

Throughout dynamic experiments the kinetics of antigen release in untreated circuits by ELISA were variable. For isolate CNM-6951 increasing absorbance values were obtained in both experiments up to 60 hours suggesting an accumulation of antigen up to this time point. However, antigen levels seem to decline from this time onwards. This may be due to a number of factors. This isolate of *F. solani* may cease to produce antigen over prolonged periods of time or degradation of the antigen may occur, causing a decline in antigen through the clearance mechanism set by the model. Alternatively, this may be related to a decline in fungal burden within the system, in which case the fungi may have entered a stationary phase of growth similar to that seen in bacterial cultures and existing cultures are cleared. For isolate CNM-7328 a noticeably lower maxima is observed in untreated circuits, whilst drug exposed circuits followed a similar dose-response pattern to CNM-6951. It has been demonstrated with *F. oxysporum* that a large amount of glucose is necessary for maximum efficiency of the initial growth phase to occur. It also is known that glucose consumption of fungi varies between both species and strains through the expression of glucose transporters (Srivastava, Pathak et al. 2011). It may be that the medium used in this model was not suitably glucose-rich or that replenishment was not sufficient in order to support the optimal growth of this isolate under flow conditions.

Clinically relevant exposures of voriconazole were achieved. Predicted $AUC_{48\text{-}72}$ values of approximately 64.9 and 85.2 and median trough values of approximately 2.41 mg/L were required to maximally suppress the antigen for isolates CNM-6951 and CNM-7328 respectively. These exposures are consistent with those achieved in experiments using *S. apiospermum* demonstrating the reproducibility of this model for the assessment of voriconazole pharmacokinetics. TDM studies suggest

that median trough concentrations of approximately 2- 5.5 mg/L are associated with maximal clinical outcome suggesting that the currently derived upper and lower limits associated with maximal voriconazole efficacy for the treatment of general IFIs may be encompassing of *F. solani*. (Pascual, Calandra et al. 2008, Myrianthefs, Markantonis et al. 2010, Dolton, Ray et al. 2012).

Isolate CNM-7328 appeared to be more susceptible to voriconazole at lower concentrations in this dynamic model compared to values obtained for MIC and static experiments. This supports the argument that the growth of this isolate in a dynamic setting may not have been fully representable of a severe invasive infection. This is further demonstrated by the low predicted AUC:MIC values associated with treatment success in this model of 14.3 compared to those predicted for *S. apiospermum*.

The work presented in this chapter describes the development of novel *in vitro* models of invasive scedosporiosis and fusariosis using the detection of surface antigens as a measure of disease progression and response to therapy. This model achieves clinically relevant drug exposures of voriconazole and can be sampled frequently to obtain a detailed pharmacokinetic dataset, a clear advantage over murine models. This, alongside the establishment of a model of invasive disease for which eradication can be directly linked to drug exposure represents a potential platform for the investigation of the PK-PD relationships for novel antifungal agents against these rare and under-studied organisms. In turn, PK-PD datasets generated using this system may help to develop optimal dosing strategies that may be taken forward to clinical trial.

CHAPTER V

The Pharmacokinetics and Pharmacodynamics of Novel Orotomide, F901318, against isolates of *Scedosporium apiospermum and Fusarium solani*

5.1 INTRODUCTION

The discovery and development of novel classes of antifungal agents has been a great challenge over the past decades. The interest from big pharma in the development of antimicrobials with novel targets has diminished due to lack of financial incentive. Therefore, small biotechnology companies have become the main contributors towards the discovery of novel antimicrobial agents. The orotomide class of agents are a novel class of antifungals. F901318 is the first and most advanced agent of the orotomides and is currently in Phase I of clinical development with F2G Ltd. F901318 was discovered via the screening of a 370,000 compound library for antifungal activity against *A. fumigatus*. Its primary target was determined to be the dihydroorotate dehydrogenase (DHODH) enzyme. The role of DHODH in the *de novo* biosynthesis of pyrimidines is well characterised in both humans and fungi. It is responsible for the conversion of dihydroorotate to orotate. As fungi such as *Aspergillus* spp. cannot salvage pyrimidines from their environment, the *de novo* biosynthesis pathway is the sole source of pyrimidines for these pathogens (Figure 1.7). Specificity of F901318 for fungal DHODH has been demonstrated and the agent exhibits a very poor inhibition of the human enzyme. The mechanism of F901318 is reversed in the presence of pyrimidine compounds however this is only at high concentrations of >5mM of which only a small fraction is present in human serum (Oliver, Law et al. 2015). F901318 also demonstrates *in vitro* activity against *S. apiospermum* and other species within its species complex (Fothergill, Wiederhold et al. 2015).

F901318 demonstrates *in vitro* activity against *S. apiospermum* and other species within the *Scedosporium- Pseudallescheria* species complex, as well as *F. solani* (Fothergill, Wiederhold et al. 2015, Fothergill, Law et al. 2016). Phase I data also suggests F901318 is safe and well tolerated at the dosages given in its first single ascending dose study in humans (Kennedy, Allen et al. 2015). An understanding of the pharmacokinetics and pharmacodynamics of novel agents such as F901318 may provide a valuable insight into the effective dosages and regimens to further study in clinical trials. The use of PK-PD is now a mandatory component of regulatory portfolios, and a critical tool that enables more streamlined approaches to the development of new antimicrobial agents (Rex, Eisenstein et al. 2013).

This chapter describes the use of previously described static and dynamic *in vitro* models of invasive scedosporiosis and fusariosis to facilitate an understanding of the exposure- response relationships for F901318 against isolates of *S. apiospermum* and *F. solani.*

5.2 METHODS

The isolates of *Pseudallescheria, Scedosporium* and *Fusarium* spp. used are detailed in Chapter IV (Section 4.21). Methods for the culture of organisms, inoculum preparation, the set -up of static and dynamic models of invasive scedosporiosis and fusariosis and the analysis of pharmacodynamics samples by ELISA are described in Chapter IV (Sections 4.21, 4.23, 4.24, 4.27 respectively).

5.21 *In vitro* susceptibility testing

Minimum inhibitory concentrations (MIC) for F901318 against *S. apiospermum* and *F. solani* isolates were determined in 5 independent experiments using both the European Committee for Antimicrobial Testing (EUCAST) and Clinical Laboratories Standards Institute (CLSI) methodologies. Concentrations for MIC testing ranged from 0.006 mg/L to 4 mg/L for F901318. The modal value, range and geometric mean were determined. The mode was used in the pharmacodynamic analyses for the determination of AUC:MIC values.

5.21 Construction of the dynamic model

The construction of the circuitry comprising the dynamic model is described in Chapter II (Section 2.251). The locations of sampling ports are detailed below (Figure 5.2).

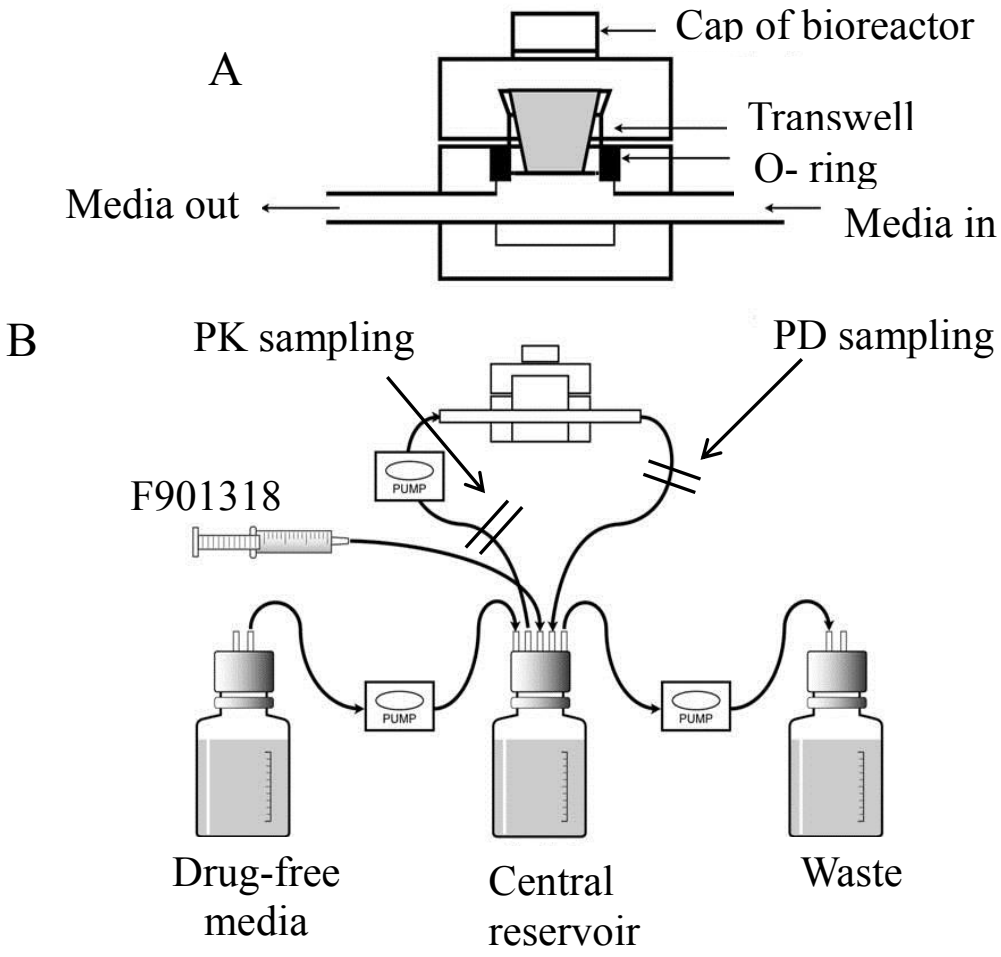

Figure 5. 1 The set-up of the dynamic in vitro model of the human alveolus specific for F901318 against *S. apiospermum* and *F. solani*.

5.22 Treatment with F901318

F901318 pure powder was dissolved in DMSO. Dilutions were prepared from known stock concentrations in DMSO in order to achieve the required concentrations for each dynamic system. For *Scedosporium* experiments, the drugs were administered directly into the central compartment as a 100 µL bolus. F901318 dosages were selected in order to obtain exposures of sub-MIC level (0.00025 mg, 0.0005 mg), the approximate MIC for isolate 8353 (0.001mg) and approximately 4 x supra- MIC (0.05 mg) as multiples of the MIC are routinely used in the assessment of antimicrobial activity (Pfaller, Sheehan et al. 2004). Dosages of 0 mg, 0.00025 mg, 0.0005 mg, 0.001 mg and 0.05 mg were administered every 12 hours to the central compartment of each corresponding circuit. For *Fusarium* experiments, dosages of 0 mg, 0.1 mg, 0.2 mg, 1 mg and 3 mg were administered as four hour infusions every 12 hours to the central compartment of each corresponding circuit. F901318 was administered directly to the central compartment of the relevant circuits. Pump speeds for controlling the clearance of drug were set in order to simulate a half-life of approximately 4-5 hours, similar to that observed in monkey PK studies. The pump connected to the fresh media and the waste Durans was run at a speed of 4.5rpm corresponding to a flow rate of approximately 24mL/hour. Pump speeds were calculated using clearance data published by the pump manufacturer. Pharmacokinetic sampling regimens were optimised using data obtained from preliminary dynamic pharmacokinetic models (data not shown).

5.23 Mass spectrometry

Mass spectrometry for pharmacokinetic analysis was performed by Joanne Goodwin and Sarah Whalley at the University of Liverpool.

F901318 concentrations were determined using a UHPLC/MS-MS triple-quadrupole 6420 mass spectrometer, (Agilent Technologies, Santa Clara, CA, USA). Instrument

parameters were optimized for F901318 (499.1 → 172.0 m/z). F901318 were extracted from DMEM media using acetonitrile and methanol (Fisher Scientific, Loughborough, UK) with IS.

HPLC separation was achieved using a Zorbax Eclipse Plus Rapid 1.8 µm C18 50 x 2.1 mm (Agilent Technologies, Santa Clara, CA, USA) column. The mobile phase consisted of 0.2% formic acid in water and 0.2% formic acid in acetonitrile at a flow rate of 0.5 ml/min, the column was maintained at 40 °C. 6, 7-Dimethyl-2,3-di(2-pyridyl) Quinoxaline (Sigma Aldrich, Dorset, UK) 100 ng/ml in methanol:acetonitrile (50:50) was used as an internal standard. The chromatographic run time for one sample was 2.5 minutes. The lower limit of quantitation of F901318 was 0.0005 mg/L. Intraday and interday coefficients of variation were <14.7% at concentrations ranging from 0.0005 to 5 mg/L.

5.24 Mathematical Modelling

A population methodology was used in order to fit a mathematical model to the data from each isolate. Version 1.2.9 of Pmetrics PK-PD analytical software was used. For pharmacodynamic datasets, data were normalised to a maxima of 1 due to variability in maximum PD values obtained in control circuits between isolates. For *Scedosporium* datasets the structural mathematical model consisted of the following two inhomogeneous ordinary differential equations:

$$dX1/dt = B(1)-(SCL/Vc)*X1 \qquad \text{Equation 1}$$

$$dN/dt = Kgmax*(1-(N/POPMAX))*N \qquad \text{Equation 2a}$$

$$*(1-(X1/Vc)^{Hg}/(X1/Vc)^{Hg}+C50g^{Hg})) \qquad \text{Equation 2b}$$

Where: B(1) is the bolus input of is the bolus input of F901318, SCL is the clearance of drug from the circuit, Vc is the volume of the circuit, N is the antigen concentration, Kgmax is the maximal rate of growth; POPMAX is the theoretical maximal density within the circuit; Hg is the slope function for the suppression of growth; and, C50g is the concentration of drug in the circuit where there is half-maximal suppression of growth.

Equation 1 describes the rate of change of drug concentrations in the circuit. Equation 2 describes the rate of change of antigen in the circuit and contains terms that describe fungal growth in the absence of drug (Equation 2a) and the drug induced suppression of growth (Equation 2b).

The structural model for the analysis of *Fusarium* datasets was identical to that described earlier, with the exception that in Equation 1. a RATEIV expression is used to describe the infusion of drug as opposed to a bolus input (Equation 1b).

$dX1/dt = -RATEIV(1)-(SCL/V_C)*X1$ Equation 1(b)

The models were fitted to the dataset of untreated and treated circuits obtained from each isolate. Each circuit was treated as an "individual". The fit of the model was assessed using the coefficient of determination (r^2) from a linear regression of the observed vs. predicted plots for both population and individual predictions, the mean and median values of parameters predicted by the model compared to those observed experimentally and the log likelihood. The Bayesian posterior estimate for each of the parameters in the model was then used to define the concentration-time profile of F901318 and the resultant effect on antigen concentrations. As no data on the PD indices best associated with antifungal efficacy were available at the

time, these parameter estimates were used to estimate the AUC that developed in each circuit and the AUC:MIC ratios.

5.3 RESULTS

5.31 Minimum Inhibitory Concentrations

The minimum inhibitory concentrations (mode, range and geometric mean) for voriconazole against isolates of *S. apiospermum, P. boydii* and *F. solani* are presented in Table 5.1.

			EUCAST			CLSI		
Drug	**Species**	**Isolate**	**Mode**	**Range**	**Mean**	**Mode**	**Range**	**Mean**
F901318	***S. apiospermum***	**8353**	**0.06**	**0.06-0.06**	**0.06**	**0.03**	**0.03-0.03**	**0.03**
F901318	***S. apiospermum***	**6322**	**0.125**	**0.06-0.125**	**0.107**	**0.06**	**0.06-0.06**	**0.06**
F901318	***S. apiospermum***	**6386**	**0.125**	**0.125-0.125**	**0.125**	**0.06**	**0.06-0.06**	**0.06**
F901318	***P. boydii***	**7935**	**0.5**	**0.5-0.5**	**0.5**	**0.015**	**0.015-0.015**	**0.015**
F901318	***P. ellipsoidea***	**13144**	**0.03**	**0.03-0.03**	**0.03**	**0.015**	**0.015-0.015**	**0.015**
F901318	***F. solani***	**CNM-6951**	**8**	**4-8**	**6.06**	**2**	**1-2**	**1.5**
F901318	***F. solani***	**CNM-7328**	**0.12**	**0.06-0.125**	**0.09**	**0.015**	**0.015-0.03**	**0.019**

Table 5. 1

Minimum inhibitory concentrations were determined in 5 independent experiments. Means displayed above are geometric means.

5.32 *Scedosporium apiospermum* models

5.321 Static models of the human alveolus

The exposure- response relationships for F901318 are described in Figures 5.2. Antigen detection was consistent for samples obtained from the static models however some variability is observed between both species and strain. Maximum absorbance values of 1-1.5 were obtained from inserts infected with *S. apiospermum* and *P. boydii* that were untreated or exposed to low doses of drug. A slightly lower maximum of approximately 0.8 was achieved for the isolate of *P. ellipsoidea*. For *S. apiospermum* 6322 and 6386 variability in data obtained from the alveolar compartment can be seen. For F901318 a concentration-dependent inhibition of antigen release was observed for isolates of *S. apiospermum, P. boydii* and *P. ellipsoidea*. For the endothelial compartments a clear exposure response relationships are defined. Concentrations of 0.5 mg/L and 0.125 mg/L were sufficient to achieve maximal suppression of antigen for *S. apiospermum* strains 8353 and 6386 respectively. For isolate 6322 maximal suppression of antigen was not achieved even at the highest concentration. Concentrations of 0.5 mg/L and 0.0125 mg/L were sufficient to suppress antigen release for isolates of *P. boydii* and *P. ellipsoidea*. The concentrations required to suppress antigen release were higher for the alveolar compartment than for the endothelial compartment in all experiments.

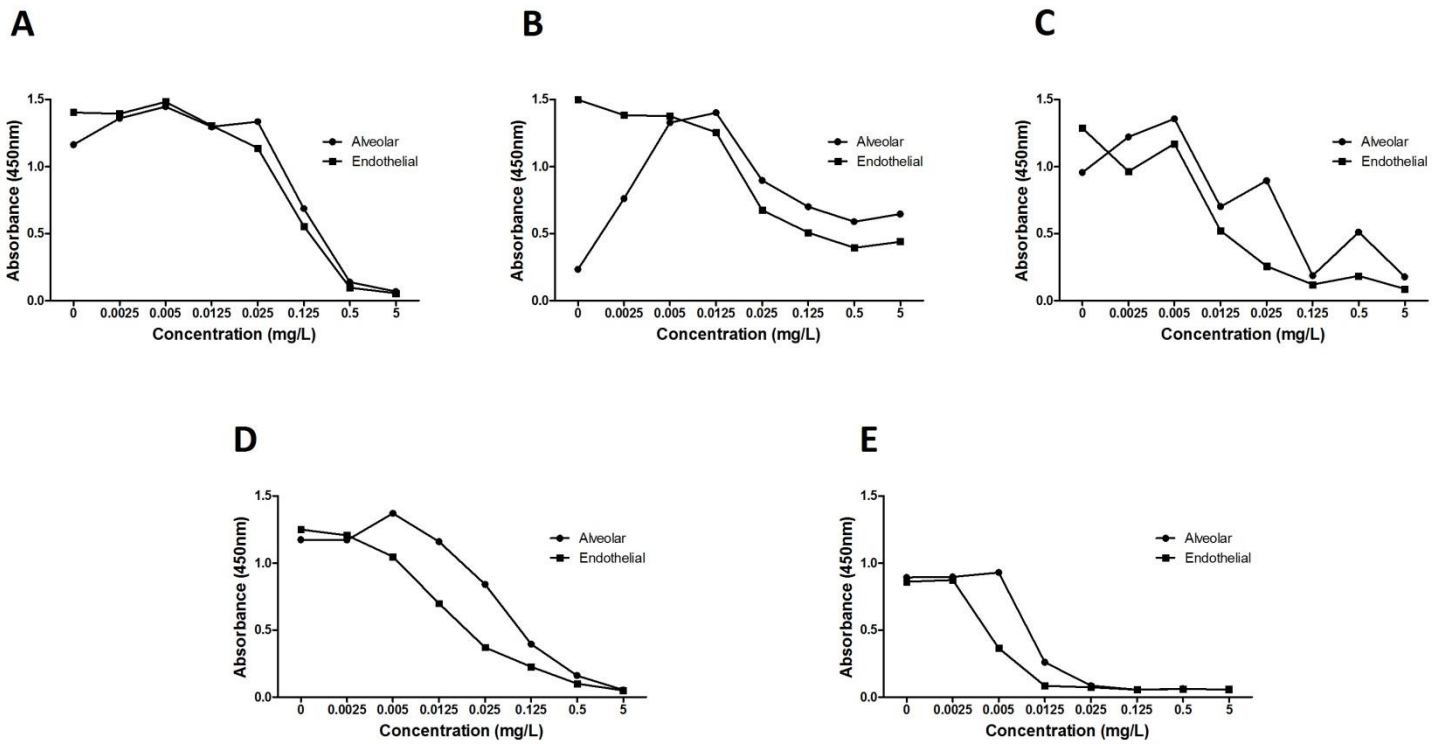

Figure 5. 2

Pharmacokinetics and pharmacodynamics of F901318 in a static model against *S. apiospermum* 8353 (A), 6322 (B), 6386 (C) , *P. boydii* 7935 (D) and *P. ellipsoidea* 13144 (E).

5.322 Dynamic models of the human alveolus

The exposure-response relationships of F901318 and *S. apiospermum* were defined for all three clinical isolates (Figures 5.3-5.5). There were differences in the PK-PD relationships between isolates. Trough concentrations within the range of 0.02 mg/L- 0.05 mg/L were sufficient to maximally suppress antigen release for isolates 8353 and 6322 using a cut-off value of 0.1. These concentrations are consistent with the MICs obtained in this study using CLSI methodology. Much lower concentrations of 0.0006 mg/L were able to successfully suppress the breakthrough of antigen for strain 6386. A minimal amount of breakthrough was observed at 108 hours post inoculation when exposed to these concentrations for strains 8353 and 6322.

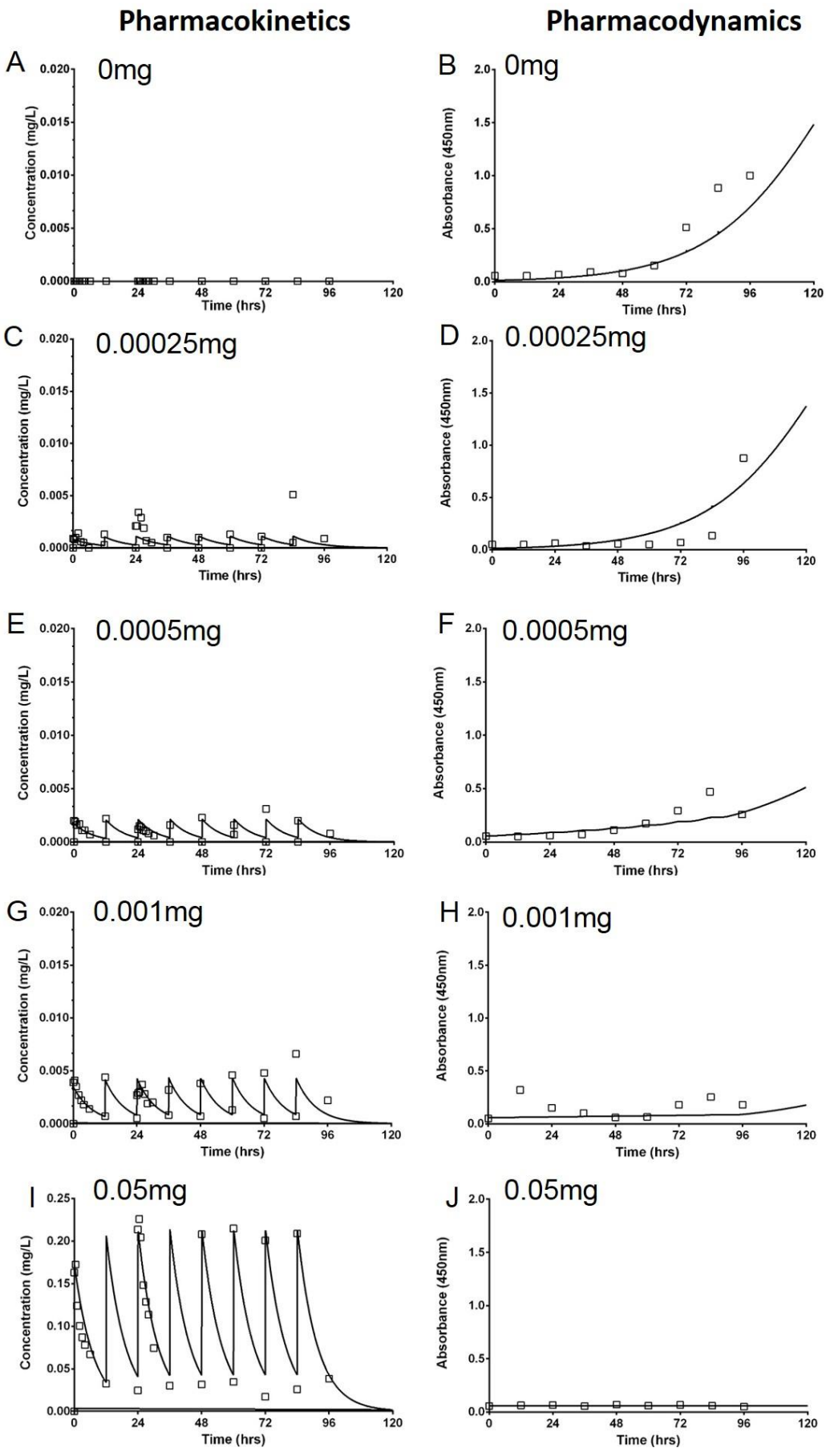

Figure 5. 3 Pharmacokinetics and pharmacodynamics of F901318 against *S. apiospermum* isolate 8353.

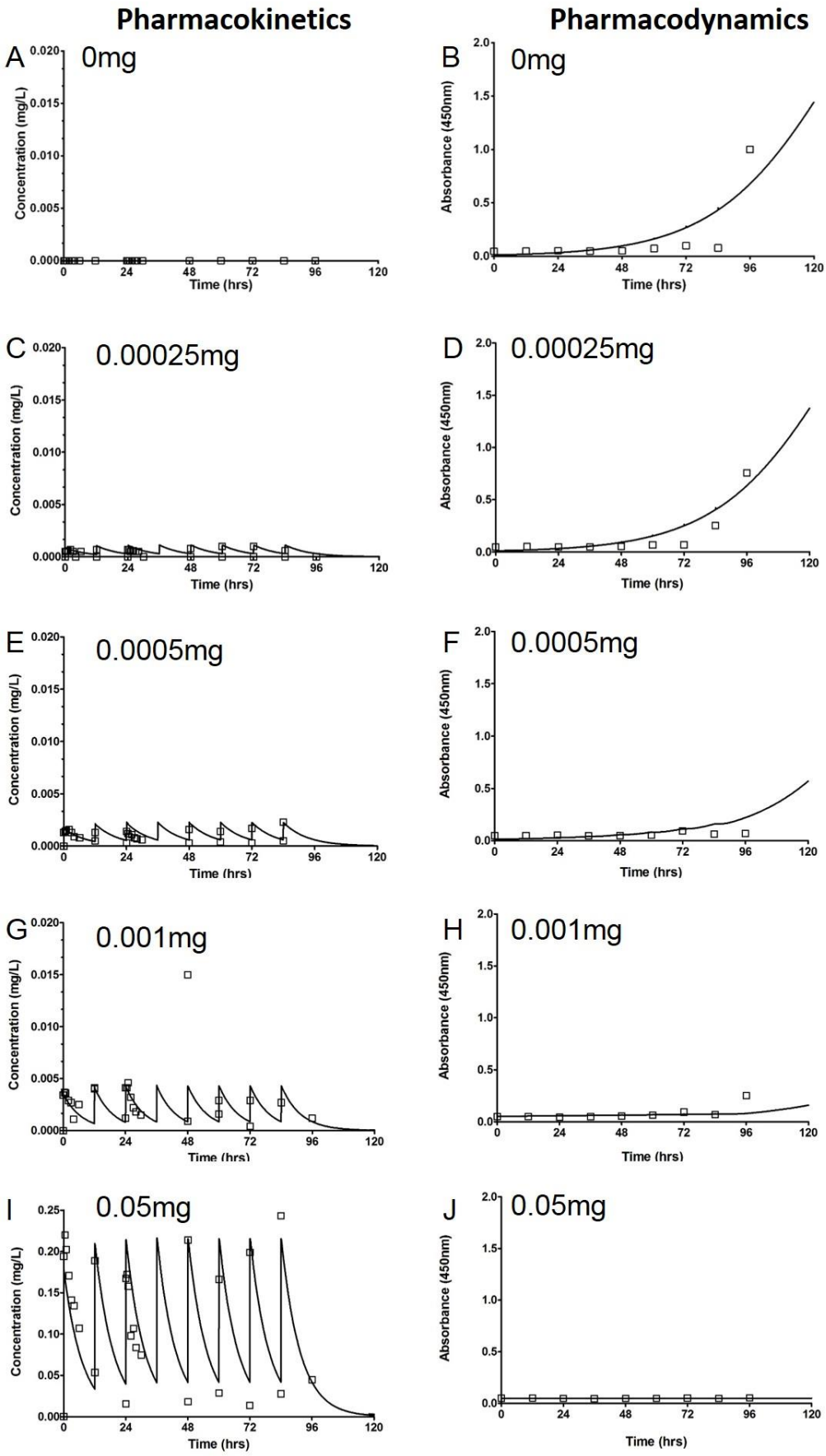

Figure 5. 4 Pharmacokinetics and pharmacodynamics of F901318 against *S. apiospermum* isolate 6322.

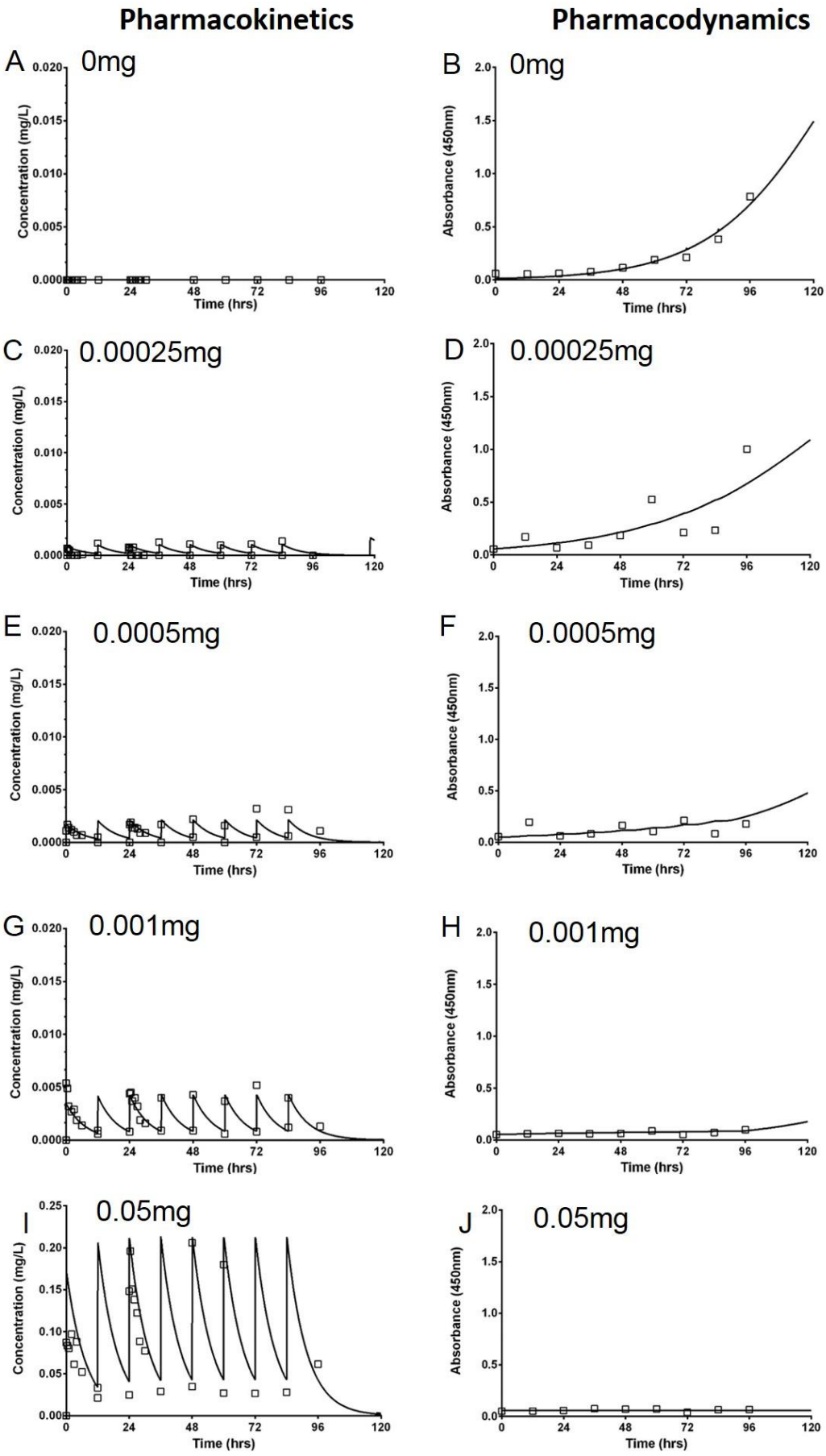

Figure 5. 5 Pharmacokinetics and pharmacodynamics of F901318 against *S. apiospermum* isolate 6386.

6.323 Mathematical modelling

The fit of the mathematical model to the data was acceptable (Figure 5.6). The fit of the Bayesian posterior estimates for each circuit is shown in Figures 5.3-5.5. Median posterior parameter estimates for each model can be seen in Table 5.2. Predicted $AUC_{72\text{-}96}$ values (mg.hr/L) for F901318 and total AUC for the antigen are displayed in Table 5.3.

A

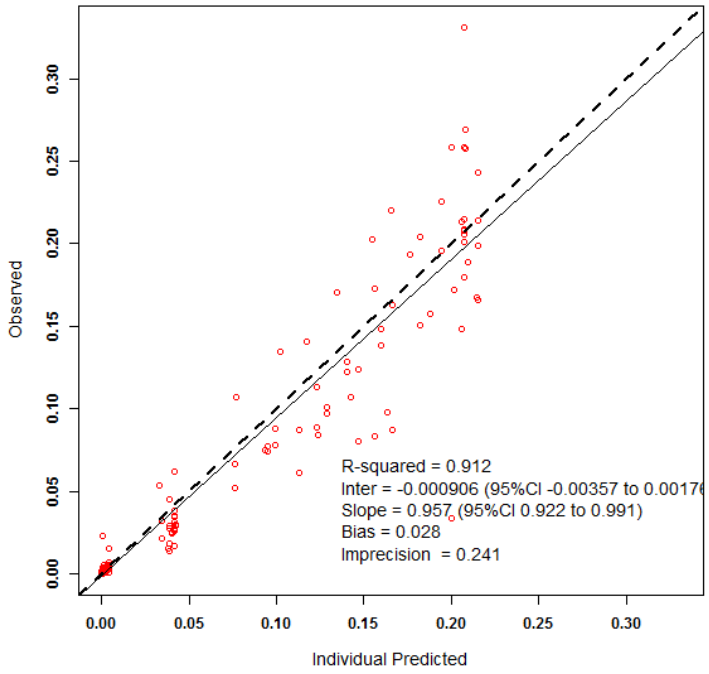

B

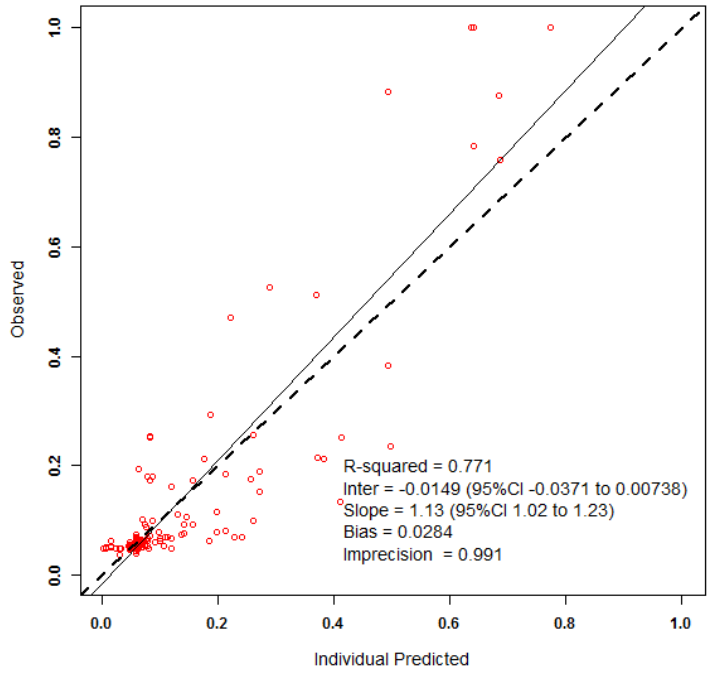

Figure 5. 6

Observed vs predicted graphs after the Bayesian step, generated using Pmetrics for (A) pharmacokinetics data from 15 individual circuits and (B) pharmacodynamics data as measured by antigen from 15 individual circuits.

Isolate	Dosage	Cl	V (L)	Kgmax	POPMAX	C50	Hg	IC1
8353	0	0.04	0.30	0.03	1.99	0.00	7.26	0.05
8353	0.00025	0.03	0.30	0.06	1.99	0.00	5.31	0.00
8353	0.0005	0.04	0.30	0.03	1.99	0.00	7.32	0.06
8353	0.001	0.04	0.30	0.03	1.99	0.00	7.32	0.06
8353	0.05	0.04	0.30	0.03	1.99	0.00	7.31	0.06
6322	0	0.03	0.30	0.06	1.99	0.00	5.28	0.00
6322	0.00025	0.03	0.30	0.06	1.99	0.00	5.31	0.00
6322	0.0005	0.03	0.30	0.03	1.99	0.00	5.32	0.02
6322	0.001	0.04	0.30	0.03	1.99	0.00	7.32	0.05
6322	0.05	0.04	0.28	0.03	1.99	0.00	7.34	0.05
6386	0	0.04	0.30	0.03	1.99	0.00	7.27	0.05
6386	0.00025	0.04	0.30	0.03	1.99	0.00	7.33	0.06
6386	0.0005	0.04	0.30	0.03	1.99	0.00	7.30	0.05
6386	0.001	0.04	0.30	0.03	1.99	0.00	7.32	0.06
6386	0.05	0.04	0.30	0.03	1.99	0.00	7.31	0.06

Table 5. 2

The median posterior parameter estimates from the mathematical model using data from 15 individual circuits. Cl represents the estimated clearance of F901318 from the ciruit; V; the estimated volume of the central compartment; Kgmax, the predicted rate of growth of *S. apiospermum* in the circuit; POPMAX, the maxima obtained from the ELISA assay; C50, the concentration of F901318 that 50% suppression of antigen is obtained; Hg, the slope function to describe *S. apiospermum* growth in both absence and presence of drug; IC1, the initial conditions for the pharmacodynamic dataset, representing background noise of the assay.

Strain	Dose (mg/ q12)	Predicted AUC_{72-96} F901318 (mg.hr/L)	Predicted AUC_{0-96} antigen
S. apiospermum 8353	0	0	23.59
	0.00025	0.019	13.78
	0.0005	0.026	13.34
	0.001	0.051	6.97
	0.05	2.559	5.64
S. apiospermum 6322	0	0	15.69
	0.00025	0.019	13.84
	0.0005	0.030	9.25
	0.001	0.051	6.69
	0.05	2.560	6.28
S. apiospermum 6386	0	0	23.61
	0.00025	0.013	24.75
	0.0005	0.026	12.40
	0.001	0.051	6.97
	0.05	2.559	5.64

Table 5. 3

Model predicted F901318 AUC_{72-96} for isolates of *S. apiospermum* for individual circuits achieved using the dynamic model.

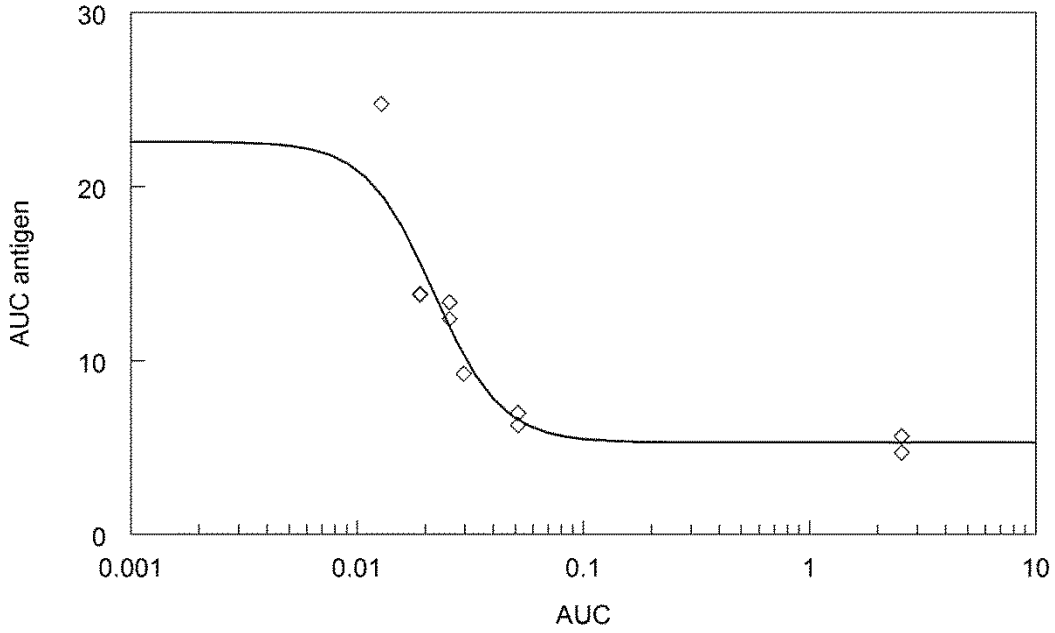

Figure 5. 7

Total AUC for *Scedosporium* specific antigen detected at 450nm, versus $AUC_{72\text{-}96}$ for F901318 (mg.hr/L). Equations were generated in ADAPT 5 using the maximum likelihood estimator.

AUCantigen = 22.58-(17.30*(AUC)^2.912)/((AUC)^2.912+0.02177^2.912)

R^2= 0.872

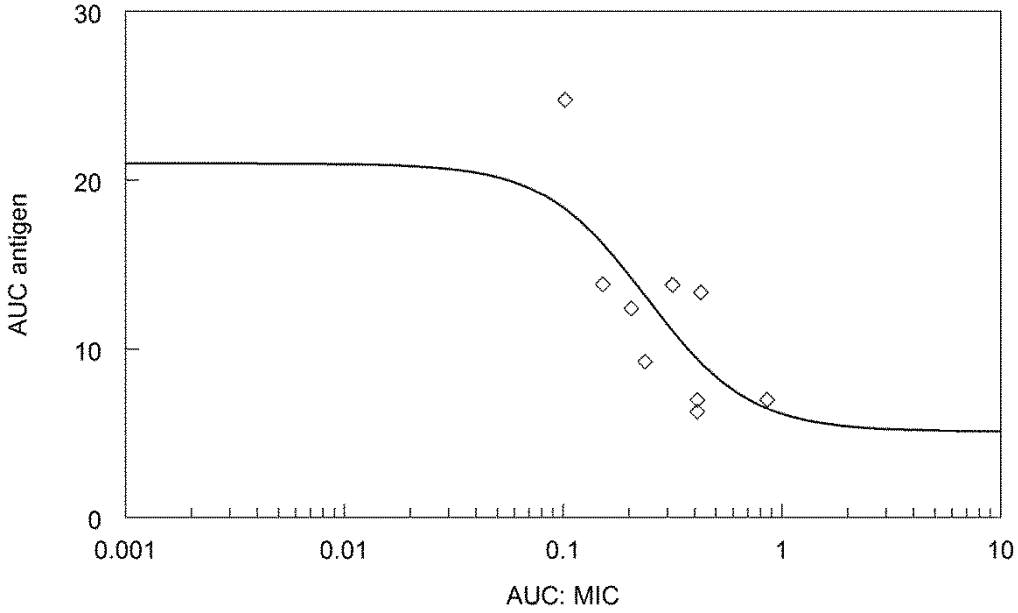

Figure 5. 8

Total AUC for *Scedosporium* specific antigen detected at 450nm, versus F901318 AUC_{72-96}: MIC (EUCAST methodology). Equations were generated in ADAPT 5 using the maximum likelihood estimator.

AUCantigen = 20.99-(15.89*(AUC:MIC)^1.862)/((AUC:MIC)^1.862+0.2405^1.862)

R^2= 0.780

5.33 *Fusarium solani* models

5.331 Static models of invasive fusariosis

The exposure- response relationships for F901318 are described in Figures 5.9. Antigen detection was consistent for samples obtained from the static model. Maximum absorbance values of approximately 1.5 were obtained from the alveolar compartments of inserts infected with *F. solani* that were untreated or exposed to low doses of drug. Slightly lower maximum absorbencies of approximately 0.8-1 were achieved from samples obtained from the endothelial compartment. F901318 demonstrated a similar concentration-dependent inhibition of antigen release was observed for both isolates of *F. solani*. For the endothelial compartments clear exposure response relationships are defined however only the top concentrations of 5 mg/L were sufficient to maximally suppress antigen release for both strains. The concentrations required to suppress antigen release were higher for the alveolar compartment than for the endothelial compartment in all experiments.

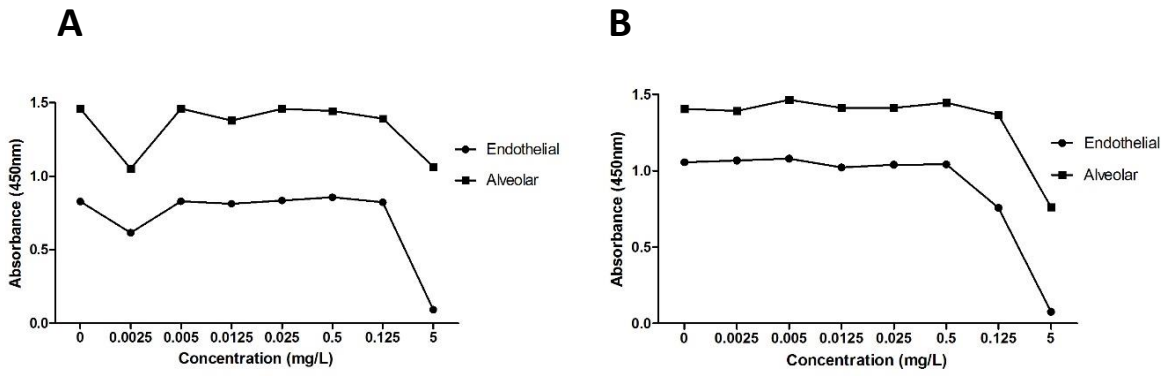

Figure 5. 9

Pharmacokinetics and pharmacodynamics of F901318 in a static model against *F. solani* isolates 6951 (A) & 7328 (B).

5.332 Dynamic models of invasive fusariosis

The exposure-response relationships of F901318 against *F. solani* were defined for both clinical isolates. There were differences in the PK-PD relationships between isolates. In this dynamic model, trough concentrations within the range of 1 mg/L- 2 mg/L and Cmax concentrations of around 4 mg/L, estimating an $AUC_{0\text{-}24}$-:MIC ratio of approximately 14 (Figure 5.10 I&J, Table 5.5) is sufficient to maximally suppress antigen release for isolate CNM-6951 using a cut-off value of 0.1 to describe complete antigen suppression. Cmax and trough concentrations of approximately 1.2 mg/L and 0.2 mg/L- 0.4 mg/L respectively equating to an AUC:MIC value of approximately 3 (Figure 5.11 G-H, Table 5.5) were sufficient to maximally suppress antigen release for isolate CNM-7328 in this model. A minimal amount of breakthrough was observed at 96 hours post inoculation when exposed to these concentrations for both strains.

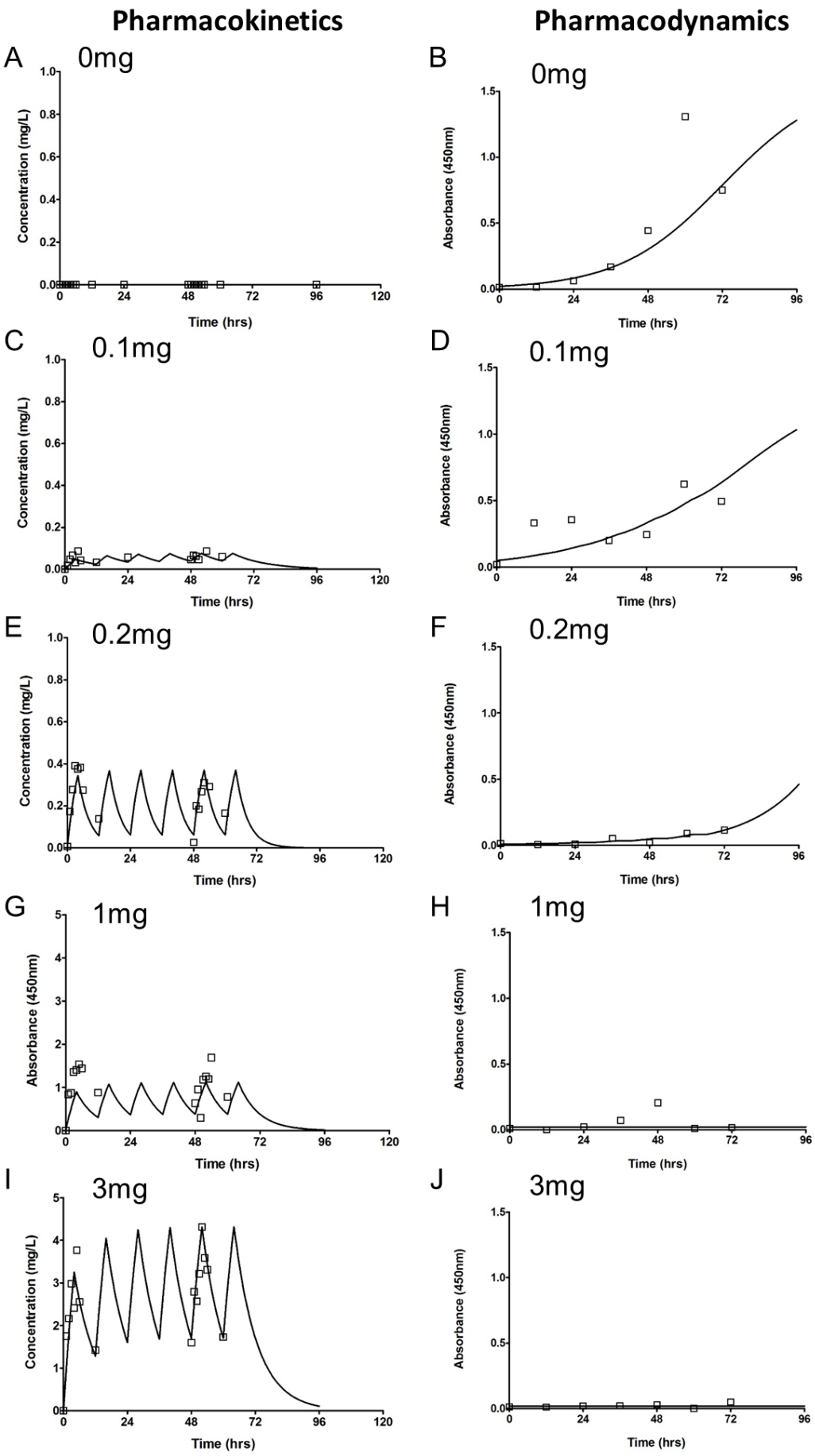

Figure 5. 10 Pharmacokinetics and pharmacodynamics of F901318 against *F. solani* CNM-6951.

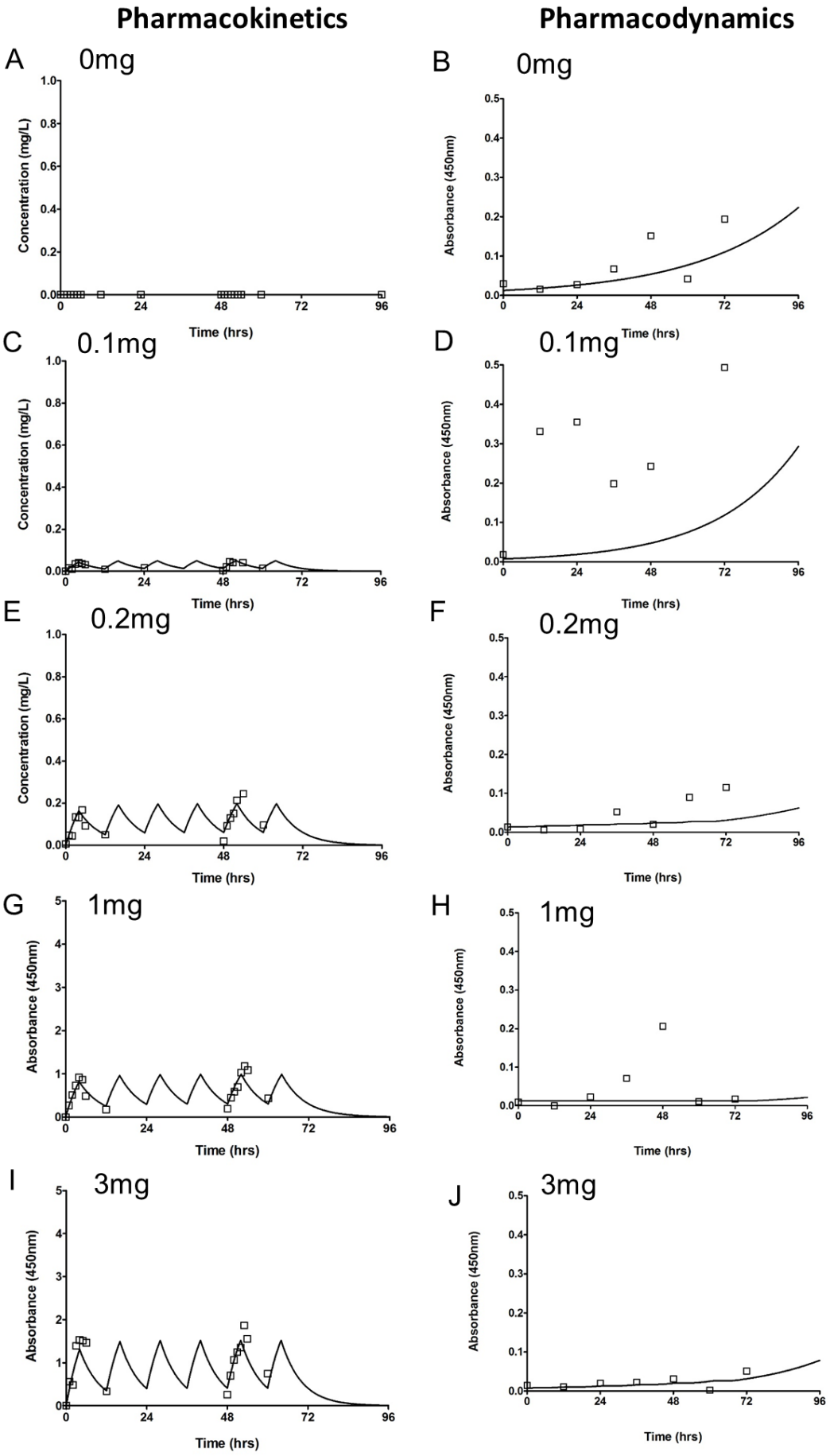

Figure 5. 11 Pharmacokinetics and pharmacodynamics of F901318 against *F. solani* CNM-7328.

6.333 Mathematical modelling

The fit of the mathematical model to the data was acceptable (Figure 5.12). The fit of the Bayesian posterior estimates for each circuit is shown in Figures 5.10-5.11. Median posterior parameter estimates for each model can be seen in Table 5.4. Predicted $AUC_{48\text{-}72}$ values (mg.hr/L) for F901318 and total AUC for the antigen are displayed in Table 5.6.

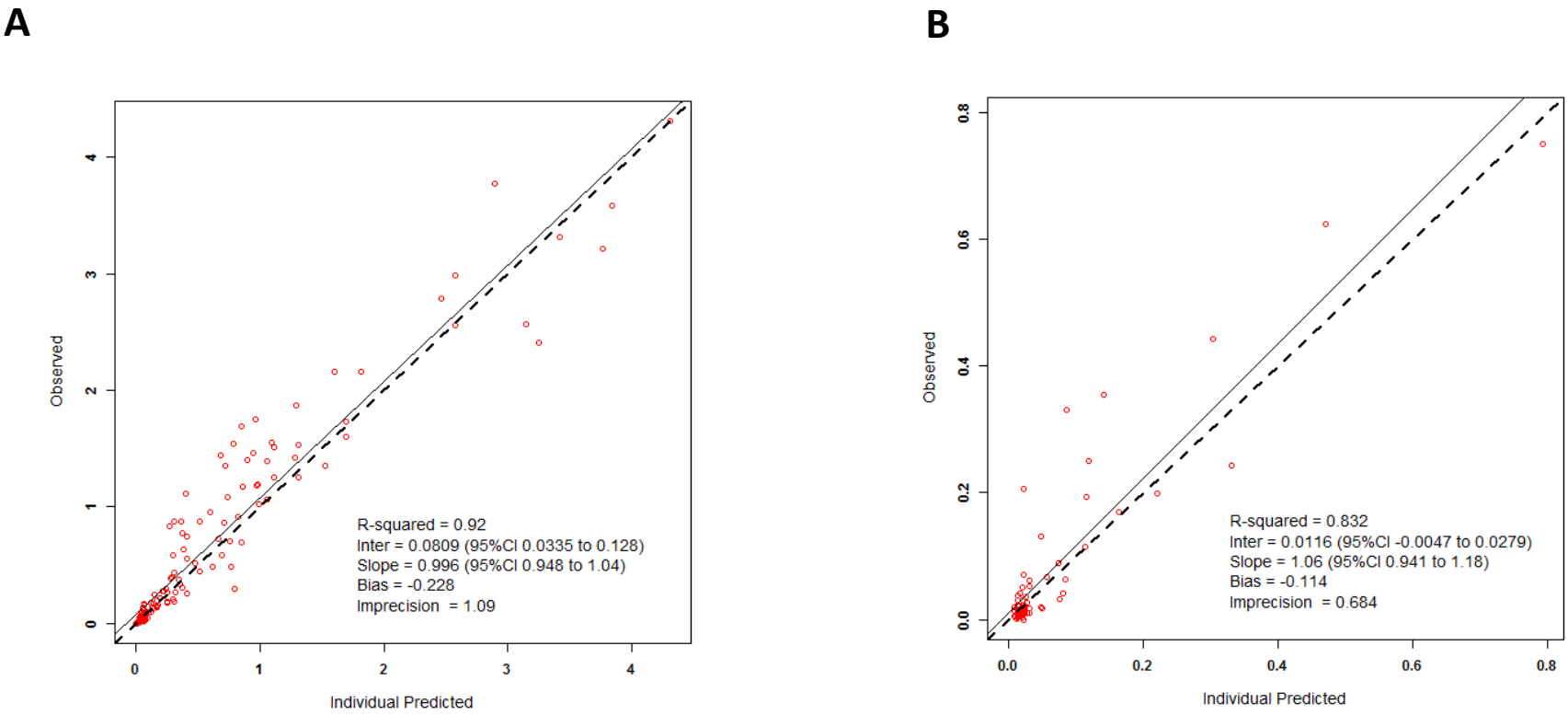

Figure 5. 12

Observed vs predicted graphs for F901318 versus *F. solani* after the Bayesian step, generated using Pmetrics for (A) pharmacokinetics data from 10 individual circuits and (B) pharmacodynamics data as measured by antigen from 10 individual circuits.

Isolate	Dosage	Cl	V (L)	Kgmax	POPMAX	C50	Hg	IC1
CNM-6951	0	0.09	0.75	0.06	1.59	0.02	24.09	0.02
CNM-6951	0.1	0.14	1.81	0.05	1.39	0.09	3.01	0.05
CNM-6951	0.2	0.09	0.38	0.06	6.97	0.22	14.81	0.01
CNM-6951	1	0.12	0.86	0.06	1.60	0.01	29.84	0.02
CNM-6951	3	0.09	0.74	0.06	1.59	0.02	23.95	0.02
CNM-7328	0	0.14	0.92	0.03	6.97	0.10	22.04	0.01
CNM-7328	0.1	0.28	1.67	0.04	6.97	0.86	11.86	0.01
CNM-7328	0.2	0.14	0.91	0.03	6.96	0.10	22.19	0.01
CNM-7328	1	0.14	0.92	0.03	6.97	0.10	22.18	0.01
CNM-7328	3	0.28	1.67	0.04	6.97	0.86	11.86	0.01

Table 5. 4

The median posterior parameter estimates from the mathematical model using data from 10 individual circuits.. Cl represents the estimated clearance of F901318 from the circuit; V; the estimated volume of the central compartment; Kgmax, the predicted rate of growth of *F. solani* in the circuit; POPMAX, the maxima obtained from the ELISA assay; C50, the concentration of F901318 that 50% suppression of antigen is obtained; Hg, the slope function to describe *F. solani* growth in both absence and presence of drug; IC1, the initial conditions for the pharmacodynamics dataset, representing background noise of the assay.

Strain	Dose (mg/ q12)	Predicted AUC_{48-72} F901318 (mg.hr/L)	Predicted AUC_{0-72} antigen
F. solani CNM-6951	0	0	3.275
	0.1	0.73	2.90
	0.2	2.96	1.50
	1	14.74	0.95
	3	21.78	1.20
F. solani CNM-7328	0	0	17.81
	0.1	1.36	17.90
	0.2	4.67	2.79
	1	17.20	1.52
	3	69.86	1.45

Table 5. 5

Model predicted F901318 AUC_{48-72} and area under antigen curves (0-72) for individual circuits achieved using the dynamic model.

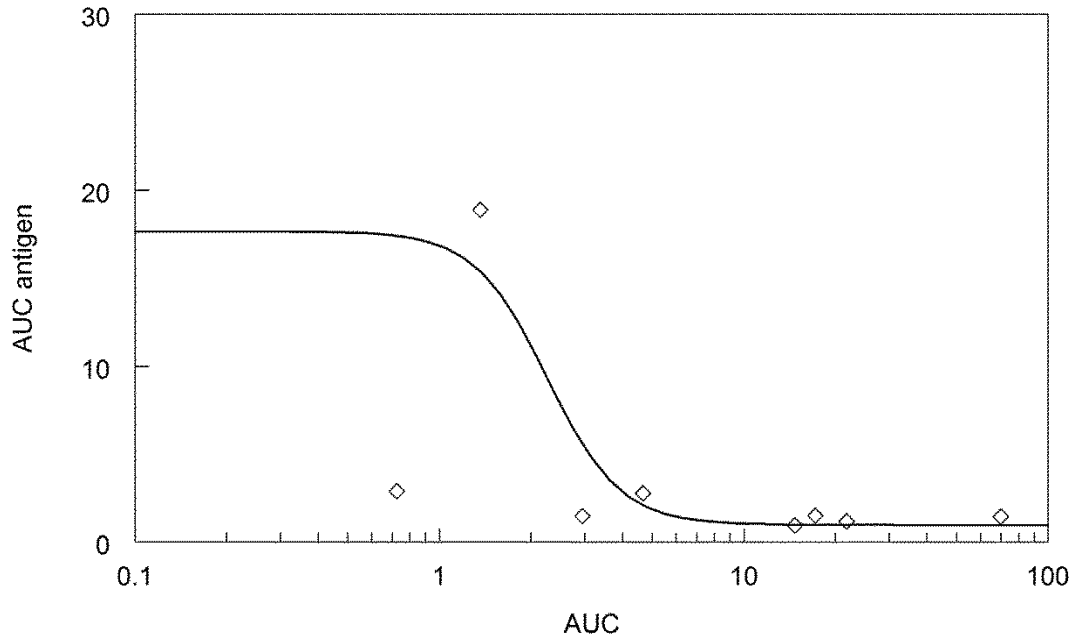

Figure 5. 13

Total AUC for *Fusarium* specific antigen detected at 450nm, versus $AUC_{48\text{-}72}$ for F901318 (mg.hr/L). Equations were generated in ADAPT 5 using the maximum likelihood estimator.

AUCantigen= 17.68-(16.69*(AUC)^3.645)/((AUC)^3.645+2.263^3.645)

R^2= 0.353

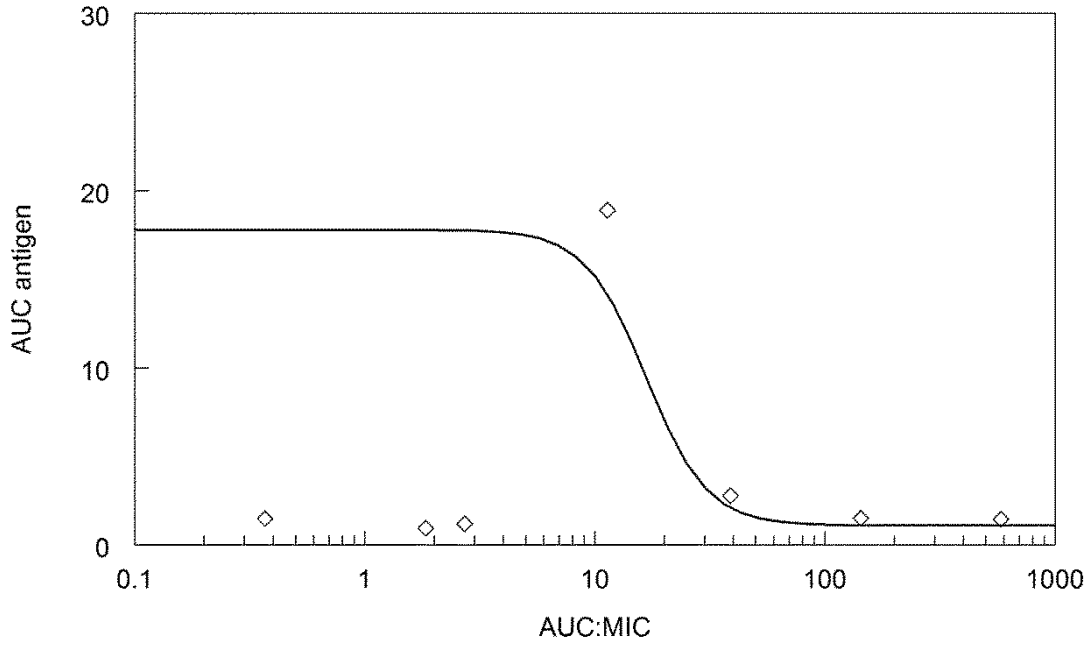

Figure 5. 14

Total AUC for *Fusarium* specific antigen detected at 450nm, versus F901318 AUC_{48-72}:MIC (EUCAST methodology). Equations were generated in ADAPT 5 using the maximum likelihood estimator.

AUCantigen = 17.8-(16.69*(AUC:MIC)^3.280)/((AUC:MIC)^3.280+16.74^3.280)

R^2= 0.055

5.4 CONCLUSIONS

Scedosporium spp. and *Fusarium* spp. are emerging fungal pathogens. Invasive diseases with these organisms have high mortality rates owing to a lack of treatment options. The development pipeline for novel antifungal agents targeting novel molecular mechanisms is severely lagging the clinical need for new drugs to treat these infections.

F901318 is a novel antifungal agent and is the most advanced member of the orotomide class of agents. F901318 demonstrates *in vitro* and *in vivo* efficacy against both wild-type and triazole resistant isolates of *A. fumigatus* (Beckmann, Binder et al. 2015, Fothergill, Wiederhold et al. 2015, Law, Oliver et al. 2015). The preclinical and clinical pharmacokinetic data from phase I studies suggest a favourable ADME profile for this agent and the agent appears well tolerated (Kennedy, Allen et al. 2015). Although primarily developed for the treatment of invasive aspergillosis, F901318 also demonstrates potent *in vitro* activity against isolates of *S. apiospermum* and *F. solani* (Fothergill, Wiederhold et al. 2015, Fothergill, Law et al. 2016). The diagnosis of invasive scedosporiosis and fusariosis is challenging. The histopathological and morphological characteristics of these fungi are often indistinguishable from those of other moulds such as *Aspergillus* spp. There are currently no clinically validated biomarkers for the diagnosis of these fatal diseases. The development of novel platforms for a quick and accurate diagnosis alongside an optimised portfolio of therapeutics could greatly improve the clinical outcomes of invasive infections with these rare species.

This investigation presents an *in vitro* PK-PD dataset for novel antifungal agent, F901318 against three isolates of *S. apiospermum* and two isolates of *F. solani.* Novel methodologies for the detection of membrane- expressed antigens specific to *Scedosporium* and *Fusairum* spp. were used as a measure of disease progression.

5.41 F901318 against isolates of *S. apiospermum*

Static studies demonstrate defined dose-response relationships for F901318 and isolates of *S. apiospermum*, *P. boydii* and *P. ellipsoidea*. There are pharmacodynamic differences between the isolates. One isolate of *S. apiospermum* demonstrated persistent growth even in the presence of the highest concentration of drug used. This is not in proportion to the MIC of 0.125 mg/L or data obtained from dynamic studies for this isolate. This is also the case for *S. apiospermum* 8353 for which an MIC of 0.006 mg/L is reported however maximal suppression of antigen is not achieved at dosages <0.5 mg/L in the static model.

The pharmacodynamic behaviour of *S. apiospermum* in untreated controls is similar to that seen in in voriconazole experiments demonstrating the reproducibility of this model in the assessment of novel antifungals. Isolates exhibit similar patterns of growth and a decreased susceptibility regardless of the agent used. As discussed in Chapter IV, starting inoculum is an important consideration when determining the severity of this model. A disease state too severe may counteract the antifungal effect of the agent used. It is also important to note that in some experiments there is a variation in the antigen concentrations measured from the alveolar compartment of the models. This may again be due to the variable amount of fungi that is extracted when flooding the surface of the alveolar layer with PBS. Another explanation may be that a destruction of the cell layer in some transwells may have allowed the antigen to pass through the porous membrane into the endothelial compartment causing variable antigen concentrations in lavage samples.

Dynamic studies present a concentration dependent reduction in antigen when treated with F901318. Phase I single ascending dose trials demonstrate that F901318 is well tolerated in healthy volunteers receiving up to 4mg/kg of drug. This dosage corresponded to total AUCs of 38.04mg.hr/L over a 120 hour period in the clinic. In this dynamic model of scedosporiosis $AUC_{72\text{-}96}$ values of approximately 2.55mg.hr/L were associated with a maximal antifungal

effect against all isolates of *S. apiospermum*, using a twice-daily dosing regimen of 0.05mg. Clinical exposures of F901318 may therefore have the potential to treat an invasive disease with these isolates. Hope et al. described the pharmacodynamics of F901318 in a murine model of aspergillosis. F901318 demonstrated time-dependent killing in this investigation. It is suggested that either T>MIC or C_{min}: MIC may be the pharmacodynamic parameters that best predict *in vivo* efficacy. C_{min}: MIC ratios of 10-30, corresponding to C_{min} values of approximately 1 mg/L were associated with near maximal reduction in galactomannan in this study (Hope, Livermore et al. 2015). Dynamic studies suggest that isolates of *S. apiospermum* were readily treatable with F901318 trough levels of 0.02 mg/L- 0.05 mg/L. These estimates are markedly lower than those suggested for the treatment of aspergillosis from murine studies. This dynamic model simulates an early invasive disease and provides direct exposure of fungi to drug in the absence of immunological effectors which may explain the augmented antifungal effect seen here. It is also important to note that the pharmacodynamic study by Hope et al. used isolates of *A. fumigatus* that demonstrated a range of susceptibilities. Whereas the isolates of *S. apiospermum* studied here are largely representative of a susceptible population (Table 5.1). There was a lesser correlation between the decline in antigen (total AUC) and the AUC of F901318 ($R^2 = 0.872$) compared to that seen with voriconazole ($R^2 = 0.986$), a known AUC driven drug. This association became weaker when the MIC was incorporated ie. the AUC:MIC ($R^2 = 0.78$) suggesting that this pharmacodynamic parameter may not be predictive of antifungal effect in this model. This further supports that, consistent with PK-PD studies done in animals F901318 may exhibit time-dependent killing in this model.

6.42 F901318 against isolates of *F. solani*

Static studies demonstrated a clear concentration dependent decline in antigen upon exposure to F901318 against both isolates of *F. solani*. Concentrations of approximately 5 mg/L were sufficient to suppress the antigen in this model. These findings in contrast to ≥16 mg/L for voriconazole are encouraging for the potential use of F901318 to treat infections with isolates that are not susceptible to voriconazole using current dosing strategies. Maximum absorbency values in untreated transwells for each of these experiments were all around 1.5 indicating successful invasion of *F. solani* through the cellular bilayer.

In a dynamic setting, low absorbance values were obtained from untreated circuits using isolate CNM-7328. The low antigen levels detected in a dynamic setting using this isolate were consistent with voriconazole data and may be due to the incapacity of this isolate to grow in the absence of high amounts of glucose (Srivastava, Pathak et al. 2011). CNM-6951 antigen concentrations decline after 60 hours consistently between models. This may due to a reduced expression of the antigen at high fungal densities or clearance of the fungi by the model during a stationary phase of growth.

As F901318 progressed from preclinical to clinical evaluation, data relating to the clinical dosing regimen had become available. In this model of fusariosis, F901318 was administered as a four-hour infusion twice-daily. Predicted $AUC_{48\text{-}72}$ values of 14.74 and 17.20 mg.hr/L, corresponding to total AUCs of 44.22 and 51.60 mg.hr/L, were associated with maximal antifungal effect against isolates 6951 and 7328 respectively in this model. These values are slightly higher than exposures seen in single ascending dose trials (38.04 mg.hr/L) at the highest dose administered suggesting that higher dosages or a different dosing regimen may be necessary for the treatment of *F. solani* invasive disease in the clinic.

The pharmacodynamic association between the AUC_{48-72} of F901318 and antifungal efficacy in this model was poor. C_{min} values within the range of the respective MIC values were observed to suppress antigen release for both isolates suggesting the MIC may be a good predictor of dose response in these experiments. However, upon further analysis there was no relationship between the AUC:MIC and efficacy in this model (Figure 5.15, R^2= 0.055) and a noticeably weakened association was seen compared to AUC alone (Figure 5.14, R^2= 0.353). These pharmacodynamic analyses support that the AUC: MIC may not be an important predictor of antifungal effect for this agent.

These analyses represent the first *in vitro* PK-PD dataset for novel antifungal agent, F901318, against isolates of *S. apiospermum* and *F. solani*. These models are able to link clinically relevant exposures to the pharmacodynamic behaviour of fungi whilst accounting for key interactions such as protein binding (eg. the use of 2% protein). Their use for the delineation of PK-PD relationships may be an important advancement in the assessment of novel antifungal agents and may provide a basis for the further investigation into the development of F901318 for the treatment of these rare and emerging mycoses. This work also contributes towards a further understanding into the presentation and detection of the antigens described by Thornton et al. under flow conditions and may assist in their efforts to develop these assays as a clinical product.

CHAPTER VI

General conclusions

The general aims of this thesis were comprised of two key components. Firstly, to develop *in vitro* models of invasive fungal infections that can successfully mimic the human PK of antifungal agents. Secondly, to refine these models for the establishment of key PK-PD relationships of new and existing agents that may guide the use of antifungal therapy in the clinic.

The models simulated human-like PK of isavuconazole and voriconazole, a marked advantage over animal models using these agents. Furthermore, mathematical modelling provided a link between the dose-exposure (PK) and suppression of antigen (PD) in these models. This allowed for the estimation of the PD indexes associated with maximal antifungal efficacy, in terms of the AUC: MIC.

PK-PD investigations for novel agents should be carried out in *in vitro* models such as those described, animal models and in patient populations. Datasets should be cross-validated for the recommendation of accurate PD targets. The bridging of experimental data to clinical populations using PK-PD simulation may help to delineate patient response to therapy to specific organisms provided the clinical datasets are sufficiently empowered. Clinical datasets describing the use of isavuconazole in patient populations are now available. The bridging of these experimental data may help to guide antifungal dosing for the potential individualisation of isavuconazole therapy in the future. A key limitation to these studies is the absence of immune- mediated suppression of organism. Therefore, the physiological response to disease and the resultant clearance of organism seen in humans is not accounted for. However, the absence of immune function allows for the direct estimation of antifungal suppression that can be attributed to drug. Another important consideration is the difference in protein levels that were used in the models compared to those present in humans (2% vs ~40. It would be necessary to incorporate the effect of protein binding into the

models when bridging to humans in order to properly translate the experimental findings into a clinical context.

Limited data on the human PK of F901318 were available at the time of this study. It is therefore undetermined whether the exposures of drug achieved using these models are clinically relevant. The exposure-response relationships were defined at the dosages tested and contribute to our understanding of the minimum exposures that may be necessary to achieve in the treatment of invasive disease with *S. apiospermum* and *F. solani*. Whether these levels are exceeded in the clinic is yet to be determined. As only the highest dose of F901318 generated levels of drug that were above the MIC for any significant amount of time, dose- fractionation studies for the further investigation into the PD targets, in terms of the T>MIC, would be necessary.

REFERENCES

1. Ader, F., A. L. Bienvenu, B. Rammaert and S. Nseir (2009). "Management of invasive aspergillosis in patients with COPD: rational use of voriconazole." Int J Chron Obstruct Pulmon Dis **4**: 279-287.
2. Adler-Moore, J. P. and R. T. Proffitt (2008). "Amphotericin B lipid preparations: what are the differences?" Clinical Microbiology and Infection **14**: 25-36.
3. Al-Maqtoofi, M. and C. R. Thornton (2016). "Detection of human pathogenic Fusarium species in hospital and communal sink biofilms by using a highly specific monoclonal antibody." Environmental Microbiology: n/a-n/a.
4. Al-Maqtoofi, M. and C. R. Thornton (2016). "Detection of human pathogenic Fusarium species in hospital and communal sink biofilms by using a highly specific monoclonal antibody." Environ Microbiol.
5. Al-Nakeeb, Z., V. Petraitis, J. Goodwin, R. Petraitiene, T. J. Walsh and W. W. Hope (2015). "Pharmacodynamics of Amphotericin B Deoxycholate, Amphotericin B Lipid Complex, and Liposomal Amphotericin B against Aspergillus fumigatus." Antimicrob Agents Chemother **59**(5): 2735-2745.
6. Al-Nakeeb, Z., A. Sudan, A. R. Jeans, L. Gregson, J. Goodwin, P. A. Warn, T. W. Felton, S. J. Howard and W. W. Hope (2012). "Pharmacodynamics of Itraconazole against Aspergillus fumigatus in an In Vitro Model of the Human Alveolus: Perspectives on the Treatment of Triazole-Resistant Infection and Utility of Airway Administration." Antimicrob Agents Chemother **56**(8): 4146-4153.
7. Al-Saigh, R., A. Elefanti, A. Velegraki, L. Zerva and J. Meletiadis (2012). "In Vitro Pharmacokinetic/Pharmacodynamic Modeling of Voriconazole Activity against Aspergillus Species in a New In Vitro Dynamic Model." Antimicrob Agents Chemother **56**(10): 5321-5327.
8. Alastruey-Izquierdo, A., M. Cuenca-Estrella, A. Monzon, E. Mellado and J. L. Rodriguez-Tudela (2008). "Antifungal susceptibility profile of clinical Fusarium spp. isolates identified by molecular methods." J Antimicrob Chemother **61**(4): 805-809.
9. Alekseeva, L., D. Huet, F. Femenia, I. Mouyna, M. Abdelouahab, A. Cagna, D. Guerrier, V. Tichanne-Seltzer, A. Baeza-Squiban, R. Chermette, J. P. Latge and N. Berkova (2009). "Inducible expression of beta defensins by human respiratory epithelial cells exposed to Aspergillus fumigatus organisms." Bmc Microbiology **9**.
10. Ally, R., D. Schurmann, W. Kreisel, G. Carosi, K. Aguirrebengoa, B. Dupont, M. Hodges, P. Troke, A. J. Romero and G. Esophageal Candidiasis Study (2001). "A randomized, double-blind, double-dummy, multicenter trial of voriconazole and fluconazole in the treatment of esophageal candidiasis in immunocompromised patients." Clin Infect Dis **33**(9): 1447-1454.
11. Andes, D., K. Marchillo, T. Stamstad and R. Conklin (2003). "In vivo pharmacokinetics and pharmacodynamics of a new triazole, voriconazole, in a murine candidiasis model." Antimicrob Agents Chemother **47**(10): 3165-3169.
12. Arendrup, M. C., M. Cuenca-Estrella, C. Lass-Florl, W. Hope and A. Eucast (2012). "EUCAST technical note on the EUCAST definitive document EDef 7.2: method for the determination of broth dilution minimum inhibitory concentrations of antifungal agents for yeasts EDef 7.2 (EUCAST-AFST)." Clin Microbiol Infect **18**(7): E246-247.
13. Arendrup, M. C., R. H. Jensen, K. Grif, M. Skov, T. Pressler, H. K. Johansen and C. Lass-Flörl (2012). "In Vivo Emergence of Aspergillus terreus with Reduced Azole Susceptibility and a Cyp51a M217I Alteration." Journal of Infectious Diseases **206**(6): 981-985.

14. Auberger, J., C. Lass-Flörl, M. Aigner, J. Clausen, G. Gastl and D. Nachbaur (2012). "Invasive fungal breakthrough infections, fungal colonization and emergence of resistant strains in high-risk patients receiving antifungal prophylaxis with posaconazole: real-life data from a single-centre institutional retrospective observational study." Journal of Antimicrobial Chemotherapy **67**(9): 2268-2273.
15. Bahar, F. G., K. Ohura, T. Ogihara and T. Imai (2012). "Species difference of esterase expression and hydrolase activity in plasma." Journal of Pharmaceutical Sciences **101**(10): 3979-3988.
16. Bal, A. M. (2010). "The echinocandins: three useful choices or three too many?" International Journal of Antimicrobial Agents **35**(1): 13-18.
17. Beckmann, N., U. Binder, C. Lass- Florl, W. Hopre, J. Livermore, J. Oliver, G. Sibley, M. Birch and D. Law (2015). Activity of F901318, a Member of the New Orotomide Class of Antifungal Agents, against Clinical Aspergillus Isolates from the UK and Austria. Interscience Conference for Antimicrobial Agents and Chemotherapy. San Diego, U.S.
18. Bellanger, A. P., L. Millon, K. Khoufache, D. Rivollet, I. Bieche, I. Laurendeau, M. Vidaud, F. Botterel and S. Bretagne (2009). "Aspergillus fumigatus germ tube growth and not conidia ingestion induces expression of inflammatory mediator genes in the human lung epithelial cell line A549." J Med Microbiol **58**(Pt 2): 174-179.
19. Blanco, J. L., R. Hontecillas, E. Bouza, I. Blanco, T. Pelaez, P. Munoz, J. P. Molina and M. E. Garcia (2002). "Correlation between the elastase activity index and invasiveness of clinical isolates of Aspergillus fumigatus." Journal of Clinical Microbiology **40**(5): 1811-1813.
20. Bocanegra, R., L. K. Najvar, S. Hernandez, D. I. McCarthy and J. R. Graybill (2005). "Caspofungin and liposomal amphotericin B therapy of experimental murine scedosporiosis." Antimicrob Agents Chemother **49**(12): 5139-5141.
21. Boutati, E. I. and E. J. Anaissie (1997). "Fusarium, a Significant Emerging Pathogen in Patients With Hematologic Malignancy: Ten Years' Experience at a Cancer Center and Implications for Management." Blood **90**(3): 999-1008.
22. Box, H., J. Livermore, A. Johnson, L. McEntee, T. W. Felton, S. Whalley, J. Goodwin and W. W. Hope (2016). "Pharmacodynamics of Isavuconazole in a Dynamic In Vitro Model of Invasive Pulmonary Aspergillosis." Antimicrobial Agents and Chemotherapy **60**(1): 278-287.
23. Bruggemann, R. J., N. M. Blijlevens, D. M. Burger, B. Franke, P. F. Troke and J. P. Donnelly (2010). "Pharmacokinetics and safety of 14 days intravenous voriconazole in allogeneic haematopoietic stem cell transplant recipients." J Antimicrob Chemother **65**(1): 107-113.
24. Calvo, E., F. J. Pastor, V. Salas, E. Mayayo and J. Guarro (2012). "Combined Therapy of Voriconazole and Anidulafungin in Murine Infections by Aspergillus flavus." Mycopathologia **173**(4): 251-257.
25. Campa-Thompson, M. M., J. A. West, J. M. Guileyardo, C. W. Spak, L. M. Sloan and S. G. Beal (2014). "Clinical and morphologic findings in disseminated Scedosporium apiospermum infections in immunocompromised patients." Proc (Bayl Univ Med Cent) **27**(3): 253-256.
26. Campo, M., R. E. Lewis and D. P. Kontoyiannis (2010). "Invasive fusariosis in patients with hematologic malignancies at a cancer center: 1998–2009." Journal of Infection **60**(5): 331-337.
27. Capilla, J. and J. Guarro (2004). "Correlation between in vitro susceptibility of Scedosporium apiospermum to voriconazole and in vivo outcome of scedosporiosis in guinea pigs." Antimicrob Agents Chemother **48**(10): 4009-4011.
28. Capilla, J., E. Mayayo, C. Serena, F. J. Pastor and J. Guarro (2004). "A novel murine model of cerebral scedosporiosis: lack of efficacy of amphotericin B." J Antimicrob Chemother **54**(6): 1092-1095.
29. Capilla, J., C. Serena, F. J. Pastor, M. Ortoneda and J. Guarro (2003). "Efficacy of voriconazole in treatment of systemic scedosporiosis in neutropenic mice." Antimicrob Agents Chemother **47**(12): 3976-3978.

30. Castiglioni, B., D. A. Sutton, M. G. Rinaldi, J. Fung and S. Kusne (2002). "Pseudallescheria boydii (Anamorph Scedosporium apiospermum). Infection in solid organ transplant recipients in a tertiary medical center and review of the literature." Medicine (Baltimore) **81**(5): 333-348.
31. Chandrasekar, P. H. and J. D. Sobel (2006). "Micafungin: A New Echinocandin." Clinical Infectious Diseases **42**(8): 1171-1178.
32. Chen, S. C.-A., M. A. Slavin and T. C. Sorrell (2011). "Echinocandin Antifungal Drugs in Fungal Infections: A Comparison." Drugs **71**(1): 11-41 10.2165/11585270-000000000-000000000.
33. Choi, J. H., E. Brummer and D. A. Stevens (2004). "Combined action of micafungin, a new echinocandin, and human phagocytes for antifungal activity against Aspergillus fumigatus." Microbes Infect **6**(4): 383-389.
34. Chotirmall, S., B. Mirkovic, G. Lavelle and N. McElvaney (2014). "Immunoevasive Aspergillus Virulence Factors." Mycopathologia **178**(5-6): 363-370.
35. Clemons, K. V., M. Espiritu, R. Parmar and D. A. Stevens (2005). "Comparative efficacies of conventional amphotericin b, liposomal amphotericin B (AmBisome), caspofungin, micafungin, and voriconazole alone and in combination against experimental murine central nervous system aspergillosis." Antimicrob Agents Chemother **49**(12): 4867-4875.
36. CLSI (2008). " M38-A2 Reference method for broth dilution antifungal susceptibility testing of filamentous fungi; approved standard CLSI document ".
37. Cornely, O. A., J. Maertens, M. Bresnik, R. Ebrahimi, A. J. Ullmann, E. Bouza, C. P. Heussel, O. Lortholary, C. Rieger, A. Boehme, M. Aoun, H. A. Horst, A. Thiebaut, M. Ruhnke, D. Reichert, N. Vianelli, S. W. Krause, E. Olavarria and R. Herbrecht (2007). "Liposomal amphotericin B as initial therapy for invasive mold infection: A randomized trial comparing a high-loading dose regimen with standard dosing (AmBiLoad trial)." Clinical Infectious Diseases **44**(10): 1289-1297.
38. Cortez, K. J., E. Roilides, F. Quiroz-Telles, J. Meletiadis, C. Antachopoulos, T. Knudsen, W. Buchanan, J. Milanovich, D. A. Sutton, A. Fothergill, M. G. Rinaldi, Y. R. Shea, T. Zaoutis, S. Kottilil and T. J. Walsh (2008). "Infections caused by Scedosporium spp." Clin Microbiol Rev **21**(1): 157-197.
39. Cuenca-Estrella, M., A. Alastruey-Izquierdo, L. Alcazar-Fuoli, L. Bernal-Martinez, A. Gomez-Lopez, M. J. Buitrago, E. Mellado and J. L. Rodriguez-Tudela (2008). "In Vitro Activities of 35 Double Combinations of Antifungal Agents against Scedosporium apiospermum and Scedosporium prolificans." Antimicrob Agents Chemother **52**(3): 1136-1139.
40. Dagenais, T. R. T. and N. P. Keller (2009). "Pathogenesis of Aspergillus fumigatus in Invasive Aspergillosis." Clinical Microbiology Reviews **22**(3): 447-465.
41. Denning, D. W. (1991). "Epidemiology and pathogenesis of systemic fungal infections in the immunocompromised host." Journal of Antimicrobial Chemotherapy **28**(suppl B): 1-16.
42. Denning, D. W. (1998). "Invasive aspergillosis." Clin Infect Dis **26**(4): 781-803; quiz 804-785.
43. Denning, D. W., P. Ribaud, N. Milpied, D. Caillot, R. Herbrecht, E. Thiel, A. Haas, M. Ruhnke and H. Lode (2002). "Efficacy and safety of voriconazole in the treatment of acute invasive aspergillosis." Clin Infect Dis **34**(5): 563-571.
44. Desai, A., Kovanda, L, Kowalski, D, Lu, Q,Townsend, R.W (2014). Isavuconazole (ISA) Population Pharmacokinetic Modeling from Phase 1 and Phase 3 Clinical Trials and Target Attainment Analysis. Interscience Conference on Antimicrobial Agents and Chemotherapy (ICAAC), Washington, DC.
45. Diekema, D. J., S. A. Messer, R. J. Hollis, R. N. Jones and M. A. Pfaller (2003). "Activities of caspofungin, itraconazole, posaconazole, ravuconazole, voriconazole, and amphotericin B against 448 recent clinical isolates of filamentous fungi." J Clin Microbiol **41**(8): 3623-3626.
46. Dignani, M. C. and E. Anaissie (2004). "Human fusariosis." Clinical Microbiology and Infection **10**: 67-75.

47. Dimopoulos, G., F. Frantzeskaki, G. Poulakou and A. Armaganidis (2012). "Invasive aspergillosis in the intensive care unit." Ann N Y Acad Sci **1272**: 31-39.
48. Docobo-Perez, F., G. L. Drusano, A. Johnson, J. Goodwin, S. Whalley, V. Ramos-Martin, M. Ballestero-Tellez, J. M. Rodriguez-Martinez, M. C. Conejo, M. van Guilder, J. Rodriguez-Bano, A. Pascual and W. W. Hope (2015). "Pharmacodynamics of fosfomycin: insights into clinical use for antimicrobial resistance." Antimicrob Agents Chemother **59**(9): 5602-5610.
49. Dolton, M. J., J. E. Ray, S. C. Chen, K. Ng, L. G. Pont and A. J. McLachlan (2012). "Multicenter study of voriconazole pharmacokinetics and therapeutic drug monitoring." Antimicrob Agents Chemother **56**(9): 4793-4799.
50. Dupont, B. (2002). "Overview of the lipid formulations of amphotericin B." Journal of Antimicrobial Chemotherapy **49**: 31-36.
51. Esnakula, A. K., I. Summers and T. J. Naab (2013). "Fatal disseminated fusarium infection in a human immunodeficiency virus positive patient." Case Rep Infect Dis **2013**: 379320.
52. Espinel-Ingroff, A. (2001). "Comparison of the E-test with the NCCLS M38-P method for antifungal susceptibility testing of common and emerging pathogenic filamentous fungi." Journal of Clinical Microbiology **39**(4): 1360-1367.
53. Espinel-Ingroff, A. (2003). "In vitro antifungal activities of anidulafungin and micafungin, licensed agents and the investigational triazole posaconazole as determined by NCCLS methods for 12,052 fungal isolates: review of the literature." Rev Iberoam Micol **20**(4): 121-136.
54. Espinel-Ingroff, A., A. Chowdhary, G. M. Gonzalez, C. Lass-Flörl, E. Martin-Mazuelos, J. Meis, T. Peláez, M. A. Pfaller and J. Turnidge (2013). "Multicenter Study of Isavuconazole MIC Distributions and Epidemiological Cutoff Values for Aspergillus spp. for the CLSI M38-A2 Broth Microdilution Method." Antimicrob Agents Chemother **57**(8): 3823-3828.
55. Espinel-Ingroff, A., E. Johnson, H. Hockey and P. Troke (2008). "Activities of voriconazole, itraconazole and amphotericin B in vitro against 590 moulds from 323 patients in the voriconazole Phase III clinical studies." J Antimicrob Chemother **61**(3): 616-620.
56. Felton, T. W., C. Baxter, C. B. Moore, S. A. Roberts, W. W. Hope and D. W. Denning (2010). "Efficacy and safety of posaconazole for chronic pulmonary aspergillosis." Clin Infect Dis **51**(12): 1383-1391.
57. Felton, T. W., J. Goodwin, L. O'Connor, A. Sharp, L. Gregson, J. Livermore, S. J. Howard, M. N. Neely and W. W. Hope (2013). "Impact of Bolus Dosing versus Continuous Infusion of Piperacillin and Tazobactam on the Development of Antimicrobial Resistance in Pseudomonas aeruginosa." Antimicrobial Agents and Chemotherapy.
58. Fera, M. T., E. La Camera and A. De Sarro (2009). "New triazoles and echinocandins: mode of action, in vitro activity and mechanisms of resistance." Expert Rev Anti Infect Ther **7**(8): 981-998.
59. Fothergill, A., N. Wiederhold, G. Sibley, A. Kennedy, J. Oliver, M. Birch and D. Law (2015). Spectrum of Activity of F901318, The First Agent from the New Orotomide Class of Antifungals. Interscience Conference Antimicrobial Agents and Chemotherapy, San Diego, U.S.
60. Fothergill, A. W., D. Law, M. Birch and N. P. Wiederhold (2016). The Novel Orotomide F901318 Demonstrates Potent In vitro Antifungal Activity Against Lomentospora and Scedosporium Species. European Congress of Clinical Microbiology and Infectious Diseases (ECCMID). Amsterdam, Netherlands.
61. Franquet, T., N. L. Muller, A. Gimenez, P. Guembe, J. de La Torre and S. Bague (2001). "Spectrum of pulmonary aspergillosis: histologic, clinical, and radiologic findings." Radiographics **21**(4): 825-837.
62. Fréalle, E., C. Noël, E. Viscogliosi, D. Camus, E. Dei-Cas and L. Delhaes (2005). "Manganese superoxide dismutase in pathogenic fungi: An issue with pathophysiological and

phylogenetic involvements." FEMS Immunology & Medical Microbiology **45**(3): 411-422.
63. Galimberti, R., A. C. Torre, M. C. Baztán and F. Rodriguez-Chiappetta (2012). "Emerging systemic fungal infections." Clinics in Dermatology **30**(6): 633-650.
64. Garcia-Effron, G., S. Park and D. S. Perlin (2009). "Correlating echinocandin MIC and kinetic inhibition of fks1 mutant glucan synthases for Candida albicans: implications for interpretive breakpoints." Antimicrob Agents Chemother **53**(1): 112-122.
65. Garnica, M., M. Oliveira da Cunha, R. Portugal, A. Maiolino, A. L. Colombo and M. Nucci (2015). "Risk Factors for Invasive Fusariosis in Patients With Acute Myeloid Leukemia and in Hematopoietic Cell Transplant Recipients." Clinical Infectious Diseases **60**(6): 875-880.
66. Gavalda, J., T. Martin, P. Lopez, X. Gomis, J. L. Ramirez, D. Rodriguez, O. Len, Y. Puigfel, I. Ruiz and A. Pahissa (2005). "Efficacy of high loading doses of liposomal amphotericin B in the treatment of experimental invasive pulmonary aspergillosis." Clin Microbiol Infect **11**(12): 999-1004.
67. Georgiadou, S. P., N. V. Sipsas, E. M. Marom and D. P. Kontoyiannis (2011). "The Diagnostic Value of Halo and Reversed Halo Signs for Invasive Mold Infections in Compromised Hosts." Clinical Infectious Diseases **52**(9): 1144-1155.
68. Gilgado, F., J. Cano, J. Gené, D. A. Sutton and J. Guarro (2008). "Molecular and Phenotypic Data Supporting Distinct Species Statuses for Scedosporium apiospermum and Pseudallescheria boydii and the Proposed New Species Scedosporium dehoogii." Journal of Clinical Microbiology **46**(2): 766-771.
69. Gloede, J., C. Scheerans, H. Derendorf and C. Kloft (2010). "In vitro pharmacodynamic models to determine the effect of antibacterial drugs." J Antimicrob Chemother **65**(2): 186-201.
70. Goddard, A. D., J. M. Stevens, F. Rao, D. A. Mavridou, W. Chan, D. J. Richardson, J. W. Allen and S. J. Ferguson (2010). "c-Type cytochrome biogenesis can occur via a natural Ccm system lacking CcmH, CcmG, and the heme-binding histidine of CcmE." J Biol Chem **285**(30): 22882-22889.
71. Gomez-Lopez, A., M. Cuenca-Estrella, A. Monzon and J. L. Rodriguez-Tudela (2001). "In vitro susceptibility of clinical isolates of Zygomycota to amphotericin B, flucytosine, itraconazole and voriconazole." J Antimicrob Chemother **48**(6): 919-921.
72. González, G., J. Márquez, R. d. Treviño-Rangel, J. Palma-Nicolás, E. Garza-González, L. Ceceñas and J. Gerardo González (2013). "Murine Model of Disseminated Fusariosis: Evaluation of the Fungal Burden by Traditional CFU and Quantitative PCR." Mycopathologia **176**(3-4): 219-224.
73. Gonzalez, G. M., R. Tijerina, L. K. Najvar, R. Bocanegra, M. G. Rinaldi, D. Loebenberg and J. R. Graybill (2003). "Activity of posaconazole against Pseudallescheria boydii: in vitro and in vivo assays." Antimicrob Agents Chemother **47**(4): 1436-1438.
74. Gray, K. C., D. S. Palacios, I. Dailey, M. M. Endo, B. E. Uno, B. C. Wilcock and M. D. Burke (2012). "Amphotericin primarily kills yeast by simply binding ergosterol." Proceedings of the National Academy of Sciences **109**(7): 2234-2239.
75. Graybill, J. R., S. Hernandez, R. Bocanegra and L. K. Najvar (2004). "Antifungal Therapy of Murine Aspergillus terreus Infection." Antimicrob Agents Chemother **48**(10): 3715-3719.
76. Gregson, L., J. Goodwin, A. Johnson, L. McEntee, C. B. Moore, M. Richardson, W. W. Hope and S. J. Howard (2013). "In Vitro Susceptibility of Aspergillus fumigatus to Isavuconazole: Correlation with Itraconazole, Voriconazole and Posaconazole." Antimicrob Agents Chemother.
77. Guinea, J., T. Pelaez, S. Recio, M. Torres-Narbona and E. Bouza (2008). "In vitro antifungal activities of isavuconazole (BAL4815), voriconazole, and fluconazole against 1,007 isolates of zygomycete, Candida, Aspergillus, Fusarium, and Scedosporium species." Antimicrob Agents Chemother **52**(4): 1396-1400.

78. Hachem, R. Y., D. P. Kontoyiannis, M. R. Boktour, C. Afif, C. Cooksley, G. P. Bodey, I. Chatzinikolaou, C. Perego, H. M. Kantarjian and Raad, II (2004). "Aspergillus terreus: an emerging amphotericin B-resistant opportunistic mold in patients with hematologic malignancies." Cancer **101**(7): 1594-1600.
79. Hayes, G. E. and D. W. Denning (2013). "Frequency, diagnosis and management of fungal respiratory infections." Curr Opin Pulm Med **19**(3): 259-265.
80. Heath, C. H., M. A. Slavin, T. C. Sorrell, R. Handke, A. Harun, M. Phillips, Q. Nguyen, L. Delhaes, D. Ellis, W. Meyer and S. C. A. Chen (2009). "Population-based surveillance for scedosporiosis in Australia: epidemiology, disease manifestations and emergence of Scedosporium aurantiacum infection." Clinical Microbiology and Infection **15**(7): 689-693.
81. Heykants, J., A. Van Peer, V. Van de Velde, P. Van Rooy, W. Meuldermans, K. Lavrijsen, R. Woestenborghs, J. Van Cutsem and G. Cauwenbergh (1989). "The clinical pharmacokinetics of itraconazole: an overview." Mycoses **32 Suppl 1**: 67-87.
82. Hohl, T. M. and M. Feldmesser (2007). "Aspergillus fumigatus: Principles of Pathogenesis and Host Defense." Eukaryotic Cell **6**(11): 1953-1963.
83. Hope, W., J. Livermore, J. Goodwin, S. Whalley, A. Johnson, L. McEntee, A. Kennedy, D. Law, M. Birch and J. Rex (2015). Pharmacokinetics and Pharmacodynamics (PK-PD) of F901318 Against Aspergillus fumigatus. Interscience Conference for Antimicrobial Agents and Chemotherapy. San Diego, U.S.
84. Hope, W. W., M. J. Kruhlak, C. A. Lyman, R. Petraitiene, V. Petraitis, A. Francesconi, M. Kasai, D. Mickiene, T. Sein, J. Peter, A. M. Kelaher, J. E. Hughes, M. P. Cotton, C. J. Cotten, J. Bacher, S. Tripathi, L. Bermudez, T. K. Maugel, P. M. Zerfas, J. R. Wingard, G. L. Drusano and T. J. Walsh (2007). "Pathogenesis of Aspergillus fumigatus and the kinetics of galactomannan in an in vitro model of early invasive pulmonary aspergillosis: implications for antifungal therapy." J Infect Dis **195**(3): 455-466.
85. Hope, W. W., M. VanGuilder, J. P. Donnelly, N. M. A. Blijlevens, R. J. M. Brüggemann, R. W. Jelliffe and M. N. Neely (2013). "Software for Dosage Individualization of Voriconazole for Immunocompromised Patients." Antimicrobial Agents and Chemotherapy **57**(4): 1888-1894.
86. Horn, D. L., A. G. Freifeld, M. G. Schuster, N. E. Azie, B. Franks and C. A. Kauffman (2014). "Treatment and outcomes of invasive fusariosis: review of 65 cases from the PATH Alliance® registry." Mycoses **57**(11): 652-658.
87. Horton, R. E. and G. Vidarsson (2013). "Antibodies and Their Receptors: Different Potential Roles in Mucosal Defense." Frontiers in Immunology **4**: 200.
88. Howard, S. J. and M. C. Arendrup (2011). "Acquired antifungal drug resistance in Aspergillus fumigatus: epidemiology and detection." Med Mycol **49 Suppl 1**: S90-95.
89. Howard, S. J., D. Cerar, M. J. Anderson, A. Albarrag, M. C. Fisher, A. C. Pasqualotto, M. Laverdiere, M. C. Arendrup, D. S. Perlin and D. W. Denning (2009). "Frequency and evolution of Azole resistance in Aspergillus fumigatus associated with treatment failure." Emerg Infect Dis **15**(7): 1068-1076.
90. Howard, S. J., C. Lass-Flörl, M. Cuenca-Estrella, A. Gomez-Lopez and M. C. Arendrup (2013). "Determination of Isavuconazole Susceptibility of Aspergillus and Candida Species by the EUCAST Method." Antimicrobial Agents and Chemotherapy **57**(11): 5426-5431.
91. Howard, S. J., J. M. Lestner, A. Sharp, L. Gregson, J. Goodwin, J. Slater, J. B. Majithiya, P. A. Warn and W. W. Hope (2011). "Pharmacokinetics and pharmacodynamics of posaconazole for invasive pulmonary aspergillosis: clinical implications for antifungal therapy." J Infect Dis **203**(9): 1324-1332.
92. Howard, S. J., I. Webster, C. B. Moore, R. E. Gardiner, S. Park, D. S. Perlin and D. W. Denning (2006). "Multi-azole resistance in Aspergillus fumigatus." International Journal of Antimicrobial Agents **28**(5): 450-453.
93. Huurneman, L. J., M. Neely, A. Veringa, F. Docobo Pérez, V. Ramos-Martin, W. J. Tissing, J.-W. C. Alffenaar and W. Hope (2016). "Pharmacodynamics of Voriconazole in Children:

Further Steps along the Path to True Individualized Therapy." Antimicrobial Agents and Chemotherapy **60**(4): 2336-2342.
94. Jacobs, F., D. Selleslag, M. Aoun, A. Sonet and A. Gadisseur (2012). "An observational efficacy and safety analysis of the treatment of acute invasive aspergillosis using voriconazole." Eur J Clin Microbiol Infect Dis **31**(6): 1173-1179.
95. Jahn, B., A. Koch, A. Schmidt, G. Wanner, H. Gehringer, S. Bhakdi and A. A. Brakhage (1997). "Isolation and characterization of a pigmentless-conidium mutant of Aspergillus fumigatus with altered conidial surface and reduced virulence." Infect Immun **65**(12): 5110-5117.
96. Jeans, A. R., S. J. Howard, Z. Al-Nakeeb, J. Goodwin, L. Gregson, J. B. Majithiya, C. Lass-Florl, M. Cuenca-Estrella, M. C. Arendrup, P. A. Warn and W. W. Hope (2012). "Pharmacodynamics of voriconazole in a dynamic in vitro model of invasive pulmonary aspergillosis: implications for in vitro susceptibility breakpoints." J Infect Dis **206**(3): 442-452.
97. Jeans, A. R., S. J. Howard, Z. Al-Nakeeb, J. Goodwin, L. Gregson, P. A. Warn and W. W. Hope (2012). "Combination of voriconazole and anidulafungin for treatment of triazole-resistant aspergillus fumigatus in an in vitro model of invasive pulmonary aspergillosis." Antimicrob Agents Chemother **56**(10): 5180-5185.
98. Joseph, J. M., R. Jain and L. H. Danziger (2007). "Micafungin: a new echinocandin antifungal." Pharmacotherapy **27**(1): 53-67.
99. Kassamali, Z., L. H. Danziger, R. C. Glowacki and D. N. Schwartz "How low can you go? Use of low- and standard-dose liposomal amphotericin B for treatment of invasive fungal infections." International Journal of Infectious Diseases(0).
100. Kennedy, A., G. Allen, J. Steiner, J. Oliver, M. Birch, G. Sibley and D. Law (2015). Pharmacokinetics of F901318 in Man from an Intravenous Single Ascending Dose Study. Interscience Conference for Antimicrobial Agents and Chemotherapy, San Diego.
101. Kontoyiannis, D. P. and R. E. Lewis (2006). "Invasive zygomycosis: update on pathogenesis, clinical manifestations, and management." Infect Dis Clin North Am **20**(3): 581-607, vi.
102. Kousha, M., R. Tadi and A. O. Soubani (2011). "Pulmonary aspergillosis: a clinical review." European Respiratory Review **20**(121): 156-174.
103. Kovanda, L. L., R. Petraitiene, V. Petraitis, T. J. Walsh, A. Desai, P. Bonate and W. W. Hope (2016). "Pharmacodynamics of isavuconazole in experimental invasive pulmonary aspergillosis: implications for clinical breakpoints." J Antimicrob Chemother **71**(7): 1885-1891.
104. Krishnan, S., E. K. Manavathu and P. H. Chandrasekar (2005). "A comparative study of fungicidal activities of voriconazole and amphotericin B against hyphae of Aspergillus fumigatus." Journal of Antimicrobial Chemotherapy **55**(6): 914-920.
105. Kwon-Chung, K. J. and J. A. Sugui (2013). "Aspergillus fumigatus—What Makes the Species a Ubiquitous Human Fungal Pathogen?" PLoS Pathogens **9**(12): e1003743.
106. Lackner, M. and J. Guarro (2013). "Pathogenesis of Scedosporium." Current Fungal Infection Reports **7**(4): 326-333.
107. Lamaris, G. A., G. Chamilos, R. E. Lewis, A. Safdar, Raad, II and D. P. Kontoyiannis (2006). "Scedosporium infection in a tertiary care cancer center: a review of 25 cases from 1989-2006." Clin Infect Dis **43**(12): 1580-1584.
108. Lass-Flörl, C., A. Alastruey-Izquierdo, M. Cuenca-Estrella, S. Perkhofer and J. L. Rodriguez-Tudela (2009). "In Vitro Activities of Various Antifungal Drugs against Aspergillus terreus: Global Assessment Using the Methodology of the European Committee on Antimicrobial Susceptibility Testing." Antimicrob Agents Chemother **53**(2): 794-795.
109. Lass-Florl, C., K. Griff, A. Mayr, A. Petzer, G. Gastl, H. Bonatti, M. Freund, G. Kropshofer, M. P. Dierich and D. Nachbaur (2005). "Epidemiology and outcome of infections due to Aspergillus terreus: 10-year single centre experience." British Journal of Haematology **131**(2): 201-207.

110. Law, D., J. Oliver, P. Warn, A. Kennedy, G. Sibley and M. Birch (2015). In Vivo Efficacy of Orally Dosed F901318, in a Murine Model of Disseminated Aspergillosis. Interscience Conference for Antimicrobial Agents and Chemotherapy. San Diego, U.S.
111. Lepak, A. J., K. Marchillo, J. VanHecker and D. R. Andes (2013). "Isavuconazole (BAL4815) Pharmacodynamic Target Determination in an In Vivo Murine Model of Invasive Pulmonary Aspergillosis against Wild-Type and cyp51 Mutant Isolates of Aspergillus fumigatus." Antimicrob Agents Chemother **57**(12): 6284-6289.
112. Lepak, A. J., K. Marchillo, J. VanHecker and D. R. Andes (2013). "Posaconazole Pharmacodynamic Target Determination against Wild-Type and Cyp51 Mutant Isolates of Aspergillus fumigatus in an In Vivo Model of Invasive Pulmonary Aspergillosis." Antimicrob Agents Chemother **57**(1): 579-585.
113. Lepak, A. J., K. Marchillo, J. VanHecker, D. Diekema and D. R. Andes (2013). "Isavuconazole pharmacodynamic target determination for Candida species in an in vivo murine disseminated candidiasis model." Antimicrob Agents Chemother **57**(11): 5642-5648.
114. Lestner, J. M., S. J. Howard, J. Goodwin, L. Gregson, J. Majithiya, T. J. Walsh, G. M. Jensen and W. W. Hope (2010). "Pharmacokinetics and pharmacodynamics of amphotericin B deoxycholate, liposomal amphotericin B, and amphotericin B lipid complex in an in vitro model of invasive pulmonary aspergillosis." Antimicrob Agents Chemother **54**(8): 3432-3441.
115. Lewis, R. E., N. P. Wiederhold and M. E. Klepser (2005). "In vitro pharmacodynamics of amphotericin B, itraconazole, and voriconazole against Aspergillus, Fusarium, and Scedosporium spp." Antimicrob Agents Chemother **49**(3): 945-951.
116. Lima, O. C., G. Larcher, P. Vandeputte, A. Lebouil, D. Chabasse, P. Simoneau and J.-P. Bouchara (2007). "Molecular cloning and biochemical characterization of a Cu,Zn-superoxide dismutase from Scedosporium apiospermum." Microbes and Infection **9**(5): 558-565.
117. Lionakis, M. S., G. Chamilos, R. E. Lewis, N. P. Wiederhold, I. I. Raad, G. Samonis and D. P. Kontoyiannis (2006). "Pentamidine Is Active in a Neutropenic Murine Model of Acute Invasive Pulmonary Fusariosis." Antimicrob Agents Chemother **50**(1): 294-297.
118. Livermore, J. and W. Hope (2012). "Evaluation of the pharmacokinetics and clinical utility of isavuconazole for treatment of invasive fungal infections." Expert Opin Drug Metab Toxicol **8**(6): 759-765.
119. Lortholary, O., G. Obenga, P. Biswas, D. Caillot, E. Chachaty, A.-L. Bienvenu, M. Cornet, J. Greene, R. Herbrecht, C. Lacroix, F. Grenouillet, I. Raad, K. Sitbon, P. Troke and a. t. F. M. S. Group (2010). "International Retrospective Analysis of 73 Cases of Invasive Fusariosis Treated with Voriconazole." Antimicrob Agents Chemother **54**(10): 4446-4450.
120. Lutsar, I., M. R. Hodges, K. Tomaszewski, P. F. Troke and N. D. Wood (2003). "Safety of voriconazole and dose individualization." Clin Infect Dis **36**(8): 1087-1088.
121. Maertens, J. A., R. Klont, C. Masson, K. Theunissen, W. Meersseman, K. Lagrou, C. Heinen, B. Crepin, J. Van Eldere, M. Tabouret, J. P. Donnelly and P. E. Verweij (2007). "Optimization of the cutoff value for the Aspergillus double-sandwich enzyme immunoassay." Clin Infect Dis **44**(10): 1329-1336.
122. Maertens, J. A., I. I. Raad, K. A. Marr, T. F. Patterson, D. P. Kontoyiannis, O. A. Cornely, E. J. Bow, G. Rahav, D. Neofytos, M. Aoun, J. W. Baddley, M. Giladi, W. J. Heinz, R. Herbrecht, W. Hope, M. Karthaus, D.-G. Lee, O. Lortholary, V. A. Morrison, I. Oren, D. Selleslag, S. Shoham, G. R. Thompson, III, M. Lee, R. M. Maher, A.-H. Schmitt-Hoffmann, B. Zeiher and A. J. Ullmann (2016). "Isavuconazole versus voriconazole for primary treatment of invasive mould disease caused by Aspergillus and other filamentous fungi (SECURE): a phase 3, randomised-controlled, non-inferiority trial." The Lancet **387**(10020): 760-769.
123. Majithiya JB, S. A., Parmar A, Denning DW, Warn PA (2008). Correlation of in vitro MIC and MFC against isavuconazole, voriconazole, and amphotericin B of Aspergillus with in

vivo outcome in mice with disseminated Aspergillosis. 18th ECCMID meeting. Barcelona**:** P1915.
124. Margalit, A. and K. Kavanagh (2015). The innate immune response to Aspergillus fumigatus at the alveolar surface.
125. Marom, E. M., A. M. Holmes, J. F. Bruzzi, M. T. Truong, P. J. O'Sullivan and D. P. Kontoyiannis (2008). "Imaging of pulmonary fusariosis in patients with hematologic malignancies." AJR Am J Roentgenol **190**(6): 1605-1609.
126. Marr K, B. E., Heinz W, Lee M, Maher R, Zeiher B, Maertens J (2014). "A Phase 3 Randomized, Double-Blind, Non-Inferiority Trial Evaluating Isavuconazole (ISA) Vs. Voriconazole (VRC) for the Primary Treatment of Invasive Mold Infection (SECURE): Outcomes in Subset of Patients with Hematologic Malignancies (HM)." *Abstr 54th Intersci Conf Antimicrob Agents Chemother (ICAAC)*, Washington, DC.
127. Marr, K. A., S. A. Balajee, L. McLaughlin, M. Tabouret, C. Bentsen and T. J. Walsh (2004). "Detection of Galactomannan Antigenemia by Enzyme Immunoassay for the Diagnosis of Invasive Aspergillosis: Variables That Affect Performance." Journal of Infectious Diseases **190**(3): 641-649.
128. Marr, K. A., R. A. Carter, M. Boeckh, P. Martin and L. Corey (2002). "Invasive aspergillosis in allogeneic stem cell transplant recipients: changes in epidemiology and risk factors." Blood **100**(13): 4358-4366.
129. Marr, K. A., M. Laverdiere, A. Gugel and W. Leisenring (2005). "Antifungal therapy decreases sensitivity of the Aspergillus galactomannan enzyme immunoassay." Clin Infect Dis **40**(12): 1762-1769.
130. Martinez, J. L., T. M. Coque and F. Baquero (2015). "What is a resistance gene? Ranking risk in resistomes." Nat Rev Micro **13**(2): 116-123.
131. Masterton, R. (2008). "The Importance and Future of Antimicrobial Surveillance Studies." Clinical Infectious Diseases **47**(Supplement 1): S21-S31.
132. Mavridou, E., R. J. Bruggemann, W. J. Melchers, J. W. Mouton and P. E. Verweij (2010). "Efficacy of posaconazole against three clinical Aspergillus fumigatus isolates with mutations in the cyp51A gene." Antimicrob Agents Chemother **54**(2): 860-865.
133. Mavridou, E., R. J. Bruggemann, W. J. Melchers, P. E. Verweij and J. W. Mouton (2010). "Impact of cyp51A mutations on the pharmacokinetic and pharmacodynamic properties of voriconazole in a murine model of disseminated aspergillosis." Antimicrob Agents Chemother **54**(11): 4758-4764.
134. McClenny, N. (2005). "Laboratory detection and identification of Aspergillus species by microscopic observation and culture: the traditional approach." Medical Mycology **43**(Supplement 1): S125-S128.
135. Meletiadis, J., J. F. Meis, J. W. Mouton, J. L. Rodriquez-Tudela, J. P. Donnelly, P. E. Verweij and E. Network (2002). "In vitro activities of new and conventional antifungal agents against clinical Scedosporium isolates." Antimicrob Agents Chemother **46**(1): 62-68.
136. Michielse, C. B. and M. Rep (2009). "Pathogen profile update: Fusarium oxysporum." Molecular Plant Pathology **10**(3): 311-324.
137. Mino, Y., T. Naito, T. Watanabe, T. Yamada, T. Yagi, H. Yamada and J. Kawakami (2013). "Hydroxy-itraconazole pharmacokinetics is similar to that of itraconazole in immunocompromised patients receiving oral solution of itraconazole." Clinica Chimica Acta **415**(0): 128-132.
138. Moriyama, B., S. Kadri, S. A. Henning, R. L. Danner, T. J. Walsh and S. R. Penzak (2015). "Therapeutic Drug Monitoring and Genotypic Screening in the Clinical Use of Voriconazole." Current fungal infection reports **9**(2): 74-87.
139. Morrissey, C. O., S. C. A. Chen, T. C. Sorrell, S. Milliken, P. G. Bardy, K. F. Bradstock, J. Szer, C. L. Halliday, N. M. Gilroy, J. Moore, A. P. Schwarer, S. Guy, A. Bajel, A. R. Tramontana, T. Spelman and M. A. Slavin (2013). "Galactomannan and PCR versus culture and histology

for directing use of antifungal treatment for invasive aspergillosis in high-risk haematology patients: a randomised controlled trial." The Lancet Infectious Diseases **13**(6): 519-528.
140. Mouton, J. W., D. F. Brown, P. Apfalter, R. Canton, C. G. Giske, M. Ivanova, A. P. MacGowan, A. Rodloff, C. J. Soussy, M. Steinbakk and G. Kahlmeter (2012). "The role of pharmacokinetics/pharmacodynamics in setting clinical MIC breakpoints: the EUCAST approach." Clin Microbiol Infect **18**(3): E37-45.
141. Muruganandan, S. and C. J. Sinal (2008). "Mice as Clinically Relevant Models for the Study of Cytochrome P450-dependent Metabolism." Clinical Pharmacology & Therapeutics **83**(6): 818-828.
142. Myrianthefs, P., S. L. Markantonis, P. Evaggelopoulou, S. Despotelis, E. Evodia, D. Panidis and G. Baltopoulos (2010). "Monitoring plasma voriconazole levels following intravenous administration in critically ill patients: an observational study." International Journal of Antimicrobial Agents **35**(5): 468-472.
143. Neely, M., A. Margol, X. Fu, M. van Guilder, D. Bayard, A. Schumitzky, R. Orbach, S. Liu, S. Louie and W. Hope (2015). "Achieving Target Voriconazole Concentrations More Accurately in Children and Adolescents." Antimicrobial Agents and Chemotherapy **59**(6): 3090-3097.
144. Neely, M. N., M. G. van Guilder, W. M. Yamada, A. Schumitzky and R. W. Jelliffe (2012). "Accurate detection of outliers and subpopulations with Pmetrics, a nonparametric and parametric pharmacometric modeling and simulation package for R." Ther Drug Monit **34**(4): 467-476.
145. Nelson, P. E., M. C. Dignani and E. J. Anaissie (1994). "Taxonomy, biology, and clinical aspects of Fusarium species." Clin Microbiol Rev **7**(4): 479-504.
146. Nucci, M. (2003). "Emerging moulds: Fusarium, Scedosporium and Zygomycetes in transplant recipients." Curr Opin Infect Dis **16**(6): 607-612.
147. Nucci, M. and E. Anaissie (2007). "Fusarium infections in immunocompromised patients." Clin Microbiol Rev **20**(4): 695-704.
148. Nucci, M., E. J. Anaissie, F. Queiroz-Telles, C. A. Martins, P. Trabasso, C. Solza, C. Mangini, B. P. Simoes, A. L. Colombo, J. Vaz, C. E. Levy, S. Costa, V. A. Moreira, J. S. Oliveira, N. Paraguay, G. Duboc, J. C. Voltarelli, A. Maiolino, R. Pasquini and C. A. Souza (2003). "Outcome predictors of 84 patients with hematologic malignancies and Fusarium infection." Cancer **98**(2): 315-319.
149. Nucci, M., K. A. Marr, F. Queiroz-Telles, C. A. Martins, P. Trabasso, S. Costa, J. C. Voltarelli, A. L. Colombo, A. Imhof, R. Pasquini, A. Maiolino, C. A. Souza and E. Anaissie (2004). "Fusarium infection in hematopoietic stem cell transplant recipients." Clin Infect Dis **38**(9): 1237-1242.
150. Nucci, M., K. A. Marr, M. J. G. T. Vehreschild, C. A. de Souza, E. Velasco, P. Cappellano, F. Carlesse, F. Queiroz-Telles, D. C. Sheppard, A. Kindo, S. Cesaro, N. Hamerschlak, C. Solza, W. J. Heinz, M. Schaller, A. Atalla, S. Arikan-Akdagli, H. Bertz, C. Galvão Castro Jr, R. Herbrecht, M. Hoenigl, G. Härter, N. E. U. Hermansen, A. Josting, L. Pagano, M. J. C. Salles, S. B. Mossad, D. Ogunc, A. C. Pasqualotto, V. Araujo, P. F. Troke, O. Lortholary, O. A. Comely and E. Anaissie (2014). "Improvement in the outcome of invasive fusariosis in the last decade." Clinical Microbiology and Infection **20**(6): 580-585.
151. Oliver, J., D. Law, G. Sibley, A. Kennedy and M. Birch (2015). F901318, a Novel Antifungal Agent from the Orotomide Class: Discovery and Mechanism of Action. Interscience Conference for Antimicrobial Agents and Chemotherapy, San Diego.
152. Olson, J. A., J. P. Adler-Moore, J. Schwartz, G. M. Jensen and R. T. Proffitt (2006). "Comparative efficacies, toxicities, and tissue concentrations of amphotericin B lipid formulations in a murine pulmonary aspergillosis model." Antimicrob Agents Chemother **50**(6): 2122-2131.

153. Ortoneda, M., F. J. Pastor, E. Mayayo and J. Guarro (2002). "Comparison of the virulence of Scedosporium prolificans strains from different origins in a murine model." J Med Microbiol **51**(11): 924-928.
154. Pagano, L., M. Caira, M. Picardi, A. Candoni, L. Melillo, L. Fianchi, M. Offidani and A. Nosari (2007). "Invasive Aspergillosis in Patients with Acute Leukemia: Update on Morbidity and Mortality—SEIFEM-C Report." Clinical Infectious Diseases **44**(11): 1524-1525.
155. Paphitou, N. I., L. Ostrosky-Zeichner, V. L. Paetznick, J. R. Rodriguez, E. Chen and J. H. Rex (2002). "In vitro activities of investigational triazoles against Fusarium species: effects of inoculum size and incubation time on broth microdilution susceptibility test results." Antimicrob Agents Chemother **46**(10): 3298-3300.
156. Park, B. J., P. G. Pappas, K. A. Wannemuehler, B. D. Alexander, E. J. Anaissie, D. R. Andes, J. W. Baddley, J. M. Brown, L. M. Brumble, A. G. Freifeld, S. Hadley, L. Herwaldt, J. I. Ito, C. A. Kauffman, G. M. Lyon, K. A. Marr, V. A. Morrison, G. Papanicolaou, T. F. Patterson, T. M. Perl, M. G. Schuster, R. Walker, J. R. Wingard, T. J. Walsh and D. P. Kontoyiannis (2011). "Invasive non-Aspergillus mold infections in transplant recipients, United States, 2001-2006." Emerging infectious diseases **17**(10): 1855-1864.
157. Parker, J., A. S. Warrilow, C. Price, J. L. Mullins, D. Kelly and S. Kelly (2014). "Resistance to antifungals that target CYP51." Journal of Chemical Biology **7**(4): 143-161.
158. Pascual, A., T. Calandra, S. Bolay, T. Buclin, J. Bille and O. Marchetti (2008). "Voriconazole Therapeutic Drug Monitoring in Patients with Invasive Mycoses Improves Efficacy and Safety Outcomes." Clinical Infectious Diseases **46**(2): 201-211.
159. Pastor, F. J. and J. Guarro (2014). "Treatment of Aspergillus terreus infections: A clinical problem not yet resolved." International Journal of Antimicrobial Agents **44**(4): 281-289.
160. Paulussen, C., G. A. V. Boulet, P. Cos, P. Delputte and L. J. R. M. Maes (2014). "Animal models of invasive aspergillosis for drug discovery." Drug Discovery Today **19**(9): 1380-1386.
161. Peman, J., M. Salavert, E. Canton, I. Jarque, E. Roma, R. Zaragoza, A. Viudes and M. Gobernado (2006). "Voriconazole in the management of nosocomial invasive fungal infections." Ther Clin Risk Manag **2**(2): 129-158.
162. Perfect, J. R., G. M. Cox, J. Y. Lee, C. A. Kauffman, L. de Repentigny, S. W. Chapman, V. A. Morrison, P. Pappas, J. W. Hiemenz, D. A. Stevens and a. t. M. S. Group (2001). "The Impact of Culture Isolation of Aspergillus Species: A Hospital-Based Survey of Aspergillosis." Clinical Infectious Diseases **33**(11): 1824-1833.
163. Perfect, J. R., K. A. Marr, T. J. Walsh, R. N. Greenberg, B. DuPont, J. de la Torre-Cisneros, G. Just-Nubling, H. T. Schlamm, I. Lutsar, A. Espinel-Ingroff and E. Johnson (2003). "Voriconazole treatment for less-common, emerging, or refractory fungal infections." Clin Infect Dis **36**(9): 1122-1131.
164. Perkhofer, S., V. Lechner, C. Lass-Florl and T. European Committee on Antimicrobial Susceptibility (2009). "In vitro activity of Isavuconazole against Aspergillus species and zygomycetes according to the methodology of the European Committee on Antimicrobial Susceptibility Testing." Antimicrob Agents Chemother **53**(4): 1645-1647.
165. Petraitiene, R., V. Petraitis, J. D. Bacher, M. A. Finkelman and T. J. Walsh (2015). "Effects of host response and antifungal therapy on serum and BAL levels of galactomannan and (1→3)-β-D-glucan in experimental invasive pulmonary aspergillosis." Medical Mycology **53**(6): 558-568.
166. Petraitis, V., R. Petraitiene, A. H. Groll, K. Roussillon, M. Hemmings, C. A. Lyman, T. Sein, J. Bacher, I. Bekersky and T. J. Walsh (2002). "Comparative antifungal activities and plasma pharmacokinetics of micafungin (FK463) against disseminated candidiasis and invasive pulmonary aspergillosis in persistently neutropenic rabbits." Antimicrob Agents Chemother **46**(6): 1857-1869.

167. Petrikkos, G. L. (2009). "Lipid formulations of amphotericin B as first-line treatment of zygomycosis." Clin Microbiol Infect **15 Suppl 5**: 87-92.
168. Pfaller, M. A., L. Boyken, R. J. Hollis, J. Kroeger, S. A. Messer, S. Tendolkar and D. J. Diekema (2009). "In vitro susceptibility of clinical isolates of Aspergillus spp. to anidulafungin, caspofungin, and micafungin: a head-to-head comparison using the CLSI M38-A2 broth microdilution method." J Clin Microbiol **47**(10): 3323-3325.
169. Pfaller, M. A., S. A. Messer, P. R. Rhomberg, R. N. Jones and M. Castanheira (2013). "In vitro activities of isavuconazole and comparator antifungal agents tested against a global collection of opportunistic yeasts and molds." J Clin Microbiol **51**(8): 2608-2616.
170. Pfaller, M. A., S. A. Messer, L. N. Woosley, R. N. Jones and M. Castanheira (2013). "Echinocandin and triazole antifungal susceptibility profiles of opportunistic yeast and mould clinical isolates (2010-2011): Application of new CLSI clinical breakpoints and epidemiological cutoff values to characterize geographic and temporal trends of antifungal resistance." Journal of Clinical Microbiology.
171. Pfaller, M. A., D. J. Sheehan and J. H. Rex (2004). "Determination of Fungicidal Activities against Yeasts and Molds: Lessons Learned from Bactericidal Testing and the Need for Standardization." Clinical Microbiology Reviews **17**(2): 268-280.
172. Pfizer. (2011). "Vfend." from http://www.pfizer.com/files/products/uspi_vfend.pdf.
173. Philip, A., Z. Odabasi, J. Rodriguez, V. L. Paetznick, E. Chen, J. H. Rex and L. Ostrosky-Zeichner (2005). "In Vitro Synergy Testing of Anidulafungin with Itraconazole, Voriconazole, and Amphotericin B against Aspergillus spp. and Fusarium spp." Antimicrob Agents Chemother **49**(8): 3572-3574.
174. Purkins, L., N. Wood, P. Ghahramani, K. Greenhalgh, M. J. Allen and D. Kleinermans (2002). "Pharmacokinetics and safety of voriconazole following intravenous- to oral-dose escalation regimens." Antimicrob Agents Chemother **46**(8): 2546-2553.
175. Raad, I. I., R. Y. Hachem, R. Herbrecht, J. R. Graybill, R. Hare, G. Corcoran and D. P. Kontoyiannis (2006). "Posaconazole as salvage treatment for invasive fusariosis in patients with underlying hematologic malignancy and other conditions." Clinical Infectious Diseases **42**(10): 1398-1403.
176. Rex, J. H., B. I. Eisenstein, J. Alder, M. Goldberger, R. Meyer, A. Dane, I. Friedland, C. Knirsch, W. R. Sanhai, J. Tomayko, C. Lancaster and J. Jackson (2013). "A comprehensive regulatory framework to address the unmet need for new antibacterial treatments." The Lancet Infectious Diseases **13**(3): 269-275.
177. Rhodes, N. J., J. L. Kuti, D. P. Nicolau, S. Van Wart, A. M. Nicasio, J. Liu, B. J. Lee, M. N. Neely and M. H. Scheetz (2016). "Defining Clinical Exposures of Cefepime for Gram-Negative Bloodstream Infections That Are Associated with Improved Survival." Antimicrobial Agents and Chemotherapy **60**(3): 1401-1410.
178. Roffey, S. J., S. Cole, P. Comby, D. Gibson, S. G. Jezequel, A. N. Nedderman, D. A. Smith, D. K. Walker and N. Wood (2003). "The disposition of voriconazole in mouse, rat, rabbit, guinea pig, dog, and human." Drug Metab Dispos **31**(6): 731-741.
179. Rudramurthy, S. M., A. Chakrabarti, E. Geertsen, J. W. Mouton and J. F. Meis (2011). "In vitro activity of isavuconazole against 208 Aspergillus flavus isolates in comparison with 7 other antifungal agents: assessment according to the methodology of the European Committee on Antimicrobial Susceptibility Testing." Diagnostic Microbiology and Infectious Disease **71**(4): 370-377.
180. Rudramurthy, S. M., M. Jatana, R. Singh and A. Chakrabarti (2013). "In vitro antifungal activity of Indian liposomal amphotericin B against clinical isolates of emerging species of yeast and moulds, and its comparison with amphotericin B deoxycholate, voriconazole, itraconazole and fluconazole." Mycoses **56**(1): 39-46.

181. Ruiz-Cendoya, M., M. M. Rodriguez, M. Marine, F. J. Pastor and J. Guarro (2008). "In vitro interactions of itraconazole and micafungin against clinically important filamentous fungi." International Journal of Antimicrobial Agents **32**(5): 418-420.
182. Rybak, J. M., K. R. Marx, A. T. Nishimoto and P. D. Rogers (2015). "Isavuconazole: Pharmacology, Pharmacodynamics, and Current Clinical Experience with a New Triazole Antifungal Agent." Pharmacotherapy: The Journal of Human Pharmacology and Drug Therapy **35**(11): 1037-1051.
183. Schelenz, S., R. A. Barnes, R. C. Barton, J. R. Cleverley, S. B. Lucas, C. C. Kibbler and D. W. Denning (2015). "British Society for Medical Mycology best practice recommendations for the diagnosis of serious fungal diseases." Lancet Infect Dis **15**(4): 461-474.
184. Schmitt-Hoffmann, A., B. Roos, M. Heep, M. Schleimer, E. Weidekamm, T. Brown, M. Roehrle and C. Beglinger (2006). "Single-ascending-dose pharmacokinetics and safety of the novel broad-spectrum antifungal triazole BAL4815 after intravenous infusions (50, 100, and 200 milligrams) and oral administrations (100, 200, and 400 milligrams) of its prodrug, BAL8557, in healthy volunteers." Antimicrob Agents Chemother **50**(1): 279-285.
185. Schmitt-Hoffmann, A., B. Roos, J. Maares, M. Heep, J. Spickerman, E. Weidekamm, T. Brown and M. Roehrle (2006). "Multiple-dose pharmacokinetics and safety of the new antifungal triazole BAL4815 after intravenous infusion and oral administration of its prodrug, BAL8557, in healthy volunteers." Antimicrob Agents Chemother **50**(1): 286-293.
186. Segal, B. H. (2009). "Aspergillosis." N Engl J Med **360**(18): 1870-1884.
187. Seyedmousavi, S., R. J. Bruggemann, J. F. Meis, W. J. Melchers, P. E. Verweij and J. W. Mouton (2015). "Pharmacodynamics of Isavuconazole in an Aspergillus fumigatus Mouse Infection Model." Antimicrob Agents Chemother **59**(5): 2855-2866.
188. Seyedmousavi, S., J. W. Mouton, W. J. G. Melchers, R. J. M. Brüggemann and P. E. Verweij (2014). "The role of azoles in the management of azole-resistant aspergillosis: From the bench to the bedside." Drug Resistance Updates **17**(3): 37-50.
189. Shalit, I., Y. Shadkchan, G. Mircus and N. Osherov (2009). "In vitro synergy of caspofungin with licensed and novel antifungal drugs against clinical isolates of Fusarium spp." Medical Mycology **47**(5): 457-462.
190. Sharma, V. and R. Bhatia (2011). "Triazoles in Antifungal Therapy: A Review." International Journal of Research in Pharmaceutical and Biomedical **2**.
191. Sinnollareddy, M., S. L. Peake, M. S. Roberts, J. Lipman and J. A. Roberts (2012). "Using pharmacokinetics and pharmacodynamics to optimise dosing of antifungal agents in critically ill patients: a systematic review." International Journal of Antimicrobial Agents **39**(1): 1-10.
192. Slavin, M., S. van Hal, T. C. Sorrell, A. Lee, D. J. Marriott, K. Daveson, K. Kennedy, K. Hajkowicz, C. Halliday, E. Athan, N. Bak, E. Cheong, C. H. Heath, C. Orla Morrissey, S. Kidd, R. Beresford, C. Blyth, T. M. Korman, J. Owen Robinson, W. Meyer and S. C. A. Chen (2015). "Invasive infections due to filamentous fungi other than Aspergillus: epidemiology and determinants of mortality." Clinical Microbiology and Infection **21**(5): 490.e491-490.e410.
193. Slesiona, S., M. Gressler, M. Mihlan, C. Zaehle, M. Schaller, D. Barz, B. Hube, I. D. Jacobsen and M. Brock (2012). "Persistence versus Escape: Aspergillus terreus and Aspergillus fumigatus Employ Different Strategies during Interactions with Macrophages." PLoS ONE **7**(2): e31223.
194. Smith, J., N. Safdar, V. Knasinski, W. Simmons, S. M. Bhavnani, P. G. Ambrose and D. Andes (2006). "Voriconazole Therapeutic Drug Monitoring." Antimicrob Agents Chemother **50**(4): 1570-1572.
195. Smith, J. A. and C. A. Kauffman (2012). "Pulmonary fungal infections." Respirology **17**(6): 913-926.
196. Soubani, A. O. and P. H. Chandrasekar (2002). "The clinical spectrum of pulmonary aspergillosis." Chest **121**(6): 1988-1999.

197. Spellberg, B., J. Schwartz, Y. Fu, V. Avanesian, J. Adler-Moore, J. E. Edwards and A. S. Ibrahim (2006). "Comparison of antifungal treatments for murine fusariosis." Journal of Antimicrobial Chemotherapy **58**(5): 973-979.
198. Srivastava, S., N. Pathak and P. Srivastava (2011). "Identification of Limiting Factors for the Optimum Growth of Fusarium Oxysporum in Liquid Medium." Toxicology International **18**(2): 111-116.
199. Steinbach, W. J., D. K. Benjamin, D. P. Kontoyiannis, J. R. Perfect, I. Lutsar, K. A. Marr, M. S. Lionakis, H. A. Torres, H. Jafri and T. J. Walsh (2004). "Infections due to Aspergillus terreus: A multicenter retrospective analysis of 83 cases." Clinical Infectious Diseases **39**(2): 192-198.
200. Stempel, J. M., S. P. Hammond, D. A. Sutton, L. M. Weiser and F. M. Marty (2015). "Invasive Fusariosis in the Voriconazole Era: Single-Center 13-Year Experience." Open Forum Infectious Diseases **2**(3): ofv099.
201. Stevens, D. A. (2012). "Advances in systemic antifungal therapy." Clinics in Dermatology **30**(6): 657-661.
202. Taccone, F. S., A.-M. Van den Abeele, P. Bulpa, B. Misset, W. Meersseman, T. Cardoso, J.-A. Paiva, M. Blasco-Navalpotro, E. De Laere, G. Dimopoulos, J. Rello, D. Vogelaers, S. I. Blot and I. C. U. S. I. on behalf of the Asp (2015). "Epidemiology of invasive aspergillosis in critically ill patients: clinical presentation, underlying conditions, and outcomes." Critical Care **19**(1): 7.
203. Takemoto, K., Y. Yamamoto and K. Kanazawa (2010). "Comparative study of the efficacy of liposomal amphotericin B and amphotericin B deoxycholate against six species of Zygomycetes in a murine lethal infection model." Journal of Infection and Chemotherapy **16**(6): 388-395.
204. Tam, V. H. and M. Nikolaou (2011). "A novel approach to pharmacodynamic assessment of antimicrobial agents: new insights to dosing regimen design." PLoS Comput Biol **7**(1): e1001043.
205. Theuretzbacher, U., F. Ihle and H. Derendorf (2006). "Pharmacokinetic/Pharmacodynamic Profile of Voriconazole." Clinical Pharmacokinetics **45**(7): 649-663.
206. Thompson, G. R., 3rd and N. P. Wiederhold (2010). "Isavuconazole: a comprehensive review of spectrum of activity of a new triazole." Mycopathologia **170**(5): 291-313.
207. Thornton, C., G. Johnson and S. Agrawal (2012). "Detection of Invasive Pulmonary Aspergillosis in Haematological Malignancy Patients by using Lateral-flow Technology." Journal of Visualized Experiments : JoVE(61): 3721.
208. Thornton, C. R. (2001). Immunological methods for fungi. Molecular and Cellular Biology of Filamentous Fungi. e. N.J. Talbot. Oxford, U.K, Oxford University Press**:** 209-226.
209. Thornton, C. R. (2008). "Development of an Immunochromatographic Lateral-Flow Device for Rapid Serodiagnosis of Invasive Aspergillosis." Clinical and Vaccine Immunology **15**(7): 1095-1105.
210. Thornton, C. R. (2009). "Tracking the emerging human pathogen Pseudallescheria boydii by using highly specific monoclonal antibodies." Clin Vaccine Immunol **16**(5): 756-764.
211. Thornton, C. R. and O. E. Wills (2015). "Immunodetection of fungal and oomycete pathogens: Established and emerging threats to human health, animal welfare and global food security." Critical Reviews in Microbiology **41**(1): 27-51.
212. Torres-Narbona, M., J. Guinea, J. Martinez-Alarcon, T. Pelaez and E. Bouza (2007). "In vitro activities of amphotericin B, caspofungin, itraconazole, posaconazole, and voriconazole against 45 clinical isolates of zygomycetes: comparison of CLSI M38-A, Sensititre YeastOne, and the Etest." Antimicrob Agents Chemother **51**(3): 1126-1129.
213. Torres, H. A., R. Y. Hachem, R. F. Chemaly, D. P. Kontoyiannis and Raad, II (2005). "Posaconazole: a broad-spectrum triazole antifungal." Lancet Infect Dis **5**(12): 775-785.

214. Tortorano, A. M., M. Richardson, E. Roilides, A. van Diepeningen, M. Caira, P. Munoz, E. Johnson, J. Meletiadis, Z. D. Pana, M. Lackner, P. Verweij, T. Freiberger, O. A. Cornely, S. Arikan-Akdagli, E. Dannaoui, A. H. Groll, K. Lagrou, A. Chakrabarti, F. Lanternier, L. Pagano, A. Skiada, M. Akova, M. C. Arendrup, T. Boekhout, A. Chowdhary, M. Cuenca-Estrella, J. Guinea, J. Guarro, S. de Hoog, W. Hope, S. Kathuria, O. Lortholary, J. F. Meis, A. J. Ullmann, G. Petrikkos and C. Lass-Florl (2014). "ESCMID and ECMM joint guidelines on diagnosis and management of hyalohyphomycosis: Fusarium spp., Scedosporium spp. and others." Clinical microbiology and infection : the official publication of the European Society of Clinical Microbiology and Infectious Diseases **20 Suppl 3**: 27-46.
215. Trifilio, S., G. Pennick, J. Pi, J. Zook, M. Golf, K. Kaniecki, S. Singhal, S. Williams, J. Winter, M. Tallman, L. Gordon, O. Frankfurt, A. Evens and J. Mehta (2007). "Monitoring plasma voriconazole levels may be necessary to avoid subtherapeutic levels in hematopoietic stem cell transplant recipients." Cancer **109**(8): 1532-1535.
216. Troke, P., K. Aguirrebengoa, C. Arteaga, D. Ellis, C. H. Heath, I. Lutsar, M. Rovira, Q. Nguyen, M. Slavin, S. C. A. Chen and o. b. o. t. G. S. S. Group (2008). "Treatment of Scedosporiosis with Voriconazole: Clinical Experience with 107 Patients." Antimicrob Agents Chemother **52**(5): 1743-1750.
217. Troke, P. F., H. P. Hockey and W. W. Hope (2011). "Observational study of the clinical efficacy of voriconazole and its relationship to plasma concentrations in patients." Antimicrob Agents Chemother **55**(10): 4782-4788.
218. Turnidge, J. and D. L. Paterson (2007). "Setting and revising antibacterial susceptibility breakpoints." Clin Microbiol Rev **20**(3): 391-408, table of contents.
219. Ueda, K., Y. Nannya, K. Kumano, A. Hangaishi, T. Takahashi, Y. Imai and M. Kurokawa (2009). "Monitoring trough concentration of voriconazole is important to ensure successful antifungal therapy and to avoid hepatic damage in patients with hematological disorders." Int J Hematol **89**(5): 592-599.
220. Ullmann A, S. S., Huang W, Mujais S (2014). "A Phase 3 Randomized, Double-Blind, Non-Inferiority Trial Evaluating Isavuconazole (ISA) vs. Voriconazole (VRC) for the Primary Treatment of Invasive Fungal Disease (IFD) Caused by Aspergillus spp. or other Filamentous Fungi (SECURE): Outcomes by Malignancy Status." *Abstr 54th Intersci Conf AntimicrobAgents and Chemother (ICAAC)*, Washington, DC
221. Vazquez, J. A. (2005). "Anidulafungin: A new echinocandin with a novel profile." Clinical Therapeutics **27**(6): 657-673.
222. Verdaguer, V., T. J. Walsh, W. Hope and K. J. Cortez (2006). "Galactomannan antigen detection in the diagnosis of invasive aspergillosis." Expert Review of Molecular Diagnostics **7**(1): 21-32.
223. Verweij, P. E. and M. A. S. H. Mennink-Kersten (2006). "Issues with galactomannan testing." Medical Mycology **44**(Supplement 1): S179-S183.
224. Vyas, S. P. and S. Gupta (2006). "Optimizing efficacy of amphotericin B through nanomodification." Int J Nanomedicine **1**(4): 417-432.
225. Walsh, T. J., P. Pappas, D. J. Winston, H. M. Lazarus, F. Petersen, J. Raffalli, S. Yanovich, P. Stiff, R. Greenberg, G. Donowitz, M. Schuster, A. Reboli, J. Wingard, C. Arndt, J. Reinhardt, S. Hadley, R. Finberg, M. Laverdiere, J. Perfect, G. Garber, G. Fioritoni, E. Anaissie, J. Lee, A. National Institute of and G. Infectious Diseases Mycoses Study (2002). "Voriconazole compared with liposomal amphotericin B for empirical antifungal therapy in patients with neutropenia and persistent fever." N Engl J Med **346**(4): 225-234.
226. Walsh, T. J., H. Teppler, G. R. Donowitz, J. A. Maertens, L. R. Baden, A. Dmoszynska, O. A. Cornely, M. R. Bourque, R. J. Lupinacci, C. A. Sable and B. E. dePauw (2004). "Caspofungin versus liposomal amphotericin B for empirical antifungal therapy in patients with persistent fever and neutropenia." N Engl J Med **351**(14): 1391-1402.

227. Wang, T., J. Xie, Y. Wang, X. Zheng, J. e. Lei, X. Wang, H. Dong, Q. Yang, L. Chen, J. Xing and Y. Dong (2015). "Pharmacokinetic and Pharmacodynamic Properties of Oral Voriconazole in Patients with Invasive Fungal Infections." Pharmacotherapy: The Journal of Human Pharmacology and Drug Therapy **35**(9): 797-804.
228. Warn PA, S. A., Denning DW (2008). Dose response in neutropenic mice with disseminated infection of multiple strains of Aspergillus fumigatus with widely varying MIC and MFC values treated with isavuconazole. 17th ECCMID meeting. Munich.
229. Warn, P. A., A. Sharp, J. Mosquera, J. Spickermann, A. Schmitt-Hoffmann, M. Heep and D. W. Denning (2006). "Comparative in vivo activity of BAL4815, the active component of the prodrug BAL8557, in a neutropenic murine model of disseminated Aspergillus flavus." J Antimicrob Chemother **58**(6): 1198-1207.
230. Warn, P. A., A. Sharp, A. Parmar, J. Majithiya, D. W. Denning and W. W. Hope (2009). "Pharmacokinetics and pharmacodynamics of a novel triazole, isavuconazole: mathematical modeling, importance of tissue concentrations, and impact of immune status on antifungal effect." Antimicrob Agents Chemother **53**(8): 3453-3461.
231. Wasylnka, J. A., M. I. Simmer and M. M. Moore (2001). "Differences in sialic acid density in pathogenic and non-pathogenic Aspergillus species." Microbiology (Reading, England) **147**(Pt 4): 869-877.
232. Wiederhold, N. P., D. P. Kontoyiannis, J. Chi, R. A. Prince, V. H. Tam and R. E. Lewis (2004). "Pharmacodynamics of caspofungin in a murine model of invasive pulmonary aspergillosis: evidence of concentration-dependent activity." J Infect Dis **190**(8): 1464-1471.
233. Willems, L., R. van der Geest and K. de Beule (2001). "Itraconazole oral solution and intravenous formulations: a review of pharmacokinetics and pharmacodynamics." J Clin Pharm Ther **26**(3): 159-169.
234. Woodcock, J. (2012). "Evidence vs. Access: Can Twenty-First-Century Drug Regulation Refine the Tradeoffs?" Clinical Pharmacology & Therapeutics **91**(3): 378-380.
235. Zhang, Y. Y., X. Zhou and M. National Collaborative Group of Sequential Itraconazole Treatment for Invasive Pulmonary (2011). "Efficacy and safety of intravenous itraconazole followed by oral itraconazole solution in the treatment of invasive pulmonary mycosis." Chin Med J (Engl) **124**(20): 3415-3419.